HAL open science

Fay's identity in the theory of integrable systems

Caroline Kalla

To cite this version:

Caroline Kalla. Fay's identity in the theory of integrable systems. General Mathematics [math.GM]. Université de Bourgogne, 2011. English. NNT : 2011DIJOS020 . tel-00622289v2

HAL Id: tel-00622289

https://theses.hal.science/tel-00622289v2

Submitted on 1 Mar 2012

HAL is a multi-disciplinary open access archive for the deposit and dissemination of scientific research documents, whether they are published or not. The documents may come from teaching and research institutions in France or abroad, or from public or private research centers.

L'archive ouverte pluridisciplinaire **HAL**, est destinée au dépôt et à la diffusion de documents scientifiques de niveau recherche, publiés ou non, émanant des établissements d'enseignement et de recherche français ou étrangers, des laboratoires publics ou privés.

UNIVERSITE DE BOURGOGNE
IMB
INSTITUT DE MATHEMATIQUES DE BOURGOGNE
UMR 5584 du CNRS

THESE

soutenue le 27 juin 2011 pour l'obtention du grade de

Docteur de l'Université de Bourgogne

(Specialité Mathématiques)

par

Caroline KALLA

Fay's identity in the theory of integrable systems

Devant le jury composé des Professeurs :

Président du jury :	**VAN MOERBEKE Pierre** *(Université catholique de Louvain)*
Rapporteurs :	**KOROTKIN Dmitry** *(Université Concordia, Montréal)* **PREVIATO Emma** *(Université de Boston)*
Examinateurs :	**MATVEEV Vladimir** *(Université de Bourgogne)* **SHRAMCHENKO Vasilisa** *(Université de Sherbrooke)*
Directeur de thèse :	**KLEIN Christian** *(Université de Bourgogne)*

Résumé

Un outil puissant dans le cadre des solutions algébro-géométriques des équations intégrables est l'identité de Fay sur des surfaces de Riemann compactes. Cette relation généralise une identité bien connue pour la fonction birapport dans le plan complexe. Elle permet d'établir des relations entre les fonctions theta et leurs dérivées. Cela offre une approche complémentaire aux solutions algébro-géométriques des équations intégrables avec certains avantages par rapport à l'utilisation des fonctions de Baker-Akhiezer. Cette méthode a été appliquée avec succès par Mumford et al. aux équations Korteweg-de Vries, Kadomtsev-Petviashvili et sine-Gordon.

Selon cette approche, nous construisons des solutions algébro-géométriques des équations de Camassa-Holm et de Dym, ainsi que des solutions de l'équation de Schrödinger non linéaire à plusieurs composantes et des équations de Davey-Stewartson. Les limites solitoniques de ces solutions sont étudiées lorsque le genre de la surface de Riemann associée tombe à zéro. De plus, nous présentons une évaluation numérique des solutions algébro-géométriques des équations intégrables lorsque la surface de Riemann associée est réelle.

Remerciements

Je remercie chaleureusement mon directeur de thèse Christian Klein pour le sujet qu'il m'a proposé, ainsi que pour son soutien, son écoute et sa gentillesse. Je ne remercierai jamais assez Dmitry Korotkin et Vasilisa Shramchenko pour toutes les discussions mathématiques que nous avons pu avoir, mais aussi pour tous ces "instants chocolat" partagés... Merci à Vladimir Matveev pour son attention et tout ce savoir qu'il partage et transmet. Je remercie B. Dubrovin et T. Grava de m'avoir invitée à l'institut de recherche SISSA à Trieste, ainsi que pour le temps qu'ils ont bien voulu m'accorder. Merci également à A. Kokotov, E. Previato et A. Treibich que j'ai eu le plaisir de rencontrer lors de mes diverses missions à l'étranger, et merci au professeur van Moerbeke d'avoir accepté d'être le président de mon jury.

Je tiens à remercier tous les enseignants et chercheurs que j'ai pu cotoyer depuis le début de ma scolarité à l'université de Bourgogne, et plus particulièrement les intervenants de la préparation à l'agrégation. Merci également aux secrétaires du laboratoire Caro, Anissa et Gladys. Ce travail n'aurait pu s'effectuer sans le soutien logistique et financier de l'IMB, de l'École Doctorale Carnot et sans la bourse de thèse que la région Bourgogne m'a attribuée.

J'ai eu la chance et le plaisir d'effectuer mes heures d'enseignement au sein d'une équipe formidable, celle des professeurs de l'IUT src, merci à N. Noirot et coucou à F. Vachey. Je salue et remercie tous les thésards, dont ceux de ma génération: Muriel, Rafa, Jérome, Etienne, Kristelle, Aymen, Bilel, Gautier et Gabriel.

Merci à mon professeur de violon Gérard Montmayeur qui m'a tant apporté, ainsi qu'à tous mes amis d' "Archets pour un Espoir" avec lesquels nous partageons des moments magiques. Merci pour tout à Patrick Gabriel. Une grosse bise à mon amie Myrine Perrin qui a préféré le soleil marseillais à la pluie dijonnaise (coucou à Popo, Garfield, etc...). J'embrasse très fort toute ma famille, et plus particulièrement mes parents et mon frère sans qui je ne serais que poussière.

To you

Contents

List of Figures **xi**

List of Symbols **xiii**

1 Introduction **1**

1.1 Introduction to the theory of integrable systems 1
1.1.1 What does integrability mean? 1
1.1.2 The discovery of solitary waves 3
1.1.3 An algebro-geometric approach to integrable systems 4
1.1.4 Reality problems in soliton theory 7
1.2 Outline of the thesis 8

I Theta functions, Fay's identity and real Riemann surfaces **15**

2 Theta functions and Fay's identity **17**

2.1 Riemann surfaces 17
2.1.1 Riemann surfaces and non-singular algebraic curves 17
2.1.2 Holomorphic mappings and coverings 18
2.1.3 Homology group and intersection index 19
2.1.4 Abelian differentials and their periods 21
2.2 Multi-dimensional theta functions 23
2.2.1 Definition and properties 23
2.2.2 Theta divisor and Jacobi inversion problem 24
2.2.3 Construction of functions and differentials on a Riemann surface 25
2.3 Fay's identity 26
2.3.1 Fay's identity and generalization of the cross-ratio to Riemann surfaces . . 27
2.3.2 Previously known degenerated versions of Fay's identity 27
2.3.3 Applications to integrable systems - Mumford's approach 29

3 Real Riemann surfaces **33**

3.1 Topological type of a real Riemann surface 33
3.2 Action of τ on the homology group $H_1(\mathcal{R}_g)$ 34

3.3 Action of τ on $H_1(\mathcal{R}_g \setminus \{a,b\})$ and $H_1(\mathcal{R}_g, \{a,b\})$ 35
3.3.1 Case $\tau a = b$ 35
3.3.2 Case $\tau a = a$ and $\tau b = b$ 36
3.4 Action of τ on the Jacobian and theta divisor 38

II Camassa-Holm and Dym type equations 41

4 Algebro-geometric solutions via Fay's identity 43
4.1 Solutions of the Camassa-Holm equation 43
4.1.1 Identities between theta functions 44
4.1.2 Real-valued solutions and smoothness conditions 46
4.2 Solutions of the Dym-type equation 50
4.2.1 Theta-functional identities 50
4.2.2 Real-valued solutions and smoothness conditions 53

5 Solitonic limit 55
5.1 Degeneracy of hyperelliptic Riemann surfaces 55
5.1.1 Degeneracy of hyperelliptic normalized Abelian differentials 55
5.1.2 Degeneration of hyperelliptic theta functions 57
5.2 Soliton-like solutions 59
5.2.1 Soliton-like solutions of the CH equation 59
5.2.2 Soliton-like solutions of the Dym-type equation 60
5.3 Peakon solutions 61
5.3.1 Peakon solutions of the CH equation 61
5.3.2 Peakon solutions of the Dym-type equation 63

III Generalized nonlinear Schrödinger equations 65

6 Algebro-geometric solutions via Fay's identity 67
6.1 New degeneration of Fay's identity 67
6.2 Computation of the argument of the fundamental scalar $q_2(a,b)$ 69
6.2.1 Integral representation for $q_2(a,b)$ 69
6.2.2 Argument of $q_2(a,b)$ when $\tau a = b$ 70
6.2.3 Argument of $q_2(a,b)$ when $\tau a = a$ and $\tau b = b$ 72
6.3 Algebro-geometric solutions of the multi-component NLS equation 73
6.3.1 Solutions of the complexified n-NLS equation 73
6.3.2 Reality conditions 75
6.3.3 Solutions of n-NLS$^+$ and n-NLS$^-$ 78
6.3.4 Stationary solutions of n-NLS 83
6.3.5 Reduction of n-NLS to $(n-1)$-NLS 84
6.3.6 Hyperelliptic solutions of n-NLS 85
6.3.7 Relationship between solutions of KP1 and solutions of n-NLS 87

6.4 Algebro-geometric solutions of the Davey-Stewartson equations 88
6.4.1 Solutions of the complexified Davey-Stewartson equations 89
6.4.2 Reality condition and solutions of the DS1$^\rho$ equation 90
6.4.3 Reality condition and solutions of the DS2$^\rho$ equation 92
6.4.4 Reduction of the DS1$^\rho$ equation to the NLS equation 95

7 Degeneration of algebro-geometric solutions 97
7.1 Fay's identity and degenerate Riemann surfaces 97
7.1.1 Uniformization map and degeneration to genus zero 98
7.1.2 Degenerate theta function 99
7.1.3 Constants in the limit 100
7.2 Degenerate algebro-geometric solutions of n-NLS 102
7.2.1 Determinantal solutions of the complexified n-NLS equation 102
7.2.2 Multi-solitonic solutions of n-NLS 104
7.2.3 Breather and rational breather solutions of n-NLS 108
7.3 Degenerate algebro-geometric solutions of the DS equations 116
7.3.1 Determinantal solutions of the complexified DS equations 116
7.3.2 Multi-solitonic solutions of the DS equations 117
7.3.3 Breather and rational breather solutions of the DS equations 120
7.3.4 Dromion and lump solutions of the DS equations 123
7.4 Outlook 129

8 On the numerical evaluation of algebro-geometric solutions 131
8.1 Hyperelliptic case 131
8.1.1 Computation on real hyperelliptic curves 131
8.1.2 Solutions to the DS equations 134
8.1.3 Solutions to the n-NLS^s equation 139
8.2 General real algebraic curves 142
8.2.1 Symplectic transformation 142
8.2.2 Trott curve 146
8.2.3 Dividing curves without real branch point 149
8.2.4 Fermat curve 151
8.3 Outlook 151

Outlook 153

Bibliography 155

Index 165

List of Figures

6.1 Hurwitz diagram of the covering $\mathcal{R}_{g,n+1}$ 79

6.2 Homology basis on the covering $\mathcal{R}^{+}_{g,n+1}$ when the genus g is odd 80

6.3 Homology basis on the covering $\mathcal{R}^{+}_{g,n+1}$ when the genus g is even 80

6.4 Closed contour $\tau\tilde{\ell}_n - \tilde{\ell}_n \in H_1\big(\mathcal{R}^{+}_{g,n+1} \setminus \{a_{n+1}, a_n\}\big)$ 81

6.5 Homology basis on the covering $\mathcal{R}^{-}_{g,n+1}$ 82

6.6 Closed contour $\tau\tilde{\ell}_n - \tilde{\ell}_n \in H_1\big(\mathcal{R}^{-}_{g,n+1} \setminus \{a_{n+1}, a_n\}\big)$ 83

7.1 Dark 2-soliton of 4-NLS^{+-+-} 106

7.2 Bright 2-soliton of 4-NLS^{++++} 108

7.3 Breather of 4-NLS^{--+-} 110

7.4 2-breather of 4-NLS^{-++-} 111

7.5 Rational breather of 4-NLS^{++++} 114

7.6 2-rational breather of 4-NLS^{++++} 115

7.7 Dark 3-soliton of DS1^{-} 118

7.8 Bright 2-soliton of DS2^{-} 120

7.9 2-breather of DS1^{-} 121

7.10 2-rational breather of DS1^{-} 123

7.11 Interaction between a line rational breather and a rational breather of DS1^{-} (same direction of propagation) 124

7.12 Interaction between a line rational breather and a rational breather of DS1^{-} (transversal propagations) 125

7.13 A dromion solution of DS1^{-} 127

7.14 A lump solution of DS2^{-} 128

8.1 Homology basis on real hyperelliptic curves 132

8.2 Solution of DS1$^+$ on a genus 2 hyperelliptic curve with real branch points on the left; the almost solitonic limit on the right . . . 134
8.3 Solution of DS2$^+$ on a genus 2 hyperelliptic curve with real branch points on the left; the almost solitonic limit on the right . . . 135
8.4 Solution of DS1$^+$ on a genus 4 hyperelliptic curve with real branch points on the left; the almost solitonic limit on the right . . . 135
8.5 Solution of DS2$^+$ on a genus 4 hyperelliptic curve with real branch points on the left; the almost solitonic limit on the right . . . 136
8.6 Solution of DS1$^-$ on a genus 2 hyperelliptic curve with pairwise conjugate branch points . . . 136
8.7 Solution of DS1$^-$ on a genus 4 hyperelliptic curve with pairwise conjugate branch points . . . 137
8.8 Solution of DS2$^-$ on a genus 2 hyperelliptic curve with pairwise conjugate branch points . . . 137
8.9 Solution of DS2$^-$ on a genus 4 hyperelliptic curve with pairwise conjugate branch points . . . 138
8.10 Solution of 2-NLS^{--} on a genus 2 hyperelliptic curve with real branch points on the left; the almost solitonic limit on the right . . . 139
8.11 Solution of 2-NLS^{+-} on a genus 2 hyperelliptic curve with real branch points on the left; the almost solitonic limit on the right . . . 139
8.12 Solution of 4-NLS^{+-+-} on the left, solution of 4-NLS^{-+--} on the right, on a genus 4 hyperelliptic curve with real branch points . . . 140
8.13 Solution of 2-NLS^{++} on a genus 2 hyperelliptic curve with conjugate pairwise branch points . . . 140
8.14 Solution of 4-NLS^{++++} on a genus 4 hyperelliptic curve with conjugate pairwise branch points . . . 141
8.15 Solution of 3-NLS^{+--} on the Trott curve . . . 148
8.16 Solution of DS1$^+$ on the Trott curve . . . 148
8.17 Solution of DS2$^+$ on the Trott curve . . . 149
8.18 Solution of 3-NLS^{+++} on a genus 3 dividing curve . . . 150
8.19 Solution of DS1$^-$ on a genus 3 dividing curve . . . 150
8.20 Solution of DS2$^-$ on the Fermat curve of genus 3 . . . 152

List of Symbols

∇	Gradient operator	17
$\mathcal{R}_g$	Compact Riemann surface of genus g	18
$H_1(\mathcal{R}_g)$	First homology group of the Riemann surface $\mathcal{R}_g$	19
$\circ$	Intersection index	20
$\delta_{i,j}$	Kronecker symbol	20
$\mathcal{A}_j, \mathcal{B}_j$	Cycles of a canonical homology basis	20
$\mathbb{I}_g$	$g \times g$ unit matrix	20
$\Omega_a^{(N)}$	Abelian differential of the second kind	21
$k_a(.)$	Local parameter in a neighbourhood of point a	21
Ω_{b-a}	Abelian differential of the third kind	21
$\mathbb{B}$	Riemann matrix	22
Λ	Periods lattice	23
$J(\mathcal{R}_g)$	Jacobian	23
$\Pi(.)$	Abel map	23
$\int_a^b$	Abel map between points a and b	23
$\Theta[\delta](.)$	Theta function with characteristic δ	23
$\Theta(.)$	Theta function with zero characteristic	23
$\langle .,. \rangle$	Euclidian inner product	23
Diag(.)	Column vector of the diagonal entries	24
$E(.,.)$	Prime form	25
$\Omega(.,.)$	Bidifferential	26
D_a, D'_a, D''_a	Directional derivatives along the vector $\mathbf{V}_a, \mathbf{W}_a, \mathbf{U}_a$ respectively	28
τ	Anti-holomorphic involution	33
$\mathcal{R}_g(\mathbb{R})$	Set of fixed points of an anti-holomorphic involution	33
$\mathbb{H}$	$g \times g$ matrix defined by the action of τ on $H_1(\mathcal{R}_g)$	34
diag(.)	Column vector of diagonal elements of a square matrix	35
$H_1(\mathcal{R}_g \setminus \{a,b\})$	First homology group of the punctured Riemann surface $\mathcal{R}_g \setminus \{a,b\}$	35
$H_1(\mathcal{R}_g, \{a,b\})$	Relative homology group	35
$\mathcal{S}_a$	Positively oriented small contour around point a	35
Re(.)	Real part	38
σ	Hyperelliptic involution	43
arg{.}	Argument of a complex scalar	69
Im(.)	Imaginary part	71
$\mathcal{R}_{g,n+1}$	$(n+1)$-sheeted branched covering of $\mathbb{CP}^1$	78
sign(.)	Sign of a real scalar	94

Chapter 1

Introduction

1.1 Introduction to the theory of integrable systems

The modern theory of integrable systems has considerably enlarged the class of exactly solvable equations. It has also led to the discovery and understanding of new physical phenomena as solitons and breathers. Among the most powerful solution generating methods are techniques from algebraic geometry which lead to solutions in terms of multi-dimensional theta functions on certain Riemann surfaces. In the seventies, almost periodic solutions to the Korteweg-de Vries (KdV), the Kadomtsev-Petviashvili (KP), the sine-Gordon equations and others were constructed in terms of multi-dimensional theta functions. These are entire transcendental functions which are in general defined as Fourier series with certain periodicity properties.

1.1.1 What does integrability mean?

The notion of integrable system arose in the framework of mechanical systems for which the equations of motion are solvable by quadratures, i.e., only algebraic operations, integrations as well as applications of the inverse function theorem are needed. A reference of particular value is the book [19] on Hamiltonian systems. In classical Hamiltonian mechanics, a mechanical system with n degrees of freedom is described by a phase space parametrized by $2n$ coordinates q_i, p_i, $i = 1, \ldots, n$, and the evolution of these coordinates is given by the following equations of motion:

$$\frac{\mathrm{d}q_i}{\mathrm{d}t} = \frac{\partial H}{\partial p_i}, \qquad \frac{\mathrm{d}p_i}{\mathrm{d}t} = -\frac{\partial H}{\partial q_i}, \qquad i = 1, \ldots, n,$$

where $H = H(q_i, p_i)$ is called the Hamilton function of the system. The first main result in this context is due to Liouville (who essentially applied Hamilton's result) and is known as Liouville's theorem. The latter states that if a mechanical system of the above form has n independent functions in involution (independent in the sense that their gradients are linearly independent), one of which being H, then it can be solved by quadratures. Recall that two functions f and g are said to be in involution if their Poisson bracket $\{f, g\}$ vanishes, where

$$\{f, g\} = \sum_{i=1}^{n} \left(\frac{\partial f}{\partial q_i} \frac{\partial g}{\partial p_i} - \frac{\partial f}{\partial p_i} \frac{\partial g}{\partial q_i} \right).$$

Moreover, f is called a first integral of the system if f and H are in involution.

This yields the notion of integrability in the sense of Liouville. Among Liouville integrable systems, let us mention a few integrable tops such as the Euler top, the Lagrange top or the Kowalevskaya top, the free motion of a particle on an ellipsoid (Jacobi), and the motion of a rigid body in an ideal fluid (Clebsch, Kirchhoff and Steklov case). To prove Liouville integrability of these systems and to solve them by quadrature was often a fastidious work. Solutions expressed in terms of the two-dimensional theta function arose in the most complicated cases. The emergence of algebraic geometry in the theory of integrable systems motivated the use of Riemann's and Abel's works developed in the beginning of the 19th century. However, for about 60 years no progress was made in this context for the following reasons: firstly, Poincaré proved that a general mechanical system of the above Hamiltonian form is not Liouville integrable as, for instance, the famous three body problem, and secondly, the domain of complex analysis and algebraic geometry developed the theory of theta functions and Abelian varieties without direct link with the theory of integrable systems.

One of the significant advances in mathematical physics at the end of the 20th century has been the discovery in 1967 by Gardner, Greene, Kruskal and Miura of a new method to solve nonlinear evolution equations. This method, called the inverse scattering method, was applied to solve the Cauchy problem for the Korteweg-de Vries (KdV) equation in the case of rapidly decaying initial data. It follows that nonlinear equations integrable via the inverse scattering method possess a Hamiltonian formulation having an infinite number of independent first integrals in involution. This allows to consider these systems as integrable systems with an infinite number of degrees of freedom. Later this method succeeded in the framework of finite dimensional systems, firstly investigated by Flaschka, Manakov and Moser. The study of one-dimensional periodic problems solvable by this method reveals connections with algebraic geometry and Riemann surfaces.

In 1968, Lax [106] introduced the concept of the Lax pair for the KdV equation to construct exact solutions by the method of inverse scattering (see, for instance, [4]). The KdV equation was in fact considered as the compatibility condition for a pair of commuting linear operators. More generally, the notion of a Lax pair consists in presenting the equations of motion of the system in the form $\partial_t L(\lambda) = [M(\lambda), L(\lambda)]$, where the matrices $L(\lambda)$ and $M(\lambda)$ depend on the dynamical variables and on a parameter λ called the spectral parameter; here the bracket $[.,.]$ denotes the commutator of matrices. It is a remarkable fact that the Lax equation is an isospectral evolution equation for the Lax matrix $L(\lambda)$. As a consequence, the algebraic curve defined by the equation $det(L(\lambda) - \mu I) = 0$ is time-independent and is called the spectral curve. The integrals of motion of the system arise as eigenvalues of the linear operator $L(\lambda)$. The Lax-pair representation of a system allows to linearize the flow on the Jacobi variety of the spectral curve. However, there is no systematic way to establish the existence of a Lax pair with spectral parameter, and there is no algorithm for finding it, even if the system is known to be integrable or even if a Lax pair without spectral parameter is already known explicitly.

In 1972, Zakharov and Shabat [154] showed that the underlying method indeed worked for another physically significant nonlinear evolution equation, namely, the nonlinear Schrödinger equation. This was indeed an important discovery, not only because it was a second nonlinear evolution equation solvable by this technique, but also because the associated linear eigenvalue problem that one has to consider is not in this case the linear Schrödinger operator. Using these ideas, Ablowitz et al. [1, 2] extended the inverse scattering method to a matrix system and found new equations which turned out to be solvable by this method. The inverse scattering method was extended to a spatially discrete system by Flaschka and Manakov [61], [110] who

independently developed a Lax formalism of the Toda lattice. Generalization of the inverse scattering method to systems with two spatial dimensions was made by Zakharov and Shabat [155]. A typical example is the Kadomtsev-Petviashvili (KP) equation, a $2+1$ dimensional version of the KdV equation.

Several new techniques were invented in the seventies, in particular, the direct method (bilinearization) of R. Hirota, the algebro-geometric method of B.A. Dubrovin, A.R. Its, I.M. Krichever, V.B. Matveev, P. Van Moerbeke, S.P. Novikov, as well as the group-theoretical (or Lie-algebraic) method due to M. Adler, B. Kostant, W.W. Symes, A.G. Reyman and M.A. Semenov-Tian-Shansky which emerged in the second half of the seventies.

1.1.2 The discovery of solitary waves

The remarkable phenomenon of solitary wave was first observed by J. Scott Russel [139] in 1834:

> "I was observing the motion of a boat which was rapidly drawn along a narrow channel by a pair of horses, when the boat suddenly stopped – not so the mass of water in the channel which it had put in motion; it accumulated round the prow of the vessel in a state of violent agitation, then suddenly leaving it behind, rolled forward with greater velocity, assuming the form of a large solitary elevation, a rounded, smooth and well-defined heap of water, which continued its course along the channel apparently without change of form or diminution of speed. I followed it on horseback, and overtook it still rolling on at a rate of some eight or nine miles an hour, preserving its original figure some thirty feet long and a foot to a foot and a half in height. Its height gradually diminished, and after a chase of one or two miles I lost it in the windings of the channel. Such, in the month of August 1834, was my first chance interview with that singular and beautiful phenomenon... "

In 1895, Korteweg and de Vries [93] derived the equation

$$4\,u_t = 6\,uu_x + u_{xxx}, \tag{1.1.1}$$

where $u = u(x,t)$ is a function of two variables, to model the wave propagation of water in a shallow channel. They obtained solitary wave solutions (see e.g. [122]), namely, solutions for which the shape is maintained when travelling. Such a solution is of the form

$$u(x,t) = 2\,c^2\,\mathrm{sech}^2\left(c\,(x + c^2 t) + d\right),$$

for some $c, d \in \mathbb{R}$. Viewing t as a time parameter, these solutions can be described as having a single localized "hump" of height $2\,c^2$ travelling to the left at speed c^2, with the position at time $t = 0$ being determined by the value of d. Notice that waves with smaller amplitudes travel more slowly than waves with larger amplitudes.

The modern theory of soliton equations started with the famous numerical computation of the interaction of solitary waves of the KdV equation by Zabusky and Kruskal [152] in 1965. The authors coined the word soliton to describe these solitary waves which behave like particles and may collide without changing shape. These observations stimulated theoretical researches and soon led in 1967 to the discovery by Gardner, Greene, Kruskal and Miura [70] of exact "multi-soliton" solutions and the Inverse Scattering Transform method (IST) that produces those solutions which have no analogue for linear partial differential equations. The most important

physical property of solitons is that they are localized wave packets which survive collisions with other solitons without change of shape. For a guide to the vast literature on solitons, see, for instance, [126, 42].

Existence of solitonic solutions to the nonlinear Schrödinger equation (NLS)

$$\mathrm{i}\,\frac{\partial\psi}{\partial t}+\frac{\partial^2\psi}{\partial x^2}+2\rho\,|\psi|^2\,\psi=0, \tag{1.1.2}$$

where $\rho=\pm1$, was proved by Zakharov and Shabat [154] using a modification of the IST. The N-soliton solutions to both the (self-)focusing NLS equation ($\rho=1$), as well as the defocusing NLS equation ($\rho=-1$), can also be computed by Darboux transformations [114], Hirota's bilinear method (see, e.g., [77, 130, 33]) or Wronskian techniques (see [69, 123, 68]). Hirota's method is based on a transformation of the underlying equation to a bilinear equation. The resulting multi-soliton solutions are expressed in the form of polynomials in exponential functions. Wronskian techniques formulate the N-soliton solutions in terms of the Wronskian determinant of N functions. This method allows a straightforward direct check that the obtained functions satisfy the equation since differentiation of a Wronskian is simple. On the other hand, multi-soliton solutions of (1.1.2) can be directly derived from algebro-geometric solutions when the associated hyperelliptic Riemann surface degenerates into a Riemann surface of genus zero, see, for instance, [23].

1.1.3 An algebro-geometric approach to integrable systems

Algebraic geometry appears in the theory of integrable systems in the inverse problem for the KdV equation with periodic initial data, for which the inverse scattering transform method failed. The inverse spectral problem for linear operators with periodic coefficients (potentials) remained unsolved for a long time, and was to some extent solved by the consideration of so-called finite-gap potentials. These are potentials for which the number of intervals forming the spectrum, and thus the number of gaps separating these intervals, is finite.

The history of periodic spectral theory starts with the investigations of Sturm and Liouville on the eigenvalues of certain differential operators of second order with given boundary conditions, now referred to as Sturm-Liouville theory. Contrary to the case were the potential is rapidly decaying, in the periodic problem there is no simple asymptotic behavior, resulting in a theory which is more technical and less explicit, investigated by Dubrovin, Matveev, Novikov, Van Moerbeke, Its and others (see, for instance, [50, 126, 118]).

Development of the finite-gap potential theory started with the works of Novikov (1974) and Lax (1975) (see [124] and [107]). Novikov proposed a solution of the inverse periodic spectral problem for finite-gap potentials which is not effective in the sense that he described all finite-gap potentials as solutions of the stationary higher KdV equations (Novikov's equation). An other approach (see [48, 23]) which is more effective consists in introducing Abelian functions, a generalization of elliptic functions to more than one variable, which are expressed as ratios of homogeneous polynomials of Riemann's theta function. It turns out that all finite-gap potentials are Abelian functions. The starting point of this approach is that the description of finite-gap potentials is reduced to a Jacobi inversion problem on a Riemann surface.

Fundamental algebraic-geometric tools in the theory of finite-gap linear operators and in the algebraic-geometric version of the inverse scattering method are the so-called Baker-Akhiezer functions which solve the auxiliary linear partial differential equations with "finite-gap" coefficients. Clebsh and Gordan first considered a generalization of the exponential function on the

Riemann sphere to Riemann surfaces of higher genus. Baker-Akhiezer functions are special functions with essential singularities on a Riemann surface and can be expressed in terms of the so-called theta function, which, in the present context, yields almost periodic solutions of the underlying equation. These functions were introduced in [97] as a generalization of the analytic properties of Bloch eigenfunctions of operators with periodic and almost periodic coefficients.

Let us illustrate this theory in the case of the Kadomtsev-Petviashvili (KP) equation. Two versions of this equation exist:

1. the stable version (also called the KP2 equation)

$$\begin{aligned} \frac{3}{4}\, u_y &= w_x, \\ w_y &= u_t - \frac{1}{4}\,(6\, u u_x + u_{xxx}), \end{aligned} \tag{1.1.3}$$

2. the unstable version (the KP1 equation)

$$\begin{aligned} \frac{3}{4}\, u_y &= w_x, \\ w_y &= u_t - \frac{1}{4}\,(6\, u u_x - u_{xxx}), \end{aligned} \tag{1.1.4}$$

where u, w are functions of the variables x, y, t. Notice that the change of variables $(x, y, t) \to (\mathrm{i}x, \mathrm{i}y, \mathrm{i}t)$ transforms the KP2 equation into the KP1. Equation (1.1.3) can be written as the compatibility condition of the auxiliary linear problem

$$[\partial_y - L, \partial_t - A] = 0,$$

where L and A are differential operators given by

$$L = \partial_x^2 + u, \qquad A = \partial_x^3 + \frac{3}{4}\,(u\partial_x + \partial_x u) + w. \tag{1.1.5}$$

The Baker-Akhiezer functions in this case are defined for each Riemann surface $\mathcal{R}_g$ of finite genus g with a fixed point p_0 on it, and a local parameter k^{-1} in a neighbourhood of this point, $k^{-1}(p_0) = 0$. For any set of points $\{p_j\}_{j=1}^g$ there exists a unique function $\Psi(x, y, t, p)$, with $p \in \mathcal{R}_g$, such that:

1. Ψ is meromorphic on $\mathcal{R}_g \setminus \{p_0\}$ and has no more than simple poles at the points p_j (if they are distinct),

2. at the point p_0 it has an essential singularity of the form:

$$\Psi(x, y, t, p) = \left(1 + \sum_{n=1}^{\infty} \xi_n(x, y, t)\, k^{-n}\right) \exp\left\{kx + k^2 y + k^3 t\right\}, \tag{1.1.6}$$

   where $k = k(p)$ for any p lying in a neighbourhood of p_0.

For any formal series (1.1.6) there exist unique operators L and A of the form (1.1.5) such that the following relations hold near point p_0

$$\begin{aligned}(\partial_y - L)\Psi &= O(k^{-1}) \exp\left\{kx + k^2 y + k^3 t\right\}, \\ (\partial_t - A)\Psi &= O(k^{-1}) \exp\left\{kx + k^2 y + k^3 t\right\}. \end{aligned} \tag{1.1.7}$$

From (1.1.7) it can be seen that the coefficient $u(x, y, t)$ of these operators reads

$$u(x, y, t) = -2\,\xi_{1,x}(x, y, t). \tag{1.1.8}$$

Now notice that the left hand sides of (1.1.7) define functions having the same analytical properties except at p_0 as Ψ, and behave as (1.1.7) near this point. The uniqueness of the Baker-Akhiezer function Ψ implies that they are equal to zero, namely,

$$(\partial_y - L)\Psi = 0, \qquad (\partial_t - A)\Psi = 0.$$

It follows that function u (1.1.8) is a solution of the KP equation. The explicit construction of Baker-Akhiezer functions in terms of Riemann theta functions and Abelian differentials allows to write the solutions (1.1.8) of the KP equation in terms of theta functions:

$$u(x, y, t) = 2\,\partial_x^2 \ln \Theta(\mathbf{Z}(x, y, t) - \mathbf{d}) + \gamma, \tag{1.1.9}$$

for some $\mathbf{d} \in \mathbb{C}^g$, where the vector $\mathbf{Z} \in \mathbb{C}^g$ is a linear function of the variables x, y, t whose vector coefficients depend on the associated Riemann surface and the marked point p_0, as well as the constant $\gamma \in \mathbb{C}$. For any $\mathbf{z} \in \mathbb{C}^g$, $\Theta(\mathbf{z})$ denotes the multi-dimensional theta function (2.2.1) with zero characteristic.

The construction was proposed in [97, 96] and was developed in different ways for various types of integrable equations in remarkable works by Novikov, Dubrovin, Matveev, Its, Van Moerbeke, who constructed algebraic geometrical solutions of the KdV equation, sine-Gordon equation and some other Lax-type equations (see, for instance, [98, 48, 105, 23]).

Parallely, in 1973, Fay [60] discovered the so-called trisecant identity which is an important and special identity satisfied by theta functions. It is a far-reaching generalization of the addition theorem for elliptic theta functions. This identity states that, for any points a, b, c, d on a compact Riemann surface of genus $g > 0$, and for any $\mathbf{z} \in \mathbb{C}^g$, there exist constants γ_1, γ_2 and γ_3 such that

$$\gamma_1\,\Theta\Big(\mathbf{z} + \int_c^a\Big)\,\Theta\Big(\mathbf{z} + \int_b^d\Big) + \gamma_2\,\Theta\Big(\mathbf{z} + \int_b^a\Big)\,\Theta\Big(\mathbf{z} + \int_c^d\Big) = \gamma_3\,\Theta(\mathbf{z})\,\Theta\Big(\mathbf{z} + \int_{c+b}^{a+d}\Big); \tag{1.1.10}$$

here and below we use the notation $\int_a^b$ for the Abel map (2.1.13) between a and b. This identity plays an important role in various domains of mathematics, as for example in the theory of Jacobian varieties [17], in conformal field theory [137], and in operator theory [116].

A few years later, Mumford [121] realized that theta-functional solutions of certain integrable equations such as KdV, KP, and Sine-Gordon, may be derived from Fay's trisecant identity and its degenerations. It is a remarkable fact that algebro-geometric solutions of these integrable equations, previously obtained by the use of Baker-Akhiezer functions, arise as a degeneration of a purely algebro-geometric identity. The aim of this thesis is to extend this approach to other integrable equations such as the Camassa-Holm and Dym type equations, as well as generalizations of the NLS equation (1.1.2) namely, the multi-component NLS equation and the Davey-Stewartson equations.

1.1.4 Reality problems in soliton theory

Solutions of integrable equations (or soliton equations) are physically meaningful if they can be applied to describe actual physical phenomena. This is not the case in general without restrictions on the associated data. Therefore, it is often necessary to select physically or geometrically relevant classes of solutions corresponding to the studied problem: for instance solutions that satisfy certain reality conditions, smooth solutions, or bounded solutions. Let us mention a few famous examples in the algebro-geometric framework.

The KP1 (1.1.4) and KP2 (1.1.3) equations may be applied to the description of various interesting phenomena in plasma physics and hydrodynamics. In both cases only real non-singular solutions are physically relevant. A solution is called non-singular if it is non-singular on the whole real Abel torus. This problem was solved by Dubrovin and Natanzon in [51]. It turns out that the Riemann surface $\mathcal{R}_g$ of genus g associated to algebro-geometric solutions is real, namely there exists an anti-holomorphic involution $\tau : \mathcal{R}_g \to \mathcal{R}_g$, $\tau^2 = \mathrm{id}$ on it. Moreover, Dubrovin and Natanzon proved that solutions of KP1 and KP2 are non-singular for a given topological type of the associated real Riemann surface.

The nonlinear Schrödinger equation (1.1.2) can be solved by introducing its complexified version

$$\begin{aligned} \mathrm{i}\,\frac{\partial\psi}{\partial t} + \frac{\partial^2\psi}{\partial x^2} + 2\,\psi^2\,\psi^* &= 0, \\ -\,\mathrm{i}\,\frac{\partial\psi^*}{\partial t} + \frac{\partial^2\psi^*}{\partial x^2} + 2\,\psi^{*2}\,\psi &= 0, \end{aligned} \tag{1.1.11}$$

where ψ and ψ^* are complex valued functions of the real variables x and t. This system has two natural real reductions: the defocusing NLS equation, obtained by imposing the reality condition $\psi^* = -\,\psi$, and the focusing NLS equation under the condition $\psi^* = \psi$. These reality conditions constrain the associated (hyperelliptic) spectral curve to be real. More precisely, it was proved by Its [79] (see also [23]) that the spectral curve associated to solutions of the defocusing NLS equation is a hyperelliptic curve with real branch points only, whereas the hyperelliptic curve for the focusing case has pairwise conjugate branch points being all non-real. Physical applications such as light propagation in fiber optics, where the sign $+$ or $-$ is determined by the dispersion relation, require non-singular solutions.

The sine-Gordon equation was derived in the end of the nineteenth century. It describes for instance immersions of negative curvature surfaces into $\mathbb{R}^3$. In the light-cone variables (ξ, η), the sine-Gordon equation reads

$$u_{\xi\eta} = \sin(u). \tag{1.1.12}$$

Assume that an asymptotic coordinate system is chosen (a coordinate system such that coordinate lines have zero normal curvature). Thus the angle between the coordinate lines satisfies (1.1.12). This means that only real non-singular solutions such that $u(\xi, \eta) \neq 0 \pmod{\pi}$ are relevant. According to [94] and [80], the spectral curve associated to real-valued solutions consists of a hyperelliptic curve having either only nonpositive real branch points or pairwise conjugate non-real branch points. However, no ideas were proposed where the poles are located on the Riemann surface. For this reason, the theory of periodic finite-gap solutions of the sine-Gordon equation lacked applications for a long time. The problem was solved by Cherednik [34] in 1980; he proved that any real solution is in fact non-singular.

1.2 Outline of the thesis

Chapter 2, 3. Chapter 2 contains various algebraic tools related to the theory of Riemann surfaces, theta functions and Abelian differentials. For further details, the reader is referred, for instance, to [24, 58, 48, 23]. Fay's identity obtained in [60] is presented as a generalization to Riemann surfaces of the well-known identity for the cross-ratio function in the complex plane. Following Mumford's approach [121], we explain how algebro-geometric solutions of the KdV, KP, sine-Gordon and the Toda lattice equations arise from Fay's identity.

As mentioned in Section 1.1.4, various tools dealing with the theory of real Riemann surfaces are necessary to construct physically meaningful algebro-geometric solutions of integrable systems. In Chapter 3, we recall basic facts concerning the topological type of a real Riemann surface. We introduce a canonical homology basis (used in [150]) adapted to the anti-holomorphic involution τ. This canonical homology basis has particular properties with respect to τ and will be used in the whole thesis. An explicit description of the real and imaginary parts of the Jacobian is given according to the works of Vinnikov [150] and Dubrovin-Natanzon [51]. Moreover, we study both actions of the anti-holomorphic involution τ on the homology group $H_1(\mathcal{R}_g \setminus \{a,b\})$ of the punctured Riemann surface $\mathcal{R}_g \setminus \{a,b\}$, and on its dual, the relative homology group $H_1(\mathcal{R}_g, \{a,b\})$, where a, b are two distinct points lying on $\mathcal{R}_g$. These technical results allow to construct in Chapter 4 real-valued and smooth algebro-geometric solutions of the Camassa-Holm and Dym type equations, as well as smooth algebro-geometric solutions of the multi-component nonlinear Schrödinger equation and the Davey-Stewartson equations in Chapter 6.

Chapter 4, 5. Algebro-geometric solutions of the Camassa-Holm and Dym type equations are obtained from theta-functional identities. Real-valuedness and smoothness of the solutions are studied from a topological point of view. In Chapter 5 these solutions are considered on surfaces degenerated to genus 0 to get special solutions such as solitons, cuspons as well as peakons.

At the end of the twentieth century, special attention was given to a shallow water equation (first discovered by means of geometric considerations by Fokas and Fuchssteiner [62]) investigated by Camassa and Holm in [31] (see also [32]):

$$u_t + 3\,uu_x = u_{xxt} + 2\,u_x u_{xx} + uu_{xxx} - 2k\,u_x, \tag{1.2.1}$$

where the function u of the real variables x and t represents the fluid velocity in x-direction measured at time t by an observer moving at speed k. In this context, only real-valued solutions are physically meaningful. They showed that for all k, the Camassa-Holm equation (CH) (1.2.1) is integrable, and for $k = 0$, it has travelling solutions of the form $u(x,t) = c\,\exp\{-|x - vt|\}$ (v is the speed), which are called peakons because they have a discontinuous first derivative at the wave peak. In particular, they described the dynamics of the peakons in terms of a finite-dimensional completely integrable Hamiltonian system, namely, each peakon solution is associated to a mechanical system of moving particles. The class of mechanical systems of this type was further extended by Calogero and Françoise in [28, 29]. Multi-peakon solutions were studied using different approaches in a series of papers [20, 21, 22, 30]. Periodic solutions of the shallow water equation were discussed in [117].

In Chapter 4, we also study the Dym type equation (DH)

$$u_{xxt} + 2\,u_x u_{xx} + uu_{xxx} - 2k\,u_x = 0, \tag{1.2.2}$$

which is a member of the Dym hierarchy (see [78] and [9, 10]). An important feature of equations (1.2.1) and (1.2.2) is that the corresponding Abel–Jacobi mapping is not standard. Namely, the holomorphic differentials that are involved do not form a basis on the hyperelliptic spectral curve, moreover, it involves a meromorphic differential. In contrast to the well known cases of KdV, NLS and sine-Gordon equations, complex solutions of the CH and Dym equations are not meromorphic functions of (x, t) but have several branches. This is due to the presence of an implicit function $y(x, t)$ of the variables x and t in the argument of the theta function appearing in the solutions. This monodromy effect is present in the profile of real-valued solutions such as cusps and peakons solutions.

Algebro-geometric solutions of the Camassa-Holm equation and their properties are studied in [7, 8, 9, 11, 12, 13, 14]. Finite-gap solutions of the Dym equation were studied by Dmitrieva [43] and Novikov [125] in relation to the KdV equation, by introducing an additional phase function. Soliton solutions of Dym type equations were studied by Dmitrieva [44]. Notice that the solitary waves are orbitally stable, i.e., their shape is stable under small perturbations, both for the smooth solitons and for the peakons.

Our own approach to the construction of algebro-geometric solutions of the CH equation (resp. Dym equation) differs from the ones studied in [12, 13, 14]. While the latter references employ the trace formula for the function u in terms of (projections of) auxiliary divisors, and used generalized theta functions and generalized Jacobians (going back to investigations of Clebsch and Gordan [36]), we derive our solutions from a purely algebraic identity satisfied by the theta function, namely, Fay's trisecant identity. The spectral data consist of a hyperelliptic curve of the form $\mu^2 = \prod_{j=1}^{2g+2}(\lambda - \lambda_j)$, and a set of marked points. For the CH equation, there are three marked points: two of them are interchanged under the involution $\sigma(\lambda, \mu) = (\lambda, -\mu)$, and the third is a ramification point $(\lambda_{j_0}, 0)$; whereas for the Dym equation, these marked points consist of two ramification points of the underlying hyperelliptic curve. We start by introducing new identities satisfied by the theta function associated to these spectral data. These identities, corollaries of Fay's famous trisecant identity (1.1.10), allow us to derive and describe complex finite-gap solutions of equations (1.2.1) and (1.2.2).

Our construction of real-valued solutions is based on the description of the real and imaginary part of the Jacobian associated to a real hyperelliptic curve (i.e., the branch points λ_j are real or pairwise conjugate non-real). It turns out that real-valued solutions are either smooth or admit an infinite number of singularities which correspond to cusps.

In Chapter 5 we consider different degenerations of algebro-geometric solutions of the CH and Dym equations when the spectral curve becomes singular and its genus drops to zero. The solutions are then expressed in terms of purely elementary functions which by an appropriate choice of parameters describe interactions between solitons and cuspons. This representation also yields the existence of peakons in a special limiting case.

Chapter 6. We prove a new degenerated version of Fay's trisecant identity (1.1.10). Following Mumford's approach, the new identity is applied to construct new algebro-geometric solutions of the multi-component nonlinear Schrödinger equation. This approach also provides an independent derivation of known algebro-geometric solutions to the Davey-Stewartson equations.

The first main result of this chapter is a new degeneration of Fay's identity (1.1.10). This new identity holds for two distinct points a, b on a compact Riemann surface of genus $g > 0$:

$$D_a' \ln \frac{\Theta(\mathbf{z} + \int_a^b)}{\Theta(\mathbf{z})} + D_a^2 \ln \frac{\Theta(\mathbf{z} + \int_a^b)}{\Theta(\mathbf{z})} + \Big(D_a \ln \frac{\Theta(\mathbf{z} + \int_a^b)}{\Theta(\mathbf{z})} - K_1 \Big)^2 + 2\, D_a^2 \ln \Theta(\mathbf{z}) + K_2 = 0, \quad (1.2.3)$$

for any $\mathbf{z} \in \mathbb{C}^g$, where K_1 and K_2 are scalars independent of $\mathbf{z}$ but dependent on the points a and b; here D_a and D'_a denote operators of directional derivatives along the vectors $\mathbf{V}_a$ and $\mathbf{W}_a$ (2.3.3). In particular, this identity implies that the following function of the variables x and t

$$\psi(x,t) = A\,\frac{\Theta(\mathbf{Z}-\mathbf{d}+\int_a^b)}{\Theta(\mathbf{Z}-\mathbf{d})}\,\exp\left\{\mathrm{i}\,(-K_1\,x+\,K_2\,t)\right\}, \tag{1.2.4}$$

where $\mathbf{Z} = \mathrm{i}\,\mathbf{V}_a\,x + \mathrm{i}\,\mathbf{W}_a\,t$, and where $A \in \mathbb{C}$, $\mathbf{d} \in \mathbb{C}^g$ are constant, is a solution of the linear Schrödinger equation

$$\mathrm{i}\,\frac{\partial\psi}{\partial t} + \frac{\partial^2\psi}{\partial x^2} + 2\,u\,\psi = 0, \tag{1.2.5}$$

with the potential $u(x,t) = D_a^2 \ln\Theta(\mathbf{Z}-\mathbf{d})$. When this potential is related to the function ψ by $u(x,t) = \rho\,|\psi|^2$, with $\rho = \pm 1$, the function ψ (1.2.4) becomes a solution of the nonlinear Schrödinger equation (1.1.2). This is the starting point of our construction of algebro-geometric solutions of the multi-component nonlinear Schrödinger equation and the Davey-Stewartson equations. The nonlinear Schrödinger equation (1.1.2) is a famous nonlinear dispersive partial differential equation with many applications, e.g. in hydrodynamics (deep water waves), plasma physics and nonlinear fiber optics. Integrability of this equation was established by Zakharov and Shabat in [154]. Algebro-geometric solutions of (1.1.2) were found by Its in [79]; the geometric theory of these solutions was developed by Previato [132].

There exist various ways to generalize the NLS equation. The first is to increase the number of dependent variables in (1.1.2). This leads to the multi-component nonlinear Schrödinger equation

$$\mathrm{i}\,\frac{\partial\psi_j}{\partial t} + \frac{\partial^2\psi_j}{\partial x^2} + 2\left(\sum_{k=1}^{n} s_k|\psi_k|^2\right)\psi_j = 0, \qquad j = 1,\ldots,n, \tag{1.2.6}$$

denoted by n-NLS^s, where $s = (s_1,\ldots,s_n)$, $s_k = \pm 1$. Here $\psi_j(x,t)$ are complex valued functions of the real variables x and t. The case $n = 1$ corresponds to the NLS equation. The two-component NLS equation ($n = 2$) is relevant in the study of electromagnetic waves in optical media in which the electric field has two nontrivial components. Integrability of the two-component NLS equation in the case $s = (1,1)$ was first established by Manakov [109]. In optical fibers, for arbitrary $n \geq 2$, the components ψ_j in (1.2.6) correspond to components of the electric field transverse to the direction of wave propagation. These components of the transverse field form a basis of the polarization states. Integrability for the multi-component case with any $n \geq 2$ and $s_k = \pm 1$ was established in [136]. Algebro-geometric solutions of the two-component NLS equation with signature $(1,1)$ were investigated in [55] using the Lax formalism and Baker-Akhiezer functions; these solutions are expressed in terms of theta functions of special trigonal spectral curves.

The second main result of this chapter is the construction of smooth algebro-geometric solutions of the multi-component nonlinear Schrödinger equation (1.2.6) for arbitrary $n \geq 2$, obtained by using (1.2.3). We first find solutions to the complexified system

$$\begin{aligned}
&\mathrm{i}\,\frac{\partial\psi_j}{\partial t} + \frac{\partial^2\psi_j}{\partial x^2} + 2\left(\sum_{k=1}^{n}\psi_k\,\psi_k^*\right)\psi_j = 0,\\
&-\mathrm{i}\,\frac{\partial\psi_j^*}{\partial t} + \frac{\partial^2\psi_j^*}{\partial x^2} + 2\left(\sum_{k=1}^{n}\psi_k\,\psi_k^*\right)\psi_j^* = 0, \qquad j = 1,\ldots,n,
\end{aligned} \tag{1.2.7}$$

where $\psi_j(x,t)$ and $\psi_j^*(x,t)$ are complex valued functions of the real variables x and t. This system reduces to the n-NLS^s equation (1.2.6) under the reality conditions

$$\psi_j^* = s_j\,\overline{\psi_j}, \qquad j = 1,\dots,n. \tag{1.2.8}$$

Algebro-geometric data associated to the solutions of (1.2.7) are given by $\{\mathcal{R}_g, f, z_a\}$, where $\mathcal{R}_g$ is a compact Riemann surface of genus $g > 0$, f is a meromorphic function of degree $n+1$ on $\mathcal{R}_g$ and $z_a \in \mathbb{CP}^1$ is a non critical value of the meromorphic function f such that $f^{-1}(z_a) = \{a_1,\dots,a_{n+1}\}$. Then the solutions ψ_j, ψ_j^*, $j = 1,\dots,n$, of system (1.2.7) read

$$\begin{aligned}
\psi_j(x,t) &= A_j\,\frac{\Theta(\mathbf{Z}-\mathbf{d}+\int_{a_{n+1}}^{a_j})}{\Theta(\mathbf{Z}-\mathbf{d})}\,\exp\left\{\mathrm{i}\,(-E_j\,x+\,F_j\,t)\right\},\\
\psi_j^*(x,t) &= \frac{q_2(a_{n+1},a_j)}{A_j}\,\frac{\Theta(\mathbf{Z}-\mathbf{d}-\int_{a_{n+1}}^{a_j})}{\Theta(\mathbf{Z}-\mathbf{d})}\,\exp\left\{\mathrm{i}\,(E_j\,x-\,F_j\,t)\right\},
\end{aligned}$$

where the scalars $E_j, F_j, q_2(a_{n+1},a_j)$ depend on the points $a_{n+1}, a_j \in \mathcal{R}_g$, and where $A_j \in \mathbb{C}$, $\mathbf{d} \in \mathbb{C}^g$ are constant; here the g-dimensional vector $\mathbf{Z}$ is a linear function of the variables x and t. Imposing the reality conditions (1.2.8), we describe explicitly solutions for the focusing case $s = (1,\dots,1)$ and the defocusing case $s = (-1,\dots,-1)$ associated to a real branched covering of the Riemann sphere. In particular, our solutions of the focusing case are associated to a covering without real branch point. Our general construction, being applied to the two-component case, gives solutions with more independent parameters than in [55] for fixed genus of the spectral curve. Moreover, we provide smoothness conditions for our solutions.

Another way to generalize the NLS equation is to increase the number of spatial dimensions to two. This leads to the Davey-Stewartson equations (DS),

$$\begin{aligned}
\mathrm{i}\,\psi_t + \psi_{xx} - \alpha^2\,\psi_{yy} + 2\,(\Phi + \rho\,|\psi|^2)\,\psi &= 0,\\
\Phi_{xx} + \alpha^2\,\Phi_{yy} + 2\rho\,|\psi|^2_{xx} &= 0,
\end{aligned} \tag{1.2.9}$$

where $\alpha = \mathrm{i}$ or $\alpha = 1$, and $\rho = \pm 1$; $\psi(x,y,t)$ and $\Phi(x,y,t)$ are functions of the real variables x, y and t, the latter being real-valued and the former being complex valued. In what follows, DS1$^\rho$ denotes the Davey-Stewartson equation when $\alpha = \mathrm{i}$, and DS2$^\rho$ the Davey-Stewartson equation when $\alpha = 1$. The Davey-Stewartson equation (1.2.9) was introduced in [38] to describe the evolution of a three-dimensional wave package on water of finite depth. Complete integrability of the equation was shown in [16]. If solutions ψ and Φ of (1.2.9) do not depend on the variable y the first equation in (1.2.9) reduces to the NLS equation (1.1.2) under appropriate boundary conditions for the function $\Phi + \rho\,|\psi|^2$ when x tends to infinity.

Algebro-geometric solutions of the Davey-Stewartson equations (1.2.9) were previously obtained in [112] using the formalism of Baker-Akhiezer functions. In both [112] and the present thesis, solutions of (1.2.9) are constructed from solutions of the complexified system which, after the change of coordinates $\xi = \frac{1}{2}(x - \mathrm{i}\alpha\,y)$ and $\eta = \frac{1}{2}(x + \mathrm{i}\alpha\,y)$, with $\alpha = \mathrm{i}$ or 1, reads

$$\begin{aligned}
\mathrm{i}\,\psi_t + \frac{1}{2}(\psi_{\xi\xi} + \psi_{\eta\eta}) + 2\,\varphi\,\psi &= 0,\\
-\,\mathrm{i}\,\psi_t^* + \frac{1}{2}(\psi_{\xi\xi}^* + \psi_{\eta\eta}^*) + 2\,\varphi\,\psi^* &= 0,\\
\varphi_{\xi\eta} + \frac{1}{2}((\psi\psi^*)_{\xi\xi} + (\psi\psi^*)_{\eta\eta}) &= 0,
\end{aligned} \tag{1.2.10}$$

where $\varphi := \Phi + \psi\psi^*$. This system reduces to (1.2.9) under the reality condition:

$$\psi^* = \rho\,\overline{\psi}. \tag{1.2.11}$$

The third main result of this chapter is an independent derivation of the solutions [112] using the degenerated Fay identity (1.2.3). Algebro-geometric data associated to these solutions are $\{\mathcal{R}_g, a, b, k_a, k_b\}$, where $\mathcal{R}_g$ is a compact Riemann surface of genus $g > 0$, a and b are two distinct points on $\mathcal{R}_g$, and k_a, k_b are arbitrary local parameters near a and b. These solutions read

$$\begin{aligned}
\psi(\xi,\eta,t) &= A\,\frac{\Theta(\mathbf{Z}-\mathbf{d}+\int_a^b)}{\Theta(\mathbf{Z}-\mathbf{d})}\,\exp\left\{\mathrm{i}\left(-G_1\,\xi - G_2\,\eta + G_3\,\tfrac{t}{2}\right)\right\},\\
\psi^*(\xi,\eta,t) &= -\,\frac{\kappa_1\kappa_2\,q_2(a,b)}{A}\,\frac{\Theta(\mathbf{Z}-\mathbf{d}-\int_a^b)}{\Theta(\mathbf{Z}-\mathbf{d})}\,\exp\left\{\mathrm{i}\left(G_1\,\xi + G_2\,\eta - G_3\,\tfrac{t}{2}\right)\right\},\\
\varphi(\xi,\eta,t) &= \frac{1}{2}\,(\ln\,\Theta(\mathbf{Z}-\mathbf{d}))_{\xi\xi} + \frac{1}{2}\,(\ln\,\Theta(\mathbf{Z}-\mathbf{d}))_{\eta\eta} + \frac{h}{4},
\end{aligned}$$

where the scalars $G_i, q_2(a,b)$ depend on the points $a, b \in \mathcal{R}_g$, and $\kappa_1, \kappa_2, A, h \in \mathbb{C}$, $\mathbf{d} \in \mathbb{C}^g$ are arbitrary constants; the g-dimensional vector $\mathbf{Z}$ is a linear function of the variables ξ, η and t. The reality condition (1.2.11) imposes constraints on the associated algebro-geometric data. In particular, the Riemann surface $\mathcal{R}_g$ has to be real. The approach used in [112] to study reality conditions (1.2.11) is based on properties of Baker-Akhiezer functions. Our present approach based on identity (1.2.3) allows to construct solutions of DS1$^\rho$ and DS2$^\rho$ corresponding to Riemann surfaces of more general topological type than in [112].

Chapter 7. In this chapter, we construct solutions in terms of elementary functions of the multi-component NLS equation (1.2.6), and the Davey-Stewartson equation (1.2.9). The solutions of n-NLS and DS presented here are obtained by degenerating algebro-geometric solutions constructed in Chapter 6. This method for finding solutions in terms of elementary functions has not been applied to n-NLS and DS so far. It provides a unified approach to various solutions of n-NLS and DS expressed in terms of a simple determinantal form, and allows to present new solutions to the multi-component NLS equation in terms of elementary functions.

Multi-soliton solutions of (1.2.6) were considered in a series of papers, see for instance [109, 133, 134, 88, 3]. Here we present a family of dark and bright multi-solitons, breather and rational breather solutions to the multi-component NLS equation. It appears to be the first time that breathers and rational breathers are given for the multi-component case. The notion of a dark soliton refers to the fact that the solution tends asymptotically to a non-zero constant, i.e., it describes a darkening on a bright background, whereas the bright soliton is a localized bright spot being described by a solution that tends asymptotically to zero. The name 'breather' reflects the behavior of the profile which is periodic in time or space and localized in space or time. It is remarkable that degenerations of algebro-geometric solutions to the multi-component NLS equation lead to the breather solutions, well known in the context of the one-component case as the soliton on a finite background [5] (breather periodic in space), the Ma breather [108] (breather periodic in time) and the rational breather [129]. In the NLS framework, these solutions have been suggested as models for a class of extreme, freak or rogue wave events (see e.g. [76, 127, 15]). A family of rational solutions to the focusing NLS equation was constructed in [54] and was rediscovered recently in [46] via Wronskian techniques. Here we give for the first

time a family of breather and rational breather solutions of the multi-component NLS equation. For the one component case, our solutions consist of the well known breather and Peregrine breather of the focusing NLS equation. For the multi-component case, we find new profiles of breathers and rational breathers which do not exist in the scalar case.

The second main result of this chapter is the construction of particular solutions of the DS equations such as solitons, breathers, dromion and lump, obtained by degenerating the algebro-geometric solutions given in Chapter 6. A main feature of equations in $1+1$ dimensions is the existence of soliton solutions which are localized in one dimension. Solutions of the $2+1$ dimensional integrable equations which are localized only in one dimension (plane solitons) were constructed in [4, 18]. Moreover, various recurrent solutions (the growing-and-decaying mode, breather and rational growing-and-decaying mode solutions) were investigated in [143]. The spectral theory of soliton type solutions to the DS1 equation (called dromions) with exponential fall off in all directions on the plane, and their connection with the initial-boundary value problem, have been studied by different methods in a series of papers [26, 63, 140, 135]. The lump solution (a rational non-singular solution) to the DS2$^-$ equation was discovered in [18].

Here we present a family of dark multi-soliton solutions of the DS1 and DS2$^+$ equations, as well as a family of bright multi-solitons for the DS1 and DS2$^-$ equations, obtained by degenerating algebro-geometric solutions. Moreover, a class of breather and rational breather solutions of the DS1 equation is given. These solutions have a very similar appearance to those in $1+1$ dimensions. Moreover, it is shown how the simplest solutions, the dromion and the lump solutions can be derived from algebro-geometric solutions.

Chapter 8. It is well known that physically meaningful almost periodic solutions to certain integrable partial differential equations are given in terms of multi-dimensional theta functions associated to real Riemann surfaces. In this chapter we study typical analytical problems in the numerical evaluation of these solutions. To illustrate that, we discuss solutions to the multi-component nonlinear Schrödinger equation as well as solutions to the Davey-Stewartson equations, investigated in Chapter 6.

Novikov criticized the practical relevance of theta functions since no numerical algorithms existed at the time to actually compute the found solutions. He suggested an effective treatment of theta functions (see, for instance, [48]) by a suitable parametrization of the characteristic quantities of a Riemann surface, i.e., the periods of holomorphic and certain meromorphic differentials on the given surface. This program is limited to genera smaller than 4 since so-called Schottky relations exist for higher genus between the components of the period matrix of a Riemann surface. The task to find such relations is known as the Schottky problem. This led to the famous Novikov conjecture for the Schottky problem that a Riemann matrix (a symmetric matrix with negative definite real part) is the matrix of $\mathcal{B}$-periods of the normalized holomorphic differentials of a Riemann surface if and only if Krichever's formula with this matrix yields a solution to the KP equation. The conjecture was finally proven by Shiota [141].

First plots of KP solutions appeared in [121] and via Schottky uniformizations in [25]. Since all compact Riemann surfaces can be defined via non-singular plane algebraic curves of the form

$$F(x,y) := \sum_{n=1}^{N}\sum_{m=1}^{M} a_{mn}x^m y^n = 0, \quad x,y \in \mathbb{C}, \tag{1.2.12}$$

with constant complex coefficients a_{nm}, Deconinck and van Hoeij developed an approach to the symbolic-numerical treatment of algebraic curves. This approach is distributed as the *algcurves*

package with Maple, see [39, 40, 41]. A purely numerical approach to real hyperelliptic Riemann surfaces was given in [65, 66], and for general Riemann surfaces in [67]. For a review of computational approaches to Riemann surfaces the reader is referred to [24].

In this chapter we want to address typical analytical problems appearing in the numerical study of theta-functional solutions to integrable PDEs, and we present the state of the art of the field by considering concrete examples. The case of hyperelliptic Riemann surfaces ($N = 2$ in (1.2.12)) is the most accessible, since equation (1.2.12) can be solved explicitly for y, and since a basis for differentials and homology can be given a priori. Families of hyperelliptic curves can be conveniently parametrized by their branch points. The codes [65, 66] are in principle able to treat numerically collisions of branch points, a limit in which certain periods of the corresponding hyperelliptic surface diverge. If the limiting Riemann surface has genus 0, the theta series breaks down to a finite sum which, for an appropriate choice of the characteristic, gives well known solitonic solutions to the studied equation.

For solutions defined on general real algebraic curves, i.e., curves (1.2.12) with all a_{nm} real, an important point in applications are reality and smoothness conditions. These are conveniently formulated for a homology basis for which the $\mathcal{A}$-cycles are invariant under the action of the anti-holomorphic involution. However, the existing algorithms for the computational treatment of algebraic curves produce a basis of the homology that is in general not related to possible automorphisms of the curve. To implement the reality and smoothness requirements, a transformation to the basis for which the conditions are formulated has to be constructed. We study the necessary symplectic transformations and give explicit relations for so-called M-curves, curves with the maximum number of real ovals.

To illustrate these concepts, we have studied for the first time numerically theta-functional solutions to integrable equations from the family of NLS equations, namely, the multi-component nonlinear Schrödinger equation (1.2.6) and the Davey-Stewartson equations (1.2.9). To ensure the correct numerical implementation of the formulae obtained in Chapter 6, we check for each point in the spacetime whether certain identities for theta functions are satisfied. Since these identities are not used in the code, they provide a strong test for the computed quantities. Numerically the identities are never exactly satisfied, but to high precision. The code reports a warning if the residual of the test relations is larger than 10^{-6} which is well below plotting accuracy. Typically the conditions are satisfied to machine precision[1]. In addition we compute the solutions on a numerical grid and numerically differentiate them. We check in this way for low genus that the solutions to n-NLS^s and DS in terms of multi-dimensional theta functions satisfy the respective equations to better than 10^{-6}. These two completely independent tests ensure that the presented plots are showing the correct solutions to better than plotting accuracy.

[1]We work with double precision, i.e., a precision of 10^{-16}; due to rounding errors this is typically reduced to 10^{-12} to 10^{-14}.

Part I

Theta functions, Fay's identity and real Riemann surfaces

Chapter 2

Theta functions and Fay's identity

The importance of Riemann surfaces for the construction of almost periodic solutions to various integrable partial differential equations (PDEs) was realized at the beginning of the 1970s by Novikov, Dubrovin and Its, Matveev, Van Moerbeke. The latter found the Its-Matveev formula for the Korteweg-de Vries equation in terms of multi-dimensional theta functions on hyperelliptic Riemann surfaces. Similar formulae were later obtained for other integrable PDEs as nonlinear Schrödinger and sine-Gordon equations. For the history of the topic the reader may refer, for instance, to the reviews [23] and [48]. It turns out that most theta-functional solutions of integrable equations can be directly derived from Fay's identity, an identity satisfied by the multi-dimensional theta function.

2.1 Riemann surfaces

A Riemann surface is a connected one-complex-dimensional analytic manifold. The most important examples of Riemann surfaces consist of non-singular algebraic curves, since one can introduce a natural complex structure on it. The theory of compact Riemann surfaces and the theory of algebraic curves over $\mathbb{C}$ are very well developed and exceedingly rich. In this part we follow the line of the Chapter 1 in [24].

2.1.1 Riemann surfaces and non-singular algebraic curves

An algebraic curve $\mathcal{C}$ is a subset in $\mathbb{C}^2$ defined by

$$\mathcal{C} = \{(\lambda, \mu) \in \mathbb{C}^2 \,|\, P(\lambda, \mu) = 0\},$$

where P is an irreducible polynomial in λ and μ of the form

$$P(\lambda, \mu) = \sum_{i=0}^{N} \sum_{j=0}^{M} p_{ij}\, \mu^i \lambda^j,$$

with coefficients $p_{ij} \in \mathbb{C}$. The curve $\mathcal{C}$ is called non-singular if $\nabla P(\lambda, \mu)\big|_{\mathcal{C}} \neq 0$, where

$$\nabla P = \left(\frac{\partial P}{\partial \lambda}, \frac{\partial P}{\partial \mu} \right).$$

On a non-singular algebraic curve, one can introduce a complex structure as follows: in a neighbourhood of the points where $\partial P/\partial\mu \neq 0$, one chooses the local parameter to be the projection on the λ-plane, and near the points where $\partial P/\partial\lambda \neq 0$, one chooses the local parameter to be the projection on the μ-plane. Holomorphic compatibility of the underlying local parameters can be checked using a complex version of the implicit function theorem.

Example 2.1.1. *Let $N \in \mathbb{N}$ such that $N \geq 3$. The polynomial equation*

$$\mu^2 = \prod_{j=1}^{N}(\lambda - \lambda_j), \tag{2.1.1}$$

where $\lambda_j \in \mathbb{C}$, describes a non-singular algebraic curve $\mathcal{C}$ if $\lambda_i \neq \lambda_k$ for $i \neq k$; such a curve is called hyperelliptic. The local parameter in a neighbourhood of a point (λ_0, μ_0) with $\lambda_0 \neq \lambda_j$ is given by the homeomorphism $(\lambda, \mu) \to \lambda$, and the local parameter in a neighbourhood of each point $(\lambda_j, 0)$ is defined by the homeomorphism $(\lambda, \mu) \to (\lambda - \lambda_j)^{1/2}$. Moreover, if N is odd, $\hat{\mathcal{C}} = \mathcal{C} \cup \{\infty\}$ describes a compact Riemann surface with local parameter $(\lambda, \mu) \to \lambda^{-1/2}$ near the infinity point ∞; otherwise, if N is even, $\hat{\mathcal{C}} = \mathcal{C} \cup \{\infty^{\pm}\}$ describes a compact Riemann surface with local parameters $(\lambda, \mu) \to \lambda^{-1}$ near the infinity points $\infty^{\pm}$.

For compact Riemann surfaces, a single non-negative integer yields a complete topological classification:

Theorem 2.1.1. *(and Definition) Any compact Riemann surface is homeomorphic to a sphere with handles. The number $g \in \mathbb{N}$ of handles is called the genus of the Riemann surface.*

For instance, every surface of genus zero is topologically a sphere, while a surface of positive genus g can be obtained topologically by identifying pairwise appropriate sides of a $4g$-sided polygon.

Example 2.1.2. *The genus of the compactification $\hat{\mathcal{C}}$ of the hyperelliptic curve (2.1.1) with $N = 2g + 1$ or $N = 2g + 2$ equals g.*

It is a remarkable but nontrivial result that any compact Riemann surface can be realized via a compactified algebraic curve. In the whole thesis we deal with compact Riemann surfaces of genus g that we denote by $\mathcal{R}_g$. If not stated otherwise, we let $\mathcal{R}_g$ denote both the non-singular compactified algebraic curve and its compact Riemann surface.

2.1.2 Holomorphic mappings and coverings

A mapping $f : \mathcal{M} \to \mathcal{N}$ between Riemann surfaces is called holomorphic if, for every local parameter (U, z) on $\mathcal{M}$ and every local parameter (V, w) on $\mathcal{N}$, with $U \cap f^{-1}(V) \neq \emptyset$, the mapping

$$w \circ f \circ z^{-1} : z(U \cap f^{-1}(V)) \longrightarrow w(V)$$

is holomorphic. Moreover, locally the mapping $F = w \circ f \circ z^{-1}$ behaves as $F(z) = z^n$, for some $n \in \mathbb{N}$. A holomorphic mapping into $\mathbb{C}$ is called a holomorphic function, and a holomorphic mapping into $\mathbb{CP}^1$ is called a meromorphic function.

Non-constant holomorphic mappings between Riemann surfaces are also called holomorphic coverings. Let $f : \mathcal{M} \to \mathcal{N}$ be a holomorphic covering. A point $p \in \mathcal{M}$ is called a branch point of f if it has no neighbourhood U (containing point p) such that $f|_U$ is injective. A covering with branch points is called ramified or branched covering (unramified otherwise).

Theorem 2.1.2. *Let $f : \mathcal{M} \to \mathcal{N}$ be a non-constant holomorphic mapping between two compact Riemann surfaces. Then there exists $m \in \mathbb{N}$ such that f takes every value $c \in \mathcal{N}$ precisely m times (counting multiplicities).*

The number m above is called the degree of f. The covering $f : \mathcal{M} \to \mathcal{N}$ is called m-sheeted. For any $a \in \mathcal{M}$, the number $b_f(a) = n_a - 1$ is called the branch number of f at a, where $n_a \in \mathbb{N}$ denotes the multiplicity of f at a. In particular, for a non-constant meromorphic function on a compact Riemann surface, the number m corresponds to the number of its poles (counting multiplicities).

Example 2.1.3. *Let us consider the compactification $\hat{\mathcal{C}}$ of the hyperelliptic curve (2.1.1) together with the meromorphic function $f : (\lambda, \mu) \to \lambda$ of degree 2. The function f allows to consider $\hat{\mathcal{C}}$ as a two-sheeted branched covering of $\mathbb{CP}^1$ where branch points are given by:*

$$\begin{array}{llll} (\lambda_j, 0),\ j = 1, \ldots, N & \textit{and} \quad \infty & \textit{for} & N = 2g+1, \\ (\lambda_j, 0),\ j = 1, \ldots, N & & \textit{for} & N = 2g+2, \end{array}$$

with the branch number $b_f = 1$ at these points.

2.1.3 Homology group and intersection index

In this work we use the notion of an intersection index on a compact Riemann surface. Intersection indices are well defined by introducing equivalence relations related to homology groups.

First homology group. Here we consider an oriented triangulation of a compact Riemann surface $\mathcal{R}$. Formal sums of points p_i, $\sum n_i p_i$, of oriented edges γ_i, $\gamma = \sum n_i \gamma_i$, and of oriented triangles D_i, $D = \sum n_i D_i$, with $n_i \in \mathbb{Z}$, are called 0-chains, 1-chains and 2-chains respectively. Let us denote these sets by C_0, C_1 and C_2. A 1-chain γ with $\delta\gamma = 0$ is called a cycle, and a 1-chain γ of the form $\gamma = \delta D$ is called a boundary; here δ denotes the boundary operator. Denote by Z the subgroup of cycles and by B the subgroup of boundaries:

$$Z = \{\gamma \in C_1 \,|\, \delta\gamma = 0\}, \qquad B = \delta C_2.$$

Due to $\delta^2 = 0$, every boundary is a cycle and we have $B \subset Z \subset C_1$. One can introduce an equivalence relation between elements of C_1: two 1-chains are called *homologous* if their difference is a boundary, namely,

$$\gamma_1 \sim \gamma_2 \quad \Longleftrightarrow \quad (\gamma_1 - \gamma_2 \in B, \text{ i.e. } \exists\, D \in C_2 : \delta D = \gamma_1 - \gamma_2)\,,$$

for any $\gamma_1, \gamma_2 \in C_1$. The factor group

$$H_1(\mathcal{R}) = H_1(\mathcal{R}, \mathbb{Z}) = Z/B$$

is called the first homology group of $\mathcal{R}$. For a compact Riemann surface $\mathcal{R}_g$ of genus g, this is a free abelian group of rank $2g$. A standard set of generators for this group can be obtained using a certain representation of $\mathcal{R}_g$ as a polygon with $4g$ sides, appropriately identified in pairs. We denote these generators by $\mathcal{A}_1, \mathcal{B}_1, \ldots, \mathcal{A}_g, \mathcal{B}_g$.

Intersection index. To introduce intersection numbers of elements of the first homology group, it is convenient to represent them by smooth cycles. Moreover, given two elements of $H_1(\mathcal{R}_g)$, one can represent them by smooth cycles intersecting transversally in a finite number of points. Let γ_1 and γ_2 be two smooth cycles intersecting transversally at the point p. One associates to this point a number $(\gamma_1 \circ \gamma_2)_p = \pm 1$, where the sign is determined by the orientation of the basis $(\gamma_1'(p), \gamma_2'(p))$; here $\gamma_i'(p)$ denotes the tangent vector of γ_i at p. More generally, let γ_1, γ_2 be two smooth cycles intersecting transversally at the finite set of their intersection points. Then the intersection index of γ_1 and γ_2 is defined by

$$\gamma_1 \circ \gamma_2 = \sum_{p \in \text{Intersection set}} (\gamma_1 \circ \gamma_2)_p.$$

The intersection number is a bilinear skew symmetric map:

$$\circ : H_1(\mathcal{R}_g) \times H_1(\mathcal{R}_g) \longrightarrow \mathbb{Z}.$$

Canonical homology basis. A homology basis $(\mathcal{A}, \mathcal{B}) := (\mathcal{A}_1, \ldots, \mathcal{A}_g, \mathcal{B}_1, \ldots, \mathcal{B}_g)$ of a compact Riemann surface $\mathcal{R}_g$ of genus g with the following intersection indices

$$\mathcal{A}_i \circ \mathcal{B}_j = \delta_{i,j} \qquad \mathcal{A}_i \circ \mathcal{A}_j = \mathcal{B}_i \circ \mathcal{B}_j = 0,$$

is called canonical basis of cycles. If the Riemann surface $\mathcal{R}_g$ is cut along this basis, one obtains a $4g$-gon where each cycle corresponds to a pair of the sides $\mathcal{A}_i, \mathcal{A}_i^{-1}, \mathcal{B}_i, \mathcal{B}_i^{-1}$ which are identified on $\mathcal{R}_g$. In the whole thesis, the notation $\mathcal{A}$ (resp. $\mathcal{B}$) will also be used to denote the vector $(\mathcal{A}_1, \ldots, \mathcal{A}_g)^t$ (resp. $(\mathcal{B}_1, \ldots, \mathcal{B}_g)^t$).

Change of canonical homology basis. Canonical homology basis are related via a symplectic transformation. Let $(\mathcal{A}, \mathcal{B})$ and $(\tilde{\mathcal{A}}, \tilde{\mathcal{B}})$ be arbitrary canonical homology basis defined on $\mathcal{R}_g$, represented here by $2g$-dimensional vectors. Then there exists a symplectic matrix $M = \begin{pmatrix} A & B \\ C & D \end{pmatrix} \in Sp(2g, \mathbb{Z})$ such that

$$\begin{pmatrix} A & B \\ C & D \end{pmatrix} \begin{pmatrix} \tilde{\mathcal{A}} \\ \tilde{\mathcal{B}} \end{pmatrix} = \begin{pmatrix} \mathcal{A} \\ \mathcal{B} \end{pmatrix}. \tag{2.1.2}$$

Recall that a symplectic matrix $M \in Sp(2g, \mathbb{Z})$ satisfies $M^t J_g M = J_g$, with the matrix J_g given by $J_g = \begin{pmatrix} 0 & \mathbb{I}_g \\ -\mathbb{I}_g & 0 \end{pmatrix}$, where $\mathbb{I}_g$ denotes the $g \times g$ unit matrix. Symplectic matrices $M = \begin{pmatrix} A & B \\ C & D \end{pmatrix} \in Sp(2g, \mathbb{Z})$ are characterized by the following system of matrix equations:

$$A^t D - C^t B = \mathbb{I}_g, \tag{2.1.3}$$

$$A^t C = C^t A, \tag{2.1.4}$$

$$D^t B = B^t D. \tag{2.1.5}$$

Moreover, the inverse matrix M^{-1} is given by $M^{-1} = \begin{pmatrix} D^t & -B^t \\ -C^t & A^t \end{pmatrix}$.

2.1.4 Abelian differentials and their periods

An Abelian differential on a compact Riemann surface $\mathcal{R}_g$ is a meromorphic 1-form ω given on $\mathcal{R}_g$. In other words, locally ω reads $f(z)\,\mathrm{d}z$, where f is a meromorphic function of z in its domain. Zeros and poles of Abelian differentials are well defined, as well as the notions of multiplicity and residue.

First, second and third kind differentials. One distinguishes three kinds of Abelian differentials: holomorphic differentials (first kind), meromorphic differentials with residues equal to zero at all singular points (second kind), and meromorphic differentials of general form (third kind). Note that for differentials of the third kind, the sum of residues equals zero. Let $a \in \mathcal{R}_g$, and $N \in \mathbb{N}$ with $N > 1$. We denote by $\Omega_a^{(N)}$ the differential of the second kind having only one singularity at point a of the form

$$\Omega_a^{(N)}(p) = \left(\frac{1}{k_a(p)^N} + O(1)\right) \mathrm{d}k_a(p), \quad p \in \mathcal{R}_g, \tag{2.1.6}$$

where k_a is a local parameter in a neighbourhood of a. Note that the differential $\Omega_a^{(N)}$ depends on the choice of the local parameter k_a near the point a. Now assume that $a, b \in \mathcal{R}_g$ are connected by a contour which does not intersect basic cycles. Hence we can define the meromorphic differential of the third kind Ω_{b-a} which has residue 1 at b and residue -1 at a.

Theorem 2.1.3. *Let $\mathcal{R}_g$ be a compact Riemann surface of genus $g > 0$. The dimension of the complex vector space of holomorphic differentials given on $\mathcal{R}_g$ equals g.*

Example 2.1.4. *For a hyperelliptic curve of the form (2.1.1), a basis of holomorphic differentials is given by*

$$\omega_j = \frac{\lambda^{j-1}}{\mu}\,\mathrm{d}\lambda, \qquad j = 1, \ldots, g, \tag{2.1.7}$$

where g, the genus of the surface, is equal to $N/2 - 1$ for even N, and to $(N-1)/2$ for odd N.

Periods of Abelian differentials. Let $(\mathcal{A}, \mathcal{B})$ be a canonical homology basis on $\mathcal{R}_g$. Periods of an Abelian differential ω of the first or second kind are defined by

$$A_k = \int_{\mathcal{A}_k} \omega, \qquad B_k = \int_{\mathcal{B}_k} \omega, \qquad k = 1, \ldots, g.$$

For an Abelian differential Ω of the third kind having simple poles at $p_j \in \mathcal{R}_g$, $j = 1, \ldots, n$, there exist additional periods called polar periods, defined by

$$C_j = \int_{\gamma_j} \Omega, \qquad j = 1, \ldots, n,$$

where γ_j is a small cycle homologous to zero in $H_1(\mathcal{R}_g)$ encircling the pole p_j only. For any two Abelian differentials ω and ω', the following Riemann's bilinear identity holds:

$$\int_{\mathcal{R}_g} \omega \wedge \omega' = \sum_{k=1}^{g} \left(A_k B_k' - A_k' B_k\right), \tag{2.1.8}$$

where A_k, B_k and A_k', B_k' denote the $\mathcal{A}$ and $\mathcal{B}$-periods of the differentials ω and ω' respectively.

Normalized Abelian differentials. It follows from identity (2.1.8) that the $g \times g$ matrix of $\mathcal{A}$-periods of a basis of holomorphic differentials $(\omega_1, \ldots, \omega_g)$, with entries

$$A_{kj} = \int_{\mathcal{A}_k} \omega_j, \qquad j, k = 1, \ldots, g,$$

is invertible. This allows to define normalized holomorphic differentials as follows. Let $(\mathcal{A}, \mathcal{B})$ be a canonical basis of $H_1(\mathcal{R}_g)$. The dual basis of holomorphic differentials ω_j normalized by

$$\int_{\mathcal{A}_k} \omega_j = 2\mathrm{i}\pi\delta_{j,k}, \qquad j, k = 1, \ldots, g, \tag{2.1.9}$$

is uniquely defined and is called canonical.

Abelian differentials of the second and third kind are normalized by imposing the condition that all $\mathcal{A}$-periods vanish. It follows that normalized Abelian differentials of the second kind $\Omega_a^{(N)}$ and of the third kind Ω_{b-a} are uniquely defined.

The $\mathcal{B}$-periods of normalized Abelian differentials $\Omega_a^{(N)}$ and Ω_{b-a} are related to normalized holomorphic differentials via the Riemann's bilinear identity. Namely, the choice $\omega = \omega_j$ and $\omega' = \Omega_a^{(N)}$ with $N > 1$ in (2.1.8) leads to

$$\int_{\mathcal{B}_j} \Omega_a^{(N)} = \frac{1}{N-1}\, \alpha_{j,N-2}, \qquad j = 1, \ldots, g, \tag{2.1.10}$$

where the scalar $\alpha_{j,N-2}$ is defined by the following expansion of the normalized holomorphic differential ω_j near the point a:

$$\omega_j = \sum_{i=0}^{\infty} \alpha_{j,i}\, k_a^i\, \mathrm{d}k_a,$$

where k_a denotes a local parameter in a neighbourhood of a. For the choice $\omega = \omega_j$ and $\omega' = \Omega_{b-a}$ one gets

$$\int_{\mathcal{B}_j} \Omega_{b-a} = \int_a^b \omega_j, \qquad j = 1, \ldots, g, \tag{2.1.11}$$

where the integration path connecting a and b does not cross the $\mathcal{A}$ and $\mathcal{B}$-cycles.

Riemann matrix. The $g \times g$ matrix of $\mathcal{B}$-periods $\mathbb{B}$ of the normalized holomorphic differentials $\omega_1, \ldots, \omega_g$, with entries given by

$$\mathbb{B}_{kj} = \int_{\mathcal{B}_k} \omega_j, \qquad j, k = 1, \ldots, g, \tag{2.1.12}$$

is called the Riemann matrix of $\mathcal{R}_g$. From the Riemann's bilinear identity (2.1.8) it can be deduced that the Riemann matrix $\mathbb{B}$ is symmetric and has a negative definite real part (more generally, a Riemann matrix is a symmetric matrix with negative definite real part). These properties of the matrix $\mathbb{B}$ ensure that the so-called theta function, defined in the next section, is an entire function on $\mathbb{C}^g$.

Jacobian, Abel map and divisors. Let Λ be the lattice $\Lambda = 2\mathrm{i}\pi\mathbb{Z}^g + \mathbb{B}\mathbb{Z}^g$ generated by the $\mathcal{A}$ and $\mathcal{B}$-periods of the normalized holomorphic differentials $\omega_1, \ldots, \omega_g$. The complex torus $J(\mathcal{R}_g) = \mathbb{C}^g/\Lambda$ is called the Jacobian of the Riemann surface $\mathcal{R}_g$. Let us denote by Π the Abel map $\Pi : \mathcal{R}_g \to J(\mathcal{R}_g)$ defined by

$$\Pi(p) = \int_{p_0}^{p} \omega, \tag{2.1.13}$$

for any $p \in \mathcal{R}_g$, where $p_0 \in \mathcal{R}_g$ is the base point of the application, and $\omega = (\omega_1, \ldots, \omega_g)^t$ is the vector of normalized holomorphic differentials. In the whole thesis we use the notation $\int_a^b = \Pi(b) - \Pi(a)$.

A divisor $\mathcal{D}$ on a Riemann surface $\mathcal{R}_g$ is a formal symbol $\mathcal{D} = \sum_{k=1}^{N} n_k\, p_k$, for some $n_k \in \mathbb{Z}$ and $N \in \mathbb{N}\backslash\{0\}$, where $p_k \in \mathcal{R}_g$. The degree of $\mathcal{D}$ is defined by $\deg \mathcal{D} = \sum_{k=1}^{N} n_k$. The Abel map can be extended linearly to all divisors on $\mathcal{R}_g$. A divisor $\mathcal{D}$ is called principal if it describes the set of zeros and poles (counting multiplicities) of a meromorphic function f on $\mathcal{R}_g$. In this case we use the notation $\mathcal{D} = (f)$ (note that $\deg(f) = 0$). This allows to define a linear equivalence relation on the set of divisors: two divisors $\mathcal{D}$ and $\mathcal{D}'$ are called linearly equivalent if the divisor $\mathcal{D} - \mathcal{D}'$ is principal. The following Abel theorem provides necessary and sufficient conditions for a divisor to be principal:

Theorem 2.1.4. *A divisor $\mathcal{D}$ is principal if and only if $\deg \mathcal{D} = 0$ and $\Pi(\mathcal{D}) \equiv 0$.*

It follows that the Abel map defines a map on linear equivalence classes of divisors.

2.2 Multi-dimensional theta functions

This part is devoted to the theory of theta functions associated to Riemann surfaces, and explores some of its numerous applications. Following the line of the Chapter 2 in [23], we recall how meromorphic functions and normalized Abelian differentials on a compact Riemann surface of arbitrary genus are constructed explicitly in terms of the multi-dimensional theta functions. We discuss also the important role of the zeros of the theta function in the Jacobi inversion problem. The question is whether we can find a divisor, i.e., the preimage under the Abel map, for an arbitrary point in the Jacobian. Theta functions are of great importance in mathematical physics due to their role in the inverse problem for periodic and quasi-periodic flows.

2.2.1 Definition and properties

The theta function with (half integer) characteristic $\delta = [\delta_1, \delta_2]$ is defined by

$$\Theta_{\mathbb{B}}[\delta](\mathbf{z}) = \sum_{\mathbf{m}\in\mathbb{Z}^g} \exp\left\{\tfrac{1}{2}\langle \mathbb{B}(\mathbf{m}+\delta_1), \mathbf{m}+\delta_1\rangle + \langle \mathbf{m}+\delta_1, \mathbf{z}+2\mathrm{i}\pi\delta_2\rangle\right\} \tag{2.2.1}$$

for any $\mathbf{z} \in \mathbb{C}^g$; here $\mathbb{B}$ is the Riemann matrix with entries (2.1.12), and $\delta_1, \delta_2 \in \left\{0, \frac{1}{2}\right\}^g$ are the vectors of the characteristic; $\langle .,. \rangle$ denotes the scalar product $\langle \mathbf{u}, \mathbf{v}\rangle = \sum_i u_i\, v_i$ for any $\mathbf{u}, \mathbf{v} \in \mathbb{C}^g$. If not stated otherwise, we denote by $\Theta[\delta](\mathbf{z})$ the theta function (2.2.1) associated to the Riemann matrix $\mathbb{B}$. The theta function with characteristic is related to the theta function with zero characteristic (denoted by Θ) as follows:

$$\Theta[\delta](\mathbf{z}) = \Theta(\mathbf{z} + 2\mathrm{i}\pi\delta_2 + \mathbb{B}\delta_1)\, \exp\left\{\tfrac{1}{2}\langle \mathbb{B}\delta_1, \delta_1\rangle + \langle \mathbf{z} + 2\mathrm{i}\pi\delta_2, \delta_1\rangle\right\}. \tag{2.2.2}$$

The theta function $\Theta[\delta](\mathbf{z})$ is even if the characteristic δ is even, i.e, $4\langle\delta_1,\delta_2\rangle$ is even, and odd if the characteristic δ is odd, i.e., $4\langle\delta_1,\delta_2\rangle$ is odd. An even characteristic is called non-singular if $\Theta[\delta](0)\neq 0$, and an odd characteristic is called non-singular if the gradient $\nabla\Theta[\delta](0)$ is non-zero.

Algebro-geometric solutions of integrable systems are expressed in terms of Abelian functions (i.e., meromorphic functions in g complex variables having $2g$ independent periods) on the Jacobian $J(\mathcal{R}_g)$ with period lattice Λ. The theta function with characteristic (2.2.1) is not an Abelian function on $J(\mathcal{R}_g)$ since it has the following quasi-periodicity property with respect to the lattice Λ:

$$\Theta[\delta](\mathbf{z}+2\mathrm{i}\pi\mathbf{N}+\mathbb{B}\mathbf{M})=\Theta[\delta](\mathbf{z})\exp\left\{-\tfrac{1}{2}\langle\mathbb{B}\mathbf{M},\mathbf{M}\rangle-\langle\mathbf{z},\mathbf{M}\rangle+2\mathrm{i}\pi(\langle\delta_1,\mathbf{N}\rangle-\langle\delta_2,\mathbf{M}\rangle)\right\}, \tag{2.2.3}$$

for any $\mathbf{N},\mathbf{M}\in\mathbb{Z}^g$. It turns out that from (2.2.3), we construct Abelian functions on $J(\mathcal{R}_g)$ as a quotient of theta functions, namely, the function

$$f(\mathbf{z})=\prod_{i=1}^{n}\frac{\Theta(\mathbf{z}+\mathbf{a}_i)}{\Theta(\mathbf{z}+\mathbf{b}_i)}, \tag{2.2.4}$$

where the vectors $\mathbf{a}_i,\mathbf{b}_i\in\mathbb{C}^g$ are such that $\sum_{i=1}^n\mathbf{a}_i\equiv\sum_{i=1}^n\mathbf{b}_i \pmod{2\mathrm{i}\pi\mathbb{Z}^g}$, is meromorphic on the torus $J(\mathcal{R}_g)=\mathbb{C}^g/\Lambda$.

For the formulation of solutions to physically relevant integrable equations in terms of multi-dimensional theta functions, there is typically a preferred homology basis in which the solution takes a simple form. Let $(\mathcal{A},\mathcal{B})$ and $(\tilde{\mathcal{A}},\tilde{\mathcal{B}})$ be arbitrary canonical homology basis defined on $\mathcal{R}_g$. Under the change of homology basis (2.1.2), the theta function transforms as:

$$\Theta_{\mathbb{B}}[\delta](\mathbf{z})=\kappa\sqrt{\det\tilde{\mathbb{K}}}\,\exp\left\{\tfrac{1}{2}\,\tilde{\mathbf{z}}^t\,(\tilde{\mathbb{K}}^t)^{-1}B\,\tilde{\mathbf{z}}\right\}\,\Theta_{\tilde{\mathbb{B}}}[\tilde{\delta}](\tilde{\mathbf{z}}), \tag{2.2.5}$$

where $\tilde{\mathbb{K}}=2\mathrm{i}\pi A+B\,\tilde{\mathbb{B}}$, and where

$$\mathbb{B}=2\mathrm{i}\pi\,(2\mathrm{i}\pi\,C+D\,\tilde{\mathbb{B}})\,\tilde{\mathbb{K}}^{-1}, \tag{2.2.6}$$

$$\tilde{\mathbf{z}}=(2\mathrm{i}\pi)^{-1}\,\tilde{\mathbb{K}}^t\,\mathbf{z}, \tag{2.2.7}$$

$$\begin{pmatrix}\delta_1\\ \delta_2\end{pmatrix}=\begin{pmatrix}A & -B\\ -C & D\end{pmatrix}\begin{pmatrix}\tilde{\delta}_1\\ \tilde{\delta}_2\end{pmatrix}+\frac{1}{2}\,\mathrm{Diag}\begin{pmatrix}B\,A^t\\ D\,C^t\end{pmatrix}, \tag{2.2.8}$$

for any $\mathbf{z}\in\mathbb{C}^g$, where Diag(.) denotes the column vector of the diagonal entries of the matrix. Here κ is a constant independent of $\mathbf{z}$ and $\tilde{\mathbb{B}}$ (the exact value of κ is not needed for our purposes).

2.2.2 Theta divisor and Jacobi inversion problem

The general Jacobi inversion problem consists, for a given point $\zeta=(\zeta_1,\ldots,\zeta_g)^t\in J(\mathcal{R}_g)$, in finding g points $p_1,\ldots,p_g$ on $\mathcal{R}_g$ such that the following identity holds in the Jacobian:

$$\sum_{k=1}^{g}\int_{p_0}^{p_k}\omega\equiv\zeta\,; \tag{2.2.9}$$

here $\omega=(\omega_1,\ldots,\omega_g)^t$ denotes the vector of normalized holomorphic differentials and $p_0\in\mathcal{R}_g$ is an arbitrary point.

In the case $g = 1$, this problem reduces to the inversion of an elliptic integral, which leads to elliptic functions, i.e., doubly periodic meromorphic functions having poles at a lattice of points in the complex plane. The theory of elliptic functions and their relation to the elliptic theta function was developed by Jacobi in his great treatise "Fundamenta nova theoriae functionum ellipticarum" (1829), and later papers. In his work, Jacobi discovered that elliptic functions can be expressed as quotients of theta functions.

In 1832, Jacobi formulated the inversion problem for hyperelliptic integrals [83], i.e., integrals over a rational function $R(x, W(x))$, where $W(x)$ is the square root of a polynomial of degree $2g+1$ or $2g+2$ with $g \geq 2$. In the case $g = 2$, this problem was solved by Göpel [72] and Rosenhain [138], generalizing Jacobi's theta functions to theta functions depending on two variables.

The basic problem for a more complicated algebraic integral was to find an expression for the inverse of the transformation defined by a complete set of integrals of the first kind. This problem is known as the Jacobi inversion problem, and its solution, involving theta functions of several variables, was found by Riemann and Weierstrass (see, for instance, [142, 95, 121]). The following theorem by Riemann gives a solution to the Jacobi inversion problem (2.2.9):

Theorem 2.2.1. *Let $(\mathcal{A}, \mathcal{B})$ be a canonical homology basis and choose $p_0 \in \mathcal{R}_g$. Denote by $\mathbf{K} = (K_1, \ldots, K_g)^t$ the vector of Riemann constants defined by*

$$K_j = \frac{2\mathrm{i}\pi + \mathbb{B}_{jj}}{2} - \frac{1}{2\mathrm{i}}\pi \sum_{k \neq j} \left(\int_{\mathcal{A}_k} \omega_k(p) \int_{p_0}^{p} \omega_j \right), \qquad j = 1, \ldots, g. \tag{2.2.10}$$

Let $\zeta \in J(\mathcal{R}_g)$ such that the Riemann theta function, defined by $F(p) = \Theta(\Pi(p) - \zeta - \mathbf{K})$ for any $p \in \mathcal{R}_g$, does not vanish identically on $\mathcal{R}_g$. Then the function $F(p)$ has on $\mathcal{R}_g$ exactly g zeros $p_1, \ldots, p_g$ that give a solution to the Jacobi inversion problem (2.2.9). Moreover, the points $p_1, \ldots, p_g$ are defined by (2.2.9) uniquely up to a permutation.

This theorem provides also information on the theta divisor, the set of zeros of the theta function:

Corollary 2.2.1. *For a non-special divisor $\mathcal{D} = p_1 + \ldots + p_g$ (i.e., there exists a non-constant function f with $(f) \geq -\mathcal{D}$), the function F defined by*

$$F(p) = \Theta\left(\Pi(p) - \Pi(\mathcal{D}) - \mathbf{K}\right)$$

for any $p \in \mathcal{R}_g$, has exactly g zeros $p_1, \ldots, p_g$.

2.2.3 Construction of functions and differentials on a Riemann surface

In this part we construct meromorphic functions and normalized Abelian differentials of the second and third kinds in terms of the multi-dimensional theta function (2.2.1). The results presented here are based on Riemann's fundamental theorem (Theorem 2.2.1). This representation of Abelian differentials in terms of theta functions is crucial for a numerical study of the solutions of the studied integrable equations.

Let us first introduce the prime form which is a generalization of the function $x - y$ on $\mathbb{C}^2$ to a Riemann surface of genus $g > 0$. Let $a, b \in \mathcal{R}_g$ be distinct points. Then the prime form is defined by

$$E(a, b) = \frac{\Theta[\delta](\int_b^a)}{h_\delta(a) h_\delta(b)}; \tag{2.2.11}$$

here $h_\delta(a)$ is a spinor given by $h_\delta^2(a) = \sum_{j=1}^g \frac{\partial\Theta[\delta]}{\partial z_j}(0)\,\omega_j(a)$, where δ is a non-singular odd characteristic. Note that the prime form is independent of the choice of the characteristic δ. From the basic properties of the prime form (see [60] for more details), it can be checked that:

i) if the divisor $\mathcal{D} = \sum_{i=1}^n a_i - b_i$ is principal, then the map $f : \mathcal{R}_g \to \mathbb{CP}^1$ defined by

$$f(p) = \prod_{i=1}^n \frac{E(p, a_i)}{E(p, b_i)} \tag{2.2.12}$$

is a single-valued meromorphic function on $\mathcal{R}_g$ having zeros at a_i and poles at b_i;

ii) for two distinct points $a, b \in \mathcal{R}_g$, the normalized third kind differential Ω_{b-a} reads

$$\Omega_{b-a}(p) = \mathrm{d}_p \ln \frac{E(p, b)}{E(p, a)}, \quad p \in \mathcal{R}_g; \tag{2.2.13}$$

iii) the bidifferential $\Omega(p, q)$ which has zero $\mathcal{A}$-periods and is decomposed according to

$$\Omega(p, q) = \left(\frac{1}{(k(p) - k(q))^2} + O(1) \right) \mathrm{d}k(p)\,\mathrm{d}k(q),$$

for any p, q in the same neighbourhood, k being a local parameter defined on this neighbourhood, admits the representation:

$$\Omega(p, q) = \mathrm{d}_p\,\mathrm{d}_q \ln E(p, q); \tag{2.2.14}$$

iv) the normalized second kind differential $\Omega_a^{(N)}$ is thus given by

$$\Omega_a^{(N)}(p) = \partial_{k_x} \Omega(p, x)\Big|_{x=a} \tag{2.2.15}$$

for any $p \in \mathcal{R}_g$, where k_x denotes a local parameter in a neighbourhood of $x \in \mathcal{R}_g$.

2.3 Fay's identity

The well known trisecant identity discovered by Fay is a far-reaching generalization of the addition theorem for elliptic theta functions to multi-dimensional theta functions (see [60]). It can also be seen as a generalization of the identity satisfied by the cross-ratio to Riemann surfaces.

Fay's identity plays an important role in various domains of mathematics, for instance, in the theory of Jacobian varieties [17], in conformal field theory [137], and in operator theory [116]. Moreover, as discovered by Mumford [121], theta-functional solutions of certain integrable equations such as Korteweg-de Vries (KdV), Kadomtsev-Petviashvili (KP), or Sine-Gordon equations may be derived from Fay's trisecant identity and its degenerations.

2.3.1 Fay's identity and generalization of the cross-ratio to Riemann surfaces

Let $a, b, c, d \in \mathcal{R}_g$ be arbitrary points on a compact Riemann surface $\mathcal{R}_g$ of genus $g > 0$. Then for any $\mathbf{z} \in \mathbb{C}^g$, Fay's trisecant identity has the form

$$\begin{aligned} E(a,b)E(c,d)\,\Theta\Big(\mathbf{z}+\int_c^a\Big)\,\Theta\Big(\mathbf{z}+\int_b^d\Big) \\ + E(a,c)E(d,b)\,\Theta\Big(\mathbf{z}+\int_b^a\Big)\,\Theta\Big(\mathbf{z}+\int_c^d\Big) \\ = E(a,d)E(c,b)\,\Theta(\mathbf{z})\,\Theta\Big(\mathbf{z}+\int_c^a+\int_b^d\Big), \end{aligned} \tag{2.3.1}$$

where all integration contours do not intersect cycles of the canonical homology basis (recall that $\int_a^b$ denotes the Abel map (2.1.13) between a and b); here Θ denotes the theta function (2.2.1) with zero characteristic, and $E(a,b)$ the prime form introduced in (2.2.11). Proofs of this formula may be found in Fay [60], Mumford [121], Farkas [59], or Gunning [74].

More recently [131], identity (2.3.1) was proved using cross-ratio functions on Riemann surfaces. This point of view allows to consider Fay's identity as a generalization of the identity satisfied by the cross-ratio on the sphere to Riemann surfaces. Namely, let us denote by

$$\lambda_0(a,b,c,d) = \frac{(a-b)\,(c-d)}{(a-d)\,(c-b)}$$

the cross-ratio of four points a, b, c, d on the Riemann sphere. Then it is well known that λ_0 satisfies the following identity:

$$\lambda_0(a,b,c,d) + \lambda_0(a,c,b,d) = 1. \tag{2.3.2}$$

The cross-ratio function on an arbitrary compact Riemann surface $\mathcal{R}_g$ of genus $g > 0$ is in fact characterized by its divisor, its symmetries, and its transformation laws (see [131] for more details). We denote the cross-ratio function on $\mathcal{R}_g$ by $\lambda_g(a,b,c,d)$, for $a, b, c, d \in \mathcal{R}_g$. Therefore, according to the properties of the prime form and characterizations of the cross-ratio function, the function $\lambda_g(a,b,c,d)$ can be written with Riemann's theorem as

$$\lambda_g(a,b,c,d) = \frac{E(a,b)\,E(c,d)}{E(a,d)\,E(c,b)}.$$

The cross-ratio functions $\lambda_g(a,b,c,d)$ and $\lambda_g(a,c,b,d)$ are then related by identity (2.3.1) which thus generalizes identity (2.3.2) to Riemann surfaces.

2.3.2 Previously known degenerated versions of Fay's identity

Let us now discuss degenerations of identity (2.3.1). Let $k_a(p)$ denote a local parameter near $a \in \mathcal{R}_g$, where p lies in a neighbourhood of a. For $j = 1, \ldots, g$, consider the following expansion of the normalized holomorphic differentials ω_j near a:

$$\omega_j(p) = \left(V_{a,j} + W_{a,j}\,k_a(p) + U_{a,j}\,\frac{k_a(p)^2}{2!} + o\left(k_a(p)^2\right)\right)\,\mathrm{d}k_a(p), \tag{2.3.3}$$

where $V_{a,j}, W_{a,j}, U_{a,j} \in \mathbb{C}$. Let us denote by D_a the operator of directional derivative along the vector $\mathbf{V}_a = (V_{a,1}, \ldots, V_{a,g})^t$:

$$D_a F(\mathbf{z}) = \sum_{j=1}^{g} \partial_{z_j} F(\mathbf{z})\, V_{a,j} = \langle \nabla F(\mathbf{z}), \mathbf{V}_a \rangle \,, \tag{2.3.4}$$

where $F : \mathbb{C}^g \longrightarrow \mathbb{C}$ is an arbitrary function; denote by D'_a the operator of directional derivative along the vector $\mathbf{W}_a = (W_{a,1}, \ldots, W_{a,g})^t$, and by D''_a the directional derivative along the vector $\mathbf{U}_a = (U_{a,1}, \ldots, U_{a,g})^t$.

Differentiating identity (2.3.1) with respect to the local parameter k_d near point d, and considering the limit when d tends to b, one gets the first degenerated version of Fay's identity derived in [121]:

$$D_b \ln \frac{\Theta(\mathbf{z} + \int_c^a)}{\Theta(\mathbf{z})} \;=\; p_1(a,b,c) + p_2(a,b,c)\, \frac{\Theta(\mathbf{z} + \int_b^a)\, \Theta(\mathbf{z} + \int_c^b)}{\Theta(\mathbf{z} + \int_c^a)\, \Theta(\mathbf{z})} \,, \tag{2.3.5}$$

which holds for any distinct points $a, b, c \in \mathcal{R}_g$ and any $\mathbf{z} \in \mathbb{C}^g$; functions p_1 and p_2 of the variables a, b, c are given by:

$$p_1(a,b,c) = D_b \ln \frac{\Theta[\delta](\int_c^b)}{\Theta[\delta](\int_a^b)} \,, \tag{2.3.6}$$

$$p_2(a,b,c) = \frac{\Theta[\delta](\int_c^a)}{\Theta[\delta](\int_b^a)\, \Theta[\delta](\int_b^c)}\, D_b\, \Theta[\delta](0), \tag{2.3.7}$$

where δ is a non-singular odd characteristic. Note that the p_i for $i = 1, 2$, depend on the choice of local parameters near the points a, b, c. From representations (2.2.13) and (2.2.11) in terms of multi-dimensional theta functions of the differential Ω_{c-a} and the prime form, one gets:

$$\Omega_{c-a}(b) = p_1(a,b,c)\; \mathrm{d}k_b, \tag{2.3.8}$$

$$\frac{E(c,a)}{E(b,a)\, E(c,b)} = p_2(a,b,c)\; \mathrm{d}k_b, \tag{2.3.9}$$

where k_b denotes a local parameter near point b.

Analogously, differentiating (2.3.5) with respect to the local parameter k_c near point c, and considering the limit when c tends to a, one gets

$$D_a D_b \ln \Theta(\mathbf{z}) \;=\; q_1(a,b) \;+\; q_2(a,b)\, \frac{\Theta(\mathbf{z} + \int_a^b)\, \Theta(\mathbf{z} - \int_a^b)}{\Theta(\mathbf{z})^2} \,, \tag{2.3.10}$$

which holds for any distinct points $a, b \in \mathcal{R}_g$ and any $\mathbf{z} \in \mathbb{C}^g$; functions q_1 and q_2 of the variables a and b depend on the choice of local parameters near these points and are given by:

$$q_1(a,b) = D_a D_b \ln \Theta[\delta](\textstyle\int_a^b) \,, \tag{2.3.11}$$

$$q_2(a,b) = \frac{D_a\, \Theta[\delta](0)\, D_b\, \Theta[\delta](0)}{\Theta[\delta](\int_a^b)^2}, \tag{2.3.12}$$

where δ is a non-singular odd characteristic. From (2.2.14) and (2.2.11) one easily gets:

$$\Omega(a,b) = -\, q_1(a,b)\ \mathrm{d}k_a\, \mathrm{d}k_b, \tag{2.3.13}$$

$$E(a,b)^{-2} = q_2(a,b)\ \mathrm{d}k_a\, \mathrm{d}k_b, \tag{2.3.14}$$

where k_c denotes a local parameter near point $c \in \{a,b\}$.

The third degenerated version of Fay's identity derived in [121] is obtained from (2.3.10) in the limit when b tends to a. Namely, let b be in a neighbourhood of a, put $k_a(b) = t$, and expand identity (2.3.10) in terms of the variable t. Then it can be checked that the first nontrivial term, which is the t^4 term, reads

$$D_a^4 \ln\Theta(\mathbf{z}) + 6\left[D_a^2 \ln\Theta(\mathbf{z})\right]^2 - 2D_a D_a'' \ln\Theta(\mathbf{z}) + 3\left(D_a'\right)^2 \ln\Theta(\mathbf{z}) + c_1 D_a^2 \ln\Theta(\mathbf{z}) + c_2 = 0, \tag{2.3.15}$$

where the scalars c_1 and c_2 depend on the coefficients appearing in the expansion with respect to the variable t of $q_1(a,b)$ and $q_2(a,b)$ (knowledge of the exact value of c_1 and c_2 is not needed for our purpose).

In Section 6.1, we shall present a new degenerated version of Fay's identity obtained by differentiating identity (2.3.1) twice (instead of once) with respect to the local parameter k_d near point d, and by considering the limit when d tends to b.

2.3.3 Applications to integrable systems - Mumford's approach

In the early 80's, Mumford observed [121] that integrable equations like KdV, KP or sine-Gordon, are 'hidden' in Fay's trisecant formula (2.3.1). Mumford's approach, based on degenerated versions of Fay's identity, shows how algebro-geometric solutions of integrable equations arise from a degeneration of a purely algebro-geometric identity.

KP and KdV equations. Historically, the Korteweg-de Vries equation (KdV)

$$4\, u_t = 6\, u u_x + u_{xxx}, \tag{2.3.16}$$

and its generalization to two spatial variables, the Kadomtsev-Petviashvili equation (KP2),

$$3\, u_{yy} = (4\, u_t - (6\, u u_x + u_{xxx}))_x, \tag{2.3.17}$$

were the most important examples of applications of algebraic-geometric methods in the 1970's, see for instance [23]. Algebro-geometric solutions of the KP equation were first constructed by Krichever [96]. Here we show how these solutions can be derived from Fay's identity following Mumford's approach.

Let $\mathcal{R}_g$ be a compact Riemann surface of genus $g > 0$ and take $a \in \mathcal{R}_g$. Choose $\mathbf{d} \in \mathbb{C}^g$ and define the function

$$u(x,y,t) = 2\, D_a^2 \ln\Theta(\mathbf{V}_a\, x + \mathbf{W}_a\, y + \mathbf{U}_a\, t/2 - \mathbf{d}) + c_1/6, \tag{2.3.18}$$

where the scalar c_1 was introduced in (2.3.15), and where the vectors $\mathbf{V}_a, \mathbf{W}_a, \mathbf{U}_a$ are defined in (2.3.3). Then the function u satisfies the KP equation (2.3.17). Indeed, this can be checked directly by applying the second directional derivative D_a^2 to identity (2.3.15). Finally, solutions (2.3.18) of the KP equation obtained via Mumford's approach coincide with the ones (1.1.9) constructed by using Baker-Akhiezer functions.

Algebro-geometric solutions of the KdV equation are deduced from (2.3.18) when the Riemann surface is hyperelliptic. Namely, assume that $\mathcal{R}_g$ is a hyperelliptic curve of the form (2.1.1), and denote by σ the hyperelliptic involution defined by $\sigma(\lambda,\mu) = (\lambda,-\mu)$. Let a be one of the ramification points of the curve and choose a local parameter k_a near a satisfying $k_a(\sigma(p)) = -k_a(p)$ for any p lying in a neighbourhood of a. Let us check that the vector $\mathbf{W}_a$ vanishes. Denote by σ^* the action of σ lifted to the space of holomorphic differentials, namely, $\sigma^*\omega(p) = \omega(\sigma p)$ for any $p \in \mathcal{R}_g$. Then, using the following action of σ on the normalized holomorphic differentials ω_j,

$$\sigma^*\omega_j = -\omega_j, \qquad j = 1,\dots,g, \tag{2.3.19}$$

by (2.3.3) it follows that $W_{a,j} = 0$. In this case the function $u(x,t)$ defined in (2.3.18) is solution of the KdV equation (2.3.16).

Sine-Gordon equation. Analogously, let us show how algebro-geometric solutions of the sine-Gordon equation arise from Fay's identity. In light-cone coordinates $(x,t) = (\xi+\eta,\xi-\eta)$, the sine-Gordon equation

$$u_{tt} - u_{xx} = \sin(u), \tag{2.3.20}$$

has the form:

$$u_{\xi\eta} = \sin(u). \tag{2.3.21}$$

Theta-functional solutions of the sine-Gordon equation were found in [94] and [80] following the line of the spectral approach applied to the KdV equation.

Let $\mathcal{R}_g$ be a hyperelliptic curve of the form (2.1.1) and let $a,b \in \mathcal{R}_g$ be two distinct ramification points. First let us prove that the vector $\mathbf{r} = \int_a^b \omega$ reads

$$\mathbf{r} = \frac{1}{2}(2\mathrm{i}\pi\mathbf{n} + \mathbb{B}\mathbf{m}), \tag{2.3.22}$$

for some $\mathbf{n},\mathbf{m} \in \mathbb{Z}^g$. Consider the hyperelliptic curve as a two-sheeted covering of the Riemann sphere, denote by ℓ a path connecting points a and b on one sheet, and consider a copy $\tilde{\ell}$ of this contour connecting points b and a, which lies on the other sheet of $\mathcal{R}_g$. Then by (2.3.19) we deduce that

$$\mathbf{r} = \int_\ell \omega = \int_{\tilde{\ell}} \omega. \tag{2.3.23}$$

Since the contour $\ell + \tilde{\ell}$ is closed, it consists of a linear combination of $\mathcal{A}$ and $\mathcal{B}$-cycles. In other words, there exist $\mathbf{n},\mathbf{m} \in \mathbb{Z}^g$ such that

$$\int_{\ell+\tilde{\ell}} \omega = 2\mathrm{i}\pi\mathbf{n} + \mathbb{B}\mathbf{m},$$

which by (2.3.23) leads to (2.3.22). Therefore, from identity (2.3.10) and the quasi-periodicity (2.2.3) of the theta function, we deduce

$$D_aD_b \ln\frac{\Theta(\mathbf{z}+\mathbf{r})}{\Theta(\mathbf{z})} = q_2(a,b)\, e^{-\frac{1}{2}\langle\mathbb{B}\mathbf{m},\mathbf{m}\rangle}\left(\frac{\Theta(\mathbf{z})^2}{\Theta(\mathbf{z}+\mathbf{r})^2}\, e^{-\phi(\mathbf{z})} - \frac{\Theta(\mathbf{z}+\mathbf{r})^2}{\Theta(\mathbf{z})^2}\, e^{\phi(\mathbf{z})}\right), \tag{2.3.24}$$

for any $\mathbf{z} \in \mathbb{C}^g$, where $\phi(\mathbf{z}) = \langle \mathbf{z}+\mathbf{r},\mathbf{m}\rangle$. Let us define the function

$$u(\mathbf{z}) = 2\mathrm{i}\ln\frac{\Theta(\mathbf{z}+\mathbf{r})}{\Theta(\mathbf{z})} + \mathrm{i}\phi(\mathbf{z}). \tag{2.3.25}$$

Thus (2.3.24) becomes

$$D_a D_b\, u(\mathbf{z}) = \frac{c}{2\mathrm{i}} \left(e^{\mathrm{i}u(\mathbf{z})} - e^{-\mathrm{i}u(\mathbf{z})} \right) = c\, \sin(u(\mathbf{z})), \tag{2.3.26}$$

where $c = q_2(a,b)\, \exp\{-\frac{1}{2}\, \langle \mathbb{B}\mathbf{m}, \mathbf{m} \rangle\}$. Hence, putting $\mathbf{z} = c^{-1/2}\, (\mathbf{V}_a\, \xi + \mathbf{V}_b\, \eta) - \mathbf{d}$ in (2.3.25), where vectors $\mathbf{V}_a, \mathbf{V}_b$ are defined in (2.3.3), and $\mathbf{d} \in \mathbb{C}^g$ is arbitrary, one gets that function $u(\xi, \eta)$ is a solution of the sine-Gordon equation (2.3.21).

Toda lattice equations. The Toda lattice equation (1D Toda)

$$\partial_x^2 u_n = e^{u_{n-1} - u_n} - e^{u_n - u_{n+1}}, \tag{2.3.27}$$

is one of the most famous integrable nonlinear lattice equations, see [61] and [145]; here $u_n(x)$, for $x \in \mathbb{R}$ and $n \in \mathbb{Z}$, is a dynamical function on a one-dimensional lattice. The Toda lattice equation describes the dynamics of a one-dimensional physical lattice, the masses of which are subject to an interaction potential of exponential type. This equation admits numerous extensions having applications in various other physical and mathematical contexts, see, e.g., [146, 52, 57, 144]. It should also be mentioned that the Toda equation can be viewed as a discrete version of the KdV equation (see [145] or [128]). Periodic problems for the Toda chain and a discrete version of the KdV equation were studied by Kac and Van Moerbeke in a series of papers (see, for instance, [84]).

Equation (2.3.27) admits a two-dimensional integrable version, the 2D Toda lattice equation:

$$\partial_x \partial_y u_n = e^{u_{n-1} - u_n} - e^{u_n - u_{n+1}}, \tag{2.3.28}$$

where the function $u_n(x,y)$ depends on two dynamical variables x, y and a discrete variable $n \in \mathbb{Z}$. Note that 2-periodic solutions of (2.3.28), namely, solutions which satisfy $u_{n+2} = u_n$, are solutions of the sine-Gordon equation (2.3.21) after a suitable change of variables.

The first results on algebro-geometric solutions of the Toda equation were given by Date and Tanaka [37]. Further important contributions were made by Krichever [99]-[104], Van Moerbeke and Mumford [119, 120]. Algebro-geometric solutions of the 2D Toda lattice are constructed from the algebro-geometric data $\{\mathcal{R}_g, a, b\}$, where $\mathcal{R}_g$ is a compact Riemann surface of genus g and $a, b \in \mathcal{R}_g$ are two distinct points. Analogously to the KP and KdV equations, if we restrict these algebro-geometric data to $\{\mathcal{R}_g, \sigma, a, b\}$ where $\mathcal{R}_g$ is a hyperelliptic curve with σ the hyperelliptic involution, and $a, b \in \mathcal{R}_g$ satisfy $\sigma(a) = b$, the 2D Toda lattice reduces to the 1D Toda lattice.

Now let us construct algebro-geometric solutions of (2.3.28) using Mumford's approach. From (2.3.10) one has:

$$D_a D_b \ln \Theta(\mathbf{z} + (n-1)\, \mathbf{r}) \;=\; q_1 \;+\; q_2\, \frac{\Theta(\mathbf{z} + n\, \mathbf{r})\, \Theta(\mathbf{z} + (n-2)\, \mathbf{r})}{\Theta(\mathbf{z} + (n-1)\, \mathbf{r})^2}, \tag{2.3.29}$$

$$D_a D_b \ln \Theta(\mathbf{z} + n\, \mathbf{r}) \;=\; q_1 \;+\; q_2\, \frac{\Theta(\mathbf{z} + (n+1)\, \mathbf{r})\, \Theta(\mathbf{z} + (n-1)\, \mathbf{r})}{\Theta(\mathbf{z} + n\, \mathbf{r})^2}, \tag{2.3.30}$$

for any $\mathbf{z} \in \mathbb{C}^g$, $n \in \mathbb{Z}$; here q_i for $i = 1, 2$ denotes the scalar $q_i(a,b)$ and $\mathbf{r} = \int_a^b \omega$. Substracting (2.3.29) and (2.3.30) one gets:

$$D_a D_b \ln \frac{\Theta(\mathbf{z} + (n-1)\, \mathbf{r})}{\Theta(\mathbf{z} + n\, \mathbf{r})} \;= \tag{2.3.31}$$

$$q_2 \frac{\Theta(\mathbf{z}+n\,\mathbf{r})}{\Theta(\mathbf{z}+(n-1)\,\mathbf{r})}\,\frac{\Theta(\mathbf{z}+(n-2)\,\mathbf{r})}{\Theta(\mathbf{z}+(n-1)\,\mathbf{r})} - q_2 \frac{\Theta(\mathbf{z}+(n+1)\,\mathbf{r})}{\Theta(\mathbf{z}+n\,\mathbf{r})}\,\frac{\Theta(\mathbf{z}+(n-1)\,\mathbf{r})}{\Theta(\mathbf{z}+n\,\mathbf{r})},$$

which can be rewritten as

$$D_a D_b \ln \frac{\Theta(\mathbf{z}+(n-1)\,\mathbf{r})}{\Theta(\mathbf{z}+n\,\mathbf{r})} = \tag{2.3.32}$$

$$\exp\left\{\ln q_2 + \ln \frac{\Theta(\mathbf{z}+(n-2)\,\mathbf{r})}{\Theta(\mathbf{z}+(n-1)\,\mathbf{r})} - \ln \frac{\Theta(\mathbf{z}+(n-1)\,\mathbf{r})}{\Theta(\mathbf{z}+n\,\mathbf{r})}\right\}$$

$$-\exp\left\{\ln q_2 + \ln \frac{\Theta(\mathbf{z}+(n-1)\,\mathbf{r})}{\Theta(\mathbf{z}+n\,\mathbf{r})} - \ln \frac{\Theta(\mathbf{z}+n\,\mathbf{r})}{\Theta(\mathbf{z}+(n+1)\,\mathbf{r})}\right\}.$$

Now let us define the function

$$u_n(\mathbf{z}) = \alpha - n \ln q_2 + \ln \frac{\Theta(\mathbf{z}+(n-1)\,\mathbf{r})}{\Theta(\mathbf{z}+n\,\mathbf{r})} \tag{2.3.33}$$

for some $\mathbf{z} \in \mathbb{C}^g$, $n \in \mathbb{Z}$, and $\alpha \in \mathbb{C}$. Thus (2.3.32) reads

$$D_a D_b\, u_n = e^{u_{n-1}-u_n} - e^{u_n - u_{n+1}}.$$

Putting $\mathbf{z} = \mathbf{V}_a\, x + \mathbf{V}_b\, y - \mathbf{d}$ in (2.3.33), where the vectors $\mathbf{V}_a, \mathbf{V}_b$ are defined in (2.3.3) and $\mathbf{d} \in \mathbb{C}^g$ is arbitrary, we obtain that the function $u_n(x,y)$ is a solution of the 2D Toda lattice equation (2.3.28).

Chapter 3

Real Riemann surfaces

In this chapter we recall some facts from the theory of real compact Riemann surfaces $\mathcal{R}_g$. Following the line of [150], we introduce a canonical homology basis adapted to the real structure of $\mathcal{R}_g$. For this choice of basic cycles, we study reality properties of various objects defined on the real Riemann surface $\mathcal{R}_g$.

3.1 Topological type of a real Riemann surface

A Riemann surface $\mathcal{R}_g$ is called real if it admits an anti-holomorphic involution $\tau : \mathcal{R}_g \to \mathcal{R}_g$, $\tau^2 = \mathrm{id}$. For this real structure, we denote by $\mathcal{R}_g(\mathbb{R})$ the set of fixed points. The connected components of the set of fixed points of the anti-involution τ are called real ovals of τ. According to Harnack's inequality [75], the number k of real ovals of a real Riemann surface of genus g cannot exceed $g+1$: $0 \leq k \leq g+1$. Curves with the maximal number $k = g+1$ of real ovals are called M-curves.

The complement $\mathcal{R}_g \setminus \mathcal{R}_g(\mathbb{R})$ has either one or two connected components. The curve $\mathcal{R}_g$ is called a *dividing* curve if $\mathcal{R}_g \setminus \mathcal{R}_g(\mathbb{R})$ has two components, and $\mathcal{R}_g$ is called *non-dividing* if $\mathcal{R}_g \setminus \mathcal{R}_g(\mathbb{R})$ is connected (notice that an M-curve is always a dividing curve).

Example 3.1.1. *Consider the hyperelliptic curve of genus g defined by the equation*

$$\mu^2 = \prod_{i=1}^{2g+2} (\lambda - \lambda_i), \tag{3.1.1}$$

where the branch points $\lambda_i \in \mathbb{R}$ are ordered such that $\lambda_1 < \ldots < \lambda_{2g+2}$. On such a curve, we can define two anti-holomorphic involutions τ_1 and τ_2, given respectively by $\tau_1(\lambda, \mu) = (\overline{\lambda}, \overline{\mu})$ and $\tau_2(\lambda, \mu) = (\overline{\lambda}, -\overline{\mu})$. Projections of real ovals of τ_1 on the λ-plane coincide with the segments $[\lambda_{2g+2}, \lambda_1], \ldots, [\lambda_{2g}, \lambda_{2g+1}]$, whereas projections of real ovals of τ_2 on the λ-plane coincide with the segments $[\lambda_1, \lambda_2], \ldots, [\lambda_{2g+1}, \lambda_{2g+2}]$. Hence the curve (3.1.1) is an M-curve with respect to both anti-involutions τ_1 and τ_2.

Example 3.1.2. *The hyperelliptic curve of genus g defined by the equation*

$$\mu^2 = -\prod_{i=1}^{g+1} (\lambda - \lambda_i)(\lambda - \overline{\lambda_i}), \quad \lambda_i \in \mathbb{C} \setminus \mathbb{R}, \tag{3.1.2}$$

does not have real ovals with respect to the anti-holomorphic involution $\tau(\lambda, \mu) = (\overline{\lambda}, \overline{\mu})$.

3.2 Action of τ on the homology group $H_1(\mathcal{R}_g)$

Denote by $(\mathcal{A}, \mathcal{B})$ the set of generators of the homology group $H_1(\mathcal{R}_g)$. According to Proposition 2.2 in [150] (see also [73]), there exists a canonical homology basis (that we call for simplicity 'Vinnikov basis' in the following) such that

$$\begin{pmatrix} \tau\mathcal{A} \\ \tau\mathcal{B} \end{pmatrix} = \begin{pmatrix} \mathbb{I}_g & 0 \\ \mathbb{H} & -\mathbb{I}_g \end{pmatrix} \begin{pmatrix} \mathcal{A} \\ \mathcal{B} \end{pmatrix}, \tag{3.2.1}$$

where $\mathbb{I}_g$ is the $g \times g$ unit matrix, and $\mathbb{H}$ is a block diagonal $g \times g$ matrix defined as follows:

1) if $\mathcal{R}_g(\mathbb{R}) \neq \emptyset$,

$$\mathbb{H} = \begin{pmatrix} 0 & 1 & & & & & & \\ 1 & 0 & & & & & & \\ & & \ddots & & & & & \\ & & & 0 & 1 & & & \\ & & & 1 & 0 & & & \\ & & & & & 0 & & \\ & & & & & & \ddots & \\ & & & & & & & 0 \end{pmatrix} \quad \text{if } \mathcal{R}_g \text{ is dividing,}$$

$$\mathbb{H} = \begin{pmatrix} 1 & & & & & \\ & \ddots & & & & \\ & & 1 & & & \\ & & & 0 & & \\ & & & & \ddots & \\ & & & & & 0 \end{pmatrix} \quad \text{if } \mathcal{R}_g \text{ is non-dividing;}$$

$\mathrm{rank}(\mathbb{H}) = g + 1 - k$ in both cases;

2) if $\mathcal{R}_g(\mathbb{R}) = \emptyset$, (i.e., the curve does not have real oval), then

$$\mathbb{H} = \begin{pmatrix} 0 & 1 & & & \\ 1 & 0 & & & \\ & & \ddots & & \\ & & & 0 & 1 \\ & & & 1 & 0 \end{pmatrix} \quad \text{or} \quad \mathbb{H} = \begin{pmatrix} 0 & 1 & & & \\ 1 & 0 & & & \\ & & \ddots & & \\ & & & 0 & 1 \\ & & & 1 & 0 \\ & & & & & 0 \end{pmatrix};$$

$\mathrm{rank}(\mathbb{H}) = g$ if g is even, $\mathrm{rank}(\mathbb{H}) = g - 1$ if g is odd.

Let us choose the homology basis satisfying (3.2.1), and let us study the action of τ on the normalized holomorphic differentials, as well as the action of the complex conjugation on the theta function with zero characteristics.

Denote by τ^* the action of τ lifted to the space of holomorphic differentials: $\tau^*\omega(p) = \omega(\tau p)$ for any $p \in \mathcal{R}_g$. By (3.2.1) the $\mathcal{A}$-cycles of the homology basis are invariant under τ. Due to

the normalization conditions (2.1.9), this leads to the following action of τ on the normalized holomorphic differentials:

$$\overline{\tau^*\omega_j} = -\,\omega_j, \tag{3.2.2}$$

Using (3.2.1) and (3.2.2) we get the following reality property for the Riemann matrix $\mathbb{B}$:

$$\overline{\mathbb{B}} = \mathbb{B} - 2\mathrm{i}\pi\,\mathbb{H}. \tag{3.2.3}$$

Moreover, according to Proposition 2.3 in [150], for any $\mathbf{z} \in \mathbb{C}^g$, relation (3.2.3) implies

$$\overline{\Theta(\mathbf{z})} = \kappa\,\Theta(\overline{\mathbf{z}} - \mathrm{i}\pi\,\mathrm{diag}(\mathbb{H})), \tag{3.2.4}$$

where κ is a complex scalar of modulus one which depends on the matrix $\mathbb{H}$ (the exact value of κ is not needed for our purpose); here $\mathrm{diag}(\mathbb{H})$ denotes the vector of diagonal elements of the matrix $\mathbb{H}$.

3.3 Action of τ on $H_1(\mathcal{R}_g \setminus \{a,b\})$ and $H_1(\mathcal{R}_g, \{a,b\})$

Let $a, b \in \mathcal{R}_g$ be two distinct points. Here we study the action of τ on the homology group $H_1(\mathcal{R}_g \setminus \{a,b\})$ of the punctured Riemann surface $\mathcal{R}_g \setminus \{a,b\}$, and the action of τ on its dual, the relative homology group $H_1(\mathcal{R}_g, \{a,b\})$.

Denote by $(\mathcal{A}, \mathcal{B}, \ell)$ the standard generators of the relative homology group $H_1(\mathcal{R}_g, \{a,b\})$, where ℓ is an oriented contour between a and b which does not intersect the canonical homology basis $(\mathcal{A}, \mathcal{B})$, and denote by $(\mathcal{A}, \mathcal{B}, \mathcal{S}_b)$ the generators of the homology group $H_1(\mathcal{R}_g \setminus \{a,b\})$, where $\mathcal{S}_b$ is a positively oriented small contour around b such that $\mathcal{S}_b \circ \ell = 1$.

In what follows, we assume that the basis of cycles $(\mathcal{A}, \mathcal{B})$ of the first homology group satisfies (3.2.1). We consider the case where $\tau a = b$, and the case where $\tau a = a$, $\tau b = b$.

3.3.1 Case $\tau a = b$

In this part we assume that $\tau a = b$.

Proposition 3.3.1. *The action of the anti-holomorphic involution τ on:*

1. *the generators $(\mathcal{A}, \mathcal{B}, \ell)$ of the relative homology group $H_1(\mathcal{R}_g, \{a,b\})$ is given by*

$$\begin{pmatrix} \tau\mathcal{A} \\ \tau\mathcal{B} \\ \tau\ell \end{pmatrix} = \begin{pmatrix} \mathbb{I}_g & 0 & 0 \\ \mathbb{H} & -\mathbb{I}_g & 0 \\ \mathbf{N}^t & 0 & -1 \end{pmatrix} \begin{pmatrix} \mathcal{A} \\ \mathcal{B} \\ \ell \end{pmatrix}, \tag{3.3.1}$$

   for some vector $\mathbf{N} \in \mathbb{Z}^g$;

2. *the generators $(\mathcal{A}, \mathcal{B}, \mathcal{S}_b)$ of the homology group $H_1(\mathcal{R}_g \setminus \{a,b\})$ is given by*

$$\begin{pmatrix} \tau\mathcal{A} \\ \tau\mathcal{B} \\ \tau\mathcal{S}_b \end{pmatrix} = \begin{pmatrix} \mathbb{I}_g & 0 & 0 \\ \mathbb{H} & -\mathbb{I}_g & \mathbf{N} \\ 0 & 0 & 1 \end{pmatrix} \begin{pmatrix} \mathcal{A} \\ \mathcal{B} \\ \mathcal{S}_b \end{pmatrix}, \tag{3.3.2}$$

where the vector $\mathbf{N} \in \mathbb{Z}^g$ is the same as in (3.3.1).

Proof. The action of τ on the $\mathcal{A}$ and $\mathcal{B}$-cycles in (3.3.1) coincides with the one (3.2.1) in $H_1(\mathcal{R}_g)$. From (3.2.1), one sees that any contour in $H_1(\mathcal{R}_g)$ which is invariant under τ is a combination of $\mathcal{A}$-cycles only. In particular, the τ-invariant closed contour $\tau\ell + \ell \in H_1(\mathcal{R}_g)$ can be written as

$$\tau\ell + \ell = \mathbf{N}^t\mathcal{A}, \tag{3.3.3}$$

for some $\mathbf{N} \in \mathbb{Z}^g$. This proves (3.3.1).

Now let us prove (3.3.2). By (3.2.1), the cycles $\tau\mathcal{A}$ admit the following decomposition in $H_1(\mathcal{R}_g \setminus \{a, b\})$:

$$\tau\mathcal{A} = \mathcal{A} + \mathbf{n}\,\mathcal{S}_b, \tag{3.3.4}$$

for some $\mathbf{n} \in \mathbb{Z}^g$. Since τ changes the orientation of $\mathcal{R}_g$, all intersection indices change their sign under the action of τ. We get from (3.3.4)

$$\begin{aligned} 0 &= \mathcal{A} \circ \ell \\ &= -\,\tau\mathcal{A} \circ \tau\ell \\ &= -\,(\mathcal{A} + \mathbf{n}\,\mathcal{S}_b) \circ \tau\ell \\ &= -\,(\mathcal{A} + \mathbf{n}\,\mathcal{S}_b) \circ (-\ell + \mathbf{N}^t\mathcal{A}), \end{aligned} \tag{3.3.5}$$

where $\mathbf{N} \in \mathbb{Z}^g$ is defined by (3.3.1). The last intersection index in (3.3.5) equals $\mathbf{n}$, which implies $\tau\mathcal{A} = \mathcal{A}$. According to (3.2.1), the action of τ on the $\mathcal{B}$-cycles in $H_1(\mathcal{R}_g \setminus \{a, b\})$ is given by

$$\tau\mathcal{B} = -\,\mathcal{B} + \mathbb{H}\mathcal{A} + \mathbf{m}\,\mathcal{S}_b, \tag{3.3.6}$$

for some $\mathbf{m} \in \mathbb{Z}^g$. Then

$$\begin{aligned} 0 &= \mathcal{B} \circ \ell \\ &= -\,\tau\mathcal{B} \circ \tau\ell \\ &= -\,(-\mathcal{B} + \mathbb{H}\mathcal{A} + \mathbf{m}\,\mathcal{S}_b) \circ \tau\ell \\ &= -\,(-\mathcal{B} + \mathbb{H}\mathcal{A} + \mathbf{m}\,\mathcal{S}_b) \circ (-\ell + \mathbf{N}^t\mathcal{A}), \end{aligned} \tag{3.3.7}$$

where $\mathbf{N}$ is defined by (3.3.1). The last intersection index in (3.3.7) equals $\mathbf{m} - \mathbf{N}$, which gives $\tau\mathcal{B} = -\,\mathcal{B} + \mathbb{H}\mathcal{A} + \mathbf{N}\,\mathcal{S}_b$. Finally, to prove that $\tau\mathcal{S}_b = \mathcal{S}_b$, we use the relation $\mathcal{S}_a + \mathcal{S}_b = 0$, where $\mathcal{S}_a$ is a positively oriented small contour around a, and the relation $\tau\mathcal{S}_b = -\,\mathcal{S}_a$. □

Using the action (3.3.2) of τ on the $\mathcal{A}$-cycles in the homology group $H_1(\mathcal{R}_g \setminus \{a, b\})$, due to the uniqueness of the normalized differential of the third kind Ω_{b-a}, we get

$$\overline{\tau^*\Omega_{b-a}} = -\,\Omega_{b-a}. \tag{3.3.8}$$

3.3.2 Case $\tau a = a$ and $\tau b = b$

Now let us assume that $a, b \in \mathcal{R}_g$ satisfy $\tau a = a$ and $\tau b = b$.

Proposition 3.3.2. *The action of the anti-holomorphic involution τ on:*

1. *the generators $(\mathcal{A}, \mathcal{B}, \ell)$ of the relative homology group $H_1(\mathcal{R}_g, \{a,b\})$ is given by*

$$\begin{pmatrix} \tau\mathcal{A} \\ \tau\mathcal{B} \\ \tau\ell \end{pmatrix} = \begin{pmatrix} \mathbb{I}_g & 0 & 0 \\ \mathbb{H} & -\mathbb{I}_g & 0 \\ \mathbf{N}^t & \mathbf{M}^t & 1 \end{pmatrix} \begin{pmatrix} \mathcal{A} \\ \mathcal{B} \\ \ell \end{pmatrix}, \tag{3.3.9}$$

where $\mathbf{N}, \mathbf{M} \in \mathbb{Z}^g$ are related by

$$2\,\mathbf{N} + \mathbb{H}\mathbf{M} = 0; \tag{3.3.10}$$

2. *the generators $(\mathcal{A}, \mathcal{B}, \mathcal{S}_b)$ of the homology group $H_1(\mathcal{R}_g \setminus \{a,b\})$ is given by*

$$\begin{pmatrix} \tau\mathcal{A} \\ \tau\mathcal{B} \\ \tau\mathcal{S}_b \end{pmatrix} = \begin{pmatrix} \mathbb{I}_g & 0 & -\mathbf{M} \\ \mathbb{H} & -\mathbb{I}_g & \mathbf{N} \\ 0 & 0 & -1 \end{pmatrix} \begin{pmatrix} \mathcal{A} \\ \mathcal{B} \\ \mathcal{S}_b \end{pmatrix}, \tag{3.3.11}$$

where the vectors $\mathbf{N}, \mathbf{M} \in \mathbb{Z}^g$ are the same as in (3.3.9).

Proof. The action of τ on the $\mathcal{A}$ and $\mathcal{B}$-cycles in (3.3.9) coincides with the one (3.2.1) in $H_1(\mathcal{R}_g)$. From (3.2.1), one sees that each contour $\mathcal{C} \in H_1(\mathcal{R}_g)$ which satisfies $\tau\mathcal{C} = -\mathcal{C}$, can be represented by

$$\mathcal{C} = \tilde{\mathbf{N}}^t \mathcal{A} + \tilde{\mathbf{M}}^t \mathcal{B}, \tag{3.3.12}$$

where $\tilde{\mathbf{N}}, \tilde{\mathbf{M}} \in \mathbb{Z}^g$ are related by $2\,\tilde{\mathbf{N}} + \mathbb{H}\tilde{\mathbf{M}} = 0$. In particular, the closed contour $\tau\ell - \ell \in H_1(\mathcal{R}_g, \{a,b\})$ can be written as

$$\tau\ell - \ell = \mathbf{N}^t \mathcal{A} + \mathbf{M}^t \mathcal{B}, \tag{3.3.13}$$

where $\mathbf{N}, \mathbf{M} \in \mathbb{Z}^g$ are related by $2\,\mathbf{N} + \mathbb{H}\mathbf{M} = 0$. This proves (3.3.9).

Now let us prove (3.3.11). By (3.2.1), the cycles $\tau\mathcal{A}$ admit the following decomposition in $H_1(\mathcal{R}_g \setminus \{a,b\})$

$$\tau\mathcal{A} = \mathcal{A} + \mathbf{n}\,\mathcal{S}_b, \tag{3.3.14}$$

for some $\mathbf{n} \in \mathbb{Z}^g$. Therefore, we get from (3.3.14)

$$\begin{aligned} 0 &= \mathcal{A} \circ \ell \\ &= -\,\tau\mathcal{A} \circ \tau\ell \\ &= -\,(\mathcal{A} + \mathbf{n}\,\mathcal{S}_b) \circ \tau\ell \\ &= -\,(\mathcal{A} + \mathbf{n}\,\mathcal{S}_b) \circ (\ell + \mathbf{N}^t\mathcal{A} + \mathbf{M}^t\,\mathcal{B}), \end{aligned} \tag{3.3.15}$$

where the vectors $\mathbf{N}, \mathbf{M} \in \mathbb{Z}^g$ are defined by (3.3.9). The last intersection index in (3.3.15) equals $-\,(\mathbf{n} + \mathbf{M})$, which gives $\tau\mathcal{A} = \mathcal{A} - \mathbf{M}\,\mathcal{S}_b$. According to (3.2.1), the action of τ on the $\mathcal{B}$-cycles in $H_1(\mathcal{R}_g \setminus \{a,b\})$ is given by

$$\tau\mathcal{B} = -\,\mathcal{B} + \mathbb{H}\mathcal{A} + \mathbf{m}\,\mathcal{S}_b, \tag{3.3.16}$$

for some $\mathbf{m} \in \mathbb{Z}^g$. Then

$$\begin{aligned} 0 &= \mathcal{B} \circ \ell \\ &= -\,\tau\mathcal{B} \circ \tau\ell \\ &= -\,(-\mathcal{B} + \mathbb{H}\mathcal{A} + \mathbf{m}\,\mathcal{S}_b) \circ \tau\ell \\ &= -\,(-\mathcal{B} + \mathbb{H}\mathcal{A} + \mathbf{m}\,\mathcal{S}_b) \circ (\ell + \mathbf{N}^t\mathcal{A} + \mathbf{M}^t\,\mathcal{B}), \end{aligned} \tag{3.3.17}$$

where $\mathbf{N}, \mathbf{M} \in \mathbb{Z}^g$ are defined by (3.3.9). The last intersection index in (3.3.17) equals $-(\mathbf{m} + \mathbf{N} + \mathbb{H}\mathbf{M})$, which by (3.3.10) implies $\tau\mathcal{B} = -\mathcal{B} + \mathbb{H}\mathcal{A} + \mathbf{N}\,\mathcal{S}_b$. Finally, since the anti-holomorphic involution τ inverses orientation we have $\tau\mathcal{S}_b = -\mathcal{S}_b$. □

Analogously to the case where $\tau a = b$, considering the action (3.3.11) of τ on the $\mathcal{A}$-cycles, we obtain the following action of τ on the normalized differential of the third kind Ω_{b-a}:

$$\overline{\tau^*\Omega_{b-a}} = \Omega_{b-a} + \sum_{k=1}^{g} M_k\,\omega_k, \tag{3.3.18}$$

where ω_k, $k = 1, \ldots, g$, are the normalized holomorphic differentials.

3.4 Action of τ on the Jacobian and theta divisor

In this part, we review known results [150], [51] about the theta divisor of real Riemann surfaces. For a given real Riemann surface $\mathcal{R}_g$, let us choose the canonical homology basis satisfying (3.2.1), and consider the Jacobian $J = J(\mathcal{R}_g)$.

The anti-holomorphic involution τ defined on $\mathcal{R}_g$ gives rise to an anti-holomorphic involution on the Jacobian: if $\mathcal{D}$ is a positive divisor of degree n on $\mathcal{R}_g$, then $\tau\,\mathcal{D}$ is the class of the point $\int_{n\,\tau p_0}^{\tau\mathcal{D}} \omega = \int_{n\,p_0}^{\mathcal{D}} \tau^*\omega$ in the Jacobian. Therefore, by (3.2.2) τ lifts to the anti-holomorphic involution on J, denoted also by τ, given by

$$\tau\zeta = -\,\overline{\zeta} + n_\zeta\,\Pi(\tau p_0), \tag{3.4.1}$$

for any $\zeta \in J$, where $n_\zeta \in \mathbb{Z}$, $n_\zeta \le g$, is the degree of the divisor $\mathcal{D}$ such that $\Pi(\mathcal{D}) = \zeta$.

Now consider the following two subsets of the Jacobian:

$$S_1 = \{\zeta \in J;\ \zeta + \tau\,\zeta = \mathrm{i}\pi\,\mathrm{diag}(\mathbb{H})\}, \tag{3.4.2}$$

$$S_2 = \{\zeta \in J;\ \zeta - \tau\,\zeta = \mathrm{i}\pi\,\mathrm{diag}(\mathbb{H})\}, \tag{3.4.3}$$

where the matrix $\mathbb{H}$ was introduced in Section 3.2. Below we study their intersections $S_1 \cap (\Theta)$ and $S_2 \cap (\Theta)$ with the theta divisor (Θ), the set of zeros of the theta function.

Let us introduce the following notation: $(e_i)_k = \delta_{ik}$, $\mathbb{B}_i = \mathbb{B}\,e_i$. The following proposition was proved in [150].

Proposition 3.4.1. *The set S_1 is the disjoint union of the tori T_v defined by*

$$T_v = \{\zeta \in J;\ \zeta = \mathrm{i}\pi\,(diag(\mathbb{H})/2 + v_1\,e_{r+1} + \ldots + v_{g-r}\,e_g) + \beta_1\,Re(\mathbb{B}_1) + \ldots + \beta_g\,Re(\mathbb{B}_g)\,,$$
$$\beta_1, \ldots, \beta_r \in \mathbb{R}/2\mathbb{Z}\,,\ \beta_{r+1}, \ldots, \beta_g \in \mathbb{R}/\mathbb{Z}\}, \tag{3.4.4}$$

where $v = (v_1, \ldots, v_{g-r}) \in (\mathbb{Z}/2\mathbb{Z})^{g-r}$ and r is the rank of the matrix $\mathbb{H}$. Moreover, if $\mathcal{R}_g(\mathbb{R}) \neq \emptyset$, then $T_v \cap (\Theta) = \emptyset$ if and only if the curve is dividing and $v = 0$.

The last statement means that among all curves which admit real ovals, the only torus T_v which does not intersect the theta divisor is the torus T_0 corresponding to dividing curves. This torus is given by

$$T_0 = \{\zeta \in J;\ \zeta = \beta_1\,\mathrm{Re}(\mathbb{B}_1) + \ldots + \beta_g\,\mathrm{Re}(\mathbb{B}_g),\ \beta_1, \ldots, \beta_r \in \mathbb{R}/2\mathbb{Z}\,,\ \beta_{r+1}, \ldots, \beta_g \in \mathbb{R}/\mathbb{Z}\}. \tag{3.4.5}$$

It is straightforward to prove that the set S_1 is the disjoint union of the tori (3.4.4). Moreover, in the case where $\mathcal{R}_g(\mathbb{R}) \neq \emptyset$ and $\mathcal{R}_g$ is non-dividing, for all v the torus T_v contains an odd half-period which yields $T_v \cap (\Theta) \neq \emptyset$. The same holds for all $v \neq 0$ in the case where the curve is dividing or does not have real ovals. Corollary 4.3 in [150] proves that if $\mathcal{R}_g$ is dividing then $T_0 \cap (\Theta) = \emptyset$.

The following proposition was proved in [51].

Proposition 3.4.2. *The set S_2 is the disjoint union of the tori $\tilde{T}_v$ defined by*

$$\tilde{T}_v = \{\zeta \in J\,;\, \zeta = 2\mathrm{i}\pi\,(\alpha_1\, e_1 + \ldots + \alpha_g\, e_g) + (v_1/2)\,\mathbb{B}_{r+1} + \ldots + (v_{g-r}/2)\,\mathbb{B}_g, \alpha_1, \ldots, \alpha_g \in \mathbb{R}/\mathbb{Z}\}, \tag{3.4.6}$$

where $v = (v_1, \ldots, v_{g-r}) \in (\mathbb{Z}/2\mathbb{Z})^{g-r}$ and r is the rank of the matrix $\mathbb{H}$. Moreover, if $\mathcal{R}_g(\mathbb{R}) \neq \emptyset$, then $\tilde{T}_v \cap (\Theta) = \emptyset$ if and only if the curve is an M-curve and $v = 0$.

The first step of the proof consists in showing that, for $\zeta \in S_2$, in the case where the number k of real ovals satisfies $1 \leq k \leq g$, the divisor $\mathcal{D}$ of degree g defined by $\zeta = \Pi(\mathcal{D}) + \mathbf{K}$ can be deformed in such a way that it contains the point p_0, the base point of the Abel map with $\tau p_0 = p_0$ (here $\mathbf{K}$ denotes the vector of Riemann constants). In this case one gets $\Theta(\zeta) = 0$. It follows that the intersection set between S_2 and (Θ) can be empty only for curves with $g+1$ real ovals. The proof is completed by noticing that in the case $k = g+1$, there exists only one connected component of the Jacobian such that $\Theta(\zeta)$ does not vanish; it consists of divisors of degree g having one point on each real oval which does not contain p_0. The image $\Pi(\mathcal{D}) + \mathbf{K}$ of such divisors in the Jacobian consists of vectors in $\tilde{T}_0$.

Proposition 3.4.2 is used in [51] to construct smooth solutions of the KP equation. In the present work, Proposition 3.4.1 and Proposition 3.4.2 are necessary to get physically meaningful smooth solutions of the studied integrable equations.

Part II

Camassa-Holm and Dym type equations

Chapter 4

Algebro-geometric solutions via Fay's identity

We give here an independent derivation of algebro-geometric solutions to the Camassa-Holm and Dym-type equations based on identities between multi-dimensional theta functions, which naturally arise from Fay's identity (2.3.1). We also give conditions for the solutions to be real and smooth. In what follows $\mathcal{R}_g$ denotes a hyperelliptic curve of genus $g > 0$, written as

$$\mu^2 = \prod_{i=1}^{2g+2} (\lambda - \lambda_i), \tag{4.0.1}$$

where the branch points $\lambda_i \in \mathbb{C}$ satisfy the relations $\lambda_i \neq \lambda_j$ for $i \neq j$. We denote by σ the hyperelliptic involution defined by $\sigma(\lambda, \mu) = (\lambda, -\mu)$.

4.1 Solutions of the Camassa-Holm equation

The Camassa-Holm equation (CH),

$$u_t + 3\,uu_x = u_{xxt} + 2\,u_x u_{xx} + uu_{xxx} - 2k\,u_x, \tag{4.1.1}$$

where $k \in \mathbb{C}$, was first obtained by Fuchssteiner and Fokas [62] using the method of recursion operators. Camassa and Holm [31] derived this equation by means of physical principles, showing that it models the propagation of unidirectional waves on shallow water, and found a Lax pair of the system. Note that the CH equation can be expressed in the following simple form,

$$m_t + u\,m_x + 2\,m\,u_x = 0, \tag{4.1.2}$$

where we put $m := u - u_{xx} + k$.

Theta-functional solutions of the CH equation (4.1.2) were first given in [14] by solving a generalized Jacobi inversion problem. Our goal here is to give an independent derivation of such solutions via Fay's trisecant identity (2.3.1). In this way, one gets purely transcendental conditions on the parameters (i.e., without reference to a divisor defined by the solution of a Jacobi inversion problem), so that solutions are real-valued and smooth.

4.1.1 Identities between theta functions

From corollaries (2.3.5) and (2.3.10) of Fay's identity, we derive the following identities, necessary in our approach to construct algebro-geometric solutions of the Camassa-Holm equation.

Proposition 4.1.1. *Let $a, b \in \mathcal{R}_g$ such that $\sigma(a) = b$ and let $e \in \mathcal{R}_g$ be a ramification point, namely, $e = (\lambda_j, 0)$ for some $j \in \{1, \dots, 2g+2\}$. Denote by g_1 and g_2 the following functions of the variable $\mathbf{z} \in \mathbb{C}^g$:*

$$g_1(\mathbf{z}) = \frac{\Theta\big(\mathbf{z} + \frac{\mathbf{r}}{2}\big)}{\Theta(\mathbf{z})}, \qquad g_2(\mathbf{z}) = \frac{\Theta\big(\mathbf{z} - \frac{\mathbf{r}}{2}\big)}{\Theta(\mathbf{z})}, \tag{4.1.3}$$

where $\mathbf{r} = \int_a^b \omega$ and ω is the vector of normalized holomorphic differentials. Then the two following identities hold:

$$D_b D_e \ln \frac{g_1}{g_2} = -\frac{p_2}{g_1 g_2} D_b \ln g_1 g_2, \tag{4.1.4}$$

$$D_b D_e \ln(g_1 g_2) = \frac{\tilde{q}_2}{\tilde{p}_2} \frac{1}{g_1 g_2} \left(D_b \ln \frac{g_1}{g_2} - 2\,\tilde{p}_1 \right) - 2\,\tilde{q}_2\, g_1 g_2. \tag{4.1.5}$$

Here we used the following notation:

$$p_2 = p_2(b, e, a), \qquad \tilde{p}_i = p_i(e, b, a), \qquad \tilde{q}_2 = q_2(b, e), \tag{4.1.6}$$

where the scalars $q_2(a, b)$ and $p_i(a, b, c)$, $i = 1, 2$, are defined in (2.3.12) and (2.3.6), (2.3.7); D_b (resp. D_e) denotes the directional derivative (2.3.4).

Proof. Under the changes of variables $(a, b, c) \to (b, e, a)$ and $\mathbf{z} \to \mathbf{z} - \mathbf{r}/2$, identity (2.3.5) becomes

$$D_e \ln \frac{g_1}{g_2} = p_1 + \frac{p_2}{g_1 g_2}. \tag{4.1.7}$$

Here we used the fact that $\int_a^e \omega = \int_e^b \omega = \mathbf{r}/2$ (use (2.3.19)). Applying the differential operator D_b to the previous equality one gets:

$$D_b D_e \ln \frac{g_1}{g_2} = -\,p_2 \frac{D_b(g_1 g_2)}{(g_1 g_2)^2} = -\frac{p_2}{g_1 g_2} D_b \ln g_1 g_2,$$

which proves (4.1.4). To prove (4.1.5), consider the change of variables $(a, b, c) \to (e, b, a)$ in (2.3.5), which leads to

$$D_b \ln g_1 = \tilde{p}_1 + \tilde{p}_2\, g_2 \frac{\Theta(\mathbf{z} + \mathbf{r})}{\Theta\big(\mathbf{z} + \frac{\mathbf{r}}{2}\big)}.$$

Changing $\mathbf{z}$ to $-\mathbf{z}$ in the last equality, one gets

$$D_b \ln g_2 = -\,\tilde{p}_1 - \tilde{p}_2\, g_1 \frac{\Theta(\mathbf{z} - \mathbf{r})}{\Theta\big(\mathbf{z} - \frac{\mathbf{r}}{2}\big)}.$$

From both previous identities, it can be deduced that

$$\frac{\Theta(\mathbf{z} + \mathbf{r})}{\Theta\big(\mathbf{z} + \frac{\mathbf{r}}{2}\big)} = (\tilde{p}_2\, g_2)^{-1} \left(D_b \ln g_1 - \tilde{p}_1\right), \tag{4.1.8}$$

$$\frac{\Theta(\mathbf{z} - \mathbf{r})}{\Theta\big(\mathbf{z} - \frac{\mathbf{r}}{2}\big)} = -\,(\tilde{p}_2\, g_1)^{-1} \left(D_b \ln g_2 + \tilde{p}_1\right). \tag{4.1.9}$$

Moreover, since

$$D_b D_e \ln(g_1 g_2) = D_b D_e \ln \Theta\Big(\mathbf{z} + \frac{\mathbf{r}}{2}\Big) + D_b D_e \ln \Theta\Big(\mathbf{z} - \frac{\mathbf{r}}{2}\Big) - 2\, D_b D_e \ln \Theta(\mathbf{z}),$$

using (2.3.10) one gets

$$D_b D_e \ln(g_1 g_2) = \frac{\tilde{q}_2}{g_1} \frac{\Theta(\mathbf{z}+\mathbf{r})}{\Theta\big(\mathbf{z}+\frac{\mathbf{r}}{2}\big)} + \frac{\tilde{q}_2}{g_2} \frac{\Theta(\mathbf{z}-\mathbf{r})}{\Theta\big(\mathbf{z}-\frac{\mathbf{r}}{2}\big)} - 2\, \tilde{q}_2\, g_1 g_2, \tag{4.1.10}$$

which by (4.1.8) and (4.1.9) leads to (4.1.5). □

From identities (4.1.4) and (4.1.5) we are now able to construct theta-functional solutions of the CH equation:

Proposition 4.1.2. *Let $a, b \in \mathcal{R}_g$ such that $\sigma(a) = b$, and let $e \in \mathcal{R}_g$ be a ramification point. Denote by ℓ an oriented contour between a and b which contains point e. Assume that ℓ does not cross cycles of the canonical homology basis. Choose arbitrary constants $\mathbf{d} \in \mathbb{C}^g$ and k, $\zeta \in \mathbb{C}$. Let $y(x,t)$ be an implicit function of the variables x, $t \in \mathbb{R}$ defined by*

$$x + \alpha_1\, y + \alpha_2\, t + \zeta = \ln \frac{\Theta\big(\mathbf{Z} - \mathbf{d} + \frac{\mathbf{r}}{2}\big)}{\Theta\big(\mathbf{Z} - \mathbf{d} - \frac{\mathbf{r}}{2}\big)}, \tag{4.1.11}$$

where $\mathbf{r} = \int_\ell \omega$. Here the vector $\mathbf{Z}$ is given by

$$\mathbf{Z}(x,t) = \mathbf{V}_e\, y(x,t) + \mathbf{V}_b\, t, \tag{4.1.12}$$

where vectors $\mathbf{V}_e$ and $\mathbf{V}_b$ are defined in (2.3.3). The scalars α_1 and α_2 satisfy

$$\alpha_1 = p_1(b,e,a), \qquad \alpha_2 = 2\, p_1(e,b,a) + k, \tag{4.1.13}$$

where the function p_1 is defined in (2.3.6). Then the following function of the variables x and t is solution of the CH equation:

$$u(x,t) = D_b \ln \frac{\Theta\big(\mathbf{Z} - \mathbf{d} + \frac{\mathbf{r}}{2}\big)}{\Theta\big(\mathbf{Z} - \mathbf{d} - \frac{\mathbf{r}}{2}\big)} - \alpha_2. \tag{4.1.14}$$

Here D_b denotes the directional derivative (2.3.4) along vector $\mathbf{V}_b$.

Proof. Let $\beta, \delta \in \mathbb{C}$ and $\alpha_1, \alpha_2 \in \mathbb{C}$ be arbitrary constants. Let us look for solutions u of CH having the following form

$$u(x,t) = \beta\, D_b \ln \frac{\Theta\big(\mathbf{Z} - \mathbf{d} + \frac{\mathbf{r}}{2}\big)}{\Theta\big(\mathbf{Z} - \mathbf{d} - \frac{\mathbf{r}}{2}\big)} + \delta = \beta\, D_b \ln \frac{g_1}{g_2} + \delta, \tag{4.1.15}$$

where $\mathbf{Z}(x,t)$ is defined in (4.1.12), and the functions g_1, g_2 were introduced in (4.1.3) with $\mathbf{z} = \mathbf{Z}(x,t) - \mathbf{d}$. By (4.1.11), the derivative with respect to the variable x of the implicit function $y(x,t)$ is given by

$$y_x = \left(D_e \ln \frac{g_1}{g_2} - \alpha_1 \right)^{-1}.$$

Assuming $\alpha_1 = p_1(b, e, a)$, by (4.1.7) the function y_x becomes

$$y_x = \frac{g_1 g_2}{p_2}. \tag{4.1.16}$$

Analogously it can be checked that

$$y_t = -\, y_x \left(\frac{u}{\beta} - \frac{\delta}{\beta} - \alpha_2 \right). \tag{4.1.17}$$

Now let us express the function $m(x,t) = u - u_{xx} + k$ introduced in (4.1.2) in terms of functions g_1 and g_2. By (4.1.4) and (4.1.16), the first derivative of the function u (4.1.15) with respect to the variable x is given by

$$u_x = -\, \beta\, D_b \ln(g_1 g_2). \tag{4.1.18}$$

By (4.1.5) and (4.1.16) we deduce the second derivative of u with respect to x:

$$u_{xx} = \beta \left(D_b \ln \frac{g_1}{g_2} - 2\, \tilde{p}_1 \right) - 2\beta\, \tilde{p}_2\, (g_1 g_2)^2\,; \tag{4.1.19}$$

here we used the identity $\tilde{q}_2 = -\, \tilde{p}_2\, p_2$ relating the scalars $\tilde{q}_2, \tilde{p}_2$ and p_2 defined in (4.1.6). Therefore, combining (4.1.15) and (4.1.19), the function m reads

$$m(x,t) = \delta + k + 2\beta\, \tilde{p}_1 + 2\beta\, \tilde{p}_2\, (g_1 g_2)^2. \tag{4.1.20}$$

Taking the derivative of m with respect to x, and the derivative of m with respect to t, one gets respectively:

$$m_x(x,t) = 4\beta\, \tilde{p}_2\, (g_1 g_2)^2\, y_x\, D_e \ln(g_1 g_2), \tag{4.1.21}$$

$$m_t(x,t) = 4\beta\, \tilde{p}_2\, (g_1 g_2)^2\, \left(y_t\, D_e \ln(g_1 g_2) + D_b \ln(g_1 g_2) \right). \tag{4.1.22}$$

Therefore, entering with the functions (4.1.15), (4.1.18), (4.1.21) and (4.1.22) into the CH equation (4.1.2) we obtain

$$\begin{aligned} &2\, \tilde{p}_2\, D_e \ln(g_1 g_2)\, y_x\, (g_1 g_2)^2 \left[u \left(1 - \frac{1}{\beta} \right) + \frac{\delta}{\beta} + \alpha_2 \right] \\ &- D_b \ln(g_1 g_2)\, \left(\delta + k + 2\beta\, \tilde{p}_1 + 2\, \tilde{p}_2\, (g_1 g_2)^2\, (\beta - 1) \right) \;=\; 0. \end{aligned}$$

In particular, the previous equality holds for $\beta = 1$, $\delta = -\, 2\, \tilde{p}_1 - k$ and $\alpha_2 = -\, \delta$, which completes the proof. □

4.1.2 Real-valued solutions and smoothness conditions

In this part, we identify real-valued and smooth solutions of the CH equation. Assume that $\mathcal{R}_g$ is a real hyperelliptic curve which admits real ovals with respect to an anti-holomorphic involution τ (see Chapter 3). Let us choose the homology basis satisfying (3.2.1). Recall that $\mathcal{R}_g(\mathbb{R})$ denotes the set of fixed points of the anti-holomorphic involution τ.

The following propositions provide reality and smoothness conditions on solutions $u(x,t)$ (4.1.14) in the case where points a and b are stable under τ, and in the case where $\tau a = b$. In particular, it is proved that, for fixed $t_0 \in \mathbb{R}$, the function $u(x, t_0)$ is smooth with respect to the real variable x when a and b are stable under τ. In the case where $\tau a = b$, the function $u(x, t_0)$ is smooth, otherwise it has cusp-like singularities.

Proposition 4.1.3. *Assume that all ramification points of $\mathcal{R}_g$ are stable under τ and denote by $e \in \mathcal{R}_g(\mathbb{R})$ one of them. Let $a, b \in \mathcal{R}_g(\mathbb{R})$ such that $\sigma(a) = b$. For any $c \in \{a, b, e\}$, choose the local parameter k_c such that $\overline{k_c(\tau p)} = k_c(p)$ for any point p lying in a neighbourhood of c. Denote by ℓ an oriented contour between a and b containing point e, which does not intersect cycles of the canonical homology basis. Choose ℓ such that the closed path $\tau\ell - \ell$ is homologous to zero in $H_1(\mathcal{R}_g)$. Take $\mathbf{d} \in \mathrm{i}\mathbb{R}^g$ and $k \in \mathbb{R}$. Choose $\zeta \in \mathbb{C}$ in (4.1.11) such that $\ln\left(\frac{\Theta(\mathbf{d}+\mathbf{r}/2)}{\Theta(\mathbf{d}-\mathbf{r}/2)}\right) - \zeta$ is real. Then solutions $u(x,t)$ of the CH equation given in (4.1.14) are real-valued, and for fixed $t_0 \in \mathbb{R}$, the function $u(x, t_0)$ is smooth with respect to the real variable x.*

Proof. Let us check that under the conditions of the proposition, the function $u(x,t)$ (4.1.14) is real-valued. First of all, invariance with respect to the anti-involution τ of the points e and b implies

$$\overline{\mathbf{Z}} = -\mathbf{Z}, \tag{4.1.23}$$

where the vector $\mathbf{Z}$ is defined in (4.1.12). In fact, using the expansion (2.3.3) of the normalized holomorphic differentials ω_j near e (resp. b) one gets

$$\overline{\tau^*\omega_j}(e)(p) = \left(\overline{V_{e,j}} + \overline{W_{e,j}}\, k_e(p) + o\left(k_e(p)^2\right)\right) \mathrm{d}k_e(p),$$

for any point p lying in a neighbourhood of e (resp. b). Then by (3.2.2), vectors $\mathbf{V}_e$ and $\mathbf{V}_b$ appearing in the vector $\mathbf{Z}$ are purely imaginary, which leads to (4.1.23). Moreover, since the closed contour $\tau\ell - \ell$ is homologous to zero in $H_1(\mathcal{R}_g)$, from (3.2.2) one gets

$$\overline{\mathbf{r}} = -\mathbf{r}. \tag{4.1.24}$$

From (2.3.8), the scalars $p_1(b,e,a)$ and $p_1(e,b,a)$ appearing respectively in α_1 and α_2 (see 4.1.13) satisfies

$$\Omega_{a-b}(e) = p_1(b,e,a)\,\mathrm{d}k_e, \qquad \Omega_{a-e}(b) = p_1(e,b,a)\,\mathrm{d}k_b. \tag{4.1.25}$$

Therefore, from (3.3.18) it can be deduced that $p_1(b,e,a)$ and $p_1(e,b,a)$ are real, which involves

$$\overline{\alpha_1} = \alpha_1, \qquad \overline{\alpha_2} = \alpha_2. \tag{4.1.26}$$

Now let us fix $y, t \in \mathbb{R}$ and denote by h the function

$$h(y,t) = \frac{\Theta\left(\mathbf{Z} - \mathbf{d} + \frac{\mathbf{r}}{2}\right)}{\Theta\left(\mathbf{Z} - \mathbf{d} - \frac{\mathbf{r}}{2}\right)}. \tag{4.1.27}$$

By (4.1.11), x is a real-valued function of the real variables y and t if the function $\ln(h(y,t)) - \zeta$ is real, namely, if the function h is real and has a constant sign. From (3.2.4), (4.1.23) and (4.1.24) we deduce that

$$\overline{h(y,t)} = \frac{\Theta\left(\mathbf{Z} + \overline{\mathbf{d}} + \frac{\mathbf{r}}{2} + \mathrm{i}\pi\,\mathrm{diag}(\mathbb{H})\right)}{\Theta\left(\mathbf{Z} + \overline{\mathbf{d}} - \frac{\mathbf{r}}{2} + \mathrm{i}\pi\,\mathrm{diag}(\mathbb{H})\right)}. \tag{4.1.28}$$

Let us choose a vector $\mathbf{d} \in \mathbb{C}^g$ such that

$$\overline{\mathbf{d}} = -\mathbf{d} - \mathrm{i}\pi\,\mathrm{diag}(\mathbb{H}) + 2\mathrm{i}\pi\mathbf{T} + \mathbb{B}\mathbf{L}$$

for some vectors $\mathbf{T}, \mathbf{L} \in \mathbb{Z}^g$. Reality of the vector $\overline{\mathbf{d}} + \mathbf{d}$ together with (3.2.3) imply

$$\mathbf{d} = \frac{1}{2}\,\mathrm{Re}(\mathbb{B})\,\mathbf{L} + \mathrm{i}\,\mathbf{d}_I \tag{4.1.29}$$

for some $\mathbf{d}_I \in \mathbb{R}^g$, where the vectors $\mathbf{T}$ and $\mathbf{L}$ satisfy $2\,\mathbf{T} + \mathbb{H}\mathbf{L} = \mathrm{diag}(\mathbb{H})$. For this choice of vector $\mathbf{d}$, (4.1.28) becomes

$$\overline{h(y,t)} = \frac{\Theta\big(\mathbf{Z} - \mathbf{d} + \frac{\mathbf{r}}{2}\big)}{\Theta\big(\mathbf{Z} - \mathbf{d} - \frac{\mathbf{r}}{2}\big)} \exp\{-\langle \mathbf{r}, \mathbf{L}\rangle\},$$

where we used the quasi-periodicity property (2.2.3) of the theta function. Therefore, the function h is real if $\mathbf{L} = 0$, that is $\mathbf{d} \in \mathrm{i}\mathbb{R}^g$. Now let us check that h has a constant sign with respect to $y, t \in \mathbb{R}$. Since $\mathbf{Z} - \mathbf{d} \pm \frac{\mathbf{r}}{2} \in \mathrm{i}\mathbb{R}^g$, by Proposition 3.4.2 the functions $\Theta(\mathbf{Z} - \mathbf{d} \pm \frac{\mathbf{r}}{2})$ of the real variables y and t do not vanish if the hyperelliptic curve is an M-curve, i.e., if all branch points in (4.0.1) are real. Hence h is a real continuous non vanishing function with respect to the real variables y and t, which means it has a constant sign. Therefore, x is a real-valued function of y and t if the constant ζ in (4.1.11) is chosen such that $\ln(h(y,t)) - \zeta$ is real. It is straightforward to see that the solution u (4.1.14) is a real-valued function of the real variables y and t, and then is real-valued with respect to the real variables x and t.

Now fix $t_0 \in \mathbb{R}$ and let us study smoothness conditions on the function $u(x, t_0)$ with respect to the variable x. First let us check that solution u (4.1.14) is a smooth function of the real variable y. The function u is smooth with respect to y if and only if it does not have singularities. Since the theta function is entire, singularities of the solution u are situated at the zeros of its denominator. By the same argument used previously to prove the real-valuedness of u, if the curve is an M-curve and $\mathbf{d} \in \mathrm{i}\mathbb{R}^g$, the functions $\Theta(\mathbf{Z} - \mathbf{d} \pm \frac{\mathbf{r}}{2})$ and $\Theta(\mathbf{Z} - \mathbf{d})$ do not vanish. In this case, the function u is smooth with respect to the real variable y. Now let us prove that u is smooth with respect to the real variable x. By (4.1.11), the function $x(y)$ is smooth with respect to the variable y. Moreover, it can be seen from (4.1.11) and (4.1.7) that

$$x_y(y) = \frac{p_2}{g_1 g_2} = p_2 \frac{\Theta(\mathbf{Z} - \mathbf{d})^2}{\Theta\big(\mathbf{Z} - \mathbf{d} + \frac{\mathbf{r}}{2}\big)\,\Theta\big(\mathbf{Z} - \mathbf{d} - \frac{\mathbf{r}}{2}\big)}. \tag{4.1.30}$$

Since the functions $\Theta(\mathbf{Z} - \mathbf{d} \pm \frac{\mathbf{r}}{2})$ and $\Theta(\mathbf{Z} - \mathbf{d})$ do not vanish, we deduce that $x(y)$ is a strictly monotonic real function, and thus the inverse function $y(x)$ has the same property. Therefore, the function $u(x, t_0) = u(y(x))$ is a smooth real-valued function with respect to the real variable x. □

Now let us study real-valuedness and smoothness of the solutions in the case where $\tau a = b$.

Proposition 4.1.4. *Assume that all ramification points of $\mathcal{R}_g$ are stable under τ and denote by $e \in \mathcal{R}_g(\mathbb{R})$ one of them. Let $a, b \in \mathcal{R}_g$ such that $\sigma(a) = b$ and assume that $\tau a = b$. Choose the local parameters such that $\overline{k_b(\tau p)} = k_a(p)$ for any point p lying in a neighbourhood of a, and $\overline{k_e(\tau p)} = -\,k_e(p)$ for any p lying in a neighbourhood of e. Denote by ℓ an oriented contour between a and b containing point e, which does not intersect cycles of the canonical homology basis. Assume that $\mathbf{N} = 2\mathbf{L}$ for some $\mathbf{L} \in \mathbb{Z}^g$, where $\mathbf{N} \in \mathbb{Z}^g$ is defined in (3.3.1). Take $k \in \mathbb{R}$ and define $\mathbf{d} = \mathbf{d}_R + \frac{\mathrm{i}\pi}{2}\,\mathbf{N}$ for some $\mathbf{d}_R \in \mathbb{R}^g$. Choose $\zeta \in \mathbb{C}$ in (4.1.11) such that $\ln\left(\frac{\Theta(\mathbf{d}+\mathbf{r}/2)}{\Theta(\mathbf{d}-\mathbf{r}/2)}\right) - \zeta$ is real. Then solutions u (4.1.14) of the CH equation are real-valued. Moreover, for fixed $t_0 \in \mathbb{R}$, the function $u(x, t_0)$ is smooth with respect to the real variable x in the case where $\mathbf{N} = 0$, otherwise it has infinite number of singularities of the type $O\left((x - x_0)^{\frac{2n}{2n+1}}\right)$ for some $n \in \mathbb{N} \setminus \{0\}$ and $x_0 \in \mathbb{R}$, which correspond to cusps.*

Proof. Analogously to the case where a and b are stable under τ, let us prove that solutions u (4.1.14) are real-valued. First let us check that vector $\mathbf{Z}$ (4.1.12) satisfy:

$$\overline{\mathbf{Z}} = \mathbf{Z}. \tag{4.1.31}$$

From (2.3.3) and (3.2.2) one gets $\overline{\mathbf{V}_a} = -\mathbf{V}_b$ and $\overline{\mathbf{V}_e} = \mathbf{V}_e$. Moreover, by assumption vectors $\mathbf{V}_a$ and $\mathbf{V}_b$ satisfy $\mathbf{V}_a + \mathbf{V}_b = 0$ (use (2.3.19)); thus we deduce that $\overline{\mathbf{V}_b} = \mathbf{V}_b$ and $\overline{\mathbf{V}_e} = \mathbf{V}_e$ which proves (4.1.31). By (3.3.8) and (4.1.25) it can be deduced that α_1 and α_2 (4.1.13) satisfy

$$\overline{\alpha_1} = \alpha_1, \qquad \overline{\alpha_2} = \alpha_2. \tag{4.1.32}$$

Moreover, from (3.2.2) and (3.3.1) one gets:

$$\overline{\mathbf{r}} = \mathbf{r} - 2\mathrm{i}\pi\mathbf{N}, \tag{4.1.33}$$

where $\mathbf{N} \in \mathbb{Z}^g$ is defined in (3.3.1). Now fix $y, t \in \mathbb{R}$. Let us check that x (4.1.11) is a real-valued function of the real variables y and t. By (4.1.32), this holds if the function h (4.1.27) is real and has a constant sign with respect to the real variables y and t. By (3.2.4), (4.1.31) and (4.1.33) it follows that

$$\overline{h(y,t)} = \frac{\Theta\big(\mathbf{Z} - \overline{\mathbf{d}} + \frac{\mathbf{r}}{2} + \mathbf{p}\big)}{\Theta\big(\mathbf{Z} - \overline{\mathbf{d}} - \frac{\mathbf{r}}{2} + \mathbf{p}\big)}, \tag{4.1.34}$$

where $\mathbf{p} = -\mathrm{i}\pi\mathbf{N} - \mathrm{i}\pi\,\mathrm{diag}(\mathbb{H})$. Let us choose the vector $\mathbf{d} \in \mathbb{C}^g$ such that

$$\overline{\mathbf{d}} \equiv \mathbf{d} + \mathbf{p} \pmod{2\mathrm{i}\pi\mathbb{Z}^g + \mathbb{B}\mathbb{Z}^g},$$

which is, since $\overline{\mathbf{d}} - \mathbf{d}$ and $\mathbf{p}$ are purely imaginary, equivalent to $\overline{\mathbf{d}} = \mathbf{d} + \mathbf{p} + 2\mathrm{i}\pi\mathbf{T}$, for some $\mathbf{T} \in \mathbb{Z}^g$. Here we used the action (3.2.3) of the complex conjugation on the Riemann matrix $\mathbb{B}$, and the fact that $\mathbb{B}$ has a negative definite real part. Hence, the vector $\mathbf{d}$ can be written as

$$\mathbf{d} = \mathbf{d}_R + \frac{\mathrm{i}\pi}{2}(\mathbf{N} + \mathrm{diag}(\mathbb{H}) - 2\,\mathbf{T}), \tag{4.1.35}$$

for some $\mathbf{d}_R \in \mathbb{R}^g$ and $\mathbf{T} \in \mathbb{Z}^g$. For this choice of vector $\mathbf{d}$, by (4.1.34) the function h is a real-valued function of the real variables y and t. Now let us study in which cases the function h has a constant sign. The sign of the function h is constant with respect to y and t if the functions $\Theta(\mathbf{Z} - \mathbf{d} \pm \frac{\mathbf{r}}{2})$ do not vanish. By (4.1.31), (4.1.33) and (4.1.35), the vectors $\mathbf{Z} - \mathbf{d} \pm \frac{\mathbf{r}}{2}$ belong to the set S_1 introduced in (3.4.2). Hence by Proposition 3.4.1, the functions $\Theta(\mathbf{Z} - \mathbf{d} \pm \frac{\mathbf{r}}{2})$ do not vanish if the hyperelliptic curve is dividing (in this case $\mathrm{diag}(\mathbb{H}) = 0$), and if the arguments $\mathbf{Z} - \mathbf{d} \pm \frac{\mathbf{r}}{2}$ in the theta function are real (modulo $2\mathrm{i}\pi\mathbb{Z}^g$). The vector $\mathbf{Z} - \mathbf{d} + \frac{\mathbf{r}}{2}$ is real if $\mathbf{T} = 0$ in (4.1.35). With this choice of vector $\mathbf{T}$, the imaginary part of the vector $\mathbf{Z} - \mathbf{d} - \frac{\mathbf{r}}{2}$ equals $-\mathrm{i}\pi\mathbf{N}$. Therefore, the vector $\mathbf{Z} - \mathbf{d} - \frac{\mathbf{r}}{2}$ is real modulo $2\mathrm{i}\pi\mathbb{Z}^g$ if all components of the vector $\mathbf{N}$ are even. To summarize, the function $h(y,t)$ defined in (4.1.27) is a real-valued function with constant sign if the hyperelliptic curve is dividing (i.e., all ramification points are stable under τ, since the ramification point e is stable under τ), if $\mathbf{T} = 0$ and $\mathbf{N} = 2\mathbf{L}$ for some $\mathbf{L} \in \mathbb{Z}^g$, where vector $\mathbf{N} \in \mathbb{Z}^g$ is defined in (3.3.1). Analogously to the proof of Proposition 4.1.3, we conclude that x is a real-valued continuous function of the real variables y and t, and thus solutions $u(x,t)$ (4.1.14) are real-valued functions of the real variables x and t.

Now let us study smoothness conditions for fixed $t_0 \in \mathbb{R}$. Notice that function $u(y)$ (4.1.14) is a smooth function of the real variable y since the denominator does not vanish, as we have

seen before. Put $\mathbf{z} = \mathbf{Z} - \mathbf{d}$. Let us consider the function $x_y(y)$ given in (4.1.30) in both cases: $\mathbf{N} = 0$ and $\mathbf{N} \neq 0$.
- If $\mathbf{N} = 0$, the function $x_y(y)$ does not vanish, since in this case $\mathbf{z} \in \mathbb{R}^g$ which implies that the function $\Theta(\mathbf{z})$ does not vanish. Hence, analogously to the case where a and b are stable under τ, for fixed $t_0 \in \mathbb{R}$, the function $u(x, t_0)$ is smooth with respect to the real variable x.
- If $\mathbf{N} \neq 0$, the function $\Theta(\mathbf{z})$ vanishes when $\mathbf{z}$ belongs to the theta divisor. Fix $x_0, t_0 \in \mathbb{R}$ and denote by $\mathbf{z}_0$ and y_0 the corresponding values of $\mathbf{z}$ and y. Assume that $\mathbf{z}_0$ is a zero of the theta function of order $n \geq 1$. Then by (4.1.30), the function $x_y(y)$ has a zero at y_0 of order $2n$. It follows that function $x(y) - x(y_0)$ has a zero of order $2n+1$ at y_0, and then

$$y(x) - y_0 = O\left((x - x_0)^{\frac{1}{2n+1}}\right). \tag{4.1.36}$$

On the other hand, it can be seen from (4.1.4) that

$$u_y(y) = p_2 \frac{\Theta(\mathbf{z})}{\Theta\left(\mathbf{z} + \frac{\mathbf{r}}{2}\right)\Theta\left(\mathbf{z} - \frac{\mathbf{r}}{2}\right)} \left[\Theta(\mathbf{z})\,\psi(\mathbf{z}) - 2\,D_b\Theta(\mathbf{z})\right], \tag{4.1.37}$$

where $\psi(\mathbf{z}) = D_b \ln\left(\Theta(\mathbf{z} + \frac{\mathbf{r}}{2})\,\Theta(\mathbf{z} - \frac{\mathbf{r}}{2})\right)$. Identity (4.1.37) implies that function $u_y(y)$ has a zero at y_0 of order $2n-1$, namely,

$$u(y) - u(y_0) = O\left((y - y_0)^{2n}\right). \tag{4.1.38}$$

Finally, combining (4.1.36) and (4.1.38), the function $u(x, t_0)$ has an infinite number of singularities of the type $O\left((x - x_0)^{\frac{2n}{2n+1}}\right)$ which correspond to cusps. □

4.2 Solutions of the Dym-type equation

This part deals with the Dym-type equation

$$u_{xxt} + 2\,u_x u_{xx} + u u_{xxx} - 2k\,u_x = 0, \tag{4.2.1}$$

where $k \in \mathbb{C}$. Analogously to the Camassa-Holm equation, we first prove identities satisfied by the theta function and derive from them solutions of equation (4.2.1). The study of real-valued and smooth solutions follows the line of the CH equation.

4.2.1 Theta-functional identities

Here we give theta-functional identities useful to construct algebro-geometric solutions of the Dym-type equation. Recall that $\mathcal{R}_g$ denotes the hyperelliptic curve (4.0.1). The following proposition is a direct consequence of identities (2.3.5) and (2.3.10):

Proposition 4.2.1. *Let $e, f \in \mathcal{R}_g$ be two distinct ramification points. Denote by g the following function of the variable $\mathbf{z} \in \mathbb{C}^g$:*

$$g(\mathbf{z}) = \left(D_e D_f \ln \Theta(\mathbf{z}) - q_1\right)^{-1}, \tag{4.2.2}$$

where $q_1 = q_1(e, f)$ is given in (2.3.11), and denote by $\mathbf{r}' = \int_e^f \omega$, where ω is the vector of normalized holomorphic differentials. Then there exist $\mathbf{n}, \mathbf{m} \in \mathbb{Z}^g$ such that

$$\mathbf{r}' = \frac{1}{2}\left(2\mathrm{i}\pi\mathbf{n} + \mathbb{B}\mathbf{m}\right). \tag{4.2.3}$$

Moreover, the two following identities hold:

$$D_e D_f \ln \Theta(\mathbf{z}+\mathbf{r}') = \kappa^2 g(\mathbf{z}) + q_1, \tag{4.2.4}$$

$$D_e D_f^2 \ln \Theta(\mathbf{z}+\mathbf{r}') = -\,\kappa^2 g(\mathbf{z})^2\, D_e D_f^2 \ln \Theta(\mathbf{z}), \tag{4.2.5}$$

for any $\mathbf{z} \in \mathbb{C}^g$*, where* $\kappa = q_2 \exp\{-\frac{1}{2}\langle \mathbb{B}\mathbf{m}, \mathbf{m}\rangle\}$ *with* $q_i = q_i(e,f)$*,* $i = 1,2$*, defined in (2.3.11) and (2.3.12).*

Proof. As proved in (2.3.22), the vector $\mathbf{r}' = \int_e^f \omega$ satisfies (4.2.3) for some $\mathbf{n}, \mathbf{m} \in \mathbb{Z}^g$. Therefore, considering the change of variables $(a,b) = (e,f)$ in (2.3.10) and using the periodicity property (2.2.3) of the theta function, one gets

$$D_e D_f \ln \Theta(\mathbf{z}) - q_1 = q_2\, e^{-\frac{1}{2}\langle \mathbb{B}\mathbf{m},\mathbf{m}\rangle}\, \frac{\Theta(\mathbf{z}+\mathbf{r}')^2}{\Theta(\mathbf{z})^2}\, e^{\phi(\mathbf{z})}, \tag{4.2.6}$$

where $\phi(\mathbf{z}) = \langle \mathbf{z}+\mathbf{r}', \mathbf{m}\rangle$. Moreover, the change of variable $\mathbf{z} \to \mathbf{z}+\mathbf{r}'$ in (2.3.10) leads to

$$D_e D_f \ln \Theta(\mathbf{z}+\mathbf{r}') - q_1 = q_2\, e^{-\frac{1}{2}\langle \mathbb{B}\mathbf{m},\mathbf{m}\rangle}\, \frac{\Theta(\mathbf{z})^2}{\Theta(\mathbf{z}+\mathbf{r}')^2}\, e^{-\phi(\mathbf{z})}. \tag{4.2.7}$$

Combining (4.2.6) and (4.2.7), we deduce that

$$\kappa^{-1}\left(D_e D_f \ln \Theta(\mathbf{z}+\mathbf{r}') - q_1\right) = \left(\kappa^{-1}\left(D_e D_f \ln \Theta(\mathbf{z}) - q_1\right)\right)^{-1} = \kappa\, g(\mathbf{z}), \tag{4.2.8}$$

where $\kappa = q_2 \exp\{-\frac{1}{2}\langle \mathbb{B}\mathbf{m}, \mathbf{m}\rangle\}$, which proves (4.2.4). Applying the operator D_f to identity (4.2.4) one gets (4.2.5). □

Theta-functional solutions of the Dym-type equation (4.2.1) are given by:

Proposition 4.2.2. *Let* $e, f \in \mathcal{R}_g$ *be two distinct ramification points of the curve. Let* $\mathbf{d} \in \mathbb{C}^g$ *and* $\alpha_2, \zeta \in \mathbb{C}$ *be arbitrary constants. Let* $y(x,t)$ *be an implicit function of the variables* $x, t \in \mathbb{R}$ *defined by*

$$x + \alpha_1\, y + \alpha_2\, t + \zeta = D_f \ln \Theta(\mathbf{Z} - \mathbf{d}), \tag{4.2.9}$$

where $\alpha_1 = q_1(e,f)$ *and the vector* $\mathbf{Z}$ *is given by*

$$\mathbf{Z}(x,t) = \mathbf{V}_e\, y + \mathbf{V}_f\, t. \tag{4.2.10}$$

Here the scalar $q_1(e,f)$ *and the vector* $\mathbf{V}_e$ *(resp.* $\mathbf{V}_f$*) are defined in (2.3.11) and (2.3.3);* D_f *denotes the directional derivative along the vector* $\mathbf{V}_f$*. Then the following function*

$$u(x,t) = D_f^2 \ln \Theta(\mathbf{Z} - \mathbf{d}) - \alpha_2, \tag{4.2.11}$$

is solution of the Dym-type equation

$$u_{xxt} + 2\, u_x u_{xx} + u u_{xxx} + 4\, u_x = 0. \tag{4.2.12}$$

Notice that if u *is solution of (4.2.12), the function*

$$v(x,t) = -\,\frac{k}{2}\, u(x, -\tfrac{k}{2}\, t) \tag{4.2.13}$$

is solution of the Dym-type equation (4.2.1) for arbitrary $k \in \mathbb{C}^*$.

Proof. Note that equation (4.2.12) can be written in the form

$$(u_{xt} + uu_{xx})_x = -\,(4 + u_{xx})\, u_x. \tag{4.2.14}$$

Let $\beta, \delta \in \mathbb{C}$ and $\alpha_1, \alpha_2 \in \mathbb{C}$ be arbitrary constants. Let us look for solutions u of equation (4.2.14) having the following form:

$$u(x,t) = \beta\, D_f^2 \ln \Theta(\mathbf{z}) + \delta, \tag{4.2.15}$$

where $\mathbf{z} = \mathbf{Z} - \mathbf{d}$. By (4.2.9), the derivative with respect to x of the implicit function $y(x,t)$ is given by

$$y_x = \left(D_e D_f \ln \Theta(\mathbf{z}) - \alpha_1\right)^{-1};$$

assuming $\alpha_1 = q_1(e,f)$, the function y_x becomes

$$y_x = g(\mathbf{z}), \tag{4.2.16}$$

where the function g is defined in (4.2.2). Analogously, it can be checked that

$$y_t = -\,g(\mathbf{z}) \left(\frac{u}{\beta} - \frac{\delta}{\beta} - \alpha_2\right). \tag{4.2.17}$$

By (4.2.16), the first derivative of function u (4.2.15) with respect to the variable x is given by

$$u_x = \beta\, g(\mathbf{z})\, D_e D_f^2 \ln \Theta(\mathbf{z}) = \beta\, D_f \ln \left(D_e D_f \ln \Theta(\mathbf{z}) - \alpha_1\right), \tag{4.2.18}$$

which by (4.2.6) leads to

$$u_x = 2\beta\, D_f \ln \frac{\Theta(\mathbf{z} + \mathbf{r}')}{\Theta(\mathbf{z})} - \beta\, D_f \phi(\mathbf{z}). \tag{4.2.19}$$

The second derivative of u with respect to x reads

$$u_{xx} = 2\beta\, g(\mathbf{z})\, D_e D_f \ln \frac{\Theta(\mathbf{z} + \mathbf{r}')}{\Theta(\mathbf{z})},$$

where we used (4.2.16) and the fact that ϕ is a linear function of x. Moreover, from (4.2.8) we deduce that

$$D_e D_f \ln \frac{\Theta(\mathbf{z} + \mathbf{r}')}{\Theta(\mathbf{z})} = \kappa^2 g(\mathbf{z}) - g(\mathbf{z})^{-1}, \tag{4.2.20}$$

which yields

$$u_{xx} = 2\beta \left(\kappa^2 g(\mathbf{z})^2 - 1\right). \tag{4.2.21}$$

By (4.2.17) and (4.2.19), the second derivative of the function u with respect to the variables x and t reads

$$u_{xt} = -\,2\, g(\mathbf{z})\, (u - \delta - \beta\, \alpha_2)\; D_e D_f \ln \frac{\Theta(\mathbf{z} + \mathbf{r}')}{\Theta(\mathbf{z})} + 2\beta\, D_f^2 \ln \frac{\Theta(\mathbf{z} + \mathbf{r}')}{\Theta(\mathbf{z})}, \tag{4.2.22}$$

which by (4.2.20) implies

$$u_{xt} = -\,2\,(u - \delta - \beta\, \alpha_2) \left(\kappa^2 g(\mathbf{z})^2 - 1\right) + 2\beta\, D_f^2 \ln \frac{\Theta(\mathbf{z} + \mathbf{r}')}{\Theta(\mathbf{z})}. \tag{4.2.23}$$

Combining (4.2.21) and (4.2.23), we obtain

$$u_{xt} + uu_{xx} = 2\,(\kappa^2 g(\mathbf{z})^2 - 1)\,[u\,(\beta - 1) + \delta + \beta\,\alpha_2] + 2\beta\,D_f^2 \ln \frac{\Theta(\mathbf{z} + \mathbf{r}')}{\Theta(\mathbf{z})}. \tag{4.2.24}$$

Now let us choose $\beta = 1$ and $\alpha_2 = -\,\delta$. Thus (4.2.24) takes the simple form:

$$u_{xt} + uu_{xx} = 2\,D_f^2 \ln \frac{\Theta(\mathbf{z} + \mathbf{r}')}{\Theta(\mathbf{z})}. \tag{4.2.25}$$

By (4.2.25) and (4.2.5), the left hand side in (4.2.14) reads

$$(u_{xt} + uu_{xx})_x = -\,2\,g(\mathbf{z})\left(\kappa^2 g(\mathbf{z})^2 + 1\right) D_e D_f^2 \ln \Theta(\mathbf{z}). \tag{4.2.26}$$

Therefore, substituting (4.2.26), (4.2.21) and (4.2.18) in the Dym type equation (4.2.14), we conclude that function u (4.2.11) is solution of (4.2.14). □

4.2.2 Real-valued solutions and smoothness conditions

In this part, we are interested in real-valued and smooth algebro-geometric solutions obtained in the previous section. These solutions can be investigated analogously to the CH equation, therefore some details will be omitted. Assume that $\mathcal{R}_g$ is a real hyperelliptic curve which admits real ovals with respect to an anti-holomorphic involution τ. Let us choose the homology basis satisfying (3.2.1).

Proposition 4.2.3. *Assume that all ramification points of $\mathcal{R}_g$ are stable under τ. Denote by $e, f \in \mathcal{R}_g(\mathbb{R})$ two distinct ramification points. For any $c \in \{e, f\}$, choose the local parameter k_c near point c such that $\overline{k_c(\tau p)} = k_c(p)$, for any p lying in a neighbourhood of c. Take $\mathbf{d} \in \mathrm{i}\mathbb{R}^g$ and $\alpha_2, \zeta \in \mathbb{R}$. Then solutions $u(x,t)$ (4.2.11) of the Dym-type equation are real-valued. Moreover, for fixed $t_0 \in \mathbb{R}$, the function $u(x, t_0)$ is smooth with respect to the real variable x if $\mathbf{m} = 0$, where $\mathbf{m} \in \mathbb{Z}^g$ is defined in (4.2.3), otherwise it admits infinite singularities of the type $O\left((x - x_0)^{\frac{2n}{2n+1}}\right)$ for some $n \in \mathbb{N} \setminus \{0\}$ and $x_0 \in \mathbb{R}$, which correspond to cusps.*

Proof. Real-valuedness of the solutions can be proved analogously to the CH equation in the case where points a and b are stable under τ (see Proposition 4.1.3). Fix $t_0 \in \mathbb{R}$. Let us study smoothness conditions, with respect to the variable x, of the function $u(x, t_0)$. Put $\mathbf{z} = \mathbf{Z} - \mathbf{d}$ where $\mathbf{Z}$ is defined in (4.2.10). From (4.2.9) and (4.2.6), it can be seen that

$$x_y(y) = \kappa\,\frac{\Theta(\mathbf{z} + \mathbf{r}')^2}{\Theta(\mathbf{z})^2}\,e^{-\phi(\mathbf{z})}, \tag{4.2.27}$$

where $\mathbf{r}' = \int_e^f \omega = \frac{1}{2}(2\mathrm{i}\pi\mathbf{n} + \mathbb{B}\mathbf{m})$ for some $\mathbf{n}, \mathbf{m} \in \mathbb{Z}^g$. Let us consider both cases: $\mathbf{m} = 0$ and $\mathbf{m} \neq 0$.

- If $\mathbf{m} = 0$, then $\mathbf{z} + \mathbf{r}' \in \mathrm{i}\mathbb{R}^g$ and the function $x_y(y)$ does not vanish since the curve is an M-curve. By similar statements used to prove smoothness of the function $u(x, t_0)$ where u is solution of the CH equation, we conclude that the function $u(x, t_0)$ where u (4.2.11) is solution of the Dym-type equation (4.2.12) is smooth.
- If $\mathbf{m} \neq 0$, the function $x_y(y)$ vanishes each time that $\mathbf{z} + \mathbf{r}'$ belongs to the theta divisor. Fix $x_0, t_0 \in \mathbb{R}$ and denote by $\mathbf{z}_0$, y_0 the corresponding value of $\mathbf{z}$, y respectively. Assume that $\mathbf{z}_0 + \mathbf{r}'$

is a zero of the theta function of order n. Then by (4.2.27), y_0 is a zero of the function $x_y(y)$ of order $2n$, which leads to

$$y(x) - y_0 = O\left((x - x_0)^{\frac{1}{2n+1}}\right). \tag{4.2.28}$$

The derivative of function u (4.2.11) with respect to the variable y can be checked applying the operator D_e to identity (4.2.6), thus one gets

$$u_y(y) = -\kappa \frac{\Theta(\mathbf{z}+\mathbf{r}')}{\Theta(\mathbf{z})^2} e^{-\phi(\mathbf{z})} \left[\Theta(\mathbf{z}+\mathbf{r}')\,\psi(\mathbf{z}) - 2\,D_f\Theta(\mathbf{z}+\mathbf{r}')\right], \tag{4.2.29}$$

where $\psi(\mathbf{z}) = 2\,D_f \ln\Theta(\mathbf{z}) + D_f\phi(\mathbf{z})$. Identity (4.2.29) implies that the function $u_y(y)$ has a zero at y_0 of order $2n-1$, namely,

$$u(y) - u(y_0) = O\left((y - y_0)^{2n}\right). \tag{4.2.30}$$

Finally, combining (4.2.28) and (4.2.30), we conclude that the function $u(x, t_0)$ has an infinite number of singularities of the type $O\left((x - x_0)^{\frac{2n}{2n+1}}\right)$ which correspond to cusps. □

Remark 4.2.1. Analogously, if all ramification points of $\mathcal{R}_g$ are stable under τ and if one chooses local parameters such that

$$\overline{k_c(\tau p)} = -\,k_c(p),$$

for any $p \in \mathcal{R}_g$ lying in a neighbourhood of $c \in \{e, f\}$, one gets real-valued solutions for the choices $\mathbf{d} \in \mathbb{R}^g$ and $\alpha_2 \in \mathbb{R}$. In this case, solutions (4.2.11) are smooth if $\overline{\mathbf{r}'} = \mathbf{r}'$, that is $\mathbf{n} = 0$ in (4.2.3), otherwise they admit infinite number of cusps.

Chapter 5

Solitonic limit

It is well known that solitonic solutions of integrable equations arise from their algebro-geometric solutions when the associated spectral curve degenerates to a curve of genus zero. In this chapter, we study the solitonic limit of the theta-functional solutions to the Camassa-Holm and Dym-type equations investigated in Chapter 4. The obtained solitary waves maintain their shape and speed after interacting nonlinearly with other solitary waves. This method to find solitonic solutions is effective for many integrable systems, such as the focusing and defocusing nonlinear Schrödinger equations and the sine-Gordon equation, see, for instance, [23].

Here we show that solutions obtained after degeneration of the hyperelliptic spectral curve depend on the choice of the ramification points in Proposition 4.1.2 and Proposition 4.2.2. Different choices lead to different solutions such as solitons, cuspons or peakons, presented here in a simple parametric form.

5.1 Degeneracy of hyperelliptic Riemann surfaces

Degeneration of the hyperelliptic curve (4.0.1) of genus g into a genus zero algebraic curve can be done by pinching all $\mathcal{A}$-cycles of the associated Riemann surface (see [23] for more details). It consists in colliding $2g$ branch points of the curve, namely, we consider the limit

$$\lambda_{2j+1}, \lambda_{2j+2} \longrightarrow \beta_j, \qquad j = 1, \ldots, g, \tag{5.1.1}$$

where $\beta_i \neq \beta_j$ for $i \neq j$. In this limit, putting $\lambda_1 = -\alpha$ and $\lambda_2 = \alpha$ with $\alpha > 0$, the curve (4.0.1) can be written as

$$\mu^2 = (\lambda^2 - \alpha^2) \prod_{j=1}^{g} (\lambda - \beta_j)^2, \tag{5.1.2}$$

where $\beta_j \neq \alpha$. Desingularization of the curve (5.1.2) yields a Riemann surface of genus zero given by the polynomial equation

$$\mu^2 = \lambda^2 - \alpha^2, \tag{5.1.3}$$

where g pairs of points on the surface each cover a β_j in the base.

5.1.1 Degeneracy of hyperelliptic normalized Abelian differentials

Quantities entering theta-functional solutions of the CH and Dym-type equations, obtained in (4.1.14) and (4.2.11) respectively, are related to the hyperelliptic spectral curve via Abelian

differentials. Hence, before degenerating the algebro-geometric solutions constructed in Chapter 4 in the limit (5.1.1), let us first determine the limit form of the normalized Abelian differentials of the first and third kind, as well as the limit form of the bidifferential (2.2.14).

Degenerate holomorphic differentials. It is well known that a basis of normalized holomorphic differentials $(\omega_1, \ldots, \omega_g)$ on the hyperelliptic curve (4.0.1) is given by:

$$\omega_k(\lambda) = \frac{\varphi_k}{\mu}\,\mathrm{d}\lambda, \tag{5.1.4}$$

for $k = 1, \ldots, g$, where the function φ_k reads

$$\varphi_k(\lambda) = c_{k1}\lambda^{g-1} + c_{k2}\lambda^{g-2} + \ldots + c_{kg},$$

with $c_{kj} \in \mathbb{C}$; moreover, φ_k is chosen such that (2.1.9) holds. In the limit (5.1.1), the normalized holomorphic differential ω_k (5.1.4) becomes

$$\omega_k^0(\lambda) = \frac{\varphi_k^0}{\sqrt{\lambda^2 - \alpha^2}\,\prod_{j=1}^g(\lambda - \beta_j)}\,\mathrm{d}\lambda,$$

for $k = 1, \ldots, g$, where

$$\varphi_k^0(\lambda) = c_{k1}^0\lambda^{g-1} + c_{k2}^0\lambda^{g-2} + \ldots + c_{kg}^0.$$

The functions φ_k^0 are determined by the normalization conditions:

$$2\mathrm{i}\pi\delta_{j,k} = \int_{\mathcal{A}_j} \omega_k^0 = -\,2\mathrm{i}\pi\,\mathrm{Res}(\omega_k^0, \beta_j),$$

for $j, k = 1, \ldots, g$, which yields

$$\varphi_k^0(\lambda) = c_{k1}^0 \prod_{i \neq k}(\lambda - \beta_i), \qquad c_{k1}^0 = -\sqrt{\beta_k^2 - \alpha^2}, \qquad k = 1, \ldots, g.$$

Therefore, in the limit considered here, the normalized holomorphic differential ω_k (5.1.4) becomes a meromorphic differential ω_k^0 on (5.1.3) having simple poles with residue 1 and -1 at the points over β_k:

$$\omega_k^0(\lambda) = \frac{c_{k1}^0}{\sqrt{\lambda^2 - \alpha^2}\,(\lambda - \beta_k)}\,\mathrm{d}\lambda. \tag{5.1.5}$$

Degenerate meromorphic differentials. Consider the hyperelliptic curve (4.0.1) and denote by $a = \infty^-$, $b = \infty^+$ the infinity points. The normalized meromorphic differential Ω_{b-a} having a simple pole at b with residue $+1$ and a simple pole at a with residue -1, after degeneration reads

$$\Omega_{b-a}^0(\lambda) = -\,\frac{\mathrm{d}\lambda}{\mu}. \tag{5.1.6}$$

To see that, consider the local parameter $k_\infty(\lambda) = \lambda^{-1}$ in the neighbourhood of points $a = \infty^-$ and $b = \infty^+$ respectively. Using the fact that these points on the curve (5.1.3) are distinguished by the condition

$$p \to \infty^\pm \quad \Longleftrightarrow \quad \left(\frac{\mu}{\lambda} \to \pm 1 \quad \text{when} \quad \lambda \to \infty\right),$$

from (5.1.6) one has

$$\Omega^0_{b-a}(\lambda) = -\,k_\infty(\lambda)\,\frac{\lambda}{\mu}\left(-\frac{\mathrm{d}k_\infty}{k_\infty(\lambda)^2}\right),$$

which leads to

$$\Omega^0_{b-a}(\lambda) \approx \pm\,\frac{1}{k_\infty(\lambda)}\,\mathrm{d}k_\infty(\lambda), \qquad \lambda \approx \infty.$$

Now let us consider the limit form of the normalized meromorphic differential Ω_{a-e} in both cases: $e = (\lambda_2, 0)$ and $e = (\lambda_{i_0}, 0)$ with $i_0 \neq 1, 2$. In the first case, it can be checked that the differential Ω_{a-e} becomes

$$\Omega^0_{a-e} = \left(\frac{1}{\mu} - \frac{1}{\lambda-\alpha}\right)\frac{\mathrm{d}\lambda}{2}, \tag{5.1.7}$$

and in the second case,

$$\Omega^0_{a-e} = \left(\frac{1}{\mu} - \frac{\mu+\mu_{i_0}}{\lambda-\beta_{i_0}}\right)\frac{\mathrm{d}\lambda}{2}, \tag{5.1.8}$$

where the limit point $e = (\beta_{i_0}, \mu_{i_0})$ lies on the curve (5.1.3). The differential Ω_{e-f} with $e = (\lambda_2, 0)$ and $f = (\lambda_1, 0)$ becomes in the limit (5.1.1):

$$\Omega^0_{e-f} = \left(\frac{1}{\lambda-\alpha} - \frac{1}{\lambda+\alpha}\right)\frac{\mathrm{d}\lambda}{2}. \tag{5.1.9}$$

Degenerate bidifferential. Following [92], for any points $p = (\lambda_p, \mu_p)$, $q = (\lambda_q, \mu_q)$ lying on the hyperelliptic curve (5.1.3), the bidifferential $\Omega(p, q)$ is given by:

$$\Omega(p,q) = \frac{\mathrm{d}h(p)\,\mathrm{d}h(q)}{(h(p)-h(q))^2}, \tag{5.1.10}$$

where h is the uniformization map (i.e., a biholomorphic map) between the Riemann surface associated to the curve (5.1.3) and the Riemann sphere, which is defined by

$$h(p) = -\,\frac{1}{\alpha}\,(\lambda_p + \mu_p).$$

If one of the arguments of $\Omega(p, q)$ coincides with the ramification point $e = (\alpha, 0)$, says $q = e$, one gets

$$\Omega(p,e) = \frac{\Omega(p,q)}{\mathrm{d}k_e}\Big|_{q=e} = \sqrt{\frac{\alpha}{2}}\,\frac{\mathrm{d}\lambda_p}{(\lambda_p-\alpha)^{3/2}\,(\lambda_p+\alpha)^{1/2}}, \tag{5.1.11}$$

where we have chosen the local parameter k_e near the ramification point e to be $k_e(q) = \sqrt{\lambda_q - \alpha}$ for any point q lying in a neighbourhood of e.

5.1.2 Degeneration of hyperelliptic theta functions

As explained in [23] in the framework of the NLS equation, the limit (5.1.1) allows to write down the multi-dimensional theta function as a finite sum of exponential terms. The solitonic solutions of the studied equations thus arise as limiting cases of algebro-geometric solutions.

Let us first describe the behavior of the matrix $\mathbb{B}$ of $\mathcal{B}$-periods of the normalized holomorphic differentials (5.1.4) in the limit (5.1.1). From (5.1.5) one has:

$$\int_\alpha^{\beta_0} \omega_k \longrightarrow c^0_{k1}\int_\alpha^{\beta_0} \frac{\mathrm{d}\lambda}{\sqrt{\lambda^2-\alpha^2}\,(\lambda-\beta_k)} = \ln\frac{\gamma_k+\gamma_0}{\gamma_k-\gamma_0}, \tag{5.1.12}$$

where

$$\gamma_k = \sqrt{\frac{\beta_k - \alpha}{\beta_k + \alpha}} = \frac{\sqrt{\beta_k^2 - \alpha^2}}{\beta_k + \alpha}, \qquad k = 0, \dots, g. \tag{5.1.13}$$

Now assume that β_k are ordered according to

$$\mathrm{Re}(\beta_j) > \mathrm{Re}(\beta_k), \qquad j > k.$$

Therefore, the limit values $\mathbb{B}^0_{jk}$ of the non-diagonal elements of the Riemann matrix $\mathbb{B}$ become

$$\mathbb{B}^0_{jk} = 2\int_{\beta_j}^{\alpha} \omega^0_k = 2\ln\frac{\gamma_k - \gamma_j}{\gamma_k + \gamma_j}, \qquad j > k, \tag{5.1.14}$$

taking into account that $\mathbb{B}^0_{jk} = \mathbb{B}^0_{kj}$. For the diagonal elements of the matrix $\mathbb{B}$, one has the following asymptotic estimate:

$$\mathrm{Re}(\mathbb{B}_{jj}) = 2\ln|\lambda_{2j+1} - \lambda_{2j+2}| + O(1), \qquad j = 1, \dots, g,$$

which in the limit (5.1.1) yields

$$\mathrm{Re}(\mathbb{B}_{jj}) \longrightarrow -\infty, \qquad j = 1, \dots, g. \tag{5.1.15}$$

According to (5.1.15), in the limit considered here, the theta function (2.2.1) with zero characteristic tends to one. Therefore, to get nontrivial theta function, and hence nontrivial solutions of (4.1.1) and (4.2.1) after degeneration, we change the argument $\mathbf{z}$ in the theta function by $\mathbf{z}-\mathbf{D}$ with $\mathbf{D} = (1/2)\,\mathbb{B}_{jj}$, in such way that

$$\Theta(\mathbf{z} - \mathbf{D}) = \sum_{\mathbf{m}\in\mathbb{Z}^g} \exp\left\{\frac{1}{2}\sum_j \mathbb{B}_{jj} m_j(m_j - 1) + \sum_{j<k} \mathbb{B}_{jk} m_j m_k + \sum_j m_j z_j\right\}. \tag{5.1.16}$$

Now taking the limit (5.1.1) in (5.1.16), by (5.1.15) it is straightforward to see that the degenerate theta function denoted by Θ_g reads

$$\Theta_g(\mathbf{z}) = \sum_{\mathbf{m}\in\{0,1\}^g} \exp\left\{\sum_{1\le j<k\le g} \mathbb{B}^0_{jk} m_j m_k + \sum_{j=1}^{g} m_j z_j\right\}, \tag{5.1.17}$$

for any $\mathbf{z} \in \mathbb{C}^g$. Moreover, as we shall see in Proposition 7.1.1 in a more general situation, the degenerate theta function Θ_g admits the following determinantal representation:

$$\Theta_g(\mathbf{z}) = \det(\mathbb{T}), \tag{5.1.18}$$

where $\mathbb{T}$ is a $g \times g$ matrix with elements

$$(\mathbb{T})_{jk} = \delta_{j,k} + \frac{2\,\gamma_j}{\gamma_j + \gamma_k}\, e^{\frac{1}{2}(z_j + z_k)}. \tag{5.1.19}$$

5.2 Soliton-like solutions

In this section we prove that the choice $e = (\lambda_2, 0)$ in (4.1.14) and (4.2.11) leads, after degeneration (5.1.1) of the associated hyperelliptic curve, to soliton-like solutions of the CH equation (4.1.1) and the Dym-type equation (4.2.1) respectively. Here soliton-like solutions denote interactions between solitons and *cuspons*, namely, non-smooth soliton solutions with a cusp. In what follows we assume that $\beta_k \in \mathbb{R}$.

5.2.1 Soliton-like solutions of the CH equation

Let us first determine quantities independent of the physical coordinates which appear in Proposition 4.1.2, when the genus of the hyperelliptic spectral curve tends to zero, as discussed in the previous section. We keep the same notation for these quantities as before the degeneration. Let us choose $e = (\lambda_2, 0)$ in (4.1.14), $a = \infty^-$, $b = \infty^+$, and consider the limit (5.1.1). With notation introduced in (5.1.1) one has $e = (\alpha, 0)$. From (5.1.5) one gets:

$$V_{b,j} = (\beta_j + \alpha)\,\gamma_j, \qquad V_{e,j} = \sqrt{\frac{2}{\alpha}}\,\frac{1}{\gamma_j}, \qquad j = 1, \dots, g, \tag{5.2.1}$$

where γ_j is defined in (5.1.13). From (5.1.12) we deduce that

$$r_j = \int_a^b \omega_j^0 = 2 \ln \frac{\gamma_j + 1}{\gamma_j - 1}, \qquad j = 1, \dots, g. \tag{5.2.2}$$

Moreover, according to (4.1.13) and (4.1.25), from (5.1.6) and (5.1.7) we obtain

$$\alpha_1 = \sqrt{\frac{2}{\alpha}}, \qquad \alpha_2 = \alpha + k. \tag{5.2.3}$$

To get real solutions, assume that $|\beta_j| > \alpha$ for $j = 1, \dots, g$. Thus it can be seen that if $\beta_{j_0} > \alpha$ for some $j_0 \in \{1, \dots, g\}$, then one has

$$\overline{r_{j_0}} = r_{j_0} + 4\mathrm{i}\pi. \tag{5.2.4}$$

In this case, as we saw in Proposition 4.1.4, one has to choose the vector $\mathbf{d} \in \mathbb{R}^g$ appearing in (4.1.14) such that

$$\overline{d_{j_0}} = d_{j_0} + 2\mathrm{i}\pi. \tag{5.2.5}$$

Hence the degenerate solutions given in the following proposition describe interactions between soliton and cusps. It can be seen that the number of cusps which appear in this interaction equals the number of parameters β_j such that $\beta_j > \alpha$. We have proved:

Proposition 5.2.1. *Take $\alpha > 0$ and $\beta_j \in \mathbb{R}$ all distinct, such that $|\beta_j| > \alpha$. Let $\mathbf{d} \in \mathbb{R}^g$ such that d_j satisfies (5.2.5) if $\beta_j > \alpha$, and choose $\zeta, k \in \mathbb{R}$. Assume that the variables x, y, t are related by the condition*

$$x + \sqrt{\frac{2}{\alpha}}\,y + (\alpha + k)\,t + \zeta = \ln \frac{\Theta_g(\mathbf{z} + \frac{\mathbf{r}}{2})}{\Theta_g(\mathbf{z} - \frac{\mathbf{r}}{2})}, \tag{5.2.6}$$

where $\mathbf{z}(x,t) = \mathbf{V}_e\, y + \mathbf{V}_b\, t - \mathbf{d}$. *Here* Θ_g *denotes the degenerated theta function (5.1.17). Moreover, the components of the vectors* $\mathbf{V}_b$ *(resp.* $\mathbf{V}_e$*) and* $\mathbf{r}$ *are given by (5.2.1) and (5.2.2). Hence the following function*

$$u(x,t) = D_b \ln \frac{\Theta_g(\mathbf{z} + \frac{\mathbf{r}}{2})}{\Theta_g(\mathbf{z} - \frac{\mathbf{r}}{2})} - \alpha - k, \tag{5.2.7}$$

is a real-valued solution of the CH equation involving elementary functions only. It describes interaction between $g - s$ *solitons and* s *cusps, where* s *is the number of parameters* β_j *such that* $\beta_j > \alpha$.

5.2.2 Soliton-like solutions of the Dym-type equation

Analogously to the CH equation, we construct soliton-like solutions of the Dym-type equation (4.2.12). Let us choose $e = (\lambda_2, 0)$ and $f = (\lambda_1, 0)$ in (4.2.11) and consider the limit (5.1.1). Keeping the notation introduced in (5.1.1) one has $e = (\alpha, 0)$ and $f = (-\alpha, 0)$. Let us choose the local parameters k_e and k_f near e and f respectively such that

$$k_e = \sqrt{\lambda - \alpha}, \qquad k_f = \mathrm{i}\sqrt{\lambda + \alpha}. \tag{5.2.8}$$

From (5.1.5) one gets

$$V_{e,j} = \sqrt{\frac{2}{\alpha}}\,\frac{1}{\gamma_j}, \qquad V_{f,j} = -\sqrt{\frac{2}{\alpha}}\,\gamma_j, \qquad j = 1, \ldots, g, \tag{5.2.9}$$

where γ_j is defined in (5.1.13). Moreover, it is clear that

$$r'_j = -\int_{-\alpha}^{\alpha} \omega_j^0 = \pm\,\mathrm{i}\pi, \qquad j = 1, \ldots, g, \tag{5.2.10}$$

since integration of the differential ω_j^0 over a closed contour encircling the cut $[-\alpha, \alpha]$ gives a non zero polar period. Finally, from (2.3.13) and (5.1.11) it can be checked that

$$\alpha_1 = -\frac{1}{2\,\alpha}. \tag{5.2.11}$$

To get real solutions, assume that $\alpha_2 \in \mathbb{R}$ and $|\beta_j| > \alpha$ for $j = 1, \ldots, g$. Contrary to the CH equation, by (5.2.10) and Remark 4.2.1, there exists only one class of real-valued solutions without pole, which represent interaction between g solitary cusps. We have proved:

Proposition 5.2.2. *Take* $\alpha > 0$ *and* $\beta_j \in \mathbb{R}$ *all distinct such that* $|\beta_j| > \alpha$. *Choose* $\mathbf{d} \in \mathrm{i}\mathbb{R}^g$ *and* $\alpha_2, \zeta \in \mathbb{R}$. *Assume that variables* x, y, t *are related by the condition*

$$x - \frac{1}{2\,\alpha}\, y + \alpha_2\, t + \zeta = D_f \ln \Theta_g(\mathbf{z}), \tag{5.2.12}$$

where $\mathbf{z}(x,t) = \mathbf{V}_e\, y + \mathbf{V}_f\, t - \mathbf{d}$ *and vectors* $\mathbf{V}_e, \mathbf{V}_f$ *are given by (5.2.9). Hence the following function*

$$u(x,t) = D_f^2 \ln \Theta_g(\mathbf{z}) - \alpha_2, \tag{5.2.13}$$

is a real-valued solution of the Dym-type equation (4.2.1) for $k = -2$, *and describes interaction between* g *cusps. Solutions for arbitrary* $k \in \mathbb{R} \setminus \{0\}$ *follow from (4.2.13).*

5.3 Peakon solutions

Camassa and Holm [31] described a class of peaked solutions for the shallow water equation (4.1.2). These solutions, called "peakons", behave like solitons and differ from the cuspons study in Section 5.2 by their discontinuous derivatives at the peak points (a cuspon is a kind of peaked soliton whose left and right derivatives equal infinity at the cusp).

Here we explain how the choice $e = (\lambda_{i_0}, 0)$ in (4.1.14) and (4.2.11) with $i_0 \in \{3, \dots, 2g+2\}$, leads to peakon solutions when the hyperelliptic spectral curve degenerates according to (5.1.1). In what follows we assume that $\beta_k \in \mathbb{R}$.

5.3.1 Peakon solutions of the CH equation

Let us first consider the solutions for fixed $t_0 \in \mathbb{R}$. Put $a = \infty^-$, $b = \infty^+$, choose $e = (\lambda_{2g+2}, 0)$ and consider the limit (5.1.1). In this limit $e = (\beta_g, \mu_g)$ on the desingularized curve (5.1.3). Hence by (5.1.5), one has the following asymptotic estimate for the coordinate $V_{e,g}$:

$$V_{e,g} \longrightarrow \infty. \tag{5.3.1}$$

This allows to consider the following change of variable

$$y \longrightarrow \frac{\gamma}{V_{e,g}}\, y \tag{5.3.2}$$

in (4.1.11) and (4.1.14), for some $\gamma \in \mathbb{R} \setminus \{0\}$. Analogously to the soliton-like solutions investigated in Section 5.2.1, in the limit considered here one gets, for $j = 1, \dots, g$:

$$V_{b,j} = (\beta_j + \alpha)\, \gamma_j, \tag{5.3.3}$$

$$r_j = 2 \ln \frac{\gamma_j + 1}{\gamma_j - 1}, \tag{5.3.4}$$

$$\alpha_2 = \alpha + k. \tag{5.3.5}$$

Therefore, taking into account the change of variable (5.3.2), for fixed $t_0 \in \mathbb{R}$, identity (4.1.11) becomes in the limit:

$$x(y, t_0) = \ln \left\{ \frac{\Theta_g(\mathbf{z} + \frac{\mathbf{r}}{2})}{\Theta_g(\mathbf{z} - \frac{\mathbf{r}}{2})} \right\} - \alpha_2\, t_0 + d_0, \tag{5.3.6}$$

where

$$z_g = \gamma\, y + V_{b,g}\, t_0 + d_g, \qquad z_j = V_{b,j}\, t_0 + d_j, \qquad j = 1, \dots, g-1, \tag{5.3.7}$$

for some $d_k \in \mathbb{R}$, $k = 0, \dots, g$. Moreover, it can be seen that the g-dimensional theta function Θ_g defined in (5.1.17) admits a decomposition with respect to the $(g-1)$-dimensional theta function Θ_{g-1}, given by:

$$\Theta_g(\mathbf{z}) = e^{z_g}\, \Theta_{g-1}(\bar{\mathbf{z}} + \bar{\mathbb{B}}_g) + \Theta_{g-1}(\bar{\mathbf{z}}), \tag{5.3.8}$$

where $\bar{\mathbf{z}} = (z_1, \dots, z_{g-1})$ and $\bar{\mathbb{B}}_g = (\mathbb{B}_{1\,g}, \dots, \mathbb{B}_{g-1\,g})$. Hence (5.3.6) can be written as

$$x(y, \bar{\mathbf{z}}) = \ln \left\{ \frac{e^{z_g + \frac{r_g}{2}}\, \Theta_{g-1}(\bar{\mathbf{z}} + \frac{\bar{\mathbf{r}}}{2} + \bar{\mathbb{B}}_g) + \Theta_{g-1}(\bar{\mathbf{z}} + \frac{\bar{\mathbf{r}}}{2})}{e^{z_g - \frac{r_g}{2}}\, \Theta_{g-1}(\bar{\mathbf{z}} - \frac{\bar{\mathbf{r}}}{2} + \bar{\mathbb{B}}_g) + \Theta_{g-1}(\bar{\mathbf{z}} - \frac{\bar{\mathbf{r}}}{2})} \right\} - \alpha_2\, t_0 + d_0, \tag{5.3.9}$$

and the solutions obtained in (4.1.14) take the following form in the limit considered here:

$$u(y(x),\bar{\mathbf{z}}) = D_b \ln\left\{\frac{e^{z_g+\frac{r_g}{2}}\,\Theta_{g-1}(\bar{\mathbf{z}}+\frac{\bar{\mathbf{r}}}{2}+\bar{\mathbb{B}}_g)+\Theta_{g-1}(\bar{\mathbf{z}}+\frac{\bar{\mathbf{r}}}{2})}{e^{z_g-\frac{r_g}{2}}\,\Theta_{g-1}(\bar{\mathbf{z}}-\frac{\bar{\mathbf{r}}}{2}+\bar{\mathbb{B}}_g)+\Theta_{g-1}(\bar{\mathbf{z}}-\frac{\bar{\mathbf{r}}}{2})}\right\} - \alpha_2. \tag{5.3.10}$$

Now assume that

$$\beta_j < -\alpha, \qquad j = 1,\dots,g, \tag{5.3.11}$$

in such a way that the function $x_y(y,\bar{\mathbf{z}})$ does not vanish, as we saw for soliton-like solutions. This yields strict monotonicity, with respect to the real variable y, of the function $x(y,\bar{\mathbf{z}})$ and its inverse. Now by (5.3.9), in the limit $y \to \pm\infty$ it can be seen that the function $x_y(y,\bar{\mathbf{z}})$ tends to zero, whereas functions $x(y,\bar{\mathbf{z}})$ and $u(y,\bar{\mathbf{z}})$ have finite values. This means that the set $x(\mathbb{R},\bar{\mathbf{z}})$ is an interval and that the associated function $u(x,\bar{\mathbf{z}})$ is defined only on this interval, where it takes finite values. Hence, expression (5.3.10) together with (5.3.9) describes a finite piece of a solution to the CH equation for fixed $t_0 \in \mathbb{R}$, where $u(x,\bar{\mathbf{z}})$ is defined on the interval $x(\mathbb{R},\bar{\mathbf{z}})$. We denote this solution by

$$U_0(x,t_0) = \{u(x,\bar{\mathbf{z}}),\, x \in x(\mathbb{R},\bar{\mathbf{z}})\}\,. \tag{5.3.12}$$

Now let us construct globally defined solutions for fixed $t_0 \in \mathbb{R}$. To this end, note that

$$x(+\infty,\bar{\mathbf{z}}) = x(-\infty,\bar{\mathbf{z}}+\bar{\mathbb{B}}_g) + r_g, \tag{5.3.13}$$

and

$$u(+\infty,\bar{\mathbf{z}}) = u(-\infty,\bar{\mathbf{z}}+\bar{\mathbb{B}}_g). \tag{5.3.14}$$

This means that the function U_1 defined by

$$U_1(x,t_0) = \left\{u(x,\bar{\mathbf{z}}+\bar{\mathbb{B}}_g),\, x \in x(\mathbb{R},\bar{\mathbf{z}}+\bar{\mathbb{B}}_g)+r_g\right\} \tag{5.3.15}$$

is also a finite piece of solutions for fixed $t_0 \in \mathbb{R}$, and takes the same value as U_0 at their common endpoint. Moreover, it can be seen that the derivative of both pieces U_0 and U_1 takes finite but different values at this common point. Therefore, gluing these two solutions one gets an extended solution $U_0(x,t_0) \cup U_1(x,t_0)$ having a peak at this point. This construction allows to define a global solution U for all values of $x \in \mathbb{R}$ and for fixed $t_0 \in \mathbb{R}$, namely, the function

$$U(x,t_0) = \cup_{n\in\mathbb{Z}}\left\{u(x,\bar{\mathbf{z}}+n\,\bar{\mathbb{B}}_g),\, x \in x(\mathbb{R},\bar{\mathbf{z}}+n\,\bar{\mathbb{B}}_g)+n\,r_g\right\} \tag{5.3.16}$$

is defined on $\mathbb{R}$ and consists of an infinite number of pieces $U_n(x,t_0)$, $n \in \mathbb{Z}$, glued at peak points. Finally we have proved:

Proposition 5.3.1. *For fixed $t_0 \in \mathbb{R}$, peakon solutions of the CH equation consist of an infinite number of pieces $U_n(x,t_0)$, $n \in \mathbb{Z}$, glued at peak points, given in the following parametric form with $y \in \mathbb{R}$:*

$$U_n(y) = D_b \ln\left\{\frac{\Theta_g(z_g+\frac{r_g}{2},\bar{\mathbf{z}}+\frac{\bar{\mathbf{r}}}{2}+n\,\bar{\mathbb{B}}_g)}{\Theta_g(z_g-\frac{r_g}{2},\bar{\mathbf{z}}-\frac{\bar{\mathbf{r}}}{2}+n\,\bar{\mathbb{B}}_g)}\right\} - \alpha_2, \tag{5.3.17}$$

$$x(y) = \ln\left\{\frac{\Theta_g(z_g+\frac{r_g}{2},\bar{\mathbf{z}}+\frac{\bar{\mathbf{r}}}{2}+n\,\bar{\mathbb{B}}_g)}{\Theta_g(z_g-\frac{r_g}{2},\bar{\mathbf{z}}-\frac{\bar{\mathbf{r}}}{2}+n\,\bar{\mathbb{B}}_g)}\right\} - \alpha_2\,t_0 + d_0 + n\,r_g, \tag{5.3.18}$$

where $z_g = \gamma\,y + V_{b,g}\,t_0 + d_g$ and $\bar{\mathbf{z}} = \bar{\mathbf{V}}_b\,t_0 + \bar{\mathbf{d}}$ for some $\bar{\mathbf{d}} \in \mathbb{R}^{g-1}$, and $\gamma, d_0, d_g \in \mathbb{R}$.

Finally, let us consider t_0 as a variable parameter t. In this case, using (5.3.9) and (5.3.13), for any $n \in \mathbb{Z}$ we observe that the piece $U_n(x,t)$ is bounded by the curves $\mathcal{C}_n$ and $\mathcal{C}_{n+1}$ defined by

$$\mathcal{C}_n = \{x = c_n(t),\, t \in \mathbb{R}\}\,, \tag{5.3.19}$$

where

$$c_n(t) = \ln\left\{\frac{\Theta_{g-1}(\bar{\mathbf{z}} + \frac{\bar{\mathbf{r}}}{2} + n\,\bar{\mathbb{B}}_g)}{\Theta_{g-1}(\bar{\mathbf{z}} - \frac{\bar{\mathbf{r}}}{2} + n\,\bar{\mathbb{B}}_g)}\right\} - \alpha_2\, t + d_0 + n\, r_g. \tag{5.3.20}$$

Moreover, it can be seen that $U_{n-1}(x,t)$ and $U_n(x,t)$ are glued along the curve $\mathcal{C}_n$, with

$$U_n(c_n(t),t) = D_b \ln\left\{\frac{\Theta_{g-1}(\bar{\mathbf{z}} + \frac{\bar{\mathbf{r}}}{2} + n\,\bar{\mathbb{B}}_g)}{\Theta_{g-1}(\bar{\mathbf{z}} - \frac{\bar{\mathbf{r}}}{2} + n\,\bar{\mathbb{B}}_g)}\right\} - \alpha_2. \tag{5.3.21}$$

Since $U_{n-1}(x,t)$ and $U_n(x,t)$ have different partial derivatives in x and t along this curve, we conclude that a global piecewise smooth solution $U(x,t)$ has peak curves along $\mathcal{C}_n$, $n \in \mathbb{Z}$.

5.3.2 Peakon solutions of the Dym-type equation

Following the line of Section 5.3.1, we first construct globally defined peakon solutions of the Dym-type equation for fixed $t_0 \in \mathbb{R}$. Choose $e = (\lambda_{2g+2}, 0)$ and $f = (\lambda_2, 0)$, and consider the limit (5.1.1). In this limit, the point e corresponds to the point (β_g, μ_g) on the curve (5.1.3), and f corresponds to the ramification point $(\alpha, 0)$. Moreover, we have seen that the coordinate $V_{e,g}$ has the behavior (5.3.1). Therefore, we consider the change of variable (5.3.2) in (4.2.9) and (4.2.11), with $\gamma \in \mathbb{R} \setminus \{0\}$. Now assume that

$$|\beta_j| > \alpha, \qquad j = 1, \ldots, g. \tag{5.3.22}$$

Therefore, for fixed $t_0 \in \mathbb{R}$, taking into account the change of variable (5.3.2) and identity (5.3.8), the function $x(y)$ defined in (4.2.9) takes the following form:

$$\begin{aligned} x(y,\bar{\mathbf{z}}) = V_{f,g}\, &\frac{e^{z_g}\,\Theta_{g-1}(\bar{\mathbf{z}} + \bar{\mathbb{B}}_g)}{e^{z_g}\,\Theta_{g-1}(\bar{\mathbf{z}} + \bar{\mathbb{B}}_g) + \Theta_{g-1}(\bar{\mathbf{z}})} \\ &+ \sum_{k=1}^{g-1} V_{f,k}\, \frac{e^{z_g}\,\partial_{z_k}\Theta_{g-1}(\bar{\mathbf{z}} + \bar{\mathbb{B}}_g) + \partial_{z_k}\Theta_{g-1}(\bar{\mathbf{z}})}{e^{z_g}\,\Theta_{g-1}(\bar{\mathbf{z}} + \bar{\mathbb{B}}_g) + \Theta_{g-1}(\bar{\mathbf{z}})} - \alpha_2\, t_0 + d_0, \end{aligned} \tag{5.3.23}$$

where

$$z_g = \gamma\, y + V_{f,g}\, t_0 + d_g, \qquad z_j = V_{f,j}\, t_0 + d_j, \qquad j = 1, \ldots, g-1, \tag{5.3.24}$$

for some $d_k \in \mathbb{R}$, $k = 0, \ldots, g$. Notice that

$$x(+\infty, \bar{\mathbf{z}}) = x(-\infty, \bar{\mathbf{z}} + \bar{\mathbb{B}}_g) + V_{f,g}, \tag{5.3.25}$$

and

$$u(+\infty, \bar{\mathbf{z}}) = u(-\infty, \bar{\mathbf{z}} + \bar{\mathbb{B}}_g). \tag{5.3.26}$$

Moreover, it can be seen that the derivative with respect to y of the function $x(y,\bar{\mathbf{z}})$ does not vanish for finite values of y. Hence, by comparison with (5.3.13) and (5.3.14), similar statements used for the CH equation yield the construction of globally defined solutions of the Dym-type equation. These solutions are given by infinite pieces of solutions glued at peak points:

Proposition 5.3.2. *For fixed $t_0 \in \mathbb{R}$, peakon solutions of the Dym-type equation are obtained by gluing at peak points infinite pieces of solutions given in parametric form, with $y \in \mathbb{R}$, by:*

$$U_n(y) = D_f^2 \ln\left\{\Theta_g(z_g, \bar{\mathbf{z}} + n\,\bar{\mathbb{B}}_g)\right\} - \alpha_2, \tag{5.3.27}$$

$$x(y) = D_f \ln\left\{\Theta_g(z_g, \bar{\mathbf{z}} + n\,\bar{\mathbb{B}}_g)\right\} - \alpha_2\, t_0 + d_0 + n\, V_{f,g}, \tag{5.3.28}$$

where $z_g = \gamma\, y + V_{f,g}\, t_0 + d_g$ and $\bar{\mathbf{z}} = \bar{\mathbf{V}}_f\, t_0 + \bar{\mathbf{d}}$ for some $\bar{\mathbf{d}} \in \mathbb{R}^{g-1}$ and $\gamma, d_0, d_g, \alpha_2 \in \mathbb{R}$.

Now let us construct time-dependent peakon solutions. For any $n \in \mathbb{Z}$, it can be seen that the piece $U_n(x,t)$ is bounded by the curves $\mathcal{C}_n$ and $\mathcal{C}_{n+1}$ defined by

$$\mathcal{C}_n = \{x = c_n(t),\, t \in \mathbb{R}\}\,, \tag{5.3.29}$$

where

$$c_n(t) = D_f \ln\left\{\Theta_{g-1}(\bar{\mathbf{z}} + n\,\bar{\mathbb{B}}_g)\right\} - \alpha_2\, t + d_0 + n\, V_{f,g}. \tag{5.3.30}$$

Moreover, we observe that functions $U_{n-1}(x,t)$ and $U_n(x,t)$ are glued along the curve $\mathcal{C}_n$ where

$$U_n(c_n(t), t) = D_f^2 \ln\left\{\Theta_{g-1}(\bar{\mathbf{z}} + n\,\bar{\mathbb{B}}_g)\right\} - \alpha_2. \tag{5.3.31}$$

The functions $U_{n-1}(x,t)$ and $U_n(x,t)$ having different partial derivatives in x and t along this curve, we conclude that a global piecewise smooth solution $U(x,t)$ has peak curves along $\mathcal{C}_n$, with $n \in \mathbb{Z}$.

Part III

Generalized nonlinear Schrödinger equations

Chapter 6

Algebro-geometric solutions via Fay's identity

We prove a new degenerated version of Fay's trisecant identity (2.3.1). Following Mumford's approach, the new identity is applied to construct new algebro-geometric solutions of the multi-component nonlinear Schrödinger (n-NLS) equation. This approach also provides an independent derivation of known algebro-geometric solutions to the Davey-Stewartson (DS) equations.

The chapter is organized as follows: in Section 6.1 we derive a new degeneration of Fay's identity and in Section 6.2 we give an auxiliary computation required in the construction of algebro-geometric solutions of DS and n-NLS equations. With the degenerated version of Fay's trisecant identity obtained in Section 6.1, we construct in Section 6.3 new smooth theta-functional solutions of the multi-component NLS equation, and describe explicitly solutions in the focusing and defocusing cases. We also discuss the reduction from n-NLS to $(n-1)$-NLS, stationary solutions of n-NLS, hyperelliptic solutions, and the link between our solutions of n-NLS and solutions of the KP1 equation. Section 6.4 contains an independent derivation of smooth theta-functional solutions of the Davey-Stewartson equations. This approach also provides an explicit description in terms of theta functions of the constants appearing in the solutions.

6.1 New degeneration of Fay's identity

Algebro-geometric solutions of the Davey-Stewartson and the multi-component NLS equation constructed in this chapter are obtained by using the following new degenerated version of Fay's identity.

Theorem 6.1.1. *Let a, b be distinct points on a compact Riemann surface $\mathcal{R}_g$ of genus g. Fix local parameters k_a and k_b in a neighbourhood of a and b respectively. Denote by δ a non-singular odd characteristic. Then for any $\mathbf{z} \in \mathbb{C}^g$,*

$$D'_a \ln \frac{\Theta(\mathbf{z}+\int_a^b)}{\Theta(\mathbf{z})} + D_a^2 \ln \frac{\Theta(\mathbf{z}+\int_a^b)}{\Theta(\mathbf{z})} + \Big(D_a \ln \frac{\Theta(\mathbf{z}+\int_a^b)}{\Theta(\mathbf{z})} - K_1(a,b)\Big)^2 + 2\, D_a^2 \ln \Theta(\mathbf{z}) + K_2(a,b) = 0, \tag{6.1.1}$$

where the scalars $K_1(a,b)$ and $K_2(a,b)$ are given by

$$K_1(a,b) = \frac{1}{2}\, \frac{D'_a\, \Theta[\delta](0)}{D_a\, \Theta[\delta](0)} + D_a \ln \Theta[\delta]\big(\textstyle\int_a^b\big)\,, \tag{6.1.2}$$

and

$$K_2(a,b) = -\,D'_a \ln\Theta\big(\textstyle\int_a^b\big) - D_a^2 \ln\Big(\Theta\big(\textstyle\int_a^b\big)\,\Theta(0)\Big) - \Big(D_a \ln\Theta\big(\textstyle\int_a^b\big) - K_1(a,b)\Big)^2. \tag{6.1.3}$$

Proof. We start from the following lemma:

Lemma 6.1.1. *Let $b, c \in \mathcal{R}_g$ be distinct points. Fix local parameters k_b and k_c in a neighbourhood of b and c respectively. Then for any $\mathbf{z} \in \mathbb{C}^g$,*

$$D_c\left[-D'_b \ln\frac{\Theta(\mathbf{z}+\int_c^b)}{\Theta(\mathbf{z})} + D_b^2 \ln\frac{\Theta(\mathbf{z}+\int_c^b)}{\Theta(\mathbf{z})} + \Big(D_b \ln\frac{\Theta(\mathbf{z}+\int_c^b)}{\Theta(\mathbf{z})} + K_1(b,c)\Big)^2 + 2\,D_b^2 \ln\Theta(\mathbf{z})\right] = 0, \tag{6.1.4}$$

where the scalar $K_1(b,c)$ is defined in (6.1.2).

Proof of Lemma 6.1.1. Let us introduce the notation $\Theta_{ab} = \Theta(\mathbf{z} + \int_a^b \omega)$ and $\Theta = \Theta(\mathbf{z})$. Differentiating (2.3.1) twice with respect to the local parameter $k_d(p)$, where p lies in a neighbourhood of d, and taking the limit $d \to b$, we obtain

$$\begin{aligned} &D'_b \ln\Theta + D_b^2 \ln\Theta + (D_b \ln\Theta)^2 + \frac{p_3}{p_2}\,D_b \ln\Theta_{ca} - \frac{p_3}{p_2}\,D_b \ln\Theta \\ &= \frac{p_1 p_3}{p_2} - 2\,D_b \ln\Theta_{ca}\,D_b \ln\Theta_{cb} + 2\,D_b \ln\Theta\,D_b \ln\Theta_{cb} + 2\,p_1\,D_b \ln\Theta_{cb} \\ &\quad - p_4 - 2\,p_1\,D_b \ln\Theta_{ca} + D'_b \ln\Theta_{ca} + D_b^2 \ln\Theta_{ca} + (D_b \ln\Theta_{ca})^2, \end{aligned} \tag{6.1.5}$$

where we took into account the relation

$$\partial_{k_d}^2\,\Theta(\mathbf{z} + \textstyle\int_b^d)\big|_{d=b} \;=\; D'_b\,\Theta(\mathbf{z}) + D_b^2\,\Theta(\mathbf{z}).$$

The quantities $p_j = p_j(a,b,c)$ for $j = 1,2$ are defined in (2.3.6) and (2.3.7), whereas quantities $p_j = p_j(a,b,c)$ for $j = 3,4$ are given by

$$p_3(a,b,c) = -\frac{E(a,c)}{E(a,b)}\,\partial_{k_x}^2 \frac{E(b,x)}{E(c,x)}\Big|_{x=b}, \quad p_4(a,b,c) = -\frac{E(c,b)}{E(a,b)}\,\partial_{k_x}^2 \frac{E(a,x)}{E(c,x)}\Big|_{x=b}. \tag{6.1.6}$$

Differentiating (6.1.5) with respect to the local parameter $k_a(p)$, where p lies in a neighbourhood of a, and taking the limit $a \to c$, we get

$$D_c D'_b \ln\Theta + D_c D_b^2 \ln\Theta - 2\,D_c D_b \ln\Theta\,D_b \ln\frac{\Theta_{cb}}{\Theta} + 2\,q_1\,D_b \ln\frac{\Theta_{cb}}{\Theta} - \frac{p_3}{p_2}\,D_c D_b \ln\Theta + K \;=\; 0, \tag{6.1.7}$$

where the scalar K depends on the points b and c, but not on the vector $\mathbf{z} \in \mathbb{C}^g$ (knowledge of the exact value of K is not needed for our purpose). Here the scalars q_1, p_2 and p_3 are defined in (2.3.11), (2.3.7), and (6.1.6) respectively. The change of variable $\mathbf{z} \to -\mathbf{z} + \int_b^c$ in (6.1.7) leads to

$$D_c D'_b \ln\Theta_{cb} - D_c D_b^2 \ln\Theta_{cb} - 2\,D_c D_b \ln\Theta_{cb}\,D_b \ln\frac{\Theta_{cb}}{\Theta} + 2\,q_1\,D_b \ln\frac{\Theta_{cb}}{\Theta} - \frac{p_3}{p_2}\,D_c D_b \ln\Theta_{cb} + K = 0. \tag{6.1.8}$$

Now (6.1.4) is obtained by subtracting (6.1.7) and (6.1.8). □

To prove Theorem 6.1.1, make the change of variable $\mathbf{z} \to -\mathbf{z} + \int_b^c$ in (6.1.5) and add $2\,D_b^2 \ln\Theta$ to each side of the equality to get

$$-D_b' \ln\frac{\Theta_{cb}}{\Theta} + D_b^2 \ln\frac{\Theta_{cb}}{\Theta} + \left(D_b \ln\frac{\Theta_{cb}}{\Theta} + \frac{1}{2}\frac{p_3}{p_2}\right)^2 - \frac{1}{4}\left(\frac{p_3}{p_2}\right)^2 - \frac{p_1 p_3}{p_2} + 2\,D_b^2 \ln\Theta$$

$$= -D_b' \ln\frac{\Theta_{ab}}{\Theta} + D_b^2 \ln\frac{\Theta_{ab}}{\Theta} + \left(D_b \ln\frac{\Theta_{ab}}{\Theta} + \frac{1}{2}\left(\frac{p_3}{p_2} + 2\,p_1\right)\right)^2 - \frac{1}{4}\left(\frac{p_3}{p_2} + 2\,p_1\right)^2 - p_4 + 2\,D_b^2 \ln\Theta.$$

By Lemma 6.1.1, the directional derivative of the left hand side of the previous equality along the vector $\mathbf{V}_c$ equals zero. Hence for any distinct points $a, b, c \in \mathcal{R}_g$, we get

$$D_c\left[-D_b' \ln\frac{\Theta_{ab}}{\Theta} + D_b^2 \ln\frac{\Theta_{ab}}{\Theta} + \left(D_b \ln\frac{\Theta_{ab}}{\Theta} + \frac{1}{2}\left(\frac{p_3}{p_2} + 2\,p_1\right)\right)^2 + 2\,D_b^2 \ln\Theta\right] = 0. \tag{6.1.9}$$

Moreover, from (2.3.6), (2.3.7) and (6.1.6), it can be seen that the expression $\frac{1}{2}(\frac{p_3}{p_2} + 2p_1)$ does not depend on the point c and equals $K_1(b,a)$ given by (6.1.2). Now let us introduce the following function of the variable $\mathbf{z} \in \mathbb{C}^g$:

$$f_{(b,a)}(\mathbf{z}) = -D_b' \ln\frac{\Theta_{ab}}{\Theta} + D_b^2 \ln\frac{\Theta_{ab}}{\Theta} + \left(D_b \ln\frac{\Theta_{ab}}{\Theta} + K_1(b,a)\right)\Big)^2 + 2\,D_b^2 \ln\Theta.$$

Then (6.1.9) can be rewritten as $D_c\, f_{(b,a)}(\mathbf{z}) = 0$ for any $\mathbf{z} \in \mathbb{C}^g$ and for all $c \in \mathcal{R}_g$, $c \neq b$ (because also $D_a\, f_{(b,a)}(\mathbf{z}) = 0$ by Lemma 6.1.1). Since on each Riemann surface $\mathcal{R}_g$ there exists a positive divisor $d_1 + \ldots + d_g$ of degree g such that the vectors $\frac{\omega(d_1)}{\mathrm{d}k_{d_1}}, \ldots, \frac{\omega(d_g)}{\mathrm{d}k_{d_g}}$ are linearly independent (see [89], Lemma 5), the function $f_{(b,a)}(\mathbf{z})$ is constant with respect to $\mathbf{z}$; we denote this constant by $-K_2(b,a)$:

$$f_{(b,a)}(\mathbf{z}) = -K_2(b,a) \tag{6.1.10}$$

for any $\mathbf{z} \in \mathbb{C}^g$. Interchanging a and b, and changing the variable $\mathbf{z}$ by $-\mathbf{z}$ in (6.1.10) we get (6.1.1). The expression (6.1.3) for the scalar $K_2(a,b)$ follows from (6.1.10) putting $\mathbf{z} = 0$. □

6.2 Computation of the argument of the fundamental scalar $q_2(a,b)$

This section is devoted to the computation of the argument $\arg\{q_2(a,b)\}$, where $q_2(a,b)$ is defined by (2.3.12). Let $\mathcal{R}_g$ be a real compact Riemann surface of genus g with an anti-holomorphic involution τ. For two distinct points $a, b \in \mathcal{R}_g$ connected by a contour ℓ which does not intersect the basis of cycles, let us denote by $(\mathcal{A}, \mathcal{B}, \ell)$ the generators of the relative homology group $H_1(\mathcal{R}_g, \{a,b\})$ and by $(\mathcal{A}, \mathcal{B}, \mathcal{S}_b)$ the generators of the homology group $H_1(\mathcal{R}_g \setminus \{a,b\})$ (see Section 3.3). In the following we assume that the basis of cycles $(\mathcal{A}, \mathcal{B})$ satisfies (3.2.1). We compute the argument of $q_2(a,b)$ both in the case $\tau a = b$, as well as in the case $\tau a = a$, $\tau b = b$.

6.2.1 Integral representation for $q_2(a,b)$

The computation of the scalar $\arg\{q_2(a,b)\}$ is based on the following integral representation for $q_2(a,b)$. Recall that Ω_{b-a} denotes the normalized meromorphic differential of the third kind which has residue 1 at b and residue -1 at a.

Proposition 6.2.1. *Let a, b be distinct points on a compact Riemann surface $\mathcal{R}_g$ of genus g. Denote by k_a and k_b local parameters in a neighbourhood of a and b respectively. Then the scalar $q_2(a,b)$ defined in (2.3.12) admits the following integral representation*

$$q_2(a,b) = -\lim_{\substack{\tilde{b}\to b\\ \tilde{a}\to a}} \left[\Big(k_a(\tilde{a})\, k_b(\tilde{b})\Big)^{-1} \exp\left\{ \int_{\tilde{a}}^{\tilde{b}} \Omega_{b-a}(p) \right\} \right], \tag{6.2.1}$$

where the integration contour between $\tilde{a}$ and $\tilde{b}$, which in the sequel is denoted by $\tilde{\ell}$, does not cross any cycle from the canonical homology basis.

Proof. Notice that the scalar $q_2(a,b)$ does not depend on the choice of the contour $\tilde{\ell}$, assuming that $\tilde{\ell}$ lies in the fundamental polygon of the Riemann surface.

Denote by k_x a local parameter in a neighbourhood of a point $x \in \mathcal{R}_g$. To prove (6.2.1), recall that (see (2.2.13))

$$\int_{\tilde{a}}^{\tilde{b}} \Omega_{b-a}(p) = \ln \frac{\Theta[\delta](\int_b^{\tilde{b}})}{\Theta[\delta](\int_a^{\tilde{b}})} + \ln \frac{\Theta[\delta](\int_a^{\tilde{a}})}{\Theta[\delta](\int_b^{\tilde{a}})}. \tag{6.2.2}$$

Since δ is an odd non-singular characteristic, the expression $\frac{\Theta[\delta](\int_b^p)}{\Theta[\delta](\int_a^p)}$ has a simple zero at b and a simple pole at a. Therefore, if we consider $\tilde{a}$ in a neighbourhood of a, and $\tilde{b}$ in a neighbourhood of b, we get (with $\alpha_1, \beta_1 \neq 0$)

$$\frac{\Theta[\delta](\int_b^{\tilde{b}})}{\Theta[\delta](\int_a^{\tilde{b}})} = \alpha_1\, k_b(\tilde{b}) + o(k_b(\tilde{b})), \tag{6.2.3}$$

$$\frac{\Theta[\delta](\int_a^{\tilde{a}})}{\Theta[\delta](\int_b^{\tilde{a}})} = \beta_1\, k_a(\tilde{a}) + o(k_a(\tilde{a})). \tag{6.2.4}$$

Combining (6.2.2) together with (6.2.3) and (6.2.4), we obtain the following relation

$$\lim_{\substack{\tilde{b}\to b\\ \tilde{a}\to a}} \left[\Big(k_a(\tilde{a})\, k_b(\tilde{b})\Big)^{-1} \exp\left\{ \int_{\tilde{a}}^{\tilde{b}} \Omega_{b-a}(p) \right\} \right] = \alpha_1\beta_1. \tag{6.2.5}$$

Moreover, using the definition (2.3.12) of $q_2(a,b)$, it follows from (6.2.3) and (6.2.4) that $\alpha_1\beta_1 = -\,q_2(a,b)$, which by (6.2.5) completes the proof. □

6.2.2 Argument of $q_2(a,b)$ when $\tau a = b$

Here we compute the argument of the fundamental scalar $q_2(a,b)$ in the case where $\tau a = b$.

Proposition 6.2.2. *Let $(\mathcal{A}, \mathcal{B}, \ell)$ be the generators of the relative homology group $H_1(\mathcal{R}_g, \{a,b\})$. Assume that $\tau a = b$, with local parameters satisfying the relation $\overline{k_b(\tau p)} = k_a(p)$ for any point p in a neighbourhood of a. Then the scalar $q_2(a,b)$ is real, and its sign is given by:*

1. *if ℓ intersects the set of real ovals of $\mathcal{R}_g$ only once, and if this intersection is transversal, then $q_2(a,b) < 0$,*

2. if ℓ does not cross any real oval, then $q_2(a,b) > 0$.

Proof. Let $\tilde{a}, \tilde{b} \in \mathcal{R}_g$ lie in a neighbourhood of a and b respectively such that $\tau\tilde{a} = \tilde{b}$. Denote by $\tilde{\ell}$ an oriented contour connecting $\tilde{a}$ and $\tilde{b}$. First, let us check that

$$\arg\{q_2(a,b)\} = \pi(1+\alpha), \tag{6.2.6}$$

where $\alpha = (\tau\tilde{\ell}+\tilde{\ell})\circ\ell$ in the relative homology group $H_1(\mathcal{R}_g, \{a,b\})$. The integral representation (6.2.1) of $q_2(a,b)$ leads to

$$\arg\{q_2(a,b)\} = \pi + \operatorname{Im}\left(\int_{\tilde{\ell}} \Omega_{b-a}(p)\right). \tag{6.2.7}$$

By (3.3.8), the last term in the right hand side of (6.2.7) is equal to $\frac{1}{2\mathrm{i}}\int_{\tau\tilde{\ell}+\tilde{\ell}} \Omega_{b-a}(p)$. The closed contour $\tau\tilde{\ell}+\tilde{\ell}$ admits the following decomposition in $H_1(\mathcal{R}_g \setminus \{a,b\})$,

$$\tau\tilde{\ell}+\tilde{\ell} = \mathbf{N}^t\mathcal{A} + \alpha\,\mathcal{S}_b, \tag{6.2.8}$$

where $\alpha = (\tau\tilde{\ell}+\tilde{\ell})\circ\ell$ and $\mathbf{N} \in \mathbb{Z}^g$ is defined in (3.3.1). Since the differential Ω_{b-a} has vanishing $\mathcal{A}$-periods, by (6.2.8) we obtain

$$\int_{\tau\tilde{\ell}+\tilde{\ell}} \Omega_{b-a}(p) = 2\mathrm{i}\pi\alpha, \tag{6.2.9}$$

which leads to (6.2.6). Therefore, the sign of $q_2(a,b)$ depends on the parity of the intersection index $\alpha = (\tau\tilde{\ell}+\tilde{\ell})\circ\ell$.

Let us now consider cases *1.* and *2.* separately.

Case 1. Assume that each of the contours ℓ and $\tilde{\ell}$ intersects the set of real ovals of $\mathcal{R}_g$ transversally only once, and, moreover, this intersection point is the same for ℓ and $\tilde{\ell}$; we denote it by $p_0 \in \mathcal{R}_g(\mathbb{R})$. Then the closed contour $\tau\tilde{\ell}+\tilde{\ell}$ can be decomposed into a sum of two closed contours $c\tilde{\ell_1}$ and $c\tilde{\ell_2}$, having the common point p_0, and such that τ sends the set of points $\{c\tilde{\ell_1}\}$ into the set of points $\{c\tilde{\ell_2}\}$. Therefore, if the orientation of $c\tilde{\ell_1}$ and $c\tilde{\ell_2}$ is inherited from the orientation of $\tau\tilde{\ell}+\tilde{\ell}$, we have $\tau c\tilde{\ell_1} = c\tilde{\ell_2}$ as elements of $H_1(\mathcal{R}_g \setminus \{a,b\})$. Then,

$$c\tilde{\ell_1}\circ\ell = -\tau c\tilde{\ell_1}\circ\tau\ell = -c\tilde{\ell_2}\circ(-\ell+\mathbf{N}^t\mathcal{A}) = c\tilde{\ell_2}\circ\ell,$$

where we used the action (3.3.1) of τ on the contour ℓ, and the fact that the intersection index between $c\tilde{\ell_2}$ and $\mathcal{A}$-cycles is zero by (6.2.8). Hence the intersection index α satisfies

$$\alpha = (\tau\tilde{\ell}+\tilde{\ell})\circ\ell = (c\tilde{\ell_1}+c\tilde{\ell_2})\circ\ell = 2,$$

which by (6.2.6) leads to $q_2(a,b) < 0$.

Case 2. Let $\mathcal{V}$ be a ring neighbourhood of the path $\tau\tilde{\ell}+\tilde{\ell}$, bounded by two closed paths denoted by $\partial\mathcal{V}_1$ and $\partial\mathcal{V}_2$, in such way that the path ℓ lies in $\mathcal{V}$ and $\tau\{\partial\mathcal{V}_1\} = \{\partial\mathcal{V}_2\}$. We assume that $\mathcal{V}$ is chosen such that no point of $\mathcal{V}$ is invariant under τ. Then $\mathcal{V}$ can be decomposed into two connected components denoted by $\mathcal{V}_1$ and $\mathcal{V}_2$ as follows: $\mathcal{V}_1$ is bounded by $\partial\mathcal{V}_1$ and $\tau\tilde{\ell}+\tilde{\ell}$, and $\mathcal{V}_2$ is bounded by $\partial\mathcal{V}_2$ and $\tau\tilde{\ell}+\tilde{\ell}$. Then $\tau\mathcal{V}_1 = \mathcal{V}_2$ since the set of points $\{\tau\tilde{\ell}+\tilde{\ell}\}$ is invariant under τ. In particular, if $a \in \mathcal{V}_1$ then $b \in \mathcal{V}_2$. Thus the intersection index $\alpha = (\tau\tilde{\ell}+\tilde{\ell})\circ\ell$ is odd, which leads to $q_2(a,b) > 0$. □

6.2.3 Argument of $q_2(a,b)$ when $\tau a = a$ and $\tau b = b$

Now let us consider the case where a and b are invariant with respect to τ.

Proposition 6.2.3. *Let $a, b \in \mathcal{R}_g(\mathbb{R})$ with local parameters satisfying $\overline{k_a(\tau p)} = k_a(p)$ for any point p in a neighbourhood of a and $\overline{k_b(\tau p)} = k_b(p)$ for any point p in a neighbourhood of b. Let $(\mathcal{A}, \mathcal{B}, \ell)$ be the generators of the relative homology group $H_1(\mathcal{R}_g, \{a,b\})$. Choose $\tilde{a}, \tilde{b} \in \mathcal{R}_g(\mathbb{R})$ in a neighbourhood of a and b respectively, and denote by $\tilde{\ell}$ an oriented contour connecting $\tilde{a}$ and $\tilde{b}$. Then the argument of the scalar $q_2(a,b)$ is given by*

$$\arg\{q_2(a,b)\} = \arg\{k_a(\tilde{a})\, k_b(\tilde{b})\} + \pi(1+\alpha) + \frac{\pi}{2}\langle \mathbb{H}\mathbf{M}, \mathbf{M}\rangle - \frac{1}{2\mathrm{i}}\left(\langle \mathbb{B}\mathbf{M}, \mathbf{M}\rangle + 2\langle \mathbf{r}, \mathbf{M}\rangle\right), \quad (6.2.10)$$

where α equals the intersection index $(\tau\tilde{\ell} - \tilde{\ell}) \circ \ell$. Here $\mathbf{r} = \int_\ell \omega$, and $\mathbf{M} \in \mathbb{Z}^g$ is defined in (3.3.9).

Proof. From the integral representation (6.2.1) of $q_2(a,b)$ we get

$$\arg\{q_2(a,b)\} = \pi + \arg\{k_a(\tilde{a})\, k_b(\tilde{b})\} + \operatorname{Im}\left(\int_{\tilde{\ell}} \Omega_{b-a}(p)\right). \quad (6.2.11)$$

By (3.3.18) we deduce that

$$2\mathrm{i}\operatorname{Im}\left(\int_{\tilde{\ell}} \Omega_{b-a}(p)\right) = \int_{\tilde{\ell}} \Omega_{b-a} - \int_{\tau\tilde{\ell}} \Omega_{b-a} - \sum_k M_k \int_{\tau\tilde{\ell}} \omega_k.$$

The closed contour $\tau\tilde{\ell} - \tilde{\ell} \in H_1(\mathcal{R}_g)$ satisfies $\tau(\tau\tilde{\ell} - \tilde{\ell}) = -(\tau\tilde{\ell} - \tilde{\ell})$; thus by (3.3.12) it has the following decomposition in $H_1(\mathcal{R}_g \setminus \{a,b\})$

$$\tau\tilde{\ell} - \tilde{\ell} = \mathbf{N}^t\mathcal{A} + \mathbf{M}^t\mathcal{B} + \alpha\,\mathcal{S}_b, \quad (6.2.12)$$

for some $\alpha \in \mathbb{Z}$, where $\mathbf{N}, \mathbf{M} \in \mathbb{Z}^g$ are defined in (3.3.9). Hence we get

$$2\mathrm{i}\operatorname{Im}\left(\int_{\tilde{\ell}} \Omega_{b-a}(p)\right) = -\int_{\mathbf{M}^t\mathcal{B}} \Omega_{b-a} + 2\mathrm{i}\pi\alpha - \sum_k M_k\left[\int_{\tilde{\ell}} \omega_k + \sum_j (\mathbb{B}_{jk} - \mathrm{i}\pi\,\mathbb{H}_{jk})\, M_j\right], \quad (6.2.13)$$

where we used the fact that the normalized differential Ω_{b-a} has vanishing $\mathcal{A}$-periods, and that the integral over the small contour $\mathcal{S}_b$ of the holomorphic differentials is zero. Since by definition the contour ℓ does not cross any cycle of the absolute homology basis, from (2.1.11) one has

$$\int_{\mathbf{M}^t\mathcal{B}} \Omega_{b-a} = \langle \mathbf{M}, \mathbf{r}\rangle. \quad (6.2.14)$$

Hence we get

$$\operatorname{Im}\left(\int_{\tilde{\ell}} \Omega_{b-a}(p)\right) = \pi\alpha + \frac{\pi}{2}\langle \mathbb{H}\mathbf{M}, \mathbf{M}\rangle - \frac{1}{2\mathrm{i}}\left(\langle \mathbf{M}, \tilde{\mathbf{r}} + \mathbf{r}\rangle + \langle \mathbb{B}\mathbf{M}, \mathbf{M}\rangle\right), \quad (6.2.15)$$

where $\tilde{\mathbf{r}} = \int_{\tilde{\ell}} \omega$. Considering the limit when $\tilde{a}$ tends to a and $\tilde{b}$ tends to b, we obtain (6.2.10). □

6.3 Algebro-geometric solutions of the multi-component NLS equation

In this section, we derive from the degenerated Fay identity (6.1.1) new theta-functional solutions of the multi-component nonlinear Schrödinger equation (n-NLS^s)

$$\mathrm{i}\,\frac{\partial\psi_j}{\partial t}+\frac{\partial^2\psi_j}{\partial x^2}+2\left(\sum_{k=1}^{n}s_k|\psi_k|^2\right)\psi_j=0,\qquad j=1,\dots,n, \tag{6.3.1}$$

where $s=(s_1,\dots,s_n)$, $s_k=\pm1$. Here $\psi_j(x,t)$, for $j=1,\dots,n$, are complex valued functions of the real variables x and t.

6.3.1 Solutions of the complexified n-NLS equation

To construct algebro-geometric solutions of (6.3.1), let us first introduce the complexified version of the n-NLS^s equation, which is a system of $2n$ equations of $2n$ dependent variables ψ_j,ψ_j^* for $j=1,\dots,n$:

$$\begin{aligned}\mathrm{i}\,\frac{\partial\psi_j}{\partial t}+\frac{\partial^2\psi_j}{\partial x^2}+2\left(\sum_{k=1}^{n}\psi_k\,\psi_k^*\right)\psi_j&=0,\\ -\mathrm{i}\,\frac{\partial\psi_j^*}{\partial t}+\frac{\partial^2\psi_j^*}{\partial x^2}+2\left(\sum_{k=1}^{n}\psi_k\,\psi_k^*\right)\psi_j^*&=0,\qquad j=1,\dots,n,\end{aligned} \tag{6.3.2}$$

where $\psi_j(x,t)$ and $\psi_j^*(x,t)$ are complex valued functions of the real variables x and t. This system reduces to the n-NLS^s equation (6.3.1) under the *reality conditions*

$$\psi_j^*=s_j\,\overline{\psi_j},\qquad j=1,\dots,n. \tag{6.3.3}$$

Theta-functional solutions of the system (6.3.2) are given by:

Theorem 6.3.1. *Let $\mathcal{R}_g$ be a compact Riemann surface of genus $g>0$ and let f be a meromorphic function of degree $n+1$ on $\mathcal{R}_g$. Let $z_a\in\mathbb{C}$ be a non critical value of f, and consider the fiber $f^{-1}(z_a)=\{a_1,\dots,a_{n+1}\}$ over z_a. Choose the local parameters k_{a_j} near a_j as $k_{a_j}(p)=f(p)-z_a$, for any point $p\in\mathcal{R}_g$ in a neighbourhood of a_j. Let $\mathbf{d}\in\mathbb{C}^g$ and $A_j\neq0$ be arbitrary constants. Then the following functions ψ_j,ψ_j^*, $j=1,\dots,n$, give solutions of the system (6.3.2)*

$$\begin{aligned}\psi_j(x,t)&=A_j\,\frac{\Theta(\mathbf{Z}-\mathbf{d}+\mathbf{r}_j)}{\Theta(\mathbf{Z}-\mathbf{d})}\,\exp\left\{-\mathrm{i}\,(E_j\,x-F_j\,t)\right\},\\ \psi_j^*(x,t)&=\frac{q_2(a_{n+1},a_j)}{A_j}\,\frac{\Theta(\mathbf{Z}-\mathbf{d}-\mathbf{r}_j)}{\Theta(\mathbf{Z}-\mathbf{d})}\,\exp\left\{\mathrm{i}\,(E_j\,x-F_j\,t)\right\}.\end{aligned} \tag{6.3.4}$$

Here $\mathbf{r}_j=\int_{a_{n+1}}^{a_j}\omega$, where ω is the vector of normalized holomorphic differentials, and

$$\mathbf{Z}=\mathrm{i}\,\mathbf{V}_{a_{n+1}}\,x+\mathrm{i}\,\mathbf{W}_{a_{n+1}}\,t. \tag{6.3.5}$$

The vectors $\mathbf{V}_{a_{n+1}}$ and $\mathbf{W}_{a_{n+1}}$ are defined in (2.3.3), and the scalars E_j,F_j are given by

$$E_j=K_1(a_{n+1},a_j),\qquad F_j=K_2(a_{n+1},a_j)-2\sum_{k=1}^{n}q_1(a_{n+1},a_k). \tag{6.3.6}$$

The scalars $q_1(a_{n+1}, a_j)$, $q_2(a_{n+1}, a_j)$, $K_1(a_{n+1}, a_j)$ and $K_2(a_{n+1}, a_j)$ are defined in (2.3.11), (2.3.12), (6.1.2) and (6.1.3) respectively.

Proof. We start with the following technical lemma:

Lemma 6.3.1. *Let $\mathcal{R}_g$ be a compact Riemann surface of genus $g > 0$ and let $a_1, \ldots, a_{n+1}$ be distinct points on $\mathcal{R}_g$. Then the vectors $\mathbf{V}_{a_j}$ for $j = 1, \ldots, n+1$, are linearly dependent if and only if there exists a meromorphic function f of degree $n+1$ on $\mathcal{R}_g$, and $z_a \in \mathbb{CP}^1$ such that $f^{-1}(z_a) = \{a_1, \ldots, a_{n+1}\}$.*

Proof of Lemma 6.3.1. Assume that there exist $\gamma_1, \ldots, \gamma_{n+1} \in \mathbb{C}^*$ such that $\sum_{k=1}^{n+1} \gamma_k \mathbf{V}_{a_k} = 0$. By (2.1.10), the left hand side of this equality equals the vector of $\mathcal{B}$-periods of the normalized differential of the second kind $\Omega = \sum_{k=1}^{n+1} \gamma_k \, \Omega^{(2)}_{a_k}$. Hence all periods of the differential Ω vanish, which implies that the Abelian integral $p \longmapsto \int_{p_0}^{p} \Omega$ is a meromorphic function of degree $n+1$ on $\mathcal{R}_g$ having simple poles at $a_1, \ldots, a_{n+1}$.

Conversely, assume that there exists a meromorphic function f of degree $n+1$ on $\mathcal{R}_g$, and $z_a \in \mathbb{C}$ such that $f^{-1}(z_a) = \{a_1, \ldots, a_{n+1}\}$ (the case $z_a = \infty$ can be treated in the same way). The function $h(p) = (f(p) - z_a)^{-1}$ is a meromorphic function of degree $n+1$ on $\mathcal{R}_g$ having simple poles at $a_1, \ldots, a_{n+1}$ only. Therefore, all periods of the differential $\mathrm{d}h$ vanish. Let $p_0 \in \mathcal{R}_g$ satisfy $h(p_0) = 0$. Using Riemann's bilinear identity (2.1.8) one gets

$$\int_{\mathcal{R}_g} \omega_j \wedge \mathrm{d}h = \int_{\partial F_g} \omega_j \int_{p_0}^{p} \mathrm{d}h = \int_{\partial F_g} \omega_j \, h(p) = 0,$$

where F_g denotes the simply connected domain with the boundary $\partial F_g = \sum_{j=1}^{g} (\mathcal{A}_j + \mathcal{A}_j^{-1} + \mathcal{B}_j + \mathcal{B}_j^{-1})$. By Cauchy's theorem, taking local parameters k_{a_j} near a_j such that $k_{a_j}(p) = f(p) - z_a$ for any point $p \in \mathcal{R}_g$ in a neighbourhood of a_j, we deduce that $\sum_{k=1}^{n+1} \mathbf{V}_{a_k} = 0$. □

To prove Theorem 6.3.1, substitute the functions (6.3.4) in the first equation of (6.3.2) to get

$$\begin{aligned} D'_{a_{n+1}} \ln \frac{\Theta(\mathbf{z}+\mathbf{r}_1)}{\Theta(\mathbf{z})} &+ D^2_{a_{n+1}} \ln \frac{\Theta(\mathbf{z}+\mathbf{r}_1)}{\Theta(\mathbf{z})} + \left(D_{a_{n+1}} \ln \frac{\Theta(\mathbf{z}+\mathbf{r}_1)}{\Theta(\mathbf{z})} - E_1 \right)^2 \\ &+ F_1 - 2 \sum_{k=1}^{n} q_2(a_{n+1}, a_k) \, \frac{\Theta(\mathbf{z}+\mathbf{r}_k)\, \Theta(\mathbf{z}-\mathbf{r}_k)}{\Theta(\mathbf{z})^2} = 0. \end{aligned} \tag{6.3.7}$$

It can be shown that equation (6.3.7) holds as follows: in (6.1.1), let us choose $a = a_{n+1}$ and $b = a_1$ to obtain

$$D'_{a_{n+1}} \ln \frac{\Theta(\mathbf{z}+\mathbf{r}_1)}{\Theta(\mathbf{z})} + D^2_{a_{n+1}} \ln \frac{\Theta(\mathbf{z}+\mathbf{r}_1)}{\Theta(\mathbf{z})} + \left(D_{a_{n+1}} \ln \frac{\Theta(\mathbf{z}+\mathbf{r}_1)}{\Theta(\mathbf{z})} - K_1 \right)^2 \tag{6.3.8}$$

$$+ K_2 + 2\, D^2_{a_{n+1}} \ln \Theta(\mathbf{z}) = 0, \tag{6.3.9}$$

for any $\mathbf{z} \in \mathbb{C}^g$, and in particular for $\mathbf{z} = \mathbf{Z} - \mathbf{d}$; here we used the notation $K_i = K_i(a_{n+1}, a_1)$ for $i = 1, 2$. By Lemma 6.3.1 the sum $\sum_{k=1}^{n+1} \mathbf{V}_{a_k}$ equals zero, which implies

$$\sum_{k=1}^{n+1} D_{a_k} = 0.$$

Replacing $-\sum_{k=1}^{n} D_{a_k}$ with $D_{a_{n+1}}$ in (6.3.9) and using (2.3.10) we obtain (6.3.7), where

$$E_1 = K_1, \qquad F_1 = K_2 - 2\sum_{k=1}^{n} q_1(a_{n+1}, a_k).$$

In the same way, it can be proved that the functions in (6.3.4) satisfy the $2n-1$ other equations of the system (6.3.2). □

The solutions (6.3.4) of the complexified system (6.3.2) depend on the Riemann surface $\mathcal{R}_g$, the meromorphic function f of degree $n+1$, a non critical value $z_a \in \mathbb{C}$ of f, and arbitrary constants $\mathbf{d} \in \mathbb{C}^g$, $A_j \neq 0$. A transformation of the local parameters given by

$$k_{a_j} \longrightarrow \beta\, k_{a_j} + \mu\, k_{a_j}^2 + O\left(k_{a_j}^3\right), \tag{6.3.10}$$

where β, μ are arbitrary complex numbers ($\beta \neq 0$), leads to a different family of solutions of the complexified system (6.3.2). These new solutions are obtained via the following transformations:

$$\begin{aligned} \psi_j(x,t) &\longrightarrow \psi_j\left(\beta\, x + 2\beta\lambda\, t, \beta^2\, t\right) \exp\left\{-\mathrm{i}\left(\lambda\, x + \lambda^2\, t\right)\right\}, \\ \psi_j^*(x,t) &\longrightarrow \beta^2\, \psi_j^*\left(\beta\, x + 2\beta\lambda\, t, \beta^2\, t\right) \exp\left\{\mathrm{i}\left(\lambda\, x + \lambda^2\, t\right)\right\}, \end{aligned} \tag{6.3.11}$$

where $\lambda = \mu\, \beta^{-1}$.

6.3.2 Reality conditions

Algebro-geometric solutions of the n-NLS^s equation (6.3.1) are constructed from solutions (6.3.4) of the complexified system by imposing the reality conditions $\psi_j^* = s_j\, \overline{\psi_j}$.

Let $\mathcal{R}_g$ be a real compact Riemann surface with an anti-holomorphic involution τ. Denote by $\mathcal{R}_g(\mathbb{R})$ the set of fixed points of the involution τ (see Section 3.1). Let us choose the homology basis satisfying (3.2.1). A meromorphic function f on $\mathcal{R}_g$ is called real if $f(\tau p) = \overline{f(p)}$ for any point $p \in \mathcal{R}_g$.

In the next proposition we derive theta-functional solutions of the system (6.3.1). The signs s_j, which appear in the reality conditions (6.3.3), are expressed in terms of certain intersection indices on $\mathcal{R}_g$. These intersection indices are defined as follows: let f be a real meromorphic function of degree $n+1$ on $\mathcal{R}_g$. Let $z_a \in \mathbb{R}$ be a non critical value of f, and assume that the fiber $f^{-1}(z_a) = \{a_1, \ldots, a_{n+1}\}$ over z_a belongs to the set $\mathcal{R}_g(\mathbb{R})$. Let $\tilde{a}_{n+1}, \tilde{a}_j \in \mathcal{R}_g(\mathbb{R})$ lie in a neighbourhood of a_{n+1} and a_j respectively such that $f(\tilde{a}_{n+1}) = f(\tilde{a}_j)$. Denote by $\tilde{\ell}_j$ an oriented contour connecting $\tilde{a}_{n+1}$ and $\tilde{a}_j$, and having the following decomposition in $H_1(\mathcal{R}_g \setminus \{a_{n+1}, a_j\})$ (see Section 3.3.2):

$$\tau\tilde{\ell}_j = \tilde{\ell}_j + \mathbf{N}_j^t \mathcal{A} + \mathbf{M}_j^t \mathcal{B} + \alpha_j\, \mathcal{S}_{a_j}, \tag{6.3.12}$$

for some $\alpha_j \in \mathbb{Z}$, where the vectors $\mathbf{N}_j, \mathbf{M}_j \in \mathbb{Z}^g$ are the same as in (3.3.9). Then

$$\alpha_j = (\tau\tilde{\ell}_j - \tilde{\ell}_j) \circ \ell_j \tag{6.3.13}$$

is the intersection index between the closed contour $\tau\tilde{\ell}_j - \tilde{\ell}_j$ and the contour ℓ_j; this index is computed in the relative homology group $H_1(\mathcal{R}_g, \{a_{n+1}, a_j\})$.

Theta-functional solutions of (6.3.1) are given by:

Proposition 6.3.1. *Let f be a real meromorphic function of degree $n+1$ on $\mathcal{R}_g$. Let $z_a \in \mathbb{R}$ be a non critical value of f, and assume that the fiber $f^{-1}(z_a) = \{a_1, \dots, a_{n+1}\}$ over z_a belongs to the set $\mathcal{R}_g(\mathbb{R})$. Choose the local parameters k_{a_j} near a_j as $k_{a_j}(p) = f(p) - z_a$, for any point $p \in \mathcal{R}_g$ in a neighbourhood of a_j. Denote by $(\mathcal{A}, \mathcal{B}, \ell_j)$ the standard generators of the relative homology group $H_1(\mathcal{R}_g, \{a_{n+1}, a_j\})$. Let $\mathbf{d}_R \in \mathbb{R}^g$, $\mathbf{T} \in \mathbb{Z}^g$, and define $\mathbf{d} = \mathbf{d}_R + \frac{\mathrm{i}\pi}{2}(diag(\mathbb{H}) - 2\,\mathbf{T})$. Moreover, take $\theta \in \mathbb{R}$. Then the following functions ψ_j for $j = 1, \dots, n$, give solutions of n-NLS^s*

$$\psi_j(x,t) = |A_j|\, e^{\mathrm{i}\theta}\, \frac{\Theta(\mathbf{Z} - \mathbf{d} + \mathbf{r}_j)}{\Theta(\mathbf{Z} - \mathbf{d})}\, \exp\{-\mathrm{i}\,(E_j\, x - F_j\, t)\}\,, \tag{6.3.14}$$

where $\mathbf{Z} = \mathrm{i}\,\mathbf{V}_{a_{n+1}}\, x + \mathrm{i}\,\mathbf{W}_{a_{n+1}}\, t$, and

$$|A_j| = |q_2(a_{n+1}, a_j)|^{1/2}\, \exp\left\{\tfrac{1}{2}\,\langle \mathbf{d}_R, \mathbf{M}_j\rangle\right\}. \tag{6.3.15}$$

Here $\mathbf{r}_j = \int_{\ell_j} \omega$, the vectors $\mathbf{V}_{a_{n+1}}, \mathbf{W}_{a_{n+1}}$ are defined in (2.3.3), and the vector $\mathbf{M}_j \in \mathbb{Z}^g$ is defined by the action of τ on the relative homology group $H_1(\mathcal{R}_g, \{a_{n+1}, a_j\})$ (see (3.3.9)). The scalars $q_2(a_{n+1}, a_j)$ and E_j, F_j are introduced in (2.3.12) and (6.3.6) respectively. The signs $s_1, \dots, s_n$ are given by

$$s_j = \exp\{\mathrm{i}\pi(1 + \alpha_j) + \mathrm{i}\pi\,\langle \mathbf{T}, \mathbf{M}_j\rangle\}\,, \tag{6.3.16}$$

where the intersection indices $\alpha_j \in \mathbb{Z}$ are defined in (6.3.13).

Proof. Let us check that under the conditions of the theorem, the functions ψ_j and ψ_j^* (6.3.4) satisfy the reality conditions (6.3.3). First of all, invariance with respect to the anti-involution τ of the point a_{n+1} implies the reality of vector (6.3.5):

$$\overline{\mathbf{Z}} = \mathbf{Z}. \tag{6.3.17}$$

In fact, using the expansion (2.3.3) of the normalized holomorphic differentials ω_j near a_{n+1} we get

$$\overline{\tau^*\omega_j}(a_{n+1})(p) = \left(\overline{V_{a_{n+1},j}} + \overline{W_{a_{n+1},j}}\, k_{a_{n+1}}(p) + o(k_{a_{n+1}}(p))\right)\, \mathrm{d}k_{a_{n+1}}(p),$$

for any point p in a neighbourhood of a_{n+1}. Then, by (3.2.2) the vectors $\mathbf{V}_{a_{n+1}}$ and $\mathbf{W}_{a_{n+1}}$ appearing in the expression (6.3.5) satisfy

$$\overline{\mathbf{V}_{a_{n+1}}} = -\mathbf{V}_{a_{n+1}}, \quad \overline{\mathbf{W}_{a_{n+1}}} = -\mathbf{W}_{a_{n+1}}, \tag{6.3.18}$$

which leads to (6.3.17). Moreover, from (3.2.2) and (3.3.9) we get

$$\overline{\mathbf{r}_j} = -\,\mathbf{r}_j - 2\mathrm{i}\pi\mathbf{N}_j - \mathbb{B}\mathbf{M}_j, \tag{6.3.19}$$

where $\mathbf{N}_j, \mathbf{M}_j \in \mathbb{Z}^g$ are defined in (3.3.9) and satisfy

$$2\,\mathbf{N}_j + \mathbb{H}\mathbf{M}_j = 0. \tag{6.3.20}$$

From (6.1.1), it is straightforward to see that the scalars $K_1(a_{n+1}, a_j)$ and $K_2(a_{n+1}, a_j)$ defined by (6.1.2) and (6.1.3) satisfy

$$\overline{K_1(a_{n+1}, a_j)} = K_1(a_{n+1}, a_j) - \left\langle \mathbf{V}_{a_{n+1}}, \mathbf{M}_j\right\rangle, \qquad \overline{K_2(a_{n+1}, a_j)} = K_2(a_{n+1}, a_j) + \left\langle \mathbf{W}_{a_{n+1}}, \mathbf{M}_j\right\rangle.$$

Moreover, one can directly see from (2.3.10) that $q_1(a_{n+1}, a_j)$ is real. Hence we get

$$\overline{E_j} = E_j - \left\langle \mathbf{V}_{a_{n+1}}, \mathbf{M}_j \right\rangle, \qquad \overline{F_j} = F_j + \left\langle \mathbf{W}_{a_{n+1}}, \mathbf{M}_j \right\rangle. \tag{6.3.21}$$

Under the assumptions of the theorem, and by (6.2.10), the argument of $q_2(a_{n+1}, a_j)$ is given by

$$\arg\{q_2(a_{n+1}, a_j)\} = \pi(1+\alpha_j) + \frac{\pi}{2}\langle \mathbb{H}\mathbf{M}_j, \mathbf{M}_j\rangle - \frac{1}{2\mathrm{i}}\left(\langle \mathbb{B}\mathbf{M}_j, \mathbf{M}_j\rangle + 2\langle \mathbf{r}_j, \mathbf{M}_j\rangle\right). \tag{6.3.22}$$

Therefore, the reality conditions (6.3.3) together with (6.3.4) lead to

$$\begin{aligned} |A_j|^2 = s_j\,|q_2(a_{n+1}, a_j)|\, &\frac{\Theta(\mathbf{Z}-\mathbf{d}-\mathbf{r}_j)\,\Theta(\mathbf{Z}-\overline{\mathbf{d}}+\mathrm{i}\pi\,\mathrm{diag}(\mathbb{H}))}{\Theta(\mathbf{Z}-\overline{\mathbf{d}}-\mathbf{r}_j+\mathrm{i}\pi\,\mathrm{diag}(\mathbb{H}))\,\Theta(\mathbf{Z}-\mathbf{d})} \\ &\times \exp\left\{\mathrm{i}\pi(1+\alpha_j) + \tfrac{\mathrm{i}\pi}{2}\langle \mathbb{H}\mathbf{M}_j, \mathbf{M}_j\rangle + \left\langle \overline{\mathbf{d}} - \mathrm{i}\pi\,\mathrm{diag}(\mathbb{H}), \mathbf{M}_j\right\rangle\right\}, \end{aligned} \tag{6.3.23}$$

if one takes into account (3.2.4) and (2.2.3). Let us choose a vector $\mathbf{d} \in \mathbb{C}^g$ such that

$$\overline{\mathbf{d}} \equiv \mathbf{d} - \mathrm{i}\pi\,\mathrm{diag}(\mathbb{H}) \pmod{2\mathrm{i}\pi\mathbb{Z}^g + \mathbb{B}\mathbb{Z}^g}.$$

Since $\overline{\mathbf{d}} - \mathbf{d}$ is purely imaginary we have

$$\overline{\mathbf{d}} = \mathbf{d} - \mathrm{i}\pi\,\mathrm{diag}(\mathbb{H}) + 2\mathrm{i}\pi\mathbf{T}, \tag{6.3.24}$$

for some $\mathbf{T} \in \mathbb{Z}^g$, where we have used (3.2.3) and the fact that $\mathbb{B}$ has a non-degenerate real part. It follows that the vector $\mathbf{d}$ can be written as

$$\mathbf{d} = \mathbf{d}_R + \frac{\mathrm{i}\pi}{2}(\mathrm{diag}(\mathbb{H}) - 2\,\mathbf{T}), \tag{6.3.25}$$

for some $\mathbf{d}_R \in \mathbb{R}^g$ and $\mathbf{T} \in \mathbb{Z}^g$. Therefore, (6.3.23) becomes

$$|A_j|^2 = s_j\,|q_2(a_{n+1}, a_j)| \exp\left\{\mathrm{i}\pi(1+\alpha_j) + \tfrac{\mathrm{i}\pi}{2}\langle \mathbb{H}\mathbf{M}_j, \mathbf{M}_j\rangle + \langle \mathbf{d}, \mathbf{M}_j\rangle\right\}. \tag{6.3.26}$$

We deduce from (6.3.25) and (6.3.26) that

$$s_j = \exp\left\{\mathrm{i}\pi(1+\alpha_j) + \tfrac{\mathrm{i}\pi}{2}\langle \mathbb{H}\mathbf{M}_j + \mathrm{diag}(\mathbb{H}), \mathbf{M}_j\rangle - \mathrm{i}\pi\langle \mathbf{T}, \mathbf{M}_j\rangle\right\}.$$

From (6.3.20) and the definition of the matrix $\mathbb{H}$ (see Section 3.2), it can be deduced that the quantity $\frac{1}{2}\langle \mathbb{H}\mathbf{M}_j + \mathrm{diag}(\mathbb{H}), \mathbf{M}_j\rangle$ is even in each case, which yields (6.3.16) and (6.3.15). □

Functions ψ_j for $j = 1, \ldots, n$, given in (6.3.14) describe a family of algebro-geometric solutions of (6.3.1) depending on: a real Riemann surface $(\mathcal{R}_g, \tau)$, a real meromorphic function f on $\mathcal{R}_g$ of degree $n+1$, a non critical value $z_a \in \mathbb{R}$ of f such that the fiber over z_a belongs to the set $\mathcal{R}_g(\mathbb{R})$, and arbitrary constants $\mathbf{d}_R \in \mathbb{R}^g$, $\mathbf{T} \in \mathbb{Z}^g$, $\theta \in \mathbb{R}$. Note that the periodicity properties of the theta function imply without loss of generality that the vector $\mathbf{T}$ can be chosen in the set $\{0,1\}^g$. The case where the Riemann surface $\mathcal{R}_g$ is dividing and $\mathbf{T} = 0$ is of special importance, because the related solutions are smooth, as explained in the next proposition. In this case, the sign s_j (6.3.16) is given by $s_j = \exp\{\mathrm{i}\pi(1+\alpha_j)\}$.

Since the theta function is entire, singularities of the functions ψ_j can appear only at the zeros of their denominator. Following Vinnikov's result [150] we obtain

Proposition 6.3.2. *Solutions (6.3.14) are smooth if the curve $\mathcal{R}_g$ is dividing and $\mathbf{d} \in \mathbb{R}^g$. Assume that solutions (6.3.14) are smooth for any vector $\mathbf{d}$ in a component T_v (3.4.4) of the Jacobian, then the curve is dividing and $\mathbf{d} \in \mathbb{R}^g$.*

Proof. By (6.3.17) and (6.3.25), the vector $\mathbf{Z}-\mathbf{d}$ belongs to the set S_1 introduced in (3.4.2). Hence by Proposition 3.4.1, the solutions are smooth if the curve is dividing (in this case diag($\mathbb{H}$)=0), and if the argument $\mathbf{Z}-\mathbf{d}$ of the theta function in the denominator is real, which by (6.3.17) leads to the choice $\mathbf{d} \in \mathbb{R}^g$ (and then $\mathbf{T} = 0$ in Proposition 6.3.1).

The following assertions were proved in [150]: let $\mathcal{R}_g(\mathbb{R}) \neq \emptyset$; if $\mathcal{R}_g$ is non dividing, then $T_v \cap (\Theta) \neq \emptyset$ for all v, where (Θ) denotes the set of zeros of the theta function; if $\mathcal{R}_g$ is dividing, then $T_v \cap (\Theta) \neq \emptyset$ if and only if $v \neq 0$. It follows that if solutions are smooth for any vector $\mathbf{d}$ in a component T_v (3.4.4) of the Jacobian, then the curve is dividing and $v = 0$. Hence $\mathbf{d} \in T_0$ where $T_0 = \mathbb{R}^g$. □

6.3.3 Solutions of n-NLS$^+$ and n-NLS$^-$

Here, we consider the two most physically significant situations: the completely focusing multi-component system n-NLS$^+$ (which corresponds to $s = (1, \ldots, 1)$), and the completely defocusing system n-NLS$^-$ (which corresponds to $s = (-1, \ldots, -1)$).

Starting from a pair $(\mathcal{R}_g, f)$, where $\mathcal{R}_g$ is a Riemann surface of genus g, and where f is a meromorphic function of degree $n+1$ on $\mathcal{R}_g$, which has $n+1$ simple poles, we construct an $(n+1)$-sheeted branched covering of $\mathbb{CP}^1$, which we denote by $\mathcal{R}_{g,n+1}$. The ramification points of the covering correspond to critical points of f; we assume that all of them are simple. We denote by $x_1, \ldots, x_{2g+2n} \in \mathcal{R}_{g,n+1}$ the critical points of the meromorphic function f, and by $z_j = f(x_j) \in \mathbb{C}$ the critical values.

For any point $a \in \mathcal{R}_{g,n+1}$ which is not a critical point or a pole of the meromorphic function f, we use the local parameter $k_a(p) = f(p) - f(a)$, for any point p in a neighbourhood of a.

According to [53], by an appropriate choice of the set of generators $\{\gamma_j\}_{j=1}^{2g+2n}$ of the fundamental group $\pi_1(\mathbb{CP}^1 \setminus \{z_1, \ldots, z_{2g+2n}\}, z_0)$ of the base, which satisfy $\gamma_1 \ldots \gamma_{2g+2n} = id$, the covering $\mathcal{R}_{g,n+1}$ can be represented as follows: consider the hyperelliptic covering of genus g and attach to it $n-1$ spheres as shown in Figure 6.1. More precisely, the generators γ_j can be chosen in such way that the loop γ_j encircles only the point z_j; the corresponding elements $\sigma_j \in \mathbf{S}_{n+1}$ (where $\mathbf{S}_{n+1}$ denotes the symmetric group of order $n+1$) of the monodromy group of the covering are given by

$$\begin{aligned} \sigma_j &= (n+1, n), & j &= 1, \ldots, 2g+2, \\ \sigma_{2g+2k+3} = \sigma_{2g+2k+4} &= (n-k, n-k-1), & k &= 0, \ldots, n-2. \end{aligned}$$

Assume that the branch points $\{z_j\}_{j=1}^{2g+2n}$ are real or pairwise conjugate, and order them as follows:

$$\mathrm{Re}(z_1) \leq \ldots \leq \mathrm{Re}(z_{2g+2n}).$$

Let us introduce an anti-holomorphic involution τ on $\mathcal{R}_{g,n+1}$, which acts as the complex conjugation on each sheet.

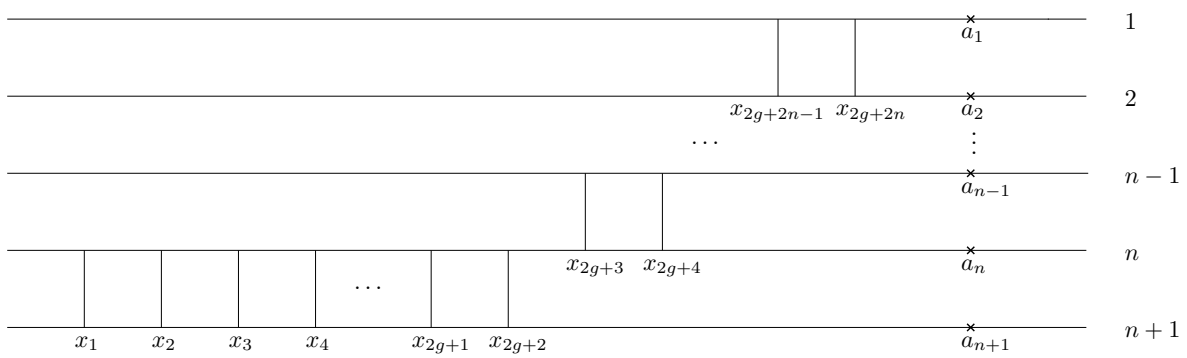

Figure 6.1: *Hurwitz diagram of the covering $\mathcal{R}_{g,n+1}$. The horizontal lines indicate copies of the Riemann sphere, and the vertical lines the ramification points of the covering $\mathcal{R}_{g,n+1}$.*

Solutions of n-NLS$^+$.

Here we construct solutions of the n-NLS$^+$ system

$$\mathrm{i}\,\frac{\partial \psi_j}{\partial t} + \frac{\partial^2 \psi_j}{\partial x^2} + 2\left(\sum_{k=1}^{n} |\psi_k|^2\right)\psi_j = 0, \qquad j = 1, \dots, n. \tag{6.3.27}$$

Let us first describe the covering and the homology basis used in the construction of the solutions.

Assume that all branch points of the covering $\mathcal{R}_{g,n+1}$ are pairwise conjugate. Denote this covering by $\mathcal{R}^+_{g,n+1}$, referring to the focusing system (6.3.27). The covering $\mathcal{R}^+_{g,n+1}$ admits two real ovals if the genus g is odd, and only one if g is even. Each of them consists of a closed contour on the covering having a real projection into the base. It is straightforward to see that the covering $\mathcal{R}^+_{g,n+1}$ is dividing (see Section 3.1): two points which have respectively a positive and a negative imaginary projection onto $\mathbb{C}$, cannot be connected by a contour which does not cross a real oval. Hence the set of fixed points of the anti-holomorphic involution τ separates the covering into two connected components.

Now let us choose the canonical homology basis such that all basic cycles belong to sheets $n+1$ and n, and such that the anti-holomorphic involution τ acts on them as in (3.2.1). By the previous topological description of $\mathcal{R}^+_{g,n+1}$, the matrix $\mathbb{H}$ in (3.2.1) reads:

$$\mathbb{H} = \begin{pmatrix} 0 & 1 & & & & \\ 1 & 0 & & & & \\ & & \ddots & & & \\ & & & 0 & 1 & \\ & & & 1 & 0 & \\ & & & & & 0 \end{pmatrix} \quad \text{if } g \text{ is odd}, \qquad \mathbb{H} = \begin{pmatrix} 0 & 1 & & \\ 1 & 0 & & \\ & & \ddots & \\ & & 0 & 1 \\ & & 1 & 0 \end{pmatrix} \quad \text{if } g \text{ is even}.$$

The canonical homology basis is described explicitly in Figure 6.2 for odd genus, and in Figure 6.3 for even genus.

As proved in the following theorem, among all coverings having a monodromy group described in Figure 6.1, only the covering $\mathcal{R}^+_{g,n+1}$ leads to algebro-geometric solutions of the focusing system (6.3.27).

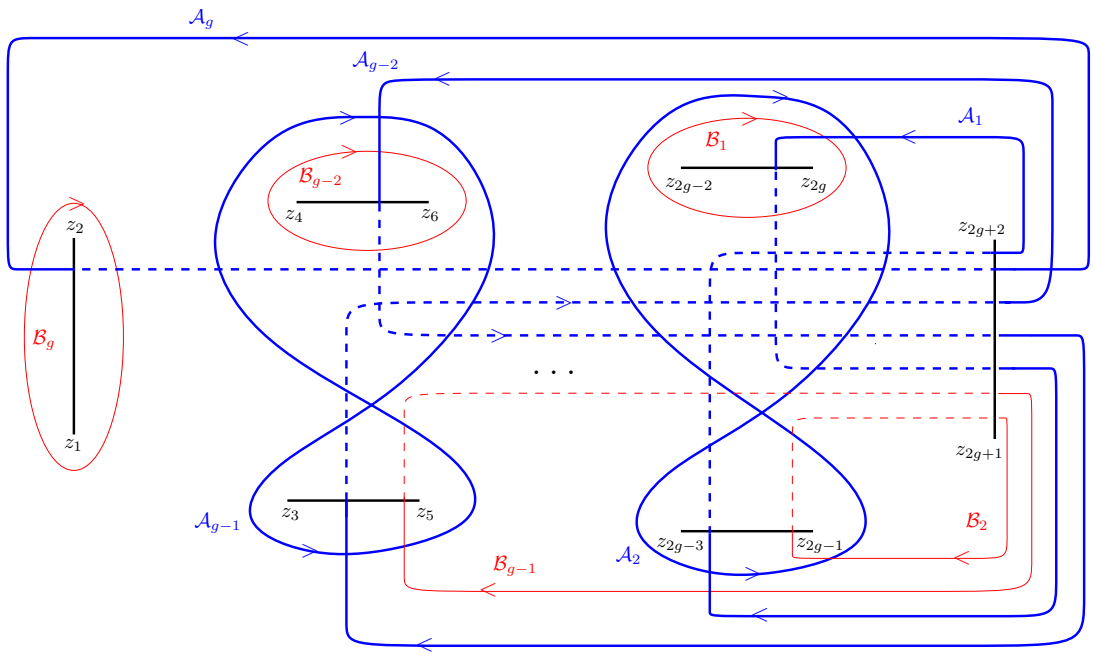

Figure 6.2: *Homology basis on the covering* $\mathcal{R}^+_{g,n+1}$ *when the genus* g *is odd. The solid line indicates the sheet* $n+1$*, and the dashed line sheet* n*.*

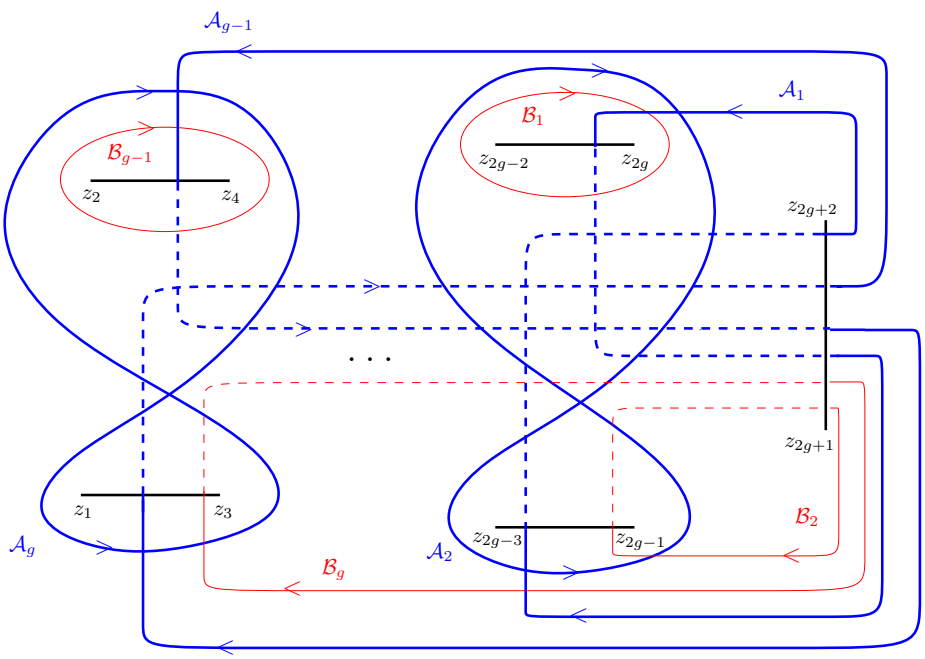

Figure 6.3: *Homology basis on the covering* $\mathcal{R}^+_{g,n+1}$ *when the genus* g *is even. The solid line indicates the sheet* $n+1$*, and the dashed line sheet* n*.*

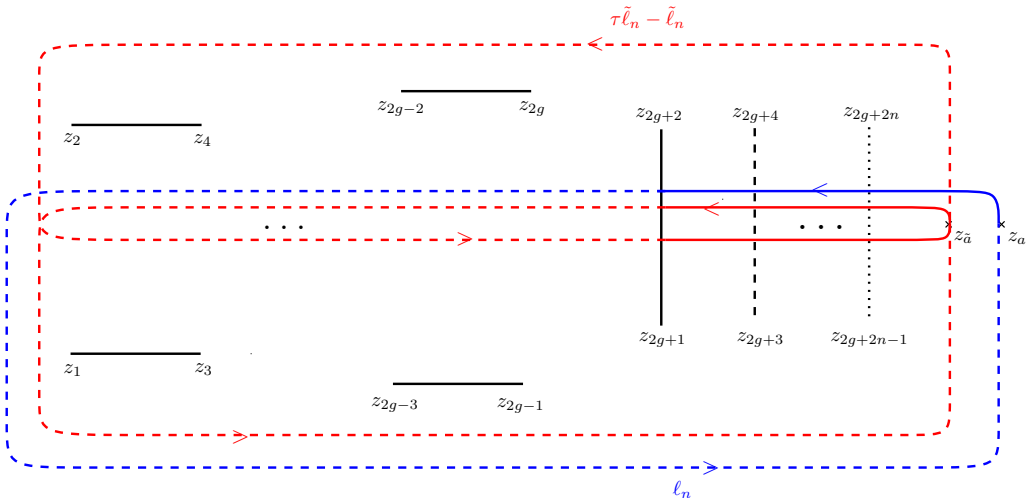

Figure 6.4: *The closed contour* $\tau\tilde{\ell}_n - \tilde{\ell}_n \in H_1\big(\mathcal{R}^+_{g,n+1} \setminus \{a_{n+1}, a_n\}\big)$ *is homologous to a closed contour which encircles the vertical cut* $[z_{2g+1}, z_{2g+2}]$, *then* $\alpha_n = (\tau\tilde{\ell}_n - \tilde{\ell}_n) \circ \ell_n = 1$.

Theorem 6.3.2. *Consider the covering* $\mathcal{R}^+_{g,n+1}$ *and the canonical homology basis discussed above. Fix* $z_a \in \mathbb{R}$ *such that* $z_a > Re(z_j)$ *for* $j = 1, \ldots, 2g+2n$. *Consider the fiber* $f^{-1}(z_a) = \{a_1, \ldots, a_{n+1}\}$ *over* z_a, *where* $a_j \in \mathcal{R}^+_{g,n+1}(\mathbb{R})$ *belongs to sheet* j *(each of the* a_j *is invariant under the involution* τ*). Let* $\mathbf{d}_R \in \mathbb{R}^g$ *and* $\theta \in \mathbb{R}$. *Then the following functions* ψ_j *for* $j = 1, \ldots, n$, *give smooth solutions of* n*-NLS*$^+$*:*

$$\psi_j(x,t) = |A_j|\, e^{\mathrm{i}\theta}\, \frac{\Theta(\mathbf{Z} - \mathbf{d}_R + \mathbf{r}_j)}{\Theta(\mathbf{Z} - \mathbf{d}_R)}\, \exp\left\{-\mathrm{i}\,(E_j\, x - F_j\, t)\right\}, \tag{6.3.28}$$

where $\mathbf{Z} = \mathrm{i}\,\mathbf{V}_{a_{n+1}}\, x + \mathrm{i}\,\mathbf{W}_{a_{n+1}}\, t$, *and the remaining notation is as in Proposition 6.3.1.*

Proof. Let us check that the conditions of the theorem imply that the functions ψ_j, $j = 1, \ldots, n$, in (6.3.14) give solutions of n-NLS^s for $s = (1, \ldots, 1)$. Since the matrix $\mathbb{H}$ associated to the covering $\mathcal{R}^+_{g,n+1}$ satisfies $\mathrm{diag}(\mathbb{H}) = 0$, and $\mathbf{d}_R \in \mathbb{R}^g$ (i.e., $\mathbf{T} = 0$ in Proposition 6.3.1), the quantity s_j defined in (6.3.16) becomes

$$s_j = \exp\left\{\mathrm{i}\pi(1 + \alpha_j)\right\}. \tag{6.3.29}$$

Let us first compute the intersection index α_n. Let $\tilde{a}_{n+1}, \tilde{a}_n \in \mathcal{R}^+_{g,n+1}(\mathbb{R})$ lie in a neighbourhood of a_{n+1} and a_n respectively such that $f(\tilde{a}_{n+1}) = f(\tilde{a}_n) = z_{\tilde{a}}$. Denote by $\tilde{\ell}_n$ an oriented contour connecting $\tilde{a}_{n+1}$ and $\tilde{a}_n$. Then the intersection index α_n between the closed contour $\tau\tilde{\ell}_n - \tilde{\ell}_n$ and the contour ℓ_n satisfies (see Figure 6.4):

$$\alpha_n = (\tau\tilde{\ell}_n - \tilde{\ell}_n) \circ \ell_n \equiv 1 \pmod 2, \tag{6.3.30}$$

which leads to $s_n = 1$. Intersection indices α_j for $j = 1, \ldots, n-1$ can be computed in the same way. Therefore

$$\alpha_1 \equiv \alpha_2 \equiv \ldots \equiv \alpha_n \equiv 1 \pmod 2,$$

which implies $s_j = 1$. By Proposition 3.4.1, smoothness of the solutions is ensured by the reality of the vector $\mathbf{Z} - \mathbf{d}_R$ and the fact that the curve is dividing. $\square$

The functions ψ_j, $j = 1, \dots, n$, given in (6.3.28) describe a family of smooth algebro-geometric solutions of the focusing multi-component NLS equation depending on $g+n$ complex parameters: $z_{2k-1} \in \mathbb{C} \setminus \mathbb{R}$ for $k = 1, \dots, g+n$; and $g+2$ real parameters: $z_a, \theta \in \mathbb{R}$, and $\mathbf{d}_R \in \mathbb{R}^g$.

Solutions of n-NLS$^-$.

Now let us construct solutions of the system n-NLS$^-$

$$\mathrm{i}\,\frac{\partial \psi_j}{\partial t} + \frac{\partial^2 \psi_j}{\partial x^2} - 2\left(\sum_{k=1}^{n} |\psi_k|^2\right)\psi_j = 0, \qquad j = 1, \dots, n. \tag{6.3.31}$$

As for the focusing case, let us first describe the covering and the homology basis used in our construction of the solutions of (6.3.31).

Assume that the branch points z_k of the covering $\mathcal{R}_{g,n+1}$ are real for $k = 1, \dots, g+2$, and that the branch points z_{2k-1}, z_{2k} are pairwise conjugate for $k = g+2, \dots, g+n$. Denote by $\mathcal{R}^-_{g,n+1}$ this covering, referring to the defocusing system (6.3.31). It is straightforward to see that such a covering is an M-curve (see Section 3.1), that is it admits a maximal number of real ovals $g+1$ with respect to the anti-holomorphic involution τ. On the other hand, it can be directly seen that $\mathcal{R}^-_{g,n+1}$ is dividing: two points which lie on the sheet $n+1$ and have respectively a positive and a negative imaginary projection onto $\mathbb{C}$ cannot be connected by a contour which does not cross a real oval.

Now let us choose the canonical homology basis such that all basic cycles belong to sheets $n+1$ and n, and which satisfies (3.2.1). Since the covering $\mathcal{R}^-_{g,n+1}$ is an M-curve, the matrix $\mathbb{H}$ involved in (3.2.1) satisfies $\mathbb{H} = 0$. Such a canonical homology basis is shown in Figure 6.5.

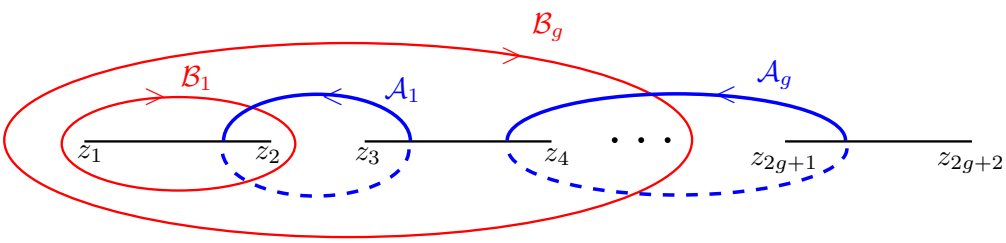

Figure 6.5: *Homology basis on the covering $\mathcal{R}^-_{g,n+1}$. The solid line indicates the sheet $n+1$, and the dashed line sheet n.*

In the following theorem, we construct algebro-geometric solutions of the defocusing system (6.3.31) associated to the covering $\mathcal{R}^-_{g,n+1}$.

Theorem 6.3.3. *Consider the covering $\mathcal{R}^-_{g,n+1}$ and the canonical homology basis discussed above. Fix $z_a \in \mathbb{R} \setminus \{z_1, \dots, z_{2g+2}\}$ such that $z_a > Re(z_j)$ for $j = 1, \dots, 2g+2n$. Consider the fiber $f^{-1}(z_a) = \{a_1, \dots, a_{n+1}\}$ over z_a, where $a_j \in \mathcal{R}^-_{g,n+1}(\mathbb{R})$ belongs to sheet j (each of the a_j is invariant under the involution τ). Let $\mathbf{d}_R \in \mathbb{R}^g$ and $\theta \in \mathbb{R}$. Then the functions ψ_j defined in (6.3.28) for $j = 1, \dots, n$ give smooth solutions of n-NLS$^-$.*

Proof. Analogously to the focusing case, one has to check that all s_j defined in (6.3.16) satisfy $s_j = -1$. Since all branch points z_k are real for $k = 1, \dots, 2g+2$, the intersection index α_n

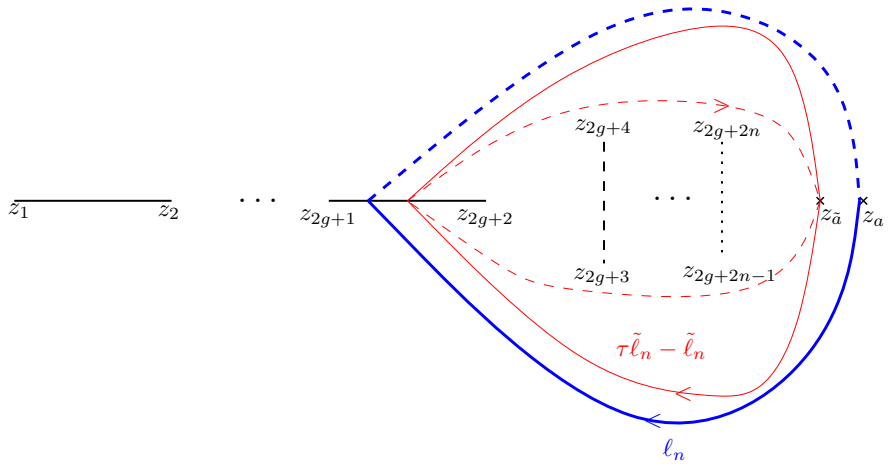

Figure 6.6: *The closed contour* $\tau\tilde{\ell}_n - \tilde{\ell}_n \in H_1\left(\mathcal{R}^-_{g,n+1} \setminus \{a_{n+1}, a_n\}\right)$ *is homologous to zero, then* $\alpha_n = (\tau\tilde{\ell}_n - \tilde{\ell}_n) \circ \ell_n = 0$.

between the closed contour $\tau\tilde{\ell}_n - \tilde{\ell}_n$ and the contour ℓ_n satisfies (see Figure 6.6)

$$\alpha_n = (\tau\tilde{\ell}_n - \tilde{\ell}_n) \circ \ell_n \equiv 0 \pmod 2, \tag{6.3.32}$$

which leads to $s_n = -1$. Intersection indices α_j for $j = 1, \ldots, n-1$ can be computed in the same way, and we get

$$\alpha_1 \equiv \alpha_2 \equiv \ldots \equiv \alpha_n \equiv 0 \pmod 2,$$

which implies $s_j = -1$. Smoothness of the solutions is ensured by the reality of the vector $\mathbf{Z} - \mathbf{d}_R$ and the fact that the curve is dividing. □

Solutions ψ_j, $j = 1, \ldots, n$, constructed here describe a family of smooth algebro-geometric solutions of the defocusing multi-component NLS equation depending on $n-1$ complex parameters: $z_{2g+2k+1} \in \mathbb{C}$ for $k = 1, \ldots, n-1$; and $3g+4$ real parameters: $z_k \in \mathbb{R}$ for $k = 1, \ldots, 2g+2$, $z_a, \theta \in \mathbb{R}$, and $\mathbf{d}_R \in \mathbb{R}^g$.

Remark 6.3.1. Smooth solutions of n-NLS^s for a vector s with mixed signs can be constructed in the same way.

6.3.4 Stationary solutions of n-NLS

It is well-known that the algebro-geometric solutions (6.3.14) on an elliptic surface describe *travelling waves*, i.e., the modulus of the corresponding solutions depends only on $x - ct$, where c is a constant. Due to the *Galilei invariance* of the multi-component NLS equation (see (6.3.11)), the invariance under transformations of the form

$$\psi_j(x,t) \longrightarrow \psi_j(x + 2\lambda\, t, t)\, \exp\left\{-\mathrm{i}\left(\lambda\, x + \lambda^2\, t\right)\right\},$$

where $\lambda = -\frac{1}{2}\, W_{a_{n+1}}\, (V_{a_{n+1}})^{-1}$, leads to stationary solutions (t-independent) in the transformed coordinates.

For arbitrary genus of the spectral curve, stationary solutions of the multi-component NLS equation are obtained from solutions (6.3.14) under the vanishing condition:

$$\mathbf{W}_{a_{n+1}} = 0. \tag{6.3.33}$$

This condition is equivalent to the existence of a meromorphic function h of degree two on $\mathcal{R}_g$, such that the point a_{n+1} is a critical point of h (this can be proved analogously to Lemma 6.3.1).

Therefore, stationary solutions of the multi-component NLS equation can be constructed from the algebro-geometric data $\{\mathcal{R}_g, f, h, z_a\}$, where:
• $\mathcal{R}_g$ is a real Riemann surface of genus g, and f is a real meromorphic function of degree $n+1$ on $\mathcal{R}_g$,
• $z_a \in \mathbb{R}$ is a non critical value of f such that $f^{-1}(z_a) = \{a_1, \dots, a_{n+1}\}$,
• h is a real meromorphic function of degree two on $\mathcal{R}_g$, and a_{n+1} is a critical point of h,
• for $j = 1, \dots, n$, local parameters k_{a_j} near a_j are chosen to be $k_{a_j}(p) = h(p) - h(a_j)$ for any point p in a neighbourhood of a_j, and $k_{a_{n+1}}(p) = (h(p) - h(a_{n+1}))^{1/2}$ for any point p in a neighbourhood of a_{n+1}.

With this choice of local parameters, we get $f(p) - z_a = \beta_j\, k_{a_j}(p) + \mu_j\, k_{a_j}(p)^2 + O\left(k_{a_j}(p)^3\right)$, for any point $p \in \mathcal{R}_g$ which lies in a neighbourhood of a_j, where $\beta_j, \mu_j \in \mathbb{R}$. Hence solutions (6.3.14) can be rewritten using this choice of local parameters and then are expressed by the use of the scalars β_j and μ_j.

Moreover, choosing a_{n+1} as a critical point of h, we get (6.3.33). In this case, the modulus of solutions (6.3.14) does not depend on the variable t.

6.3.5 Reduction of n-NLS to $(n-1)$-NLS

It is natural to wonder if starting from solutions of n-NLS we can obtain solutions of $(n-1)$-NLS for $n > 2$. Such a reduction is possible if one of the functions ψ_j solutions of n-NLS vanishes identically.

Let $\mathcal{R}^+_{g,n+1}$ be the $(n+1)$-sheeted covering introduced in Section 6.3.3; to obtain solutions of $(n-1)$-NLS$^+$ from solutions of n-NLS$^+$, we consider the following degeneration of the covering $\mathcal{R}^+_{g,n+1}$: let the branch points z_{2g+2n} and $z_{2g+2n-1}$ coalesce, in such way that the first sheet gets disconnected from the other sheets (see Figure 6.1); denote by $\mathcal{R}^+_{g,n}$ the covering obtained in this limit.

Then the normalized holomorphic differentials on $\mathcal{R}^+_{g,n+1}$ tend to normalized holomorphic differentials on $\mathcal{R}^+_{g,n}$; on the first sheet, all holomorphic differentials tend to zero. Therefore, in this limit, each component of the vector $\mathbf{V}_{a_1}$ tends to 0.

Hence by (2.3.12) and (6.3.15), the function ψ_1 tends to zero as z_{2g+2n} and $z_{2g+2n-1}$ coalesce. Functions ψ_j for $j = 2, \dots, n$ obtained in this limit give solutions of $(n-1)$-NLS$^+$ associated to the covering $\mathcal{R}^+_{g,n}$.

Remark 6.3.2. A similar degeneration produces a solution of $(n-1)$-NLS$^-$ from a solution of n-NLS$^-$. Repeating this degeneration $n-1$ times, we rediscover (see [79]) algebro-geometric solutions of the focusing (resp. defocusing) nonlinear Schrödinger equation (1.1.2) associated to a hyperelliptic curve with pairwise conjugate branch points (resp. real branch points).

6.3.6 Hyperelliptic solutions of n-NLS

In this part we construct smooth hyperelliptic theta-functional solutions of n-NLS^s. The following lemma gives an example where the vectors $\mathbf{V}_{a_1}, \ldots, \mathbf{V}_{a_{n+1}}$ defined in (2.3.3) are linearly dependent. This property ensures by Lemma 6.3.1 and Theorem 6.3.1 that we can construct hyperelliptic solutions of n-NLS^s. Let $\mathcal{R}_g$ be a hyperelliptic curve of genus $g > 0$ given in a general form by

$$\mu^2 = \prod_{k=1}^{2g+2} (\lambda - \lambda_k), \tag{6.3.34}$$

with the projection map $\pi(\lambda, \mu) \longmapsto \lambda$ of degree two on $\mathcal{R}_g$.

Lemma 6.3.2. *Let $a_j = (\lambda_{a_j}, \mu_{a_j}) \in \mathcal{R}_g$ be $n+1$ points having distinct projection, such that $\lambda_{a_j} \neq \lambda_k$, and assume $n \geq g$. Let $\gamma_{g+1}, \ldots, \gamma_n \in \mathbb{C} \setminus \{0\}$ be arbitrary constants and put $\gamma_{n+1} = 1$. Then $\det\left(\mathbf{V}_{a_1}, \ldots, \mathbf{V}_{a_g}\right) \neq 0$, and there exist $\gamma_1, \ldots, \gamma_g \in \mathbb{C} \setminus \{0\}$ such that $\sum_{k=1}^{n+1} \gamma_k \mathbf{V}_{a_k} = 0$. For $j = 1, \ldots, g$, the scalars γ_j are given by*

$$\gamma_j = -\sum_{k=g+1}^{n+1} \gamma_k \frac{\mu_{a_j}}{\mu_{a_k}} \prod_{\substack{1 \leq i \leq g \\ i \neq j}} \frac{\lambda_{a_k} - \lambda_{a_i}}{\lambda_{a_j} - \lambda_{a_i}}. \tag{6.3.35}$$

Proof. A basis of holomorphic differentials on $\mathcal{R}_g$ is given by

$$\nu = (\nu_1, \ldots, \nu_g)^t = \left(1, \lambda, \ldots, \lambda^{g-1}\right)^t \frac{\mathrm{d}\lambda}{\mu}. \tag{6.3.36}$$

Normalized holomorphic differentials $\omega = (\omega_1, \ldots, \omega_g)^t$ are obtained as follows:

$$\omega = 2\mathrm{i}\pi \left(A^t\right)^{-1} \nu, \tag{6.3.37}$$

where $A_{ij} = \int_{\mathcal{A}_i} \nu_j$. From (6.3.37) and definition (2.3.3) of the vectors $\mathbf{V}_{a_i}$ we deduce that

$$\begin{pmatrix} V_{a_1,1} & \ldots & V_{a_g,1} \\ V_{a_1,2} & \ldots & V_{a_g,2} \\ \vdots & \ldots & \vdots \\ V_{a_1,g} & \ldots & V_{a_g,g} \end{pmatrix} = 2\mathrm{i}\pi \left(A^t\right)^{-1} \begin{pmatrix} \frac{1}{\mu_{a_1}} & \ldots & \frac{1}{\mu_{a_g}} \\ \frac{\lambda_{a_1}}{\mu_{a_1}} & \ldots & \frac{\lambda_{a_g}}{\mu_{a_g}} \\ \vdots & \ldots & \vdots \\ \frac{\lambda_{a_1}^{g-1}}{\mu_{a_1}} & \ldots & \frac{\lambda_{a_g}^{g-1}}{\mu_{a_g}} \end{pmatrix}. \tag{6.3.38}$$

Since by assumptions all λ_{a_j} are distinct, equality (6.3.38) involves the linear independence of the vectors $\mathbf{V}_{a_1}, \ldots, \mathbf{V}_{a_g}$ (the determinant of the last matrix in the right hand side in (6.3.38) is a Vandermonde determinant which does not vanish). Denote by $\gamma^{(p)} := (\gamma_1, \ldots, \gamma_p)^t$. It follows that the system $\left(\mathbf{V}_{a_1}, \ldots, \mathbf{V}_{a_{n+1}}\right) \gamma^{(n+1)} = 0$, rewritten as

$$\left(\mathbf{V}_{a_1}, \ldots, \mathbf{V}_{a_g}\right) \gamma^{(g)} = -\sum_{k=g+1}^{n+1} \gamma_k \mathbf{V}_{a_k},$$

can be solved using Cramer's method. Therefore, using (6.3.38) we get, for $j = 1, \ldots, g$,

$$\gamma_j = -\sum_{k=g+1}^{n+1} \gamma_k \, \frac{\mu_{a_j}}{\mu_{a_k}} \, \frac{\mathrm{Vd}(\lambda_{a_1}, \ldots, \overbrace{\lambda_{a_k}}^{j}, \ldots, \lambda_{a_g})}{\mathrm{Vd}(\lambda_{a_1}, \ldots, \lambda_{a_g})},$$

where $\mathrm{Vd}(\lambda_{a_1}, \ldots, \lambda_{a_g}) := \prod_{1 \le i < k \le g} (\lambda_{a_k} - \lambda_{a_i})$ is the Vandermonde determinant. □

Remark 6.3.3. On the other hand, if $n < g$, the proof of Lemma 6.3.2 shows that for any points $a_1, \ldots, a_{n+1} \in \mathcal{R}_g$ having distinct projection, the vectors $\mathbf{V}_{a_1}, \ldots, \mathbf{V}_{a_{n+1}}$ cannot be linearly dependent.

Theorem 6.3.4. *Let $\mathcal{R}_g$ be a real hyperelliptic curve (6.3.34) and denote by τ an anti-holomorphic involution. Choose the canonical homology basis which satisfies (3.2.1). Take $n \ge g$ and let $a_1, \ldots, a_{n+1} \in \mathcal{R}_g(\mathbb{R})$ having distinct projection $\pi(a_j) = \lambda_{a_j}$ into the base, such that $\lambda_{a_j} \neq \lambda_k$. Denote by ℓ_j an oriented contour between a_{n+1} and a_j which does not intersect cycles of the canonical homology basis. Let $\mathbf{d}_R \in \mathbb{R}^g$, $\mathbf{T} \in \mathbb{Z}^g$, and define $\mathbf{d} = \mathbf{d}_R + \frac{\mathrm{i}\pi}{2}(diag(\mathbb{H}) - 2\,\mathbf{T})$. Take $\theta \in \mathbb{R}$ and let $\gamma_{g+1}, \ldots, \gamma_n \in \mathbb{R}$ be arbitrary constants with $\gamma_{n+1} = 1$. Put $\hat{s} = (sign(\gamma_1)\, s_1, \ldots, sign(\gamma_n)\, s_n)$ where s_j and γ_j are given in (6.3.16) and (6.3.35) respectively. Then by Lemma 6.3.2, the following functions ψ_j for $j = 1, \ldots, n$ give solutions of n-NLS$^{\hat{s}}$*

$$\psi_j(x,t) = |\gamma_j|^{1/2} \, |A_j| \, e^{\mathrm{i}\theta} \, \frac{\Theta(\mathbf{Z} - \mathbf{d} + \mathbf{r}_j)}{\Theta(\mathbf{Z} - \mathbf{d})} \, \exp\{-\mathrm{i}\,(E_j\, x - F_j\, t)\}, \tag{6.3.39}$$

where $|A_j|$ is given in (6.3.15). Here $\mathbf{r}_j = \int_{\ell_j} \omega$, and $\mathbf{Z} = \mathrm{i}\,\mathbf{V}_{a_{n+1}}\, x + \mathrm{i}\,\mathbf{W}_{a_{n+1}}\, t$, where the vectors $\mathbf{V}_{a_{n+1}}$ and $\mathbf{W}_{a_{n+1}}$ were introduced in (2.3.3). The scalars E_j, F_j are given by

$$E_j = K_1(a_{n+1}, a_j), \qquad F_j = K_2(a_{n+1}, a_j) - 2\sum_{k=1}^{n} \gamma_k \, q_1(a_{n+1}, a_k),$$

where $q_1(a_{n+1}, a_j)$, $q_2(a_{n+1}, a_j)$, $K_1(a_{n+1}, a_j)$ and $K_2(a_{n+1}, a_j)$ are respectively defined in (2.3.11), (2.3.12), (6.1.2) and (6.1.3). If $\mathcal{R}_g$ is dividing and $\mathbf{d} \in \mathbb{R}^g$, functions (6.3.39) give smooth hyperelliptic solutions of n-NLS$^{\hat{s}}$.

Example 6.3.1. *(Hyperelliptic solutions of 2-NLS$^{\hat{s}}$ in genus 2.)*
Let us construct smooth hyperelliptic theta-functional solutions of 2-NLS$^{\hat{s}}$ in genus 2, for any vector of signs $\hat{s}$. Consider the hyperelliptic curve (6.3.34) with $g = 2$ and let $a_1 = (\lambda_{a_1}, \mu_{a_1})$, $a_2 = (\lambda_{a_2}, \mu_{a_2})$ and $a_3 = (\lambda_{a_3}, \mu_{a_3})$ be three points on the curve such that $\lambda_{a_1} \neq \lambda_{a_2} \neq \lambda_{a_3}$ and $\lambda_{a_j} \neq \lambda_k$. By Lemma 6.3.2, the vectors $\mathbf{V}_{a_j}$ are related by $\mathbf{V}_{a_3} + \gamma_1 \mathbf{V}_{a_1} + \gamma_2 \mathbf{V}_{a_2} = 0$ with

$$\gamma_1 = -\frac{\mu_{a_1}}{\mu_{a_3}} \, \frac{\lambda_{a_3} - \lambda_{a_2}}{\lambda_{a_1} - \lambda_{a_2}}, \qquad \gamma_2 = -\frac{\mu_{a_2}}{\mu_{a_3}} \, \frac{\lambda_{a_3} - \lambda_{a_1}}{\lambda_{a_2} - \lambda_{a_1}}. \tag{6.3.40}$$

We consider two cases:

i) the curve has real branch points only. Let us prove that on such a curve one can construct solutions of 2-NLS$^{\hat{s}}$ for $\hat{s} = (1, -1)$, $\hat{s} = (-1, -1)$, and $\hat{s} = (-1, 1)$. Let $\lambda_1, \ldots, \lambda_6 \in \mathbb{R}$ satisfy $\lambda_1 < \ldots < \lambda_6$. First, note that in the case where a_j and a_{n+1} lie on the same sheet, or lie on different sheets, one has $\frac{\mu_{a_j}}{\mu_{a_{n+1}}}\, s_j > 0$ (see Section 6.3.3). Now assume that $\lambda_{a_3} > \lambda_{a_2} > \lambda_{a_1}$. By

(6.3.40) we deduce that $\hat{s}_1 = 1$ and $\hat{s}_2 = -1$. Hence by Theorem 6.3.4, functions (6.3.39) give smooth hyperelliptic solutions of 2-NLS$^{\hat{s}}$ where $\hat{s} = (1, -1)$. Analogously, the choice $\lambda_{a_2} > \lambda_{a_3} > \lambda_{a_1}$ leads to solutions of 2-NLS$^{\hat{s}}$ with $\hat{s} = (-1, -1)$, and the choice $\lambda_{a_2} > \lambda_{a_1} > \lambda_{a_3}$ provides solutions of 2-NLS$^{\hat{s}}$ for $\hat{s} = (-1, 1)$.

ii) the curve has all its branch points pairwise conjugate. As explained below, on such a curve one gets solutions of 2-NLS$^{\hat{s}}$ for any vector of signs $\hat{s}$. Assume that $\overline{\lambda_{2k-1}} = \lambda_{2k}$ for $k = 1, 2, 3$. First, note that if a_j and a_{n+1} lie on the same sheet, $\frac{\mu_{a_j}}{\mu_{a_{n+1}}} > 0$ and $s_j > 0$, otherwise $\frac{\mu_{a_j}}{\mu_{a_{n+1}}} < 0$ and $s_j > 0$. Following the reasoning of case i), if a_1, a_2 and a_3 lie on the same sheet, the functions (6.3.39) give smooth hyperelliptic solutions of 2-NLS$^{\hat{s}}$ with $\hat{s} = (1, -1)$, $\hat{s} = (-1, -1)$ or $\hat{s} = (-1, 1)$, depending on the projections λ_{a_j}. Now assume that a_1 and a_3 belong to the same sheet, and take a_2 on another sheet. Then, for the choice $\lambda_{a_3} > \lambda_{a_2} > \lambda_{a_1}$, the vector of signs satisfies $\hat{s} = (1, 1)$.

6.3.7 Relationship between solutions of KP1 and solutions of n-NLS

Historically, the KP equation is the first example of a system with two space variables for which it has been possible to completely solve the problem of reality of the algebro-geometric solutions.

Here we show that starting from our solutions of the multi-component NLS equation and its complexification, we can construct a subclass of complex and real solutions of the Kadomtsev-Petviashvili equation (KP1)

$$\frac{3}{4}\, u_{yy} = \left(u_t - \frac{1}{4}\,(6\, u u_x - u_{xxx}) \right)_x . \tag{6.3.41}$$

Let $\mathcal{R}_g$ be an arbitrary compact Riemann surface with marked point a, and let k_a be an arbitrary local parameter near a. Define vectors $\mathbf{V}_a$, $\mathbf{W}_a$, $\mathbf{U}_a$ as in (2.3.3) and let $\mathbf{d} \in \mathbb{C}^g$. Then, according to Krichever's theorem [96] (see also [99, 100]), the function

$$u(x, y, t) = 2\, D_a^2 \ln \Theta(\mathrm{i}\, \mathbf{V}_a\, x + \mathrm{i}\, \mathbf{W}_a\, y + \mathrm{i}\, \mathbf{U}_a\, t - \mathbf{d}) + 2\, \beta \tag{6.3.42}$$

is a solution of KP1; here the constant β is defined by the expansion near a of the normalized meromorphic differential $\Omega_a^{(2)}$ having a pole of order two at a only:

$$\Omega_a^{(2)}(p) = k_a(p)^{-2} + \beta\, k_a(p) + o(k_a(p)),$$

where p lies in a neighbourhood of a.

Let us check that if the local parameter k_a is defined by the meromorphic function f of degree $n+1$ on $\mathcal{R}_g$ as $k_a(p) = f(p) - f(a)$, then formula (6.3.42) naturally arises from our construction of solutions of the n-NLS^s system. Namely, identify a with a_{n+1}. Then, due to the fact that $\sum_{j=1}^{n+1} \mathbf{V}_{a_j} = 0$ where $\{a_1, \ldots, a_{n+1}\} = f^{-1}(z_a)$ (see Lemma 6.3.1), the solution (6.3.42) of KP1 can be rewritten as

$$u(x, y, t) = -\, 2 \sum_{j=1}^{n} D_{a_{n+1}} D_{a_j} \ln \Theta(\mathbf{z}) + 2\, \beta,$$

where $\mathbf{z} = \mathrm{i}\, \mathbf{V}_{a_{n+1}}\, x + \mathrm{i}\, \mathbf{W}_{a_{n+1}}\, y + \mathrm{i}\, \mathbf{U}_{a_{n+1}}\, t - \mathbf{d}$. Using Corollary (2.3.10) of Fay's identity, we get

$$u(x, y, t) = -\, 2 \sum_{j=1}^{n} \left(q_1(a_{n+1}, a_j) + q_2(a_{n+1}, a_j)\, \frac{\Theta(\mathbf{z} + \mathbf{r}_j)\, \Theta(\mathbf{z} - \mathbf{r}_j)}{\Theta(\mathbf{z})^2} \right) + 2\, \beta. \tag{6.3.43}$$

Now let us consider solutions ψ_j, ψ_j^* (6.3.4) of the complexified multi-component NLS equation, and make the change of variables $(x,t) \to (x,y)$ and $\mathbf{d} \to -\mathrm{i}\,\mathbf{U}_{a_{n+1}}\,t + \mathbf{d}$. Then by (6.3.43), the complex-valued solutions u (6.3.42) of KP1 and solutions ψ_j, ψ_j^* (6.3.4) of the complexified n-NLS system are related by

$$u(x,y,t) = \gamma - 2\sum_{j=1}^{n} \psi_j(x,y,t)\,\psi_j^*(x,y,t), \tag{6.3.44}$$

where

$$\gamma = -2\sum_{j=1}^{n} q_1(a_{n+1}, a_j) + 2\,\beta.$$

If we impose the reality conditions (6.3.3), we obtain real solutions of KP1 from our solutions (6.3.14) of the n-NLS^s equation:

$$u(x,y,t) = \gamma - 2\sum_{j=1}^{n} s_j\,|\psi_j(x,y,t)|^2. \tag{6.3.45}$$

Since in our construction of solutions to the multi-component NLS equation, the local parameters are defined by the meromorphic function f, complex solutions (6.3.44) and real solutions (6.3.45) of KP1 obtained in this way form only a subclass of Krichever's solutions.

6.4 Algebro-geometric solutions of the Davey-Stewartson equations

In this section we present another application of the degenerated Fay identity (6.1.1), which leads to algebro-geometric solutions of the Davey-Stewartson equations (1.2.9). Let us introduce the function $\phi := \Phi + \rho\,|\psi|^2$, where $\rho = \pm 1$, and the differential operators

$$D_1 = \partial_{xx} - \alpha^2\partial_{yy}, \quad D_2 = \partial_{xx} + \alpha^2\partial_{yy}.$$

Introduce also the characteristic coordinates

$$\xi = \frac{1}{2}(x - \mathrm{i}\alpha\,y), \quad \eta = \frac{1}{2}(x + \mathrm{i}\alpha\,y), \qquad \alpha = \mathrm{i}\,\text{or}\,1.$$

In these coordinates, the Davey-Stewartson equations (1.2.9) become

$$\begin{aligned} \mathrm{i}\,\psi_t + D_1\psi + 2\,\phi\,\psi &= 0, \\ D_2\phi + \rho\,D_1|\psi|^2 &= 0, \end{aligned} \tag{6.4.1}$$

where the differential operators D_1 and D_2 are given by

$$D_1 = \frac{1}{2}(\partial_\xi^2 + \partial_\eta^2), \quad D_2 = \partial_\xi\partial_\eta.$$

In what follows, DS1$^\rho$ denotes the Davey-Stewartson equation when $\alpha = \mathrm{i}$ (in this case ξ and η are both real), and DS2$^\rho$ the Davey-Stewartson equation when $\alpha = 1$ (in this case ξ and η are pairwise conjugate).

6.4.1 Solutions of the complexified Davey-Stewartson equations

Consider first the complexified version of the Davey-Stewartson equations:

$$\begin{aligned} \mathrm{i}\,\psi_t + \frac{1}{2}(\psi_{\xi\xi} + \psi_{\eta\eta}) + 2\,\varphi\,\psi &= 0, \\ -\mathrm{i}\,\psi_t^* + \frac{1}{2}(\psi_{\xi\xi}^* + \psi_{\eta\eta}^*) + 2\,\varphi\,\psi^* &= 0, \\ \varphi_{\xi\eta} + \frac{1}{2}((\psi\psi^*)_{\xi\xi} + (\psi\psi^*)_{\eta\eta}) &= 0, \end{aligned} \tag{6.4.2}$$

where $\varphi := \Phi + \psi\psi^*$. This system reduces to (6.4.1) under the *reality condition*:

$$\psi^* = \rho\,\overline{\psi}, \tag{6.4.3}$$

which leads to $\varphi = \phi$. Theta-functional solutions of system (6.4.2) are given by:

Theorem 6.4.1. *Let $\mathcal{R}_g$ be a compact Riemann surface of genus $g > 0$, and let $a, b \in \mathcal{R}_g$ be distinct points. Take arbitrary constants $\mathbf{d} \in \mathbb{C}^g$ and $A, \kappa_1, \kappa_2 \in \mathbb{C} \setminus \{0\}$, $h \in \mathbb{C}$. Denote by ℓ an oriented contour connecting a and b which does not intersect cycles of the canonical homology basis. Then for any $\xi, \eta, t \in \mathbb{C}$, the following functions ψ, ψ^* and φ are solutions of system (6.4.2)*

$$\begin{aligned} \psi(\xi,\eta,t) &= A\,\frac{\Theta(\mathbf{Z}-\mathbf{d}+\mathbf{r})}{\Theta(\mathbf{Z}-\mathbf{d})}\,\exp\left\{-\mathrm{i}\left(G_1\,\xi + G_2\,\eta - G_3\,\tfrac{t}{2}\right)\right\}, \\ \psi^*(\xi,\eta,t) &= -\frac{\kappa_1\kappa_2\,q_2(a,b)}{A}\,\frac{\Theta(\mathbf{Z}-\mathbf{d}-\mathbf{r})}{\Theta(\mathbf{Z}-\mathbf{d})}\,\exp\left\{\mathrm{i}\left(G_1\,\xi + G_2\,\eta - G_3\,\tfrac{t}{2}\right)\right\}, \\ \varphi(\xi,\eta,t) &= \frac{1}{2}\,(\ln\Theta(\mathbf{Z}-\mathbf{d}))_{\xi\xi} + \frac{1}{2}\,(\ln\Theta(\mathbf{Z}-\mathbf{d}))_{\eta\eta} + \frac{h}{4}. \end{aligned} \tag{6.4.4}$$

Here $\mathbf{r} = \int_\ell \omega$, where ω is the vector of normalized holomorphic differentials, and

$$\mathbf{Z} = \mathrm{i}\left(\kappa_1\mathbf{V}_a\,\xi - \kappa_2\mathbf{V}_b\,\eta + (\kappa_1^2\,\mathbf{W}_a - \kappa_2^2\,\mathbf{W}_b)\,\tfrac{t}{2}\right), \tag{6.4.5}$$

where the vectors $\mathbf{V}_a, \mathbf{V}_b$ and $\mathbf{W}_a, \mathbf{W}_b$ were introduced in (2.3.3). The scalars G_1, G_2, G_3 are given by

$$G_1 = \kappa_1\,K_1(a,b), \qquad G_2 = \kappa_2\,K_1(b,a), \tag{6.4.6}$$

$$G_3 = \kappa_1^2\,K_2(a,b) + \kappa_2^2\,K_2(b,a) + h, \tag{6.4.7}$$

and the scalars $q_2(a,b), K_1(a,b), K_2(a,b)$ are defined in (2.3.12), (6.1.2), (6.1.3) respectively.

Proof. Substitute the functions (6.4.4) in the first equation of system (6.4.2) to get

$$\begin{aligned} &\kappa_1^2\,D_a'\ln\frac{\Theta(\mathbf{Z}-\mathbf{d}+\mathbf{r})}{\Theta(\mathbf{Z}-\mathbf{d})} + \kappa_1^2\,D_a^2\ln\frac{\Theta(\mathbf{Z}-\mathbf{d}+\mathbf{r})}{\Theta(\mathbf{Z}-\mathbf{d})} + 2\,\kappa_1^2\,D_a^2\ln\Theta(\mathbf{Z}-\mathbf{d}) + G_3 - h \\ &+ \left(\kappa_1\,D_a\ln\frac{\Theta(\mathbf{Z}-\mathbf{d}+\mathbf{r})}{\Theta(\mathbf{Z}-\mathbf{d})} - G_1\right)^2 + \left(\kappa_2\,D_b\ln\frac{\Theta(\mathbf{Z}-\mathbf{d}+\mathbf{r})}{\Theta(\mathbf{Z}-\mathbf{d})} + G_2\right)^2 \\ &- \kappa_2^2\,D_b'\ln\frac{\Theta(\mathbf{Z}-\mathbf{d}+\mathbf{r})}{\Theta(\mathbf{Z}-\mathbf{d})} + \kappa_2^2\,D_b^2\ln\frac{\Theta(\mathbf{Z}-\mathbf{d}+\mathbf{r})}{\Theta(\mathbf{Z}-\mathbf{d})} + 2\,\kappa_2^2\,D_b^2\ln\Theta(\mathbf{Z}-\mathbf{d}) = 0. \end{aligned}$$

By (6.1.1), the last equality holds for any $\mathbb{Z}-\mathbf{d}\in\mathbb{C}^g$, and in particular for $\mathbb{Z}$ defined in (6.4.5). In the same way, it can be checked that functions (6.4.4) satisfy the second equation of system (6.4.2). Moreover, from (2.3.10) we get

$$(\psi\psi^*)_{\xi\xi}=\kappa_1^3\,\kappa_2\,D_a^3D_b\ln\Theta(\mathbf{Z}-\mathbf{d}),\quad (\psi\psi^*)_{\eta\eta}=\kappa_1\,\kappa_2^3\,D_aD_b^3\ln\Theta(\mathbf{Z}-\mathbf{d}).$$

Therefore, taking into account that

$$\varphi_{\xi\eta}=-\frac{1}{2}\left(\kappa_1^3\,\kappa_2\,D_a^3D_b\ln\Theta(\mathbf{Z}-\mathbf{d})+\kappa_1\,\kappa_2^3\,D_aD_b^3\ln\Theta(\mathbf{Z}-\mathbf{d})\right),$$

the functions (6.4.4) satisfy the last equation of system (6.4.2). □

The solutions (6.4.4) depend on the Riemann surface $\mathcal{R}_g$, the points $a,b\in\mathcal{R}_g$, the vector $\mathbf{d}\in\mathbb{C}^g$, the constants $\kappa_1,\kappa_2\in\mathbb{C}\setminus\{0\}$, $h\in\mathbb{C}$, and the local parameters k_a and k_b near a and b. The transformation of the local parameters given by

$$\begin{aligned}k_a&\longrightarrow\beta\,k_a+\mu_1\,k_a^2+O\left(k_a^3\right),\\ k_b&\longrightarrow\beta\,k_b+\mu_2\,k_b^2+O\left(k_b^3\right),\end{aligned}$$

where β,μ_1,μ_2 are arbitrary complex numbers ($\beta\neq0$), leads to a different family of solutions of the complexified system (6.4.2). These new solutions are obtained via the following transformations:

$$\begin{aligned}\psi(\xi,\eta,t)&\longrightarrow\psi\left(\beta\,\xi+\beta\lambda_1\,t,\beta\,\eta+\beta\lambda_2\,t,\beta^2\,t\right)\exp\left\{-\mathrm{i}\left(\lambda_1\,\xi+\lambda_2\,\eta+\left(\lambda_1^2+\lambda_2^2-\alpha\right)\tfrac{t}{2}\right)\right\},\\ \psi^*(\xi,\eta,t)&\longrightarrow\beta^2\,\psi^*\left(\beta\,\xi+\beta\lambda_1\,t,\beta\,\eta+\beta\lambda_2\,t,\beta^2\,t\right)\exp\left\{\mathrm{i}\left(\lambda_1\,\xi+\lambda_2\,\eta+\left(\lambda_1^2+\lambda_2^2-\alpha\right)\tfrac{t}{2}\right)\right\},\\ \phi(\xi,\eta,t)&\longrightarrow\beta^2\,\phi\left(\beta\,\xi+\beta\lambda_1\,t,\beta\,\eta+\beta\lambda_2\,t,\beta^2\,t\right)+\frac{\alpha}{4},\end{aligned}$$

where $\lambda_i=\kappa_i\,\mu_i\,\beta^{-1}$ for $i=1,2$, and $\alpha=h\,(1-\beta^2)$.

6.4.2 Reality condition and solutions of the DS1$^\rho$ equation

Let us consider the DS1$^\rho$ equation

$$\begin{aligned}\mathrm{i}\,\psi_t+\frac{1}{2}(\partial_\xi^2+\partial_\eta^2)\psi+2\,\phi\,\psi&=0,\\ \partial_\xi\partial_\eta\,\phi+\rho\,\frac{1}{2}(\partial_\xi^2+\partial_\eta^2)|\psi|^2&=0,\end{aligned}\tag{6.4.8}$$

where $\rho=\pm1$. Here ξ,η,t are real variables. Algebro-geometric solutions of (6.4.8) are constructed from solutions ψ,ψ^* (6.4.4) of the complexified system, under the reality condition $\psi^*=\rho\,\overline{\psi}$.

Let $\mathcal{R}_g$ be a real compact Riemann surface with an anti-holomorphic involution τ. Denote by $\mathcal{R}_g(\mathbb{R})$ the set of fixed points of the involution τ. Let us choose the homology basis satisfying (3.2.1). Then the solutions of (6.4.8) are given by:

Theorem 6.4.2. *Let $a, b \in \mathcal{R}_g(\mathbb{R})$ be distinct points with local parameters satisfying $\overline{k_a(\tau p)} = k_a(p)$ for any p in a neighbourhood of a, and $\overline{k_b(\tau p)} = k_b(p)$ for any p in a neighbourhood of b. Denote by $(\mathcal{A}, \mathcal{B}, \ell)$ the standard generators of the relative homology group $H_1(\mathcal{R}_g, \{a, b\})$ (see Section 3.3). Let $\mathbf{d}_R \in \mathbb{R}^g$, $\mathbf{T} \in \mathbb{Z}^g$, and define $\mathbf{d} = \mathbf{d}_R + \frac{\mathrm{i}\pi}{2}(diag(\mathbb{H}) - 2\,\mathbf{T})$. Moreover, take $\theta, h \in \mathbb{R}$, $\tilde{\kappa}_1, \kappa_2 \in \mathbb{R} \setminus \{0\}$ and put*

$$\kappa_1 = -\,\rho\,\tilde{\kappa}_1^2\,\kappa_2\,q_2(a,b)\,\exp\left\{\tfrac{1}{2}\,\langle \mathbb{B}\mathbf{M}, \mathbf{M}\rangle + \langle \mathbf{r} + \mathbf{d}, \mathbf{M}\rangle\right\}, \tag{6.4.9}$$

where $\mathbf{M} \in \mathbb{Z}^g$ is defined in (3.3.9). Then the following functions ψ and ϕ are solutions of the DS1$^\rho$ equation

$$\psi(\xi, \eta, t) = |A|\,e^{\mathrm{i}\theta}\,\frac{\Theta(\mathbf{Z} - \mathbf{d} + \mathbf{r})}{\Theta(\mathbf{Z} - \mathbf{d})}\,\exp\left\{-\mathrm{i}\left(G_1\,\xi + G_2\,\eta - G_3\,\tfrac{t}{2}\right)\right\}, \tag{6.4.10}$$

$$\phi(\xi, \eta, t) = \frac{1}{2}\,(\ln\Theta(\mathbf{Z} - \mathbf{d}))_{\xi\xi} + \frac{1}{2}\,(\ln\Theta(\mathbf{Z} - \mathbf{d}))_{\eta\eta} + \frac{h}{4}, \tag{6.4.11}$$

where $|A| = |\tilde{\kappa}_1\,\kappa_2\,q_2(a,b)|\,\exp\{\langle \mathbf{d}_R, \mathbf{M}\rangle\}$, and the remaining notation is as in Theorem 6.4.1.

The case where $\mathbf{V}_a + \mathbf{V}_b = 0$ and $\kappa_1 = \kappa_2$ is treated at the end of this section. It corresponds to solutions of the nonlinear Schrödinger equation.

Proof. The proof follows the lines of Section 6.3.2, where similar statements were proven for the n-NLS^s equation. Let us check that under the conditions of the theorem, the functions ψ and ψ^* (6.4.4) satisfy the reality condition (6.4.3). Take $\kappa_1, \kappa_2 \in \mathbb{R}$. First of all, invariance with respect to the anti-involution τ of the points a and b implies the reality of vector (6.4.5). Moreover, from (3.2.2) and (3.3.9) we get

$$\overline{\mathbf{r}} = -\,\mathbf{r} - 2\mathrm{i}\pi\mathbf{N} - \mathbb{B}\mathbf{M}, \tag{6.4.12}$$

where $\mathbf{N}, \mathbf{M} \in \mathbb{Z}^g$ are defined in (3.3.9) and satisfy

$$2\,\mathbf{N} + \mathbb{H}\mathbf{M} = 0. \tag{6.4.13}$$

From (6.1.1), it is straightforward to see that the scalars $K_1(a,b)$ and $K_2(a,b)$ defined by (6.1.2) and (6.1.3) satisfy

$$\overline{K_1(a,b)} = K_1(a,b) - \langle \mathbf{V}_a, \mathbf{M}\rangle, \qquad \overline{K_2(a,b)} = K_2(a,b) + \langle \mathbf{W}_a, \mathbf{M}\rangle, \tag{6.4.14}$$

which implies

$$\overline{G_1} = G_1 - \kappa_1\,\langle \mathbf{V}_a, \mathbf{M}\rangle, \quad \overline{G_2} = G_2 - \kappa_2\,\langle \mathbf{V}_b, \mathbf{M}\rangle, \quad \overline{G_3} = G_3 + \kappa_1^2\,\langle \mathbf{W}_a, \mathbf{M}\rangle + \kappa_2^2\,\langle \mathbf{W}_b, \mathbf{M}\rangle.$$

Therefore, the reality condition (6.4.3) together with (6.4.4) leads to

$$\begin{aligned} |A|^2 = -\,\rho\,\kappa_1\kappa_2\,q_2(a,b)\,&\frac{\Theta(\mathbf{Z} - \mathbf{d} - \mathbf{r})\,\Theta(\mathbf{Z} - \overline{\mathbf{d}} + \mathrm{i}\pi\,\mathrm{diag}(\mathbb{H}))}{\Theta(\mathbf{Z} - \overline{\mathbf{d}} - \mathbf{r} + \mathrm{i}\pi\,\mathrm{diag}(\mathbb{H}))\,\Theta(\mathbf{Z} - \mathbf{d})} \\ &\times \exp\left\{\tfrac{1}{2}\,\langle \mathbb{B}\mathbf{M}, \mathbf{M}\rangle + \left\langle \mathbf{r} + \overline{\mathbf{d}} - \mathrm{i}\pi\,\mathrm{diag}(\mathbb{H}), \mathbf{M}\right\rangle\right\}, \end{aligned} \tag{6.4.15}$$

taking into account the action (3.2.4) of the complex conjugation on the theta function, and the quasi-periodicity (2.2.3) of the theta function. Let us choose a vector $\mathbf{d} \in \mathbb{C}^g$ such that

$$\overline{\mathbf{d}} \equiv \mathbf{d} - \mathrm{i}\pi\,\mathrm{diag}(\mathbb{H}) \pmod{2\mathrm{i}\pi\mathbb{Z}^g + \mathbb{B}\mathbb{Z}^g},$$

which is, since $\overline{\mathbf{d}} - \mathbf{d}$ is purely imaginary, equivalent to $\overline{\mathbf{d}} = \mathbf{d} - \mathrm{i}\pi\,\mathrm{diag}(\mathbb{H}) + 2\mathrm{i}\pi\mathbf{T}$, for some $\mathbf{T} \in \mathbb{Z}^g$. Here we used the action (3.2.3) of the complex conjugation on the matrix of $\mathcal{B}$-periods $\mathbb{B}$, and the fact that $\mathbb{B}$ has a negative definite real part. Hence, the vector $\mathbf{d}$ can be written as

$$\mathbf{d} = \mathbf{d}_R + \frac{\mathrm{i}\pi}{2}(\mathrm{diag}(\mathbb{H}) - 2\,\mathbf{T}), \tag{6.4.16}$$

for some $\mathbf{d}_R \in \mathbb{R}^g$ and $\mathbf{T} \in \mathbb{Z}^g$. Therefore, all theta functions in (6.4.15) cancel and (6.4.15) becomes

$$|A|^2 = -\,\rho\,\kappa_1\kappa_2\,q_2(a,b)\,\exp\left\{\tfrac{1}{2}\,\langle\mathbb{B}\mathbf{M},\mathbf{M}\rangle + \langle\mathbf{r}+\mathbf{d},\mathbf{M}\rangle\right\}. \tag{6.4.17}$$

The reality of the right hand side of equality (6.4.17) can be deduced from formula (6.2.10) for the argument of $q_2(a,b)$. Moreover, it is straightforward to see from (6.4.16) and (6.4.13) that $\exp\{\langle\mathbf{d},\mathbf{M}\rangle\}$ is also real. Since κ_1,κ_2 are arbitrary real constants, we can choose κ_1 as in (6.4.9), which leads to

$$|A|^2 = \left(\tilde{\kappa}_1\,\kappa_2\,q_2(a,b)\,\exp\left\{\tfrac{1}{2}\,\langle\mathbb{B}\mathbf{M},\mathbf{M}\rangle + \langle\mathbf{r}+\mathbf{d},\mathbf{M}\rangle\right\}\right)^2 = |\tilde{\kappa}_1\,\kappa_2\,q_2(a,b)|^2\,\exp\left\{2\,\langle\mathbf{d}_R,\mathbf{M}\rangle\right\}. \quad \square$$

Functions ψ and ϕ given in (6.4.10) and (6.4.11) describe a family of algebro-geometric solutions of (6.4.8) depending on: a real Riemann surface $(\mathcal{R}_g,\tau)$, two distinct points $a,b \in \mathcal{R}_g(\mathbb{R})$, local parameters k_a,k_b which satisfy $\overline{k_a(\tau p)} = k_a(p)$ and $\overline{k_b(\tau p)} = k_b(p)$, and arbitrary constants $\mathbf{d}_R \in \mathbb{R}^g$, $\mathbf{T} \in \mathbb{Z}^g$, $\theta,h \in \mathbb{R}$, $\tilde{\kappa}_1,\kappa_2 \in \mathbb{R}\setminus\{0\}$. Note that because of the periodicity properties of the theta function, without loss of generality, the vector $\mathbf{T}$ can be chosen in the set $\{0,1\}^g$. The case where the Riemann surface is dividing and $\mathbf{T}=0$ is of special importance, because the related solutions are smooth, as explained in Proposition 6.3.2.

6.4.3 Reality condition and solutions of the DS2$^\rho$ equation

Let us consider the DS2$^\rho$ equation

$$\begin{aligned} &\mathrm{i}\,\psi_t + \frac{1}{2}(\partial_\xi^2 + \partial_\eta^2)\psi + 2\,\phi\,\psi = 0,\\ &\partial_\xi\partial_\eta\,\phi + \rho\,\frac{1}{2}(\partial_\xi^2 + \partial_\eta^2)|\psi|^2 = 0, \end{aligned} \tag{6.4.18}$$

where $\rho = \pm 1$. Here t is a real variable and variables ξ,η satisfy $\overline{\xi} = \eta$. Analogously to the case where ξ and η are real variables, algebro-geometric solutions of (6.4.18) are constructed from solutions ψ,ψ^* (6.4.4) of the complexified system by imposing the reality condition $\psi^* = \rho\,\overline{\psi}$.

Let $\mathcal{R}_g$ be a real compact Riemann surface with an anti-holomorphic involution τ. Let us choose the homology basis satisfying (3.2.1). Then the solutions of (6.4.18) are given by:

Theorem 6.4.3. *Let $a,b \in \mathcal{R}_g$ be distinct points such that $\tau a = b$, with local parameters satisfying $\overline{k_b(\tau p)} = k_a(p)$ for any point p in a neighbourhood of a. Denote by $(\mathcal{A},\mathcal{B},\ell)$ the standard generators of the relative homology group $H_1(\mathcal{R}_g,\{a,b\})$ (see Section 3.3). Let $\mathbf{T},\mathbf{L} \in \mathbb{Z}^g$ satisfy*

$$2\,\mathbf{T} + \mathbb{H}\mathbf{L} = \mathit{diag}(\mathbb{H}), \tag{6.4.19}$$

and define $\mathbf{d} = \frac{1}{2}\mathrm{Re}(\mathbb{B})\mathbf{L} + \mathrm{i}\mathbf{d}_I$, *for some* $\mathbf{d}_I \in \mathbb{R}^g$. *Moreover, take* $\theta, h \in \mathbb{R}$ *and* $\kappa_1, \kappa_2 \in \mathbb{C} \setminus \{0\}$ *such that* $\overline{\kappa_1} = \kappa_2$. *Let us consider the following functions* ψ *and* ϕ:

$$\psi(\xi,\eta,t) = |A|\, e^{\mathrm{i}\theta}\, \frac{\Theta(\mathbf{Z}-\mathbf{d}+\mathbf{r})}{\Theta(\mathbf{Z}-\mathbf{d})}\, \exp\left\{-\mathrm{i}\left(G_1\,\xi + G_2\,\eta - G_3\,\tfrac{t}{2}\right)\right\}, \tag{6.4.20}$$

$$\phi(\xi,\eta,t) = \frac{1}{2}\left(\ln\Theta(\mathbf{Z}-\mathbf{d})\right)_{\xi\xi} + \frac{1}{2}\left(\ln\Theta(\mathbf{Z}-\mathbf{d})\right)_{\eta\eta} + \frac{h}{4}, \tag{6.4.21}$$

where $|A| = |\kappa_1|\,|q_2(a,b)|^{1/2}\,\exp\left\{-\frac{1}{2}\langle \mathrm{Re}(\mathbf{r}), \mathbf{L}\rangle\right\}$. *Then,*

1. *if* ℓ *intersects the set of real ovals of* $\mathcal{R}_g$ *only once, and if this intersection is transversal, functions* ψ *and* ϕ *are solutions of DS2*$^\rho$ *with* $\rho = e^{\mathrm{i}\pi\langle \mathbf{N},\mathbf{L}\rangle}$,
2. *if* ℓ *does not cross any real oval, functions* ψ *and* ϕ *are solutions of DS2*$^\rho$ *with* $\rho = -\,e^{\mathrm{i}\pi\langle \mathbf{N},\mathbf{L}\rangle}$,

where $\mathbf{N} \in \mathbb{Z}^g$ *is defined in (3.3.1), and the remaining notation is as in Theorem 6.4.1.*

Proof. Analogously to the proof of Theorem 6.4.2, let us check that under the conditions of the theorem, the functions ψ and ψ^* (6.4.4) satisfy the reality condition (6.4.3). First of all, due to the fact that points a and b are interchanged by τ, the vector $\mathbf{Z}$ (6.4.5) satisfies

$$\overline{\mathbf{Z}} = -\,\mathbf{Z}. \tag{6.4.22}$$

In fact, using the expansion (2.3.3) of the normalized holomorphic differentials ω_j near a we get

$$\overline{\tau^*\omega_j}(a)(p) = \left(\overline{V_{b,j}} + \overline{W_{b,j}}\, k_a(p) + o(k_a(p))\right)\, \mathrm{d}k_a(p),$$

for any point p in a neighbourhood of a. Then by (3.2.2), the vectors $\mathbf{V}_a, \mathbf{V}_b$ and $\mathbf{W}_a, \mathbf{W}_b$ appearing in the vector $\mathbf{Z}$ satisfy

$$\overline{\mathbf{V}_a} = -\mathbf{V}_b, \quad \overline{\mathbf{W}_a} = -\mathbf{W}_b, \tag{6.4.23}$$

which leads to (6.4.22). From (3.2.2) and (3.3.1) we get

$$\overline{\mathbf{r}} = \mathbf{r} - 2\mathrm{i}\pi\mathbf{N}, \tag{6.4.24}$$

where $\mathbf{N} \in \mathbb{Z}^g$ is defined in (3.3.1). By Proposition 6.2.2, the scalar $q_2(a,b)$ is real. From (6.1.1), it is straightforward to see that the scalars $K_1(a,b)$ and $K_2(a,b)$, defined in (6.1.2) and (6.1.3), satisfy

$$\overline{K_1(a,b)} = K_1(b,a), \qquad \overline{K_2(a,b)} = K_2(b,a),$$

which leads to $\overline{G_1} = G_2$ and $G_3 \in \mathbb{R}$. Therefore, the reality condition (6.4.3) together with (6.4.4) lead to

$$|A|^2 = -\,\rho\,|\kappa_1|^2\, q_2(a,b)\, \frac{\Theta(\mathbf{Z}-\mathbf{d}-\mathbf{r})\,\Theta(\mathbf{Z}+\overline{\mathbf{d}}+\mathrm{i}\pi\,\mathrm{diag}(\mathbb{H}))}{\Theta(\mathbf{Z}+\overline{\mathbf{d}}-\mathbf{r}+\mathrm{i}\pi\,\mathrm{diag}(\mathbb{H}))\,\Theta(\mathbf{Z}-\mathbf{d})}, \tag{6.4.25}$$

taking into account (3.2.4). Let us choose a vector $\mathbf{d} \in \mathbb{C}^g$ such that

$$\overline{\mathbf{d}} = -\,\mathbf{d} - \mathrm{i}\pi\,\mathrm{diag}(\mathbb{H}) + 2\mathrm{i}\pi\mathbf{T} + \mathbb{B}\mathbf{L},$$

for some vectors $\mathbf{T}, \mathbf{L} \in \mathbb{Z}^g$. The reality of vector $\overline{\mathbf{d}} + \mathbf{d}$ together with (3.2.3) imply

$$\mathbf{d} = \frac{1}{2}\,\mathrm{Re}(\mathbb{B})\mathbf{L} + \mathrm{i}\mathbf{d}_I \tag{6.4.26}$$

for some $\mathbf{d}_I \in \mathbb{R}^g$, where $2\,\mathbf{T} + \mathbb{H}\mathbf{L} = \mathrm{diag}(\mathbb{H})$. With this choice of vector $\mathbf{d}$, (6.4.25) becomes

$$|A|^2 = -\,\rho\,|\kappa_1|^2\,q_2(a,b)\,e^{-\langle \mathbf{r},\mathbf{L}\rangle}. \tag{6.4.27}$$

Moreover, from (6.4.24) we deduce that equality (6.4.27) holds only if

$$\rho = -\,\mathrm{sign}(q_2(a,b))\,e^{-\mathrm{i}\pi\langle \mathbf{N},\mathbf{L}\rangle}.$$

The sign of $q_2(a,b)$ in the case where $\tau a = b$ is given in Proposition 6.2.2, which completes the proof. □

Corollary 6.4.1. *From Theorem 6.4.3 we deduce that:*

1. *if $\mathcal{R}_g$ is dividing and each component of the vector $\mathbf{L}$ is even, functions (6.4.20) and (6.4.21) are solutions of DS2$^+$,*

2. *if $\mathcal{R}_g$ does not have real oval and each component of the vector $\mathbf{L}$ is even, functions (6.4.20) and (6.4.21) are solutions of DS2$^-$.*

Remark 6.4.1. To construct solutions associated to non-dividing Riemann surfaces, we first observe from (6.4.19) that all components of the vector $\mathbf{L}$ cannot be even, since for non-dividing Riemann surfaces the vector $\mathrm{diag}(\mathbb{H})$ contains odd coefficients (see Section 3.2). In this case, the vector $\mathbf{N}$ has to be computed to determine the sign ρ in Theorem 6.4.3. This vector $\mathbf{N}$ is defined by the action of τ on the relative homology group $H_1(\mathcal{R}_g, \{a,b\})$ (see (3.3.1)). It follows that we do not have a general expression for this vector.

To ensure the smoothness of solutions (6.4.20) and (6.4.21) for all complex conjugate ξ, η, and $t \in \mathbb{R}$, the function $\Theta(\mathbf{Z} - \mathbf{d})$ of the variables ξ, η, t must not vanish. Following the work by Dubrovin and Natanzon [51] on smoothness of algebro-geometric solutions of the Kadomtsev-Petviashvili equation (KP1), in the case where $\mathcal{R}_g$ admits real ovals we get

Proposition 6.4.1. *Functions (6.4.20) and (6.4.21) are smooth solutions of DS2$^+$ if the curve is an M-curve and $\mathbf{d} \in \mathrm{i}\mathbb{R}^g$. Assume that the curve admits real ovals and functions (6.4.20), (6.4.21) are smooth solutions of DS2$^\rho$ for any vector $\mathbf{d}$ in a component $\tilde{T}_v$ (3.4.6) of the Jacobian, then the curve is an M-curve, $\mathbf{d} \in \mathrm{i}\mathbb{R}^g$ and $\rho = +1$.*

Proof. By (6.4.22) and (6.4.26) the vector $\mathbf{Z} - \mathbf{d}$ belongs to the set S_2 introduced in (3.4.3). Hence by Proposition 3.4.2, the solutions are smooth if the curve is an M-curve and $\mathbf{Z} - \mathbf{d} \in \mathrm{i}\mathbb{R}^g$ which implies $\mathbf{d} \in \mathrm{i}\mathbb{R}^g$ by (6.4.22) (and therefore $\mathbf{L} = \mathbf{T} = 0$). □

Remark 6.4.2. Smoothness of the solutions to the DS2$^-$ equation was investigated in [112]. It is proved that the obtained solutions are smooth if and only if the associated Riemann surface does not have real oval, and if there are no pseudo-real functions of degree $g-1$ on it (i.e., a function which satisfies $\overline{f(\tau p)} = -f(p)^{-1}$).

6.4.4 Reduction of the DS1$^\rho$ equation to the NLS equation

Solutions of the nonlinear Schrödinger equation (1.1.2) can be derived from solutions of the Davey-Stewartson equations, when the associated Riemann surface is hyperelliptic.

Proposition 6.4.2. *Let $\mathcal{R}_g$ be a hyperelliptic curve of genus $g > 0$ which admits an anti-holomorphic involution τ. Denote by σ the hyperelliptic involution defined on $\mathcal{R}_g$. Let $a, b \in \mathcal{R}_g(\mathbb{R})$ with local parameters satisfying $\overline{k_a(\tau p)} = k_a(p)$ for p near a, and $\overline{k_b(\tau p)} = k_b(p)$ for p near b. Moreover, assume that $\sigma a = b$ and $k_a(p) = k_b(\sigma p)$ for p near a. Then, taking $\kappa_1 = \kappa_2 = 1$, the function ψ defined in (6.4.10) is solution of the equation*

$$\mathrm{i}\,\psi_t + \psi_{\xi\xi} + 2\left(\rho\,|\psi|^2 + q_1(a,b) + \frac{h}{4}\right)\psi = 0, \tag{6.4.28}$$

which can be transformed to the NLS$^\rho$ equation

$$\mathrm{i}\,\tilde{\psi}_t + \tilde{\psi}_{\xi\xi} + 2\rho\,|\tilde{\psi}|^2\,\tilde{\psi} = 0,$$

by the substitution

$$\tilde{\psi}(\xi,t) = \psi(\xi,t)\,\exp\left\{-2\mathrm{i}\left(q_1(a,b) + \tfrac{h}{4}\right)t\right\}.$$

If all branch points of $\mathcal{R}_g$ are real, $\tilde{\psi}$ is a smooth solution of NLS$^-$. If they are all pairwise conjugate, $\tilde{\psi}$ is a smooth solution of NLS$^+$.

Proof. If $a, b \in \mathcal{R}_g$ are such that $\sigma a = b$ and if the local parameters satisfy $k_a(p) = k_b(\sigma p)$, one has

$$\mathbf{V}_a + \mathbf{V}_b = 0, \qquad \mathbf{W}_a + \mathbf{W}_b = 0. \tag{6.4.29}$$

To verify (6.4.29), we use the action $\sigma\mathcal{A}_k = -\mathcal{A}_k$ of the involution σ on the $\mathcal{A}$-cycles of the homology basis. Hence by (2.1.9) we have

$$2\mathrm{i}\pi\delta_{jk} = \int_{\sigma\mathcal{A}_k} \sigma^*\omega_j = -\int_{\mathcal{A}_k} \sigma^*\omega_j,$$

for $j, k = 1, \ldots, g$. It follows that the holomorphic differential $-\sigma^*\omega_j$ satisfies the normalization condition (2.1.9), which implies, by virtue of uniqueness of the normalized holomorphic differentials,

$$\sigma^*\omega_j = -\,\omega_j, \tag{6.4.30}$$

for $j = 1, \ldots, g$. Using (2.3.3) we obtain

$$\begin{aligned}\sigma^*\omega_j(a)(p) &= (V_{b,j} + W_{b,j}\,k_b(\sigma p) + o(k_b(\sigma p)))\,\mathrm{d}k_b(\sigma p)\\ &= (V_{b,j} + W_{b,j}\,k_a(p) + o(k_a(p)))\,\mathrm{d}k_a(p),\end{aligned}$$

for any p in a neighbourhood of a, which by (6.4.30) implies (6.4.29).

Therefore, when the Riemann surface associated to solutions of DS1$^\rho$ is hyperelliptic, assuming that a and b satisfy $\sigma a = b$, and $\kappa_1 = \kappa_2 = 1$, by (6.4.29) and (2.3.10), under the reality condition $\psi^* = \rho\,\overline{\psi}$, the function ϕ in (6.4.11) satisfies

$$\phi(\xi,\eta,t) = \rho\,|\psi|^2 + q_1(a,b) + \frac{h}{4}.$$

Hence the function ψ (6.4.10) becomes solution of equation (6.4.28), with $\rho = \pm 1$ depending on the reality of the branch points, as explained in Section 6.3.3. □

Solutions of the NLS equation obtained in this way coincide with those in [23].

Chapter 7

Degeneracy of algebro-geometric solutions

We present new solutions in terms of elementary functions of the multi-component nonlinear Schrödinger equations (6.3.1) and known solutions of the Davey-Stewartson equations (6.4.1) as multi-soliton, breather, dromion and lump solutions. These solutions are given in a simple determinantal form and are obtained as limiting cases in suitable degenerations of previously derived algebro-geometric solutions. In particular we present for the first time breather and rational breather solutions of the multi-component nonlinear Schrödinger equations.

The chapter is organized as follows: Section 7.1 provides technical tools for the degeneration of Riemann surfaces. We present a method which allows to degenerate algebro-geometric solutions associated to an arbitrary Riemann surface that can be applied to general integrable equations. In Section 7.2 solutions in terms of elementary functions to the complexified n-NLS equation are derived by degenerating algebro-geometric solutions; for an appropriate choice of the parameters one gets multi-solitonic solutions, and for the first time breather and rational breather solutions to the multi-component NLS equation. In Section 7.3 a similar program is carried out for the DS equations; well known solutions as multi-solitons, dromion or lump are rediscovered from an algebro-geometric approach.

7.1 Fay's identity and degenerate Riemann surfaces

It is well known that solutions in terms of theta functions are almost periodic due to the periodicity properties of the theta functions. In the limit when the Riemann surface degenerates to a surface of genus zero, periods of the surface diverge, and the theta series breaks down to elementary functions. Whereas this procedure is well-known in the case of a hyperelliptic surface, i.e., a two-sheeted branched covering of the Riemann sphere, where such a degeneration consists in colliding branch points pairwise, it has not been applied so far to theta-functional solutions on non-hyperelliptic surfaces.

We present here a method to treat this case based on the uniformization theorem for Riemann surfaces. In particular, we show that the theta function tends to a finite sum of exponentials in the limit when the arithmetic genus of the associated Riemann surface drops to zero, and explicitly provide the quantities (independent of the vector $\mathbf{z}$) appearing in identities (2.3.10) and (6.1.1) in this limit. As illustrated in Section 7.2 and 7.3, particular solutions of n-NLS

and DS such as multi-solitons, well known in the theory of soliton equations, arise from such degenerations of algebro-geometric solutions.

7.1.1 Uniformization map and degeneration to genus zero

Let us first recall some techniques used for degenerating Riemann surfaces (see [60] for more details). There exist basically two ways for degenerating a Riemann surface by pinching a cycle: a cycle homologous to zero in the first case, and a cycle non-homologous to zero in the second case. The first degeneration leads to two Riemann surfaces whose genera add up to the genus of the pinched surface, whereas the limiting situation for the second degeneration is one Riemann surface of genus $g-1$ with two points identified, g being the genus of the non-degenerated surface. In both cases, locally one can identify the pinched region to a hyperboloid

$$y^2 = x^2 - \epsilon, \tag{7.1.1}$$

where $\epsilon > 0$ is a small parameter, such that the vanishing cycle coincides with the homology class of the closed countour around the cut $[-\sqrt{\epsilon}, \sqrt{\epsilon}]$ in the x-plane. In what follows, we deal with the degeneration of the second type and make consecutive pinches until the surface degenerates to genus zero.

To degenerate the Riemann surface $\mathcal{R}_g$ of genus g into a Riemann surface $\mathcal{R}_0$ of genus zero, we pinch all $\mathcal{A}_i$-cycles into double points. After desingularization one gets $\mathcal{R}_0$, and each double point corresponds to two different points on $\mathcal{R}_0$, denoted by u_i and v_i for $i = 1, \ldots, g$. In this limit, holomorphic normalized differentials ω_i become normalized differentials of the third kind with poles at u_i and v_i. Note that the normalized differential of the second kind $\Omega_a^{(N)}$ with a pole of order $N > 1$ at a remains a differential of the second kind with the same order of the pole after degeneration to genus zero. We keep the same notation for the differential of the second kind on the degenerated surface.

The compact Riemann surface $\mathcal{R}_0$ of genus zero is conformally equivalent to the Riemann sphere with the coordinate w. This mapping between $\mathcal{R}_0$ and the w-sphere is called the uniformization map and we denote it by $w(p) = w$ for any $p \in \mathcal{R}_0$. Therefore, in what follows we let $\mathcal{R}_0$ stand also for the Riemann sphere with the coordinate w.

Meromorphic differentials on $\mathcal{R}_0$ can be constructed using the fact that in genus zero, such differentials are entirely defined by their behaviors near their singularities. This leads to the following third and second kind differentials on $\mathcal{R}_0$.

- *Differentials of the third kind:*

$$\Omega_{v_i - u_i} = \left(\frac{1}{w - w_{v_i}} - \frac{1}{w - w_{u_i}} \right) \mathrm{d}w. \tag{7.1.2}$$

- *Differentials of the second kind:*

$$\Omega_a^{(2)} = \frac{1}{k_a'(w_a)} \frac{\mathrm{d}w}{(w - w_a)^2}, \tag{7.1.3}$$

where k_a is a local parameter in a neighbourhood of $w_a \in \mathcal{R}_0$ and the prime denotes the derivative with respect to the argument. This is the differential on $\mathcal{R}_0$, obtained from $\Omega_a^{(2)}$ (2.1.6) defined on $\mathcal{R}_g$, in the limit as the surface $\mathcal{R}_g$ degenerates to $\mathcal{R}_0$. The factor $(k_a'(w_a))^{-1}$ ensures that the biresidue of $\Omega_a^{(2)}$ with respect to the local parameter k_a is 1 as before the degeneration.

7.1.2 Degenerate theta function

To study the theta function with zero characteristic in the limit when the genus tends to zero, let us first analyse the behavior of the matrix $\mathbb{B}$ of $\mathcal{B}$-periods of the normalized holomorphic differentials. Since holomorphic normalized differentials ω_i become differentials of the third kind with poles at u_i and v_i, for a small parameter $\epsilon > 0$, elements $(\mathbb{B})_{ik}$ of the matrix $\mathbb{B}$ have the following behavior:

$$\begin{aligned}(\mathbb{B})_{ik} &= \int_{u_i}^{v_i} \Omega_{v_k-u_k} + O(\epsilon), \qquad i \neq k, \\ (\mathbb{B})_{kk} &= \ln \epsilon + O(1).\end{aligned} \tag{7.1.4}$$

Therefore, the real parts of diagonal terms of the Riemann matrix tend to $-\infty$ when ϵ tends to zero, that is when the Riemann surface degenerates into the Riemann surface $\mathcal{R}_0$. It follows that the theta function (2.2.1) with zero characteristic tends to one, since only the term corresponding to the vector $\mathbf{m} = 0$ in the series may give a non-zero contribution.

To get non constant solutions of (6.3.1) and (6.4.1) after the degeneration of the Riemann surface, let us write the argument of the theta-function in the form $\mathbf{Z} - \mathbf{D}$, where $\mathbf{D}$ is a vector with components $D_k = (1/2)\,(\mathbb{B})_{kk} + d_k$, for some $d_k \in \mathbb{C}$ independent of ϵ. Hence for any $\mathbf{Z} \in \mathbb{C}^g$ one gets

$$\lim_{\epsilon\to 0} \Theta(\mathbf{Z} - \mathbf{D}) = \sum_{\mathbf{m}\in\{0,1\}^g} \exp\left\{ \sum_{1\le i<k\le g} (\mathbb{B})_{ik}\, m_i m_k + \sum_{k=1}^{g} m_k\,(Z_k - d_k) \right\}. \tag{7.1.5}$$

Here we use the same notation for the quantities $(\mathbb{B})_{ik}$ on the degenerated surface. The expression in the right hand side of (7.1.5) can be put into a determinantal form (see Proposition 7.1.1 below) which will be used in the whole chapter. This determinantal form can be obtained from the following representation of the components $(\mathbb{B})_{ik}$ after degeneration, obtained from (7.1.2) and (7.1.4),

$$(\mathbb{B})_{ik} = \ln\left\{ \frac{w_{v_i} - w_{v_k}}{w_{v_i} - w_{u_k}}\, \frac{w_{u_i} - w_{u_k}}{w_{u_i} - w_{v_k}} \right\}. \tag{7.1.6}$$

Hence, following [113] one gets:

Proposition 7.1.1. *For any $\mathbf{z} \in \mathbb{C}^g$, the following holds:*

$$\sum_{\mathbf{m}\in\{0,1\}^g} \exp\left\{ \sum_{1\le i<k\le g} (\mathbb{B})_{ik}\, m_i m_k + \sum_{k=1}^{g} m_k\, z_k \right\} = \det(\mathbb{T}), \tag{7.1.7}$$

where $\mathbb{T}$ is a $g \times g$ matrix with entries given by

$$(\mathbb{T})_{ik} = \delta_{i,k} + \frac{w_{v_i} - w_{u_i}}{w_{v_i} - w_{u_k}}\, e^{\frac{1}{2}(z_i + z_k)}. \tag{7.1.8}$$

Proof. The proof is carried out by comparing the coefficient of $\exp\{z_{k_1} + \ldots + z_{k_n}\}$ in the left and right-hand side of (7.1.7), where $k_1, \ldots, k_n$ are n different numbers taken from $1, \ldots, g$. Due to the symmetry property of the left-hand side in (7.1.7) with respect to the variables z_k, however,

it is sufficient to choose $k_1 = 1, \ldots, k_n = n$. Denote the coefficient of the term $\exp\{z_{k_1} + \ldots + z_{k_n}\}$ on the left-hand side of (7.1.7) by R_1. This term arises by taking $m_k = 1$ for $k = 1, \ldots, n$ and $m_k = 0$ for $k = n+1, \ldots, g$, and has the form:

$$R_1 = \exp\left\{ \sum_{1 \le i < k \le n} (\mathbb{B})_{ik} \right\}.$$

On the other hand, let R_2 be the corresponding coefficient on the right-hand side of (7.1.7). Since

$$\det(\mathbb{T}) = e^{\sum_{j=1}^{g} z_j} \det\left(\left\| \delta_{i,k}\, e^{-z_i} + \frac{w_{v_i} - w_{u_i}}{w_{v_i} - w_{u_k}} \right\|_{1 \le i,k \le g} \right),$$

we obtain

$$R_2 = \det\left(\left\| \frac{w_{v_i} - w_{u_i}}{w_{v_i} - w_{u_k}} \right\|_{1 \le i,k \le n} \right) = \prod_{j=1}^{n} (w_{v_j} - w_{u_j}) \det\left(\left\| \frac{1}{w_{v_i} - w_{u_k}} \right\|_{1 \le i,k \le n} \right).$$

By virtue of the formula for the Cauchy determinant:

$$\det\left(\left\| \frac{1}{w_{v_i} - w_{u_k}} \right\|_{1 \le i,k \le n} \right) = (-1)^{\frac{n(n-1)}{2}} \frac{\prod_{1 \le i < k \le n} (w_{v_k} - w_{v_i})(w_{u_k} - w_{u_i})}{\prod_{i,k=1}^{n} (w_{v_i} - w_{u_k})},$$

R_2 becomes

$$R_2 = \prod_{1 \le i < k \le n} \frac{(w_{v_k} - w_{v_i})(w_{u_k} - w_{u_i})}{(w_{u_k} - w_{v_i})(w_{v_k} - w_{u_i})} = \exp\left\{ \sum_{1 \le i < k \le n} (\mathbb{B})_{ik} \right\} = R_1,$$

which completes the proof. □

7.1.3 Constants in the limit

The next step is to give explicitly the quantities (independent of the vector $\mathbf{z}$) appearing in (2.3.10) and (6.1.1), i.e., $\mathbf{V}_a, \mathbf{W}_a, \mathbf{r} = \int_a^b \omega, q_2$, etc, after the degeneration to genus zero. We use the same notation for these quantities on the degenerated surface. For any distinct points $a, b \in \mathcal{R}_0$, it follows from (2.3.3) and (7.1.2) that:

$$V_{a,k} = \frac{1}{k_a'(w_a)} \left(\frac{1}{w_a - w_{v_k}} - \frac{1}{w_a - w_{u_k}} \right), \tag{7.1.9}$$

$$W_{a,k} = \frac{1}{k_a'(w_a)^2} \left(-\frac{1}{(w_a - w_{v_k})^2} + \frac{1}{(w_a - w_{u_k})^2} \right) - \frac{k_a''(w_a)}{k_a'(w_a)^2} V_{a,k}, \tag{7.1.10}$$

$$r_k = \ln\left\{ \frac{w_b - w_{v_k}}{w_b - w_{u_k}} \frac{w_a - w_{u_k}}{w_a - w_{v_k}} \right\}, \tag{7.1.11}$$

for $k = 1, \ldots, g$. Moreover, from the integral representation (6.2.1) of $q_2(a,b)$, using (7.1.2) one gets

$$q_2(a,b) = \frac{1}{k'(w_a)k'(w_b)(w_a - w_b)^2}\,. \tag{7.1.12}$$

Putting $\mathbf{z} = 0$ in (2.3.10) and taking the limit $\epsilon \to 0$ leads to

$$q_1(a,b) = -\,q_2(a,b), \tag{7.1.13}$$

due to the fact that the theta function tends to one and that its partial derivatives tend to zero. To compute the scalar $K_1(a,b)$ in the limit, let us first prove the following lemma:

Lemma 7.1.1. *Let a, b be distinct points on a compact Riemann surface $\mathcal{R}_g$ of genus $g > 0$. Denote by k_a and k_b local parameters in a neighbourhood of a and b respectively. Then the scalar $K_1(a,b)$ defined in (6.1.2) admits the following integral representation:*

$$K_1(a,b) = \lim_{\tilde{a}\to a}\left[\int_c^{\tilde{a}} \Omega_a^{(2)}(p) + \frac{1}{k_a(\tilde{a})}\right] - \int_c^b \Omega_a^{(2)}(p), \tag{7.1.14}$$

where c is an arbitrary point on $\mathcal{R}_g$.

Proof. Let us denote by k_x a local parameter in a neighbourhood of a point $x \in \mathcal{R}_g$. To prove (7.1.14), recall that (see (2.2.15))

$$\int_c^{\tilde{a}} \Omega_a^{(2)}(p) = \partial_{k_q} \ln \Theta[\delta]\big(\textstyle\int_q^{\tilde{a}}\big)\Big|_{q=a} - \gamma, \tag{7.1.15}$$

where $\gamma = \partial_{k_q} \ln \Theta[\delta](\int_q^c)\Big|_{q=a}$. Since δ is a non-singular odd characteristic, one has

$$\Theta[\delta]\big(\textstyle\int_q^{\tilde{a}}\big) = \gamma_1\,(k_a(\tilde{a}) - k_a(q)) + \frac{\gamma_2}{2}\,(k_a(\tilde{a}) - k_a(q))^2 + o\left((k_a(\tilde{a}) - k_a(q))^2\right) \tag{7.1.16}$$

for any $\tilde{a}$ and q in a neighbourhood of a, where $\gamma_1 \neq 0$. From (7.1.15) and (7.1.16) we deduce that

$$\int_c^{\tilde{a}} \Omega_a^{(2)}(p) = -\,\frac{1}{k_a(\tilde{a})} + \frac{1}{2}\,\frac{\gamma_2}{\gamma_1} - \gamma + O(k_a(\tilde{a})). \tag{7.1.17}$$

Moreover, by (7.1.16) it can be seen that

$$\gamma_1 = -\,\partial_{k_q}\Theta[\delta]\big(\textstyle\int_q^{\tilde{a}}\big)\Big|_{q=\tilde{a}} = D_{\tilde{a}}\,\Theta[\delta](0), \tag{7.1.18}$$

$$\gamma_2 = \partial_{k_q}^2\Theta[\delta]\big(\textstyle\int_q^{\tilde{a}}\big)\Big|_{q=\tilde{a}} = D'_{\tilde{a}}\,\Theta[\delta](0), \tag{7.1.19}$$

where we used the fact that $D_{\tilde{a}}^2\,\Theta[\delta](0) = 0$. Combining (7.1.17) with (7.1.18) and (7.1.19), the right hand side in (7.1.14) becomes

$$\frac{1}{2}\,\frac{D'_a\,\Theta[\delta](0)}{D_a\,\Theta[\delta](0)} + D_a \ln \Theta[\delta]\big(\textstyle\int_a^b\big)\,.$$

The proof is completed taking into account the definition (6.1.2) of $K_1(a,b)$. □

Therefore, from (7.1.14) and (7.1.3) we deduce that

$$K_1(a,b) = \frac{1}{k'(w_a)(w_b - w_a)} - \frac{1}{2}\frac{k''(w_a)}{k'(w_a)^2}\,. \tag{7.1.20}$$

Finally, taking the limit $\epsilon \to 0$ in (6.1.1) one gets

$$K_2(a,b) = -\Big(K_1(a,b)\Big)^2. \tag{7.1.21}$$

7.2 Degenerate algebro-geometric solutions of n-NLS

As mentioned in Section 6.3.1, one way to construct solutions of (6.3.1) is first to solve its complexified version (6.3.2) and impose reality conditions (6.3.3). Algebro-geometric solutions of the complexified system were obtained in Theorem 6.3.1. Recall that the proof of this theorem is based on the following identity:

$$\sum_{k=1}^{n+1} \mathbf{V}_{a_k} = 0, \tag{7.2.1}$$

which is satisfied by the vectors $\mathbf{V}_{a_k}$ associated to the fiber $f^{-1}(z_a) = \{a_1, \ldots, a_{n+1}\}$ over $z_a \in \mathbb{CP}^1$. We shall use this relation to construct solutions of (6.3.1) in terms of elementary functions.

Remark 7.2.1. The relationship between solutions of the KP1 equation and solutions of the multi-component NLS equation has been investigated in Section 6.3.7. This relationship implies that all solutions of the multi-component NLS equation constructed in this chapter provide also solutions of the KP1 equation.

In the next section, solutions of (6.3.2) in terms of elementary functions are derived from solutions (6.3.4) by degenerating the associated Riemann surface $\mathcal{R}_g$ into a Riemann surface of genus zero. Imposing reality conditions (6.3.3), by an appropriate choice of the parameters one gets special solutions of (6.3.1) such as multi-solitons and breathers. To the best of my knowledge, such an approach to multi-solitonic solutions of n-NLS^s has not been studied before. Moreover, breather and rational breather solutions to the multi-component case are derived here for the first time.

7.2.1 Determinantal solutions of the complexified n-NLS equation

Solutions of the complexified scalar NLS equation in terms of elementary functions were obtained in [23], when the genus of the associated hyperelliptic spectral curve tends to zero. For specific choices of parameters, they get dark and bright multi-solitons of the NLS equation, as well as quasi-periodic modulations of the plane wave solutions previously constructed in [82]. A direct generalization of this approach to the multi-component case is not obvious, due to the complexity of the associated spectral curve. To bypass this problem and to construct spectral data associated to algebro-geometric solutions (6.3.4) in the limit when the genus tends to zero, we use the uniformization map between the degenerate Riemann surface and the Riemann sphere. Details of such a degeneration have been presented in Section 7.1.

Let us discuss solutions of n-NLS in genus zero. Consider the following meromorphic function f on the sphere:

$$f(w) = \alpha \prod_{i=1}^{n+1} \frac{w - w_{a_i}}{w - w_{b_i}} \tag{7.2.2}$$

where $w_{a_j} \neq w_{b_k}$ for all j, k, $w_{a_j} \neq w_{a_k}$ for $j \neq k$, and $\alpha \in \mathbb{C}$. Without loss of generality, put $\alpha = 1$. This function is of degree $n+1$ on the sphere, hence it represents a genus zero $(n+1)$-sheeted branched covering of $\mathbb{CP}^1$. Recall that a meromorphic function f on the sphere is called real if its zeros as well as its poles are real or pairwise conjugate.

If not stated otherwise, the local parameter in a neighbourhood of a regular point w_a (i.e., $f'(w_a) \neq 0$) is chosen to be $k_a(w) = f(w) - f(w_a)$ for any w in a neighbourhood of w_a. Solutions of the complexified system (6.3.2) associated to the meromorphic function f (7.2.2) on the sphere are given by:

Proposition 7.2.1. *Let $j, k \in \mathbb{N}$ satisfy $1 \leq j \leq n$ and $1 \leq k \leq g$. Let f be a meromorphic function (7.2.2) of degree $n+1$ on the sphere, with complex zeros $\{w_{a_i}\}_{i=1}^{n+1}$ and complex poles $\{w_{b_i}\}_{i=1}^{n+1}$. Let $\mathbf{d} \in \mathbb{C}^g$ and $A_j \neq 0$ be arbitrary constants. Moreover, assume that $w_{u_k}, w_{v_k} \in \mathbb{C}$ satisfy*

$$f(w_{u_k}) = f(w_{v_k}). \tag{7.2.3}$$

Then the following functions are solutions of the complexified system (6.3.2)

$$\begin{aligned} \psi_j(x,t) &= A_j \frac{\det(\mathbb{T}_{j,1})}{\det(\mathbb{T}_{j,0})} \exp\{-\mathrm{i}\,(E_j\, x - F_j\, t)\}, \\ \psi_j^*(x,t) &= \frac{q_2(a_{n+1}, a_j)}{A_j} \frac{\det(\mathbb{T}_{j,-1})}{\det(\mathbb{T}_{j,0})} \exp\{\mathrm{i}\,(E_j\, x - F_j\, t)\}. \end{aligned} \tag{7.2.4}$$

For $\beta = -1, 0, 1$, $\mathbb{T}_{j,\beta}$ denotes the $g \times g$ matrix with entries (7.1.8) where $z_k^{(j)} = Z_k - d_k + \beta\, r_{j,k}$. Here $Z_k = \mathrm{i}\, V_{a_{n+1},k}\, x + \mathrm{i}\, W_{a_{n+1},k}\, t$, where the scalars $V_{a_{n+1},k}$ and $W_{a_{n+1},k}$ are defined in (7.1.9) and (7.1.10), and $r_{j,k}$ is defined in (7.1.11) with $w_a := w_{a_{n+1}}$ and $w_b := w_{a_j}$. The scalars E_j and F_j are given by

$$E_j = K_1(a_{n+1}, a_j), \qquad F_j = -\left(K_1(a_{n+1}, a_j)\right)^2 + 2 \sum_{k=1}^{n} q_2(a_{n+1}, a_k),$$

where $q_2(a_{n+1}, a_j)$ and $K_1(a_{n+1}, a_j)$ are defined in (7.1.12) and (7.1.20).

Proof. Consider solutions (6.3.4) associated to a Riemann surface $\mathcal{R}_g$ of genus $g > 0$, and assume $f(a_i) = 0$ for $i = 1, \ldots, n+1$. Pinch all $\mathcal{A}$-cycles of the associated Riemann surface $\mathcal{R}_g$ into double points, as explained in Section 7.1. After desingularization, the meromorphic function f of degree $n+1$ on $\mathcal{R}_g$ becomes a meromorphic function of degree $n+1$ on the sphere, given in general form by (7.2.2). In the limit considered here, the theta function tends to the determinantal form (7.1.7). Quantities defined on the degenerated surface independent of the variables x and t were constructed in Section 7.1.3 and are given in (7.1.9)-(7.1.13) and (7.1.20), (7.1.21). Condition (7.2.3) follows from the fact that double points appearing after degeneration of $\mathcal{R}_g$ are desingularized into two distinct points w_{u_k} and w_{v_k} having the same projection under the

meromorphic function f. Note that equation (7.2.1) holds in the limit, since by (7.1.9) and (7.2.2) one has:

$$\sum_{i=1}^{n+1} V_{a_i,k} = \frac{1}{f(w_{u_k})} - \frac{1}{f(w_{v_k})}, \tag{7.2.5}$$

which by (7.2.3) equals zero for $k = 1, \ldots, g$. □

Remark 7.2.2. Functions (7.2.4) give a family of solutions to the complexified multi-component NLS equation (6.3.2) depending on $3n + g + 2$ complex parameters: w_{a_i}, w_{b_i} for $1 \leq i \leq n+1$, d_k for $1 \leq k \leq g$, and A_j for $1 \leq j \leq n$.

Remark 7.2.3. The transformations (6.3.11) which leave equation (6.3.2) invariant may be useful to simplify the expressions in the obtained solutions and thus to facilitate the numerical implementation.

7.2.2 Multi-solitonic solutions of n-NLS

Imposing the reality conditions (6.3.3) on the degenerate solutions (7.2.4) of the complexified system, one gets particular solutions of (6.3.1) such as dark and bright multi-solitons. Dark and bright solitons differ by the fact that the modulus of the first tends to a non zero constant and the modulus of the second tends to zero when the spatial variable tends to infinity. Such solutions were obtained in [23] for the one component case by degenerating algebro-geometric solutions, and describe elastic collisions between solitons. Elastic means that the solitons asymptotically retain their shape and speed after interaction. The interaction of vector solitons is more complex than the one of scalar solitons because inelastic collisions can appear in all components of one solution (see, for instance, [3]).

In what follows $N \in \mathbb{N}$ with $N \geq 1$.

Dark multi-solitons of n-NLS^s, $s \neq (1, \ldots, 1)$.

Dark multi-soliton solutions of 2-NLS^s were investigated in [133]. The dark N-soliton solution derived here corresponds to elastic interactions between N dark solitons. Moreover, we show that this type of solutions does not exist for the focusing multi-component nonlinear Schrödinger equation, i.e., in the case where $s = (1, \ldots, 1)$.

Proposition 7.2.2. *Let $j, k \in \mathbb{N}$ satisfy $1 \leq j \leq n$ and $1 \leq k \leq N$. Let f be a real meromorphic function (7.2.2) of degree $n+1$ on the sphere, having $n+1$ real zeros $\{w_{a_i}\}_{i=1}^{n+1}$. Choose $\theta \in \mathbb{R}$ and $\mathbf{d} \in \mathbb{R}^N$. Moreover, assume that $w_{u_k}, w_{v_k} \in \mathbb{C}$ satisfy (7.2.3) and*

$$\overline{w_{u_k}} = w_{v_k}. \tag{7.2.6}$$

Put $s_j = sign(f'(w_{a_{n+1}})f'(w_{a_j}))$. Then the following functions define smooth dark N-soliton solutions of n-NLS^s, where $s = (s_1, \ldots, s_n)$ with $s \neq (1, \ldots, 1)$,

$$\psi_j(x,t) = A_j\, e^{\mathrm{i}\theta}\, \frac{\det(\mathbb{T}_{j,1})}{\det(\mathbb{T}_{j,0})} \exp\left\{-\mathrm{i}\,(E_j\, x - F_j\, t)\right\}. \tag{7.2.7}$$

Here $A_j = |q_2(a_{n+1}, a_j)|^{1/2}$, and the remaining notation is as in Proposition 7.2.1 with $g = N$.

Proof. Let us check that the functions ψ_j and ψ_j^* defined in (7.2.4) satisfy the reality conditions (6.3.3) with $s_j = \mathrm{sign}(f'(w_{a_{n+1}})f'(w_{a_j}))$. Put $A_j = |q_2(a_{n+1}, a_j)|^{1/2}$ in (7.2.4). Then with the above assumptions, it is straightforward to see that $\psi_j^* = s_j\,\overline{\psi_j}$ where $s_j = \mathrm{sign}(q_2(a_{n+1}, a_j))$, which by (7.1.12) leads to $s_j = \mathrm{sign}(f'(w_{a_{n+1}})f'(w_{a_j}))$. Moreover, with (7.2.6) it can be seen that condition (7.2.1) is equivalent to

$$\frac{1}{|w_{a_{n+1}} - w_{v_k}|^2} + \sum_{j=1}^{n} \frac{f'(w_{a_{n+1}})}{f'(w_{a_j})} \frac{1}{|w_{a_j} - w_{v_k}|^2} = 0, \tag{7.2.8}$$

for $k = 1, \ldots, N$. Therefore, by (7.2.8) the quantity $f'(w_{a_{n+1}})f'(w_{a_j})$ cannot be positive for all j, which yields $s \neq (1, \ldots, 1)$. The solutions are smooth since the denominator in (7.2.7) is a finite sum of real exponentials. □

Remark 7.2.4. The dark N-soliton solutions (7.2.7) depend on $N+1$ real parameters d_k, θ and a real meromorphic function f (7.2.2) defined by $2n+2$ real parameters. The solitons are dark since the modulus of the ψ_j tends to A_j when $x \in \mathbb{R}$ tends to infinity.

Example 7.2.1. *With the notation of Proposition 7.2.1 and 7.2.2, functions ψ_j (7.2.7) are given for $N = 1$ by*

$$\psi_j(x,t) = A_j \frac{1 + e^{Z_1 - d_1 + r_{j,1}}}{1 + e^{Z_1 - d_1}} e^{-\mathrm{i}\,(E_j x - F_j t)}.$$

Example 7.2.2. *Figure 7.1 shows the elastic interaction with a phase-shift between two dark soliton solutions of the 4-NLS^s equation with $s = (1, -1, 1, -1)$. It corresponds to the following choice of parameters: $w_{a_1} = 8$, $w_{a_2} = 5$, $w_{a_3} = 3$, $w_{a_4} = -4$, $w_{a_5} = -10$, $w_{b_1} = 1$, $w_{b_2} = 2$, $w_{b_3} = 17$, $w_{b_4} = 1/4$, $w_{b_5} = -1/2$, and $w_{u_1} \approx 1.51 + 2.43\mathrm{i}$ with $f(w_{u_1}) = 7$, $w_{u_2} \approx 4.41 + 3.45\mathrm{i}$ with $f(w_{u_1}) = 1$.*

Bright multi-solitons of n-NLS^s.

Bright multi-solitons of the NLS equation presented in [23] were obtained by collapsing all branch cuts of the underlying hyperelliptic curve of the algebro-geometric solutions. This way they get solutions expressed as the quotient of a finite sum of exponentials similar to dark multi-solitons, except that the modulus of the solutions tends to zero instead of a non-zero constant when the spatial variable tends to infinity. Following this approach, a family of bright multi-solitons of n-NLS^s is obtained here by further degeneration of (7.2.4).

For the multi-component case there exist two sorts of bright soliton interactions: elastic or inelastic. Inelastic collisions between bright solitons were investigated in [134] for the two component case and in [88] for the multi-component case. The family of bright multi-solitons of n-NLS^s obtained here describes the standard elastic collision with phase shift. Notice that there exist various ways to degenerate algebro-geometric solutions. Therefore, it appears possible that bright solitons with inelastic collision can be obtained by different degenerations.

Proposition 7.2.3. *Let $j \in \mathbb{N}$ satisfy $1 \leq j \leq n$. Take $w_{a_j}, \theta \in \mathbb{R}$ and choose $\hat{\mathbf{d}} \in \mathbb{C}^{2N}$ such that $\overline{\hat{d}_{2k-1}} = \hat{d}_{2k}$, $k = 1, \ldots, N$. Moreover, let $w_{u_{2k}}, w_{v_{2k-1}} \in \mathbb{C}$ satisfy*

$$\overline{w_{u_{2k}}} = w_{v_{2k-1}} \tag{7.2.9}$$

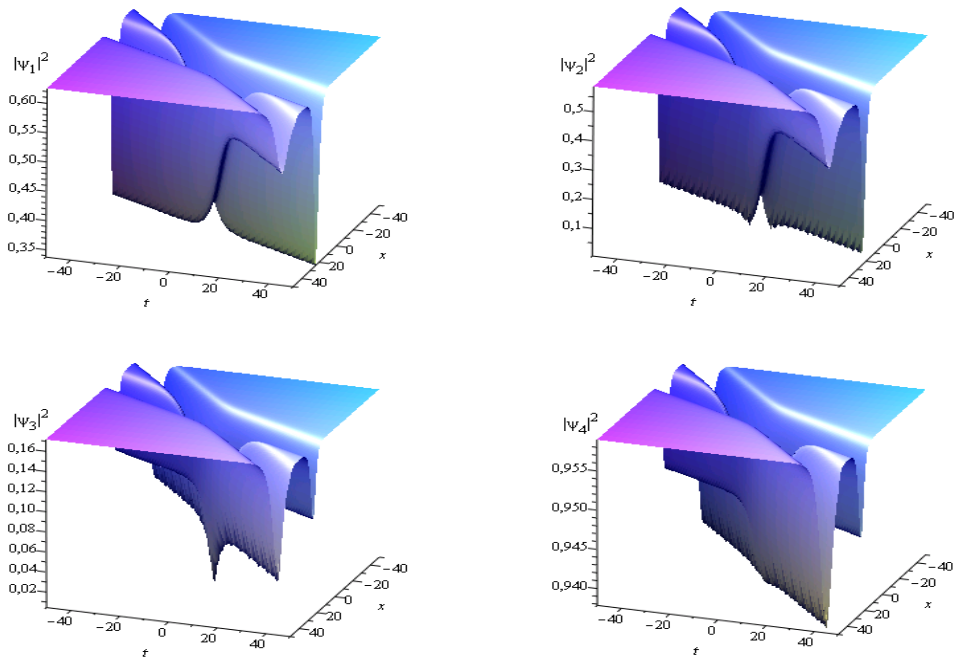

Figure 7.1: *Dark 2-soliton of 4-NLS^s with* $s = (1, -1, 1, -1)$.

for $k = 1, \ldots, N$. *Choose* $\gamma_j \in \mathbb{R}$ *and put* $s_j = sign(\gamma_j)$. *Then the following functions give bright* N*-soliton solutions of* n*-NLS^s*

$$\psi_j(x,t) = A_j\, e^{\mathrm{i}\theta}\, \frac{\det(\mathbb{K}_j)}{\det(\mathbb{M})}, \tag{7.2.10}$$

where $A_j = |\gamma_j|^{1/2}\, |w_{a_j}|^{-1}$. *Here* $\mathbb{K}_j$ *and* $\mathbb{M}$ *are* $2N \times 2N$ *matrices with entries* $(\mathbb{K}_j)_{ik}$ *and* $(\mathbb{M})_{ik}$ *given by:*

$$\begin{aligned}
\text{- for } i \text{ and } k \text{ even:} \quad (\mathbb{K}_j)_{ik} &= \delta_{2,i}\, \frac{w_{u_i}}{w_{u_k}}\, e^{\frac{1}{2}(z_2+z_k+\hat{r}_{j,2}+\hat{r}_{j,k})} + \delta_{i,k} - \delta_{2,i}\,\delta_{2,k} \\
&\quad + \delta_{2,k}\,(\delta_{2,i}-1)\, \frac{w_{u_i}}{w_{u_2}}\, e^{\frac{1}{2}(z_i-z_2+\hat{r}_{j,i}-\hat{r}_{j,2})} \\
\text{- for } i \text{ even and } k \text{ odd:} \quad (\mathbb{K}_j)_{ik} &= \alpha_{u_k}^2\, \frac{w_{u_i}}{\alpha_{v_i}-\alpha_{u_k}}\, \frac{\alpha_{v_2}-\alpha_{v_i}}{\alpha_{v_2}-\alpha_{u_k}}\, e^{\frac{1}{2}(z_i+z_k+\hat{r}_{j,i}+\hat{r}_{j,k})} \\
\text{- for } i \text{ odd and } k \text{ even:} \quad (\mathbb{K}_j)_{ik} &= \frac{w_{v_i}}{w_{v_i}-w_{u_k}}\, e^{\frac{1}{2}(z_i+z_k+\hat{r}_{j,i}+\hat{r}_{j,k})} \\
\text{- for } i \text{ and } k \text{ odd:} \quad (\mathbb{K}_j)_{ik} &= \delta_{i,k}
\end{aligned}$$

$$\begin{aligned}
\text{- for } i,k \text{ even, or } i,k \text{ odd:} \quad (\mathbb{M})_{ik} &= \delta_{i,k} \\
\text{- for } i \text{ even and } k \text{ odd:} \quad (\mathbb{M})_{ik} &= \alpha_{u_k}\,\alpha_{v_i}\, \frac{w_{u_i}}{\alpha_{v_i}-\alpha_{u_k}}\, e^{\frac{1}{2}(z_i+z_k)} \\
\text{- for } i \text{ odd and } k \text{ even:} \quad (\mathbb{M})_{ik} &= -\frac{w_{v_i}}{w_{v_i}-w_{u_k}}\, e^{\frac{1}{2}(z_i+z_k)}.
\end{aligned}$$

Here $\overline{\alpha_{v_{2k}}} = \alpha_{u_{2k-1}}$ *where*

$$\alpha_{u_{2k-1}} = \sum_{j=1}^{n} \gamma_j \left(\frac{1}{w_{a_j}} - \frac{1}{w_{a_j} - w_{v_{2k-1}}} \right). \tag{7.2.11}$$

Moreover, z_k *is a linear function of the variables* x *and* t *satisfying* $\overline{z_{2k}} = z_{2k-1}$*, given by*

$$z_{2k-1} = \mathrm{i}\, \alpha_{u_{2k-1}}\, x + \mathrm{i}\, \alpha^2_{u_{2k-1}}\, t - \hat{d}_{2k-1}.$$

The scalars $\hat{r}_{j,k}$ *satisfy* $\overline{\hat{r}_{j,2k}} = -\,\hat{r}_{j,2k-1}$ *where*

$$\hat{r}_{j,2k-1} = \ln \left\{ \frac{w_{a_j} - w_{v_{2k-1}}}{w_{a_j}\, w_{v_{2k-1}}\, \alpha_{u_{2k-1}}} \right\}.$$

Proof. Consider functions (7.2.4) obtained from (6.3.4) for the choice of local parameters k_{a_i}:

$$k_{a_i}(w) = (\gamma_i\, f'(w_{a_i}))^{-1} f(w)$$

for any w in a neighbourhood of w_{a_i}, $i = 1, \ldots, n+1$, and assume $g = 2N$. Hence condition (7.2.1) becomes

$$\sum_{i=1}^{n+1} \gamma_i \left(\frac{1}{w_{a_i} - w_{v_k}} - \frac{1}{w_{a_i} - w_{u_k}} \right) = 0 \tag{7.2.12}$$

for $k = 1, \ldots, 2N$. Now put $A_j = |q_2(a_{n+1}, a_j)|^{1/2}$ in (7.2.4), where

$$q_2(a_{n+1}, a_j) = \gamma_{n+1}\, \gamma_j\, (w_{a_{n+1}} - w_{a_j})^{-2}.$$

Choose a small parameter $\epsilon > 0$ and define $d_k = -\ln \epsilon + \hat{d}_k$, for $k = 1, \ldots, 2N$, and

$$w_{u_{2k-1}} = w_{a_{n+1}} + \epsilon^2\, \alpha^{-1}_{u_{2k-1}}, \qquad w_{v_{2k}} = w_{a_{n+1}} + \epsilon^2\, \alpha^{-1}_{v_{2k}}, \tag{7.2.13}$$

for $k = 1, \ldots, N$. Now put $\gamma_{n+1} = \epsilon^2$ and consider in the determinant $\det(\mathbb{T}_{j,1})$ appearing in (7.2.4) the substitution

$$L_{2i} \longrightarrow L_{2i} - \frac{(\mathbb{T}_{j,1})_{2i,2}}{(\mathbb{T}_{j,1})_{2,2}}\, L_2,$$

for $i = 2, \ldots, N$, where L_k denotes the line number k of the matrix $\mathbb{T}_{j,1}$, and $(\mathbb{T}_{j,1})_{i,k}$ denotes the entries of this matrix. In the limit $\epsilon \to 0$, it can be seen that the functions ψ_j given in (7.2.4) converge towards functions (7.2.10), where the following change of parameters (eliminating the parameter $w_{a_{n+1}}$) has been made:

$$w_{a_j} \to w_{a_j} + w_{a_{n+1}}, \qquad w_{u_{2k}} \to w_{u_{2k}} + w_{a_{n+1}}, \qquad w_{v_{2k-1}} \to w_{v_{2k-1}} + w_{a_{n+1}},$$

for $j = 1, \ldots, n$ and $k = 1, \ldots, N$. Analogous statements can be made for the functions ψ^*_j. By assumption, it is straightforward to see that the functions ψ_j and ψ^*_j obtained in the limit considered here satisfy the reality conditions $\psi^*_j = s_j\, \overline{\psi_j}$ with $s_j = \mathrm{sign}(\gamma_j)$. Moreover, in this limit condition (7.2.12) yields (7.2.11). □

Remark 7.2.5. The bright N-soliton solutions (7.2.10) depend on $2N$ complex parameters $\hat{d}_{2k-1}$, $w_{v_{2k-1}}$, and $2n+1$ real parameters $w_{a_j}, \gamma_j, \theta$. Moreover, all parameters appearing in (7.2.10) are free, contrary to the dark multi-solitons (7.2.7) where parameters w_{u_k} and w_{v_k} have to satisfy the polynomial equation (7.2.3). The solitons are bright since the modulus of the ψ_j tends to zero when $x \in \mathbb{R}$ tends to infinity, in contrast to the dark solitons.

Example 7.2.3. *With the notation of Proposition 7.2.3, the functions ψ_j (7.2.10) are given for $N = 1$ by*

$$\psi_j(x,t) = A_j\, e^{\mathrm{i}\theta}\, \frac{e^{\overline{z_1} - \hat{r}_{j,1}}}{1 + e^{B + 2Re(z_1)}},$$

where $B = \ln\left\{-|w_{v_1}|^2\, |\alpha_{u_1}|^2\, (4\, Im(w_{v_1})\, Im(\alpha_{u_1}))^{-1}\right\}$.

Example 7.2.4. *Figure 7.2 shows the interaction between two bright solitons solution of the 4-NLS^s equation with $s = (1,1,1,1)$. It corresponds to the following choice of parameters: $\gamma_j = 1$, $w_{a_1} = -6$, $w_{a_2} = 17$, $w_{a_3} = 3$, $w_{a_4} = 7$, and $w_{v_1} = 1 + \mathrm{i}$, $w_{v_3} = 2 - 3\mathrm{i}$, $\hat{d}_k = 0$. The resulting two-soliton solution shows the standard elastic collision with a phase-shift.*

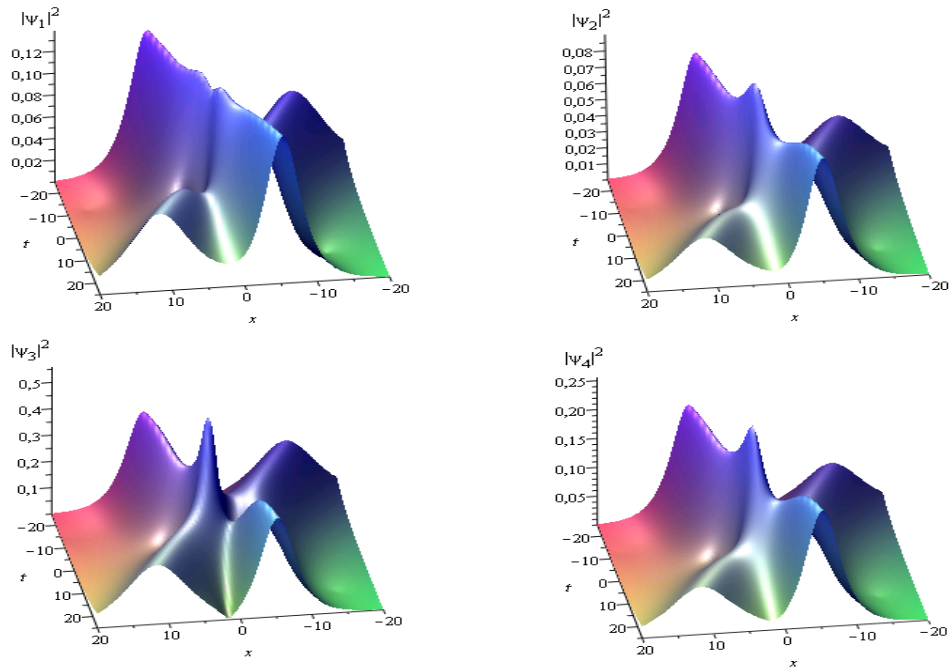

Figure 7.2: *Bright 2-soliton of 4-NLS^s with $s = (1,1,1,1)$.*

7.2.3 Breather and rational breather solutions of n-NLS

Solutions obtained here differ from the dark multi-solitons studied in Section 7.2.2 by the reality condition imposed on parameters w_{u_k} and w_{v_k} in the solutions (7.2.4) of the complexified system for $k = 1, \ldots, g$. By an appropriate choice of parameters, one gets periodic solutions (breathers) as well as rational solutions (rational breathers). The name 'breather' reflects the behavior of

the profile of the solution which is periodic in time (respectively, space) and localized in space (respectively, time). This appears to be the first time that explicit breather and rational breather solutions of n-NLS^s are given.

In what follows $N \in \mathbb{N}$ with $N \geq 1$.

Multi-Breathers of n-NLS^s.

Multi-breather solutions of n-NLS^s are given in the following proposition. The N-breather solution corresponds to an elastic interaction between N breathers.

Proposition 7.2.4. *Let $j, k \in \mathbb{N}$ satisfy $1 \leq j \leq n$ and $1 \leq k \leq N$. Let f be a real meromorphic function (7.2.2) of degree $n+1$ on the sphere, having $n+1$ real zeros $\{w_{a_i}\}_{i=1}^{n+1}$. Choose $\theta \in \mathbb{R}$ and take $\hat{\mathbf{d}} \in \mathbb{C}^{2N}$ such that $\overline{\hat{d}_{2k-1}} = \hat{d}_{2k}$. Let $w_{u_{2k}}, w_{u_{2k-1}}, w_{v_{2k}}, w_{v_{2k-1}} \in \mathbb{C}$ satisfy (7.2.3) and*

$$\overline{w_{u_{2k}}} = w_{v_{2k-1}}, \quad \overline{w_{u_{2k-1}}} = w_{v_{2k}}. \tag{7.2.14}$$

Put $s_j = sign(f'(w_{a_{n+1}})f'(w_{a_j}))$. Then the following functions define N-breather solutions of n-NLS^s

$$\psi_j(x,t) = A_j\, e^{\mathrm{i}\theta}\, \frac{\det(\mathbb{T}_{j,1})}{\det(\mathbb{T}_{j,0})}\, \exp\left\{-\mathrm{i}\,(E_j\, x - F_j\, t)\right\}, \tag{7.2.15}$$

where $A_j = |q_2(a_{n+1}, a_j)|^{1/2}$, and the remaining notation is the same as in Proposition 7.2.1 for $g = 2N$.

Remark 7.2.6. Functions (7.2.15) cover a family of breather solutions of n-NLS^s depending on N complex parameters d_k, a real parameter θ, and a real meromorphic function f (7.2.2) defined by $2n+2$ real parameters.

To simplify the computation of the solutions, we apply transformation (6.3.11) to the solutions (7.2.4), with β and λ given by

$$\beta = 1, \qquad \lambda = \frac{1}{2}\, f''(w_{a_{n+1}})\, f'(w_{a_{n+1}})^{-2}. \tag{7.2.16}$$

Hence, the quantity $f''(w_{a_{n+1}})f'(w_{a_{n+1}})^{-2}\, V_{a_{n+1},k}$ in the expression (7.1.10) for the scalar $W_{a_{n+1},k}$ disappears, as well as the quantity $\frac{1}{2}f''(w_{a_{n+1}})f'(w_{a_{n+1}})^{-2}$ in the expression (7.1.20) for the scalar $K_1(a_{n+1}, a_j)$.

Example 7.2.5. *Figure 7.3 shows a breather solution of the 4-NLS^s equation for the vector of signs $s = (-1,-1,1,-1)$. It corresponds to the following choice of parameters: $w_{a_1} = 10$, $w_{a_2} = -5$, $w_{a_3} = -1/3$, $w_{a_4} = 1/4$, $w_{a_5} = 1/2$, and $w_{u_1} \approx 0.55 - 0.11\mathrm{i}$ with $f(w_{u_1}) = 2\mathrm{i}$, $w_{u_2} \approx -0.35 + 0.07\mathrm{i}$ with $f(w_{u_2}) = -2\mathrm{i}$.*

Example 7.2.6. *Figure 7.4 shows an elastic collision between two breathers, solution of the 4-NLS^s equation with $s = (-1,1,1,-1)$. It corresponds to the following choice of parameters: $w_{a_1} = 1/3$, $w_{a_2} = 3$, $w_{a_3} = 1/7$, $w_{a_4} = 2$, $w_{a_5} = 1$, $w_{b_1} = -1$, $w_{b_2} = 4$, $w_{b_3} = -2$, $w_{b_4} = 0$, and $w_{u_1} \approx 0.55 - 0.11\mathrm{i}$ with $f(w_{u_1}) = 2\mathrm{i}$, $w_{u_2} \approx -0.35 + 0.07\mathrm{i}$ with $f(w_{u_2}) = -2\mathrm{i}$, $w_{u_3} \approx -0.91 - 0.52\mathrm{i}$ with $f(w_{u_3}) = 10 - 5\mathrm{i}$, and $w_{u_4} \approx 14.46 + 5.32\mathrm{i}$ with $f(w_{u_4}) = 10 + 5\mathrm{i}$.*

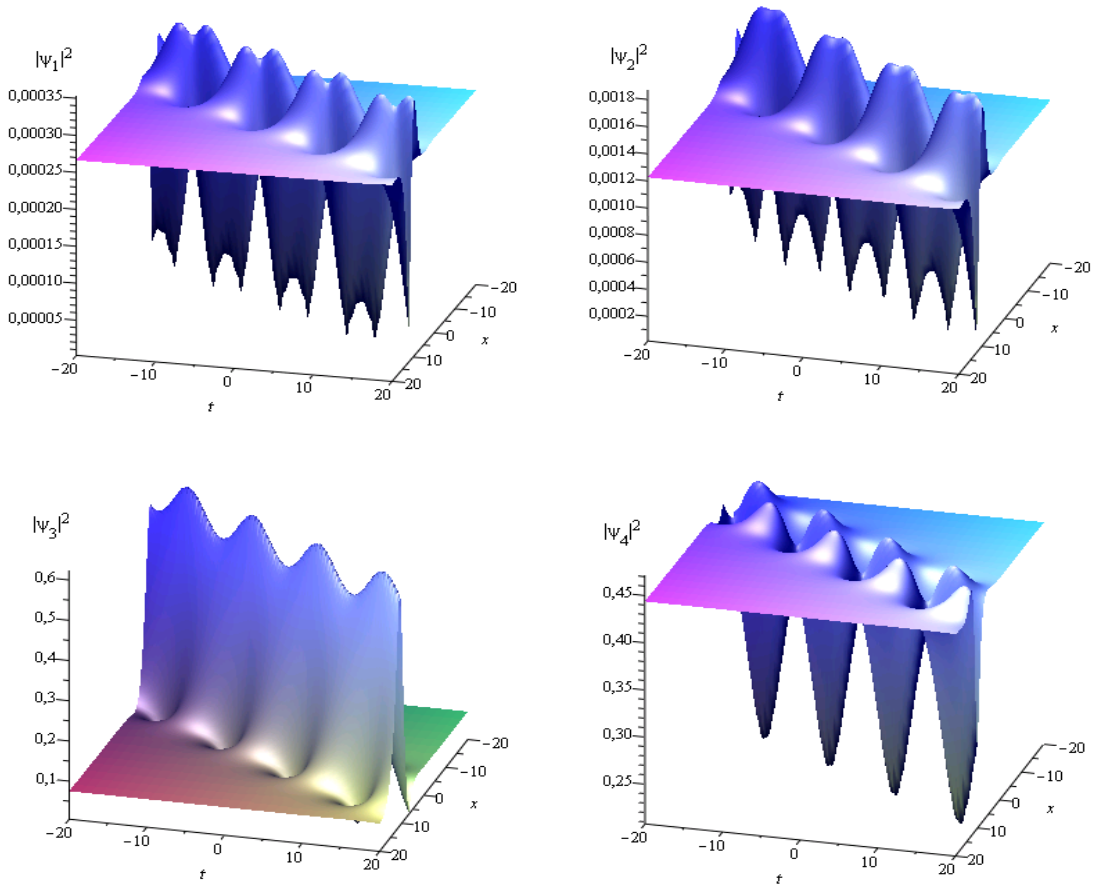

Figure 7.3: *Breather of* 4-*NLS*^{s} *with* $s = (-1, -1, 1, -1)$.

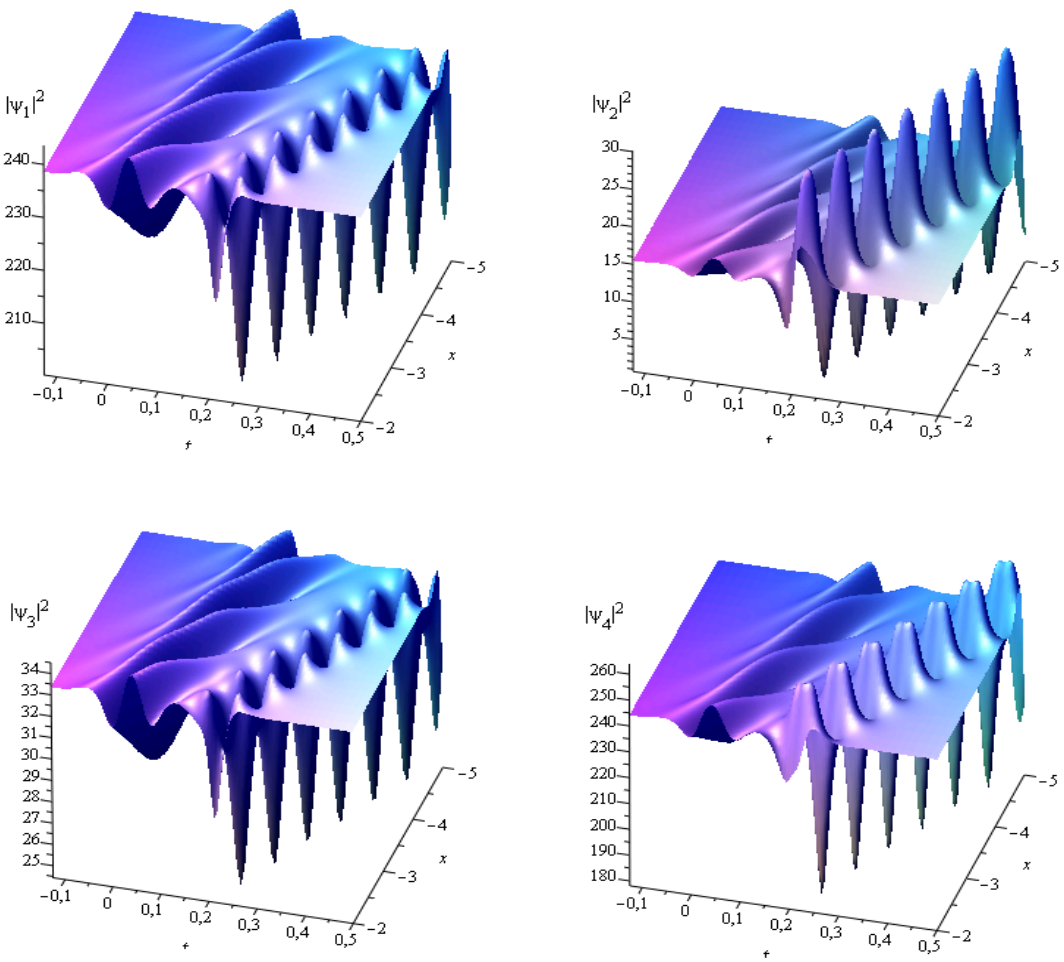

Figure 7.4: *2-breather of* 4-*NLS*^{s} *with* $s = (-1, 1, 1, -1)$.

N-rational breathers of n-NLS^s, for $1 \le N \le n$.

Here we are interested in solutions of n-NLS^s that can be expressed in the form of a ratio of two polynomials (modulo an exponential factor). These solutions, called rational breathers, are neither periodic in time nor in space, but are isolated in time and space. They are obtained from the breather solutions (7.2.15) in the limit when the parameters $w_{v_{2k-1}}$ and $w_{u_{2k-1}}$ coincide, as well as the parameters $w_{v_{2k}}$ and $w_{u_{2k}}$, for $k = 1, \dots N$. An appropriate choice of the parameters d_i in (7.2.15) for $i = 1, \dots, 2N$, leads to limits of the form '0/0' in the expression for the breather solutions. Thus, by performing a Taylor expansion of the numerator and denominator in (7.2.15), one gets a family of N-rational breather solutions of n-NLS^s.

Proposition 7.2.5. *Let $N, j \in \mathbb{N}$ satisfy $1 \le N \le n$ and $1 \le j \le n$. Let f be a real meromorphic function (7.2.2) of degree $n+1$ on the sphere, having $n+1$ real zeros $\{w_{a_i}\}_{i=1}^{n+1}$. Choose $\theta \in \mathbb{R}$ and take $\hat{\mathbf{d}} \in \mathbb{C}^{2N}$ such that $\overline{\hat{d}_{2k}} = \hat{d}_{2k-1}$ for $k = 1, \dots, N$. Moreover, let $w_{u_{2k-1}}, w_{v_{2k}} \in \mathbb{C}$, $k = 1, \dots, N$, be complex conjugate critical points of the meromorphic function f, i.e., they are solutions of $f'(w) = 0$, which is equivalent to the condition*

$$\sum_{i=1}^{n+1} \frac{1}{f'(w_{a_i})} \frac{1}{(w - w_{a_i})^2} = 0. \tag{7.2.17}$$

Put $s_j = sign(f'(w_{a_{n+1}}) f'(w_{a_j}))$. Then the following functions give N-rational breathers of n-NLS^s

$$\psi_j(x,t) = A_j \, e^{\mathrm{i}\theta} \frac{\det(\mathbb{K}_{j,1})}{\det(\mathbb{K}_{j,0})} \exp\left\{-\mathrm{i}\,(E_j\, x - F_j\, t)\right\}, \tag{7.2.18}$$

where $A_j = |q_2(a_{n+1}, a_j)|^{1/2}$. For $\beta = 0, 1$, $\mathbb{K}_{j,\beta}$ denotes a $2N \times 2N$ matrix with entries $(\mathbb{K}_{j,\beta})_{i,k}$ given by:

$$\begin{aligned}
\text{- for } i \text{ and } k \text{ even:} \quad (\mathbb{K}_{j,\beta})_{ik} &= (1-\delta_{i,k}) \frac{1}{w_{v_i} - w_{v_k}} - \delta_{i,k}\,(z_k + \beta\, \hat{r}_{j,k}) \\
\text{- for } i \text{ even and } k \text{ odd:} \quad (\mathbb{K}_{j,\beta})_{ik} &= \frac{1}{w_{v_i} - w_{u_k}} \\
\text{- for } i \text{ odd and } k \text{ even:} \quad (\mathbb{K}_{j,\beta})_{ik} &= -\frac{1}{w_{u_i} - w_{v_k}} \\
\text{- for } i \text{ and } k \text{ odd:} \quad (\mathbb{K}_{j,\beta})_{ik} &= -(1-\delta_{i,k}) \frac{1}{w_{u_i} - w_{u_k}} - \delta_{i,k}\,(z_k + \beta\, \hat{r}_{j,k}).
\end{aligned}$$

Here z_i is a linear function of the variables x and t given by

$$z_i = \mathrm{i}\, \hat{V}_{a_{n+1},i}\, x + \mathrm{i}\, \hat{W}_{a_{n+1},i}\, t - \hat{d}_i$$

for $i = 1, \dots, 2N$, where $\overline{\hat{V}_{a_{n+1},2k}} = -\hat{V}_{a_{n+1},2k-1}$ and $\overline{\hat{W}_{a_{n+1},2k}} = -\hat{W}_{a_{n+1},2k-1}$ with

$$\hat{V}_{a_{n+1},2k-1} = \frac{1}{f'(w_{a_{n+1}})} \frac{1}{(w_{a_{n+1}} - w_{u_{2k-1}})^2}, \quad \hat{W}_{a_{n+1},2k-1} = -\frac{1}{f'(w_{a_{n+1}})^2} \frac{2}{(w_{a_{n+1}} - w_{u_{2k-1}})^3}$$

for $k = 1, \dots, N$. Scalars $\hat{r}_{j,k}$ satisfy $\overline{\hat{r}_{j,2k}} = -\hat{r}_{j,2k-1}$ and are given by

$$\hat{r}_{j,2k-1} = -\frac{w_{a_{n+1}} - w_{a_j}}{(w_{a_{n+1}} - w_{u_{2k-1}})\,(w_{a_j} - w_{u_{2k-1}})}.$$

Scalars E_j, F_j are defined by

$$E_j = \frac{1}{f'(w_{a_{n+1}})\,(w_{a_j} - w_{a_{n+1}})}, \qquad F_j = -\,E_j^2 + 2\sum_{k=1}^{n} q_2(a_{n+1}, a_k).$$

Proof. To simplify the expression for the obtained solutions, apply the transformation (6.3.11) to functions (7.2.15) with β and λ as in (7.2.16). Let $\epsilon > 0$ be a small parameter and define $d_k = \epsilon\,\hat{d}_k + \mathrm{i}\pi$, for $k = 1, \ldots, 2N$. Moreover, assume

$$w_{v_{2k-1}} = w_{u_{2k-1}} + \epsilon\,\alpha_{v_{2k-1}}, \qquad w_{u_{2k}} = w_{v_{2k}} + \epsilon\,\alpha_{u_{2k}}, \tag{7.2.19}$$

for some $\alpha_{v_{2k-1}}, \alpha_{u_{2k}} \in \mathbb{C}$, where $k = 1, \ldots, N$. Note that equation number k of system (7.2.5) can be written as

$$\sum_{j=1}^{n+1} \frac{1}{f'(w_{a_j})}\,\frac{f(w_{v_k})\,f(w_{u_k})}{(w_{a_j} - w_{v_k})\,(w_{a_j} - w_{u_k})} = -\,\frac{f(w_{v_k}) - f(w_{u_k})}{w_{v_k} - w_{u_k}}\,. \tag{7.2.20}$$

Hence, in the limit $\epsilon \to 0$, equation (7.2.20) becomes

$$\sum_{j=1}^{n+1} \frac{1}{f'(w_{a_j})}\,\frac{f(w_{v_{2k-1}})^2}{(w_{a_j} - w_{v_{2k-1}})^2} = -\,f'(w_{v_{2k-1}}),$$

and

$$\sum_{j=1}^{n+1} \frac{1}{f'(w_{a_j})}\,\frac{f(w_{u_{2k}})^2}{(w_{a_j} - w_{u_{2k}})^2} = -\,f'(w_{u_{2k}}),$$

for $k = 1, \ldots, N$. Therefore, choose $w_{v_{2k-1}}$ and $w_{u_{2k}}$ to be distinct critical points of the meromorphic function f for $k = 1, \ldots N$, i.e., they are solutions of $f'(w) = 0$, in such way that equation (7.2.1) holds in the limit considered here. Since the condition $f'(w) = 0$ is equivalent to solve a polynomial equation of degree $2n$, it follows that $1 \le N \le n$. Now take the limit $\epsilon \to 0$ in (7.2.15). Note that parameters $\alpha_{v_{2k-1}}, \alpha_{u_{2k}}$ cancel in this limit, and the degenerated functions take the form (7.2.18). □

Remark 7.2.7. Functions (7.2.18) provide a family of rational breather solutions of n-NLS^s depending on N complex parameters $\hat{d}_k$, a real parameter θ, and a real meromorphic function f (7.2.2) defined by $2n+2$ real parameters, chosen such that f has complex conjugate critical points.

Example 7.2.7. *With the notation of Proposition 7.2.5 the functions ψ_j (7.2.18) for $N = 1$ are given by*

$$\psi_j(x,t) = A_j\,e^{\mathrm{i}\theta}\,\frac{B + (z_1 + \hat{r}_{j,1})(\overline{z_1} - \overline{\hat{r}_{j,1}})}{B + |z_1|^2}\,\exp\left\{-\mathrm{i}\,(E_j x - N_j t)\right\},$$

where $B = (2\,Im(w_{u_1}))^{-2}$.

Example 7.2.8. *Figure 7.5 shows a rational breather solution of the 4-NLS^s equation with $s = (1,1,1,1)$. It corresponds to the following choice of parameters: $k_{a_k}(w) = f'(w_{a_k})f(w)$ for $k = 1,\dots,n+1$, with $w_{a_1} = 3$, $w_{a_2} = 5$, $w_{a_3} = 7$, $w_{a_4} = 0$, $w_{a_5} = 4$, and $w_{u_1} \approx 4.53 + 0.56\mathrm{i}$ being a solution of $\sum_{i=1}^{n+1}(w - w_{a_i})^{-2} = 0$. We observe that the functions ψ_2 and ψ_3 coincide with the Peregrine breather well known in the scalar case [129], whereas the functions ψ_1, ψ_4 belong to a new class of rational breathers which does not exist in the scalar case. This new type of rational breathers emerges due to the higher degree of the meromorphic function associated to the solutions of n-NLS^s for $n > 1$.*

Example 7.2.9. *Figure 7.6 shows a 2-rational breather solution of the 4-NLS^s equation with $s = (1,1,1,1)$. It corresponds to the following choice of parameters: $k_{a_k}(w) = f'(w_{a_k})f(w)$ for $k = 1,\dots,n+1$, with $w_{a_1} = 3$, $w_{a_2} = 5$, $w_{a_3} = 7$, $w_{a_4} = 0$, $w_{a_5} = 4$, and $w_{u_1} \approx 4.53 + 0.56\mathrm{i}$, $w_{u_3} \approx 3.45 + 0.56\mathrm{i}$ being solutions of $\sum_{i=1}^{n+1}(w - w_{a_i})^{-2} = 0$, and $d_k = 10$. Variation of the parameters d_k leads to a displacement in the (x,t)-plane of the rational breathers appearing in each of the pictures of Figure 7.6.*

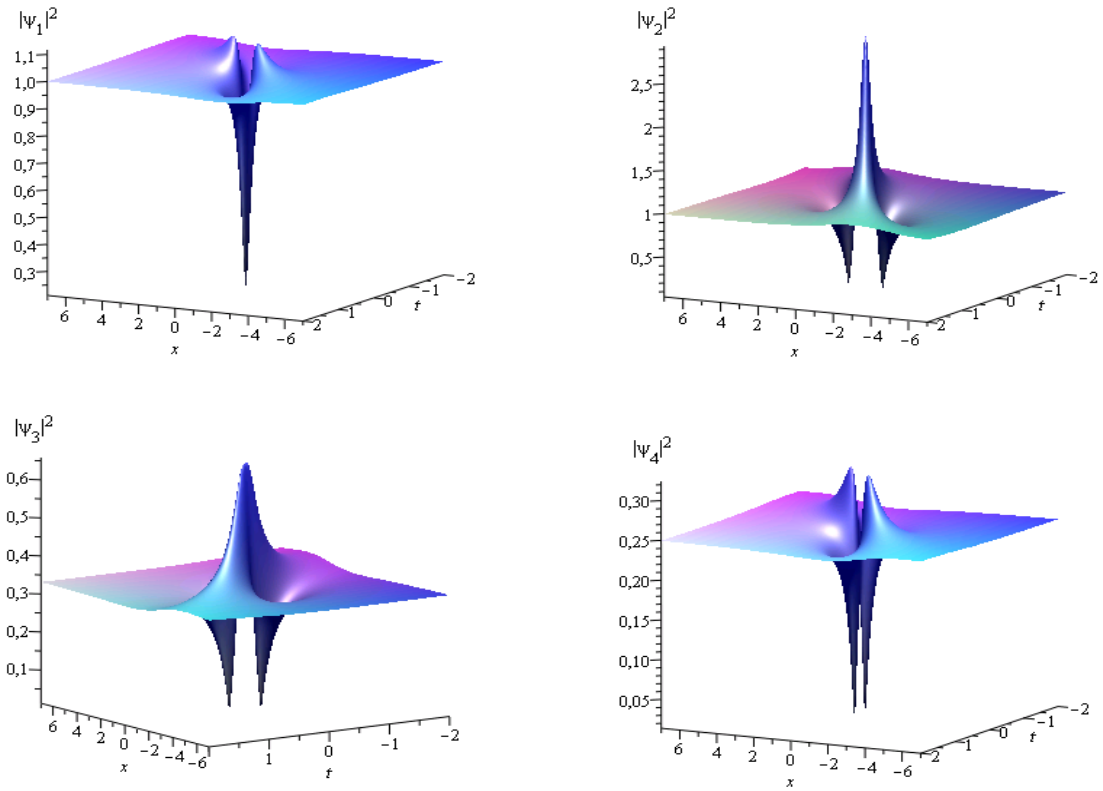

Figure 7.5: *Rational breather of 4-NLS^s with $s = (1,1,1,1)$.*

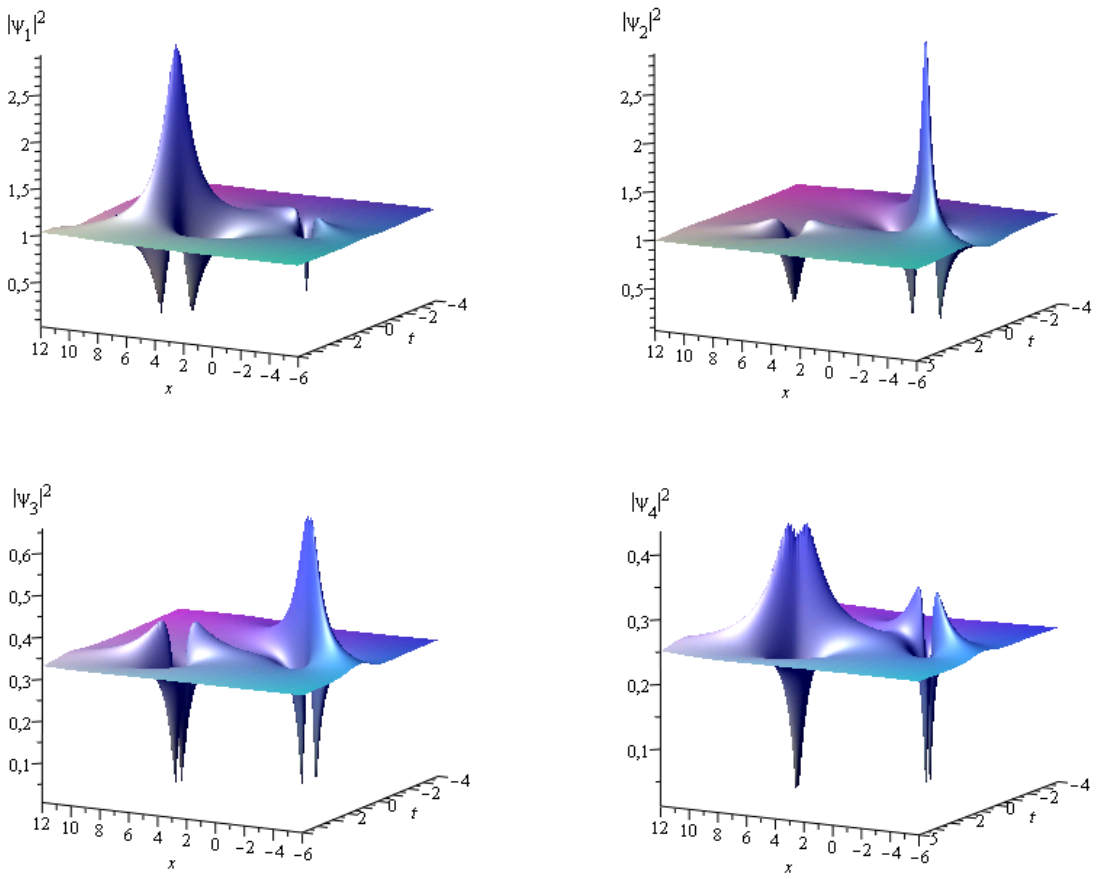

Figure 7.6: *2-rational breather of* 4-*NLS*^{s} *with* $s = (1, 1, 1, 1)$.

7.3 Degenerate algebro-geometric solutions of the DS equations

Solutions of the Davey-Stewartson equations (6.4.1) in terms of elementary functions constructed here are obtained analogously to the solutions of the n-NLS equation, therefore some details will be omitted. In this section, we study the behaviour of theta-functional solutions (6.4.4) of the complexified DS equations (6.4.2) when the Riemann surface degenerates into a Riemann surface of genus zero. Imposing the reality condition (6.4.3), for particular choices of the parameters one gets well-known solutions such as multi-soliton, breather, rational breather, dromion and lump. This appears to be the first time that such solutions of DS are derived from algebro-geometric solutions.

7.3.1 Determinantal solutions of the complexified DS equations

Here solutions of the complexified system (6.4.2) are given as a quotient of two determinants. In the next subsections, this particular form will be more convenient to produce special solutions of the DS equations (6.4.1).

Proposition 7.3.1. *Let $k \in \mathbb{N}$ satisfy $1 \leq k \leq g$. Let $w_a, w_b, w_{u_k}, w_{v_k}, h \in \mathbb{C}$, and $A, \kappa_1, \kappa_2 \in \mathbb{C} \setminus \{0\}$. Choose $\mathbf{d} \in \mathbb{C}^g$. Then the following functions give solutions of the system (6.4.2)*

$$\begin{aligned}
\psi(\xi,\eta,t) &= A\,\frac{\det(\mathbb{T}_1)}{\det(\mathbb{T}_0)}\,\exp\left\{-\mathrm{i}\,(G_1\,\xi + G_2\,\eta - G_3\,\tfrac{t}{2})\right\},\\
\psi^*(\xi,\eta,t) &= -\,\frac{\kappa_1\,\kappa_2}{A\,(w_a-w_b)^2}\,\frac{\det(\mathbb{T}_{-1})}{\det(\mathbb{T}_0)}\,\exp\left\{\mathrm{i}\,(G_1\,\xi + G_2\,\eta - G_3\,\tfrac{t}{2})\right\},\\
\varphi(\xi,\eta,t) &= \frac{1}{2}\,(\ln\det(\mathbb{T}_0))_{\xi\xi} + \frac{1}{2}\,(\ln\det(\mathbb{T}_0))_{\eta\eta} + \frac{h}{4}.
\end{aligned} \tag{7.3.1}$$

For $\beta = -1, 0, 1$, $\mathbb{T}_\beta$ denotes the $g \times g$ matrix with entries (7.1.8) with $z_k = Z_k - d_k + \beta\, r_k$. Here the scalars r_k are given in (7.1.11) and

$$\mathbf{Z} = \mathrm{i}\,\kappa_1 \mathbf{V}_a\,\xi - \mathrm{i}\,\kappa_2 \mathbf{V}_b\,\eta + \mathrm{i}\,(\kappa_1^2\,\mathbf{W}_a - \kappa_2^2\,\mathbf{W}_b)\,\frac{t}{2} \tag{7.3.2}$$

with

$$V_{c,k} = \frac{1}{w_c - w_{v_k}} - \frac{1}{w_c - w_{u_k}}, \qquad W_{c,k} = -\,\frac{1}{(w_c - w_{v_k})^2} + \frac{1}{(w_c - w_{u_k})^2}, \tag{7.3.3}$$

for $c \in \{a, b\}$. The scalars G_1, G_2, G_3 are given by

$$G_1 = \frac{\kappa_1}{w_b - w_a}, \quad G_2 = \frac{\kappa_2}{w_a - w_b}, \quad G_3 = -\,G_1^2 - G_2^2 + h. \tag{7.3.4}$$

Proof. Consider solutions (6.4.4) of system (6.4.2) in the limit when the Riemann surface degenerates to a Riemann surface of genus zero, as explained in Section 7.1.1. In this limit, choose the local parameters k_a and k_b near $a \in \mathcal{R}_0$ and $b \in \mathcal{R}_0$ to be the uniformization map between the degenerate Riemann surface $\mathcal{R}_0$ and the w-sphere. Hence, for any $w \in \mathcal{R}_0$ in a neighbourhood of $w_a \in \mathcal{R}_0$, $k_a(w) = w - w_a$. Therefore, quantities independent of variables ξ, η and t are obtained from (7.1.9)-(7.1.13) and (7.1.20), (7.1.21). □

Remark 7.3.1. Functions (7.3.1) give a family of solutions of the complexified system, involving elementary functions only. These solutions depend on $3g + 6$ complex parameters $w_a, w_b, h, A, \kappa_1, \kappa_2$ and w_{u_k}, w_{v_k}, d_k. Varying these parameters we will obtain different types of physically interesting solutions in the next subsections.

7.3.2 Multi-solitonic solutions of the DS equations

Soliton solutions of the DS equations were shown to be representable in terms of Wronskian determinants in [16]. Single soliton and multi-soliton solutions corresponding to the known one-dimensional solutions can be obtained from this representation. These solitons are pseudo-one-dimensional in the sense that in the (x, y)-plane, they have the same form as one-dimensional solitons in the (x, t)-plane, but that they move with an angle with respect to the axes. The multi-soliton solution describes the interaction of many such solitons each propagating in different directions.

In what follows $N \in \mathbb{N}$ with $N \geq 1$.

Dark multi-soliton of DS1$^\rho$ and DS2$^+$.

Here dark multi-solitons of the DS1$^\rho$ and DS2$^+$ equations are derived from functions (7.3.1) for an appropriate choice of the parameters. They were investigated in [151].

Put $g = N$ and $A = |\kappa_1\kappa_2|^{1/2}\,|w_a - w_b|^{-1}$ in (7.3.1). Moreover, assume $h \in \mathbb{R}$ and $\mathbf{d} \in \mathbb{R}^N$.

Reality condition for DS1$^\rho$. Let us check that with the following choice of parameters,

$$w_a, w_b \in \mathbb{R}, \qquad \kappa_1, \kappa_2 \in \mathbb{R} \setminus \{0\}, \qquad \overline{w_{v_k}} = w_{u_k}, \qquad k = 1, \ldots, N, \tag{7.3.5}$$

functions ψ and ψ^* in (7.3.1) satisfy the reality condition $\psi^* = \rho\,\overline{\psi}$ with $\rho = -\operatorname{sign}(\kappa_1\kappa_2)$. Indeed, this can be deduced from the fact that $G_1, G_2, G_3 \in \mathbb{R}$, and

$$\overline{\det\left(\mathbb{T}_\beta\right)} = \det\left(\overline{\mathbb{T}_\beta}\right) = \det\left(\mathbb{T}_{-\beta}\right), \tag{7.3.6}$$

since u and v can be interchanged in the proof of (7.1.7). Therefore, functions ψ and ϕ in (7.3.1) define dark multi-soliton solutions of DS1$^\rho$.

Smoothness. The dark multi-soliton solutions obtained here are smooth because the denominator $\det(\mathbb{T}_0)$ of functions ψ and ϕ (7.3.1) consists of a finite sum of real exponentials (see (7.1.7)), since ξ, η, t are real.

Remark 7.3.2. One gets a family of smooth dark multi-soliton of the DS1$^\rho$ equation, depending on $N + 6$ real parameters $w_a, w_b, h, \kappa_1, \kappa_2, d_k$, a phase θ, and N complex parameters w_{u_k}.

Reality condition for DS2$^+$. Let us check that with the following choice of parameters,

$$\overline{w_a} = w_b, \qquad \overline{\kappa_1} = \kappa_2, \qquad w_{u_k}, w_{v_k} \in \mathbb{R}, \qquad k = 1, \ldots, N, \tag{7.3.7}$$

the functions ψ and ψ^* (7.3.1) satisfy the reality condition $\psi^* = \overline{\psi}$. With (7.3.7), it is straightforward to see that (7.3.6) is also satisfied. Moreover, since $\overline{G_1} = G_2$, $G_3 \in \mathbb{R}$ and $(w_a - w_b)^2 < 0$, the functions ψ and ψ^* (7.3.1) satisfy the reality condition $\psi^* = \overline{\psi}$. Therefore, they define dark multi-soliton solutions of DS2$^+$.

Smoothness. To get smooth solutions, additional conditions are needed to ensure that $\det(\mathbb{T}_0)$ does not vanish for all complex conjugate $\xi = \bar{\eta}$. For instance, if

$$w_{v_1} < w_{u_1} < w_{v_2} < w_{u_2} < \ldots < w_{v_N} < w_{u_N},$$

the scalars $(\mathbb{B})_{ik}$ (7.1.6) are real for any $i, k \in \{1, \ldots, N\}$. Therefore, the functions ψ and ϕ (7.3.1) are smooth, since their denominator does not vanish as a finite sum of real exponentials.

Remark 7.3.3. One gets a family of smooth dark multi-soliton of the DS2$^+$ equation, depending on $3N+1$ real parameters h, w_{u_k}, w_{v_k}, d_k, a phase θ, and 2 complex parameters w_a, κ_1.

Example 7.3.1. *In the case $N = 3$, Figure 7.7 shows a collision of three dark solitons solution to the DS1$^-$ equation with the following choice of parameters: $w_a = 8$, $w_b = -10$, $w_{u_1} = 5 + 2\mathrm{i}$, $w_{u_2} = 20 + 10\mathrm{i}$, $w_{u_3} = -3 + \mathrm{i}$, $\kappa_1 = \kappa_2 = 1$, $d_k = h = 0$.*

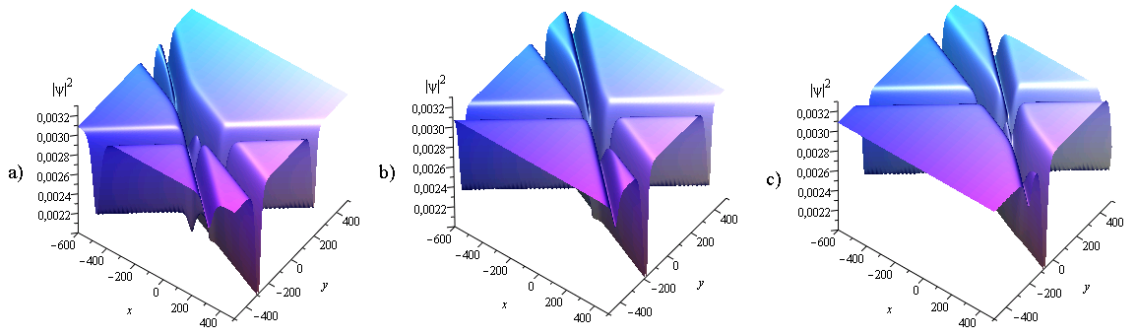

Figure 7.7: *Dark 3-soliton of DS1$^-$ at a) $t = -300$, b) $t = 0$, c) $t = 300$.*

Bright multi-soliton of DS1$^\rho$ and DS2$^-$.

In this part we construct bright multi-soliton solutions to the DS1$^\rho$ and DS2$^-$ equations. It is well known that such solutions can be written in terms of a quotient of sums of exponentials, for which the modulus tends to zero if the spatial variables tend to infinity.

To get bright multi-soliton solutions, one degenerates once more solutions (7.3.1) of the complexified system. Put $g = 2N$ and $A = |\kappa_1\kappa_2|^{1/2}\,|w_a - w_b|^{-1}$ in (7.3.1), and take $h \in \mathbb{R}$.

Degeneration. Choose a small parameter $\epsilon > 0$ and define $d_k = -\ln\epsilon + \hat{d}_k$, for $k = 1, \ldots, 2N$, and

$$\begin{aligned} w_{u_{2k-1}} &= w_a + \epsilon\,\alpha_{u_{2k-1}}^{-1}\,(w_a - w_b), & w_{v_{2k-1}} &= w_b + \epsilon\,\alpha_{v_{2k-1}}^{-1}\,(w_a - w_b), \\ w_{u_{2k}} &= w_b + \epsilon\,\alpha_{u_{2k}}^{-1}\,(w_a - w_b), & w_{v_{2k}} &= w_a + \epsilon\,\alpha_{v_{2k}}^{-1}\,(w_a - w_b), \end{aligned} \tag{7.3.8}$$

for $k = 1, \ldots, N$. Moreover, put $\kappa_1 = \epsilon\,\hat{\kappa}_1\,(w_a - w_b)$, and $\kappa_2 = \epsilon\,\hat{\kappa}_2\,(w_a - w_b)$. Consider in the determinant $\det(\mathbb{T}_1)$ appearing in (7.3.1) the substitution

$$L_{2i} \longrightarrow L_{2i} - \frac{(\mathbb{T}_1)_{2i,2}}{(\mathbb{T}_1)_{2,2}}\,L_2$$

for $i = 2, \ldots, N$, where L_k denotes the line number k of the matrix $\mathbb{T}_1$ and $(\mathbb{T}_1)_{i,k}$ the entries of this matrix. An analogous transformation has to be considered for the matrix $\mathbb{T}_{-1}$ appearing in

function ψ^*. Now take the limit $\epsilon \to 0$ in (7.3.1). The function ψ obtained in this limit has the form (7.3.11). Notice that in this limit, the dependence on the parameters w_a and w_b disappears.

Reality condition for DS1$^\rho$. It is straightforward to see that, with the following choice of parameters,

$$\hat\kappa_1, \hat\kappa_2 \in \mathbb{R} \setminus \{0\}\,, \quad \overline{\hat d_{2k-1}} = \hat d_{2k}, \quad \overline{\alpha_{u_{2k-1}}} = \alpha_{v_{2k}}, \quad \overline{\alpha_{u_{2k}}} = \alpha_{v_{2k-1}}, \qquad k = 1, \dots, N, \tag{7.3.9}$$

the functions ψ and ψ^* obtained in the limit considered here satisfy the reality condition $\psi^* = \rho\,\overline{\psi}$ with $\rho = -\operatorname{sign}(\hat\kappa_1\hat\kappa_2)$.

Reality condition for DS2$^-$. In the same way, with the following choice of parameters,

$$\overline{\hat\kappa_1} = \hat\kappa_2, \quad \overline{\hat d_{2k-1}} = \hat d_{2k}, \quad \overline{\alpha_{u_{2k-1}}} = \alpha_{u_{2k}}, \quad \overline{\alpha_{v_{2k-1}}} = \alpha_{v_{2k}}, \qquad k = 1, \dots, N, \tag{7.3.10}$$

the functions ψ and ψ^* obtained in the considered limit satisfy the reality condition $\psi^* = -\,\overline{\psi}$.

The solutions. Let $\theta \in \mathbb{R}$. With (7.3.9), the following functions of the variables ξ, η, t obtained in the considered limit, give bright N-soliton solutions of DS1$^\rho$ where $\rho = -\operatorname{sign}(\hat\kappa_1\hat\kappa_2)$ and $\gamma = 0$; because of (7.3.10) these functions define bright N-soliton solutions of DS2$^-$ where $\gamma = 1$:

$$\begin{aligned}
\psi(\xi,\eta,t) &= \hat A\, e^{\mathrm{i}\theta}\, \frac{\det(\mathbb{K})}{\det(\mathbb{M})},\\
\phi(\xi,\eta,t) &= \frac{1}{2}\,(\ln\det(\mathbb{M}))_{\xi\xi} + \frac{1}{2}\,(\ln\det(\mathbb{M}))_{\eta\eta} + \frac{h}{4},
\end{aligned} \tag{7.3.11}$$

where $\hat A = |\hat\kappa_1\hat\kappa_2|^{1/2}$. Here $\mathbb{K}$ and $\mathbb{M}$ are $2N \times 2N$ matrices with entries $(\mathbb{K})_{ik}$ and $(\mathbb{M})_{ik}$ given by:

$$\begin{aligned}
\text{- for } i \text{ and } k \text{ even:} \quad (\mathbb{K})_{ik} &= \delta_{i,k} - \delta_{2,i}\,\delta_{2,k} + \delta_{2,i}\, e^{\frac{1}{2}(z_2+z_k+\hat r_2+\hat r_k)}\\
&\quad + \delta_{2,k}\,(\delta_{2,i}-1)\, e^{\frac{1}{2}(z_i-z_2+\hat r_i-\hat r_2)}\\
\text{- for } i \text{ even and } k \text{ odd:} \quad (\mathbb{K})_{ik} &= -\,\frac{\alpha_{u_k}^2}{\alpha_{v_i}-\alpha_{u_k}}\,\frac{\alpha_{v_2}-\alpha_{v_i}}{\alpha_{v_2}-\alpha_{u_k}}\, e^{\frac{1}{2}(z_i+z_k+\hat r_i+\hat r_k)}\\
\text{- for } i \text{ odd and } k \text{ even:} \quad (\mathbb{K})_{ik} &= -\,\frac{\alpha_{v_i}\,\alpha_{u_k}}{\alpha_{v_i}-\alpha_{u_k}}\, e^{\frac{1}{2}(z_i+z_k+\hat r_i+\hat r_k)}\\
\text{- for } i \text{ and } k \text{ odd:} \quad (\mathbb{K})_{ik} &= \delta_{i,k},
\end{aligned}$$

$$\begin{aligned}
\text{- for } i,k \text{ even, or } i,k \text{ odd:} \quad (\mathbb{M})_{ik} &= \delta_{i,k}\\
\text{- otherwise:} \quad (\mathbb{M})_{ik} &= (-1)^{i+1}\,\frac{\alpha_{v_i}\,\alpha_{u_k}}{\alpha_{v_i}-\alpha_{u_k}}\, e^{\frac{1}{2}(z_i+z_k)}.
\end{aligned}$$

Here z_i, $i = 1, \dots, 2N$, is a linear function of the variables ξ, η and t given by:

$$z_{2k-1} = \mathrm{i}\,\hat\kappa_1\,\alpha_{u_{2k-1}}\,\xi + \mathrm{i}\,\hat\kappa_2\,\alpha_{v_{2k-1}}\,\eta + \mathrm{i}\left(\hat\kappa_1^2\,\alpha_{u_{2k-1}}^2 + \hat\kappa_2^2\,\alpha_{v_{2k-1}}^2\right)\frac{t}{2} - \hat d_{2k-1} + \gamma\,\frac{\mathrm{i}\pi}{2},$$

$$z_{2k} = -\,\mathrm{i}\,\hat\kappa_1\,\alpha_{v_{2k}}\,\xi - \mathrm{i}\,\hat\kappa_2\,\alpha_{u_{2k}}\,\eta - \mathrm{i}\left(\hat\kappa_1^2\,\alpha_{v_{2k}}^2 + \hat\kappa_2^2\,\alpha_{u_{2k}}^2\right)\frac{t}{2} - \hat d_{2k} + \gamma\,\frac{\mathrm{i}\pi}{2},$$

for $k = 1, \ldots, N$. Moreover, the scalars $\hat{r}_k$ are defined by

$$\hat{r}_k = (-1)^k \ln\{-\alpha_{v_k}\alpha_{u_k}\}, \qquad k = 1, \ldots, 2N.$$

Remark 7.3.4. i) With (7.3.9), functions (7.3.11) give a family of bright multi-soliton solutions of the DS1$^\rho$ equation depending on $3N$ complex parameters $\hat{d}_{2k-1}, \alpha_{u_{2k-1}}, \alpha_{u_{2k}}$ and 4 real parameters $h, \theta, \hat{\kappa}_1, \hat{\kappa}_2$.
ii) With (7.3.10), functions (7.3.11) provide a family of bright multi-soliton solutions of the DS2$^-$ equation depending on $3N+1$ complex parameters $\hat{d}_{2k-1}, \alpha_{u_{2k-1}}, \alpha_{v_{2k-1}}, \hat{\kappa}_1$ and 2 real parameters h, θ.

Example 7.3.2. *In the case $N = 2$, Figure 7.8 shows an elastic collision of two bright solitons solution of the DS2$^-$ equation with the following choice of parameters: $w_a = 10 + 20\mathrm{i}$, $w_b = 10 - 20\mathrm{i}$, $\alpha_{u_1} = 5 + 2\mathrm{i}$, $\alpha_{v_1} = 2 + \mathrm{i}$, $\alpha_{u_3} = 3 + \mathrm{i}$, $\alpha_{v_3} = 1 + 4\mathrm{i}$, $\hat{\kappa}_1 = 1$, $\hat{d}_k = h = 0$.*

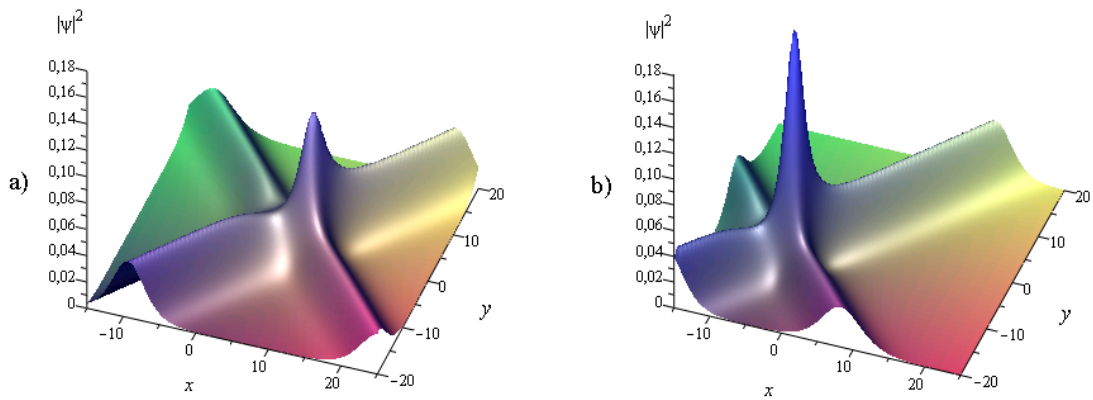

Figure 7.8: *Bright 2-soliton of DS2$^-$ at a) $t = 0$, b) $t = 50$.*

7.3.3 Breather and rational breather solutions of the DS equations

The breather solutions of the DS equation were found in [143]. Here a family of breather solutions and rational breather solutions of the DS1 equation are derived from algebro-geometric solutions. These solutions resemble their $1+1$ dimensional analogues. In particular, the profiles of the corresponding solutions of the DS equation in the (x, y, t) coordinates look in the (x, y) plane as those in the (x, t) coordinates.

Multi-Breathers of DS1$^\rho$.

The N-breather solution obtained here corresponds to an elastic interaction between N breathers. Put $g = 2N$ and $A = |\kappa_1\kappa_2|^{1/2}|w_a - w_b|^{-1}$ in (7.3.1). It is straightforward to see that with the following choice of parameters,

$$w_a, w_b, h \in \mathbb{R}, \quad \kappa_1, \kappa_2 \in \mathbb{R} \setminus \{0\}, \quad \overline{d_{2k-1}} = d_{2k}, \quad \overline{w_{v_{2k}}} = w_{u_{2k-1}}, \quad \overline{w_{v_{2k-1}}} = w_{u_{2k}}, \tag{7.3.12}$$

for $k = 1, \ldots, N$, functions ψ and ψ^* (7.3.1) satisfy the reality condition $\psi^* = \rho\overline{\psi}$ with $\rho = -\operatorname{sign}(\kappa_1\kappa_2)$. Therefore, analogously to the n-NLS equation, the functions ψ and ϕ in (7.3.1) give N-breather solutions of DS1$^\rho$.

Remark 7.3.5. One gets a family of breather solutions of DS1$^\rho$ depending on $3N$ complex parameters d_{2k-1}, $w_{u_{2k-1}}, w_{u_{2k}}$ and 6 real parameters $w_a, w_b, h, \kappa_1, \kappa_2$ and a phase θ.

Example 7.3.3. *Figure 7.9 shows the evolution in time of the 2-breather solution of DS1$^-$ with the following choice of parameters:* $w_a = 8$, $w_b = -1$, $w_{u_1} = 5 - 2\mathrm{i}$, $w_{u_2} = 2 + \mathrm{i}$, $w_{u_3} = 3 - \mathrm{i}$, $w_{u_4} = 1 + 4\mathrm{i}$, $\kappa_1 = \kappa_2 = 1$, $d_k = h = 0$.

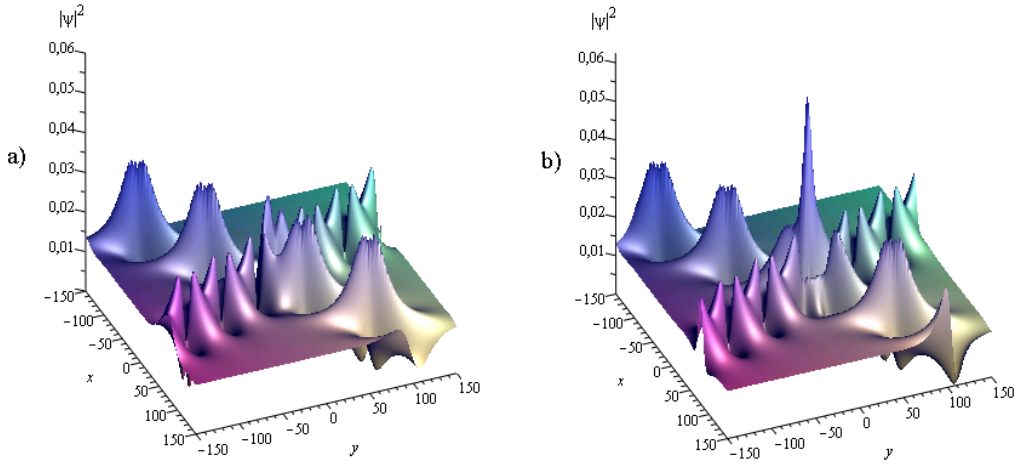

Figure 7.9: 2-*breather of DS1$^-$ at a)* $t = 0$, *b)* $t = 45$.

Multi-rational breathers of DS1$^\rho$.

In this part, we deal with rational solutions (modulo an exponential factor) of the DS1$^\rho$ equation. These solutions are obtained as limiting cases of the breather solutions. The N-rational solutions describe elastic interactions between N rational breathers, and are expressed as a quotient of two polynomials of degree N in the variables ξ, η, t.

Assume $g = 2N$ and put $A = |\kappa_1\kappa_2|^{1/2}\,|w_a - w_b|^{-1}$ in (7.3.1).

Degeneration. Let $\epsilon > 0$ be a small parameter and define $d_k = \epsilon\,\hat{d}_k + \mathrm{i}\pi$, for $k = 1, \ldots, 2N$, and

$$w_{v_{2k-1}} = w_{u_{2k-1}} + \epsilon\,\alpha_{v_{2k-1}}, \qquad w_{u_{2k}} = w_{v_{2k}} + \epsilon\,\alpha_{u_{2k}}, \tag{7.3.13}$$

for $k = 1, \ldots, N$. It is straightforward to see that $\det(\mathbb{T}_\beta) \approx \epsilon^{2N} P_\beta$, where P_β is a polynomial of degree $2N$ with respect to the variables ξ, η and t. Now take the limit $\epsilon \to 0$ in (7.3.1). The function ψ obtained in this limit is an N-rational breather solution of DS1$^\rho$ given by (7.3.15).

Reality condition. By imposing the following constraints on the parameters:

$$w_a, w_b, h \in \mathbb{R}, \quad \kappa_1, \kappa_2 \in \mathbb{R} \setminus \{0\}, \quad \overline{\hat{d}_{2k}} = \hat{d}_{2k-1}, \quad \overline{w_{u_{2k-1}}} = w_{v_{2k}}, \quad k = 1, \dots, N, \tag{7.3.14}$$

it can be seen that the functions ψ and ψ^* (7.3.1) in the considered limit satisfy the reality condition $\psi^* = \rho\,\overline{\psi}$, with $\rho = -\operatorname{sign}(\kappa_1\kappa_2)$.

The solutions. Let $\theta \in \mathbb{R}$. Then the following degenerated functions define N-rational breather solutions of DS1$^\rho$

$$\begin{aligned}
\psi(\xi,\eta,t) &= A\,e^{\mathrm{i}\theta}\,\frac{\det(\mathbb{K}_1)}{\det(\mathbb{K}_0)}\,\exp\left\{-\mathrm{i}\,(G_1\,\xi + G_2\,\eta - G_3\,\tfrac{t}{2})\right\},\\
\phi(\xi,\eta,t) &= \frac{1}{2}\,(\ln\det(\mathbb{K}_0))_{\xi\xi} + \frac{1}{2}\,(\ln\det(\mathbb{K}_0))_{\eta\eta} + \frac{h}{4},
\end{aligned} \tag{7.3.15}$$

where $\mathbb{K}_\beta$, with $\beta = 0, 1$, is a $2N \times 2N$ matrix with entries $(\mathbb{K}_\beta)_{ik}$ given by

$$\begin{aligned}
\text{- for } i \text{ and } k \text{ even:} \quad (\mathbb{K}_\beta)_{ik} &= (1-\delta_{i,k})\,\frac{1}{w_{v_i} - w_{v_k}} - \delta_{i,k}\,(z_k + \beta\,\hat{r}_k)\\
\text{- for } i \text{ even and } k \text{ odd:} \quad (\mathbb{K}_\beta)_{ik} &= \frac{1}{w_{v_i} - w_{u_k}}\\
\text{- for } i \text{ odd and } k \text{ even:} \quad (\mathbb{K}_\beta)_{ik} &= -\,\frac{1}{w_{u_i} - w_{v_k}}\\
\text{- for } i \text{ and } k \text{ odd :} \quad (\mathbb{K}_\beta)_{ik} &= -\,(1-\delta_{i,k})\,\frac{1}{w_{u_i} - w_{u_k}} - \delta_{i,k}\,(z_k + \beta\,\hat{r}_k).
\end{aligned}$$

Here z_k is a linear function of the variables ξ, η and t given by

$$z_k = \mathrm{i}\,\kappa_1\hat{V}_{a,k}\,\xi - \mathrm{i}\,\kappa_2\hat{V}_{b,k}\,\eta + \mathrm{i}\left(\kappa_1^2\,\hat{W}_{a,k} - \kappa_2^2\,\hat{W}_{b,k}\right)\frac{t}{2} - \hat{d}_k.$$

Moreover, for $c \in \{a, b\}$, the scalars $\hat{V}_{c,k}, \hat{W}_{c,k}$ and $\hat{r}_k$ satisfy $\overline{\hat{V}_{c,2k}} = \hat{V}_{c,2k-1}$, $\overline{\hat{W}_{c,2k}} = \hat{W}_{c,2k-1}$ and $\overline{\hat{r}_{2k}} = \hat{r}_{2k-1}$, and are given by:

$$\hat{V}_{c,2k-1} = \frac{1}{(w_c - w_{u_{2k-1}})^2}, \qquad \hat{W}_{c,2k-1} = -\,\frac{2}{(w_c - w_{u_{2k-1}})^3},$$

$$\hat{r}_{2k-1} = -\,\frac{w_a - w_b}{(w_a - w_{u_{2k-1}})\,(w_b - w_{u_{2k-1}})},$$

for $k = 1, \dots, N$. Constants G_1, G_2, G_3 are given in (7.3.4).

Remark 7.3.6. Functions (7.3.15) give a family of rational solutions of DS1$^\rho$ depending on $2N$ complex parameters $d_{2k-1}, w_{u_{2k-1}}$ and 6 real parameters $w_a, w_b, h, \theta, \kappa_1, \kappa_2$.

Example 7.3.4. *Figure 7.10 shows the evolution in time of the 2-rational breather solution of DS1$^-$ with the following choice of parameters:* $w_a = 2$, $w_b = 1$, $w_{u_1} = 2\mathrm{i}$, $w_{u_3} = 2 + \mathrm{i}$, $\kappa_1 = \kappa_2 = 1$, $d_k = h = 0$.

Example 7.3.5. *Figure 7.11 (resp. Figure 7.12) shows the interaction between a line rational breather and a rational breather solution of DS1$^-$ with the following choice of parameters:* $w_a = 2$, $w_b = -2$, $w_{u_1} = 3\mathrm{i}$ *(resp.* $w_{u_1} = 3\mathrm{i} + 1$*)*, $w_{u_3} = 2\mathrm{i}$, $\kappa_1 = \kappa_2 = 1$, $d_k = h = 0$. *By line rational breather we denote a growing and decaying mode localized only in one direction.*

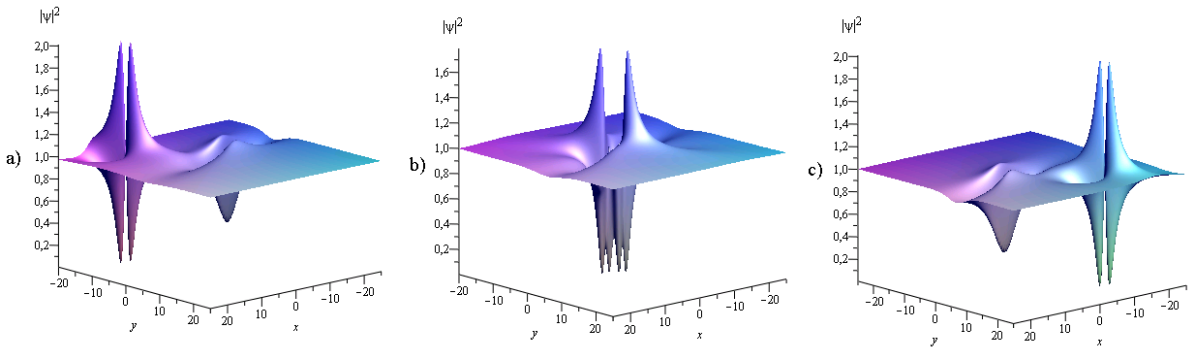

Figure 7.10: 2-*rational breather of DS1*$^-$ *at a)* $t=-5$, *b)* $t=0$, *c)* $t=5$.

7.3.4 Dromion and lump solutions of the DS equations

Here we construct the dromion solution of DS1$^\rho$ and the lump solution of DS2$^-$ which correspond to solutions with exponential decrease in all directions of the plane. Such solutions are derived by suitable degenerations of solutions (7.3.1) to the complexified system, and by imposing the reality condition $\overline{\psi^*}=\rho\,\psi$. This appears to be the first time that such solutions are obtained as limiting cases of theta-functional solutions.

Dromion of DS1$^\rho$.

Boiti et al. [26] have shown that the DS1 equation has solutions that decay exponentially in all directions. The solutions they obtained can move along any direction in the plane, and the only effect of their interactions is a shift in their position, independently of their relative initial position in the plane. Later, Fokas and Santini [63, 140] pointed out that by an appropriate choice of the boundary conditions, the localized solitons (called 'dromions') of the DS1 equation possess properties which are different from the properties of one-dimensional solitons, namely, the obtained solutions do not preserve their form upon interaction. For a particular choice of their spectral parameters, they recovered solutions previously derived by Boiti et al. For details on the theory of dromion solutions the reader is referred to [135] and references therein. In this section we explore how the simplest dromion solution can be derived from algebro-geometric solutions.

Let us consider solutions of the complexified system obtained in (7.3.1). Assume $g=4$ and put $A=|\kappa_1\kappa_2|^{1/2}\,|w_a-w_b|^{-1}$.

Degeneration. Choose a small parameter $\epsilon>0$ and define $d_k=-\ln(\epsilon)+\hat{d}_k$ for $k=1,\dots,4$, and

$$\begin{aligned}
&w_{u_1}=\epsilon\,\alpha_{u_1}, && w_{u_2}=w_a+\epsilon\,\alpha_{u_2}, && w_{u_3}=w_b+\epsilon\,\alpha_{u_3}, && w_{u_4}=\epsilon\,\alpha_{u_4},\\
&w_{v_1}=w_a+\epsilon\,\alpha_{v_1}, && w_{v_2}=\epsilon\,\alpha_{v_2}, && w_{v_3}=\epsilon\,\alpha_{v_3}, && w_{v_4}=w_b+\epsilon\,\alpha_{v_4}.
\end{aligned}\tag{7.3.16}$$

Moreover, put $\kappa_1=\epsilon\,\hat{\kappa}_1\,\alpha_{v_1}$ and $\kappa_2=\epsilon\,\hat{\kappa}_2\,\alpha_{u_3}$. Now consider the limit $\epsilon\to 0$ in (7.3.1). The functions ψ and ϕ obtained in this limit are given by (7.3.18).

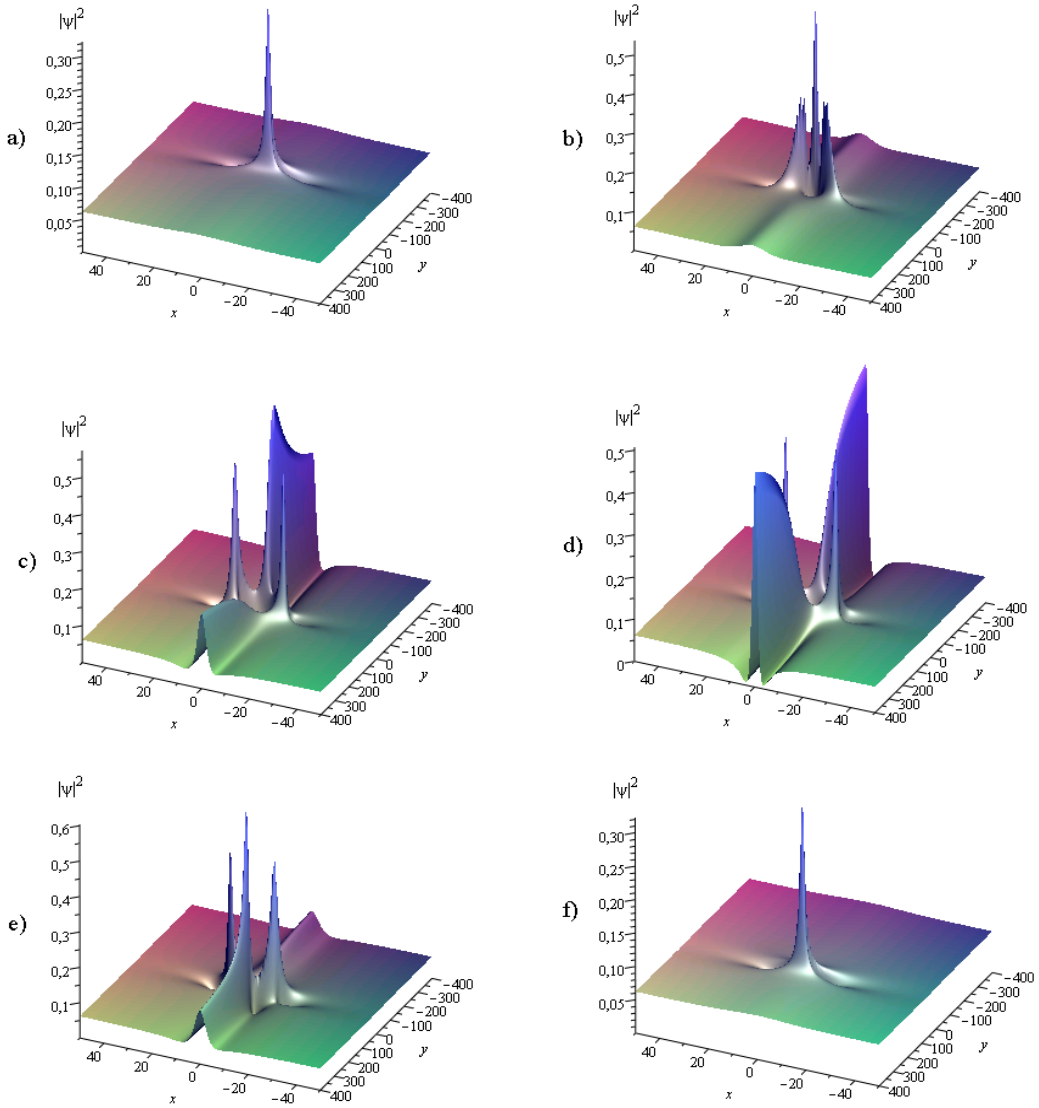

Figure 7.11: *Interaction between a line rational breather and a rational breather of DS1⁻ at a)* $t = -50$, *b)* $t = -20$, *c)* $t = -5$, *d)* $t = 0$, *e)* $t = 10$, *f)* $t = 50$. *The rational breather propagates in the same direction as the line breather.*

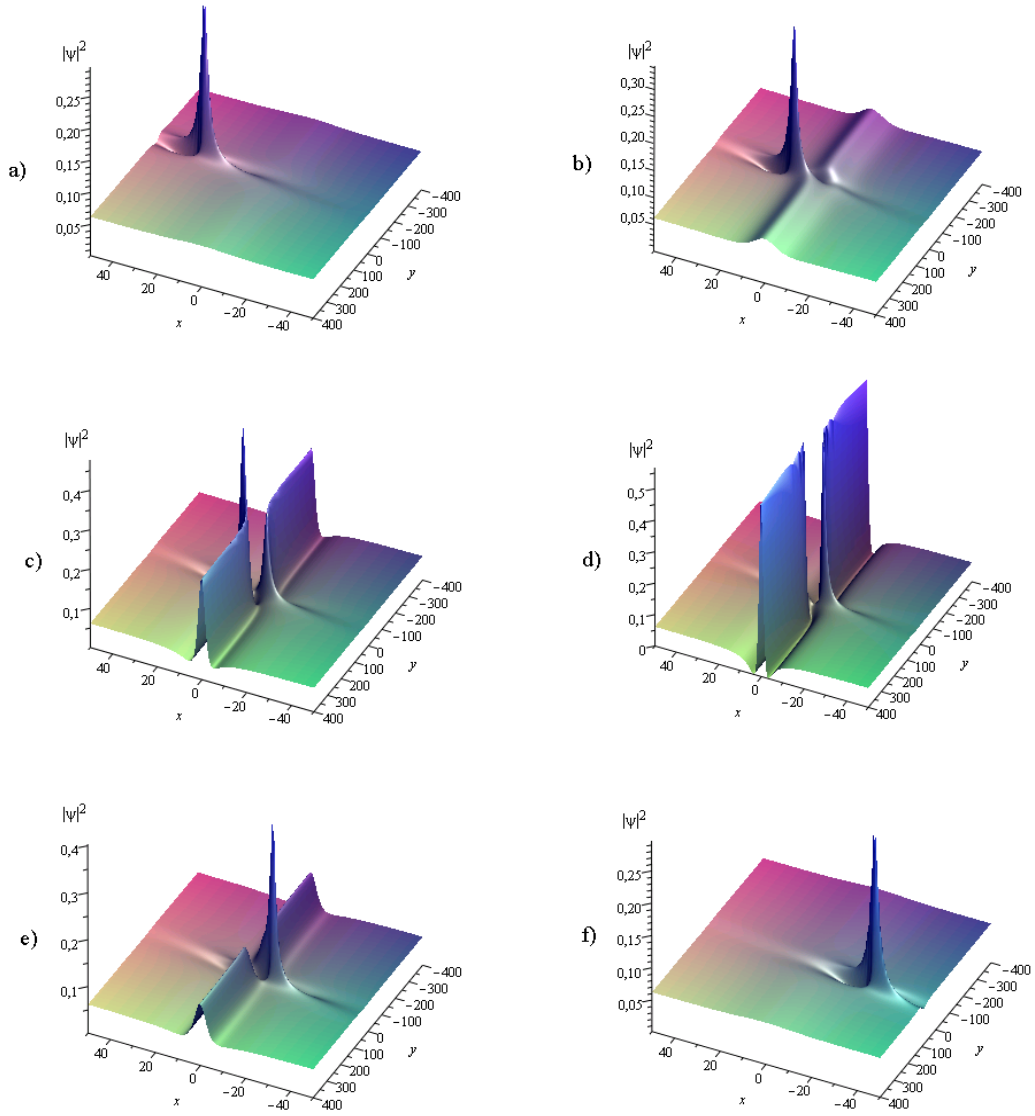

Figure 7.12: *Interaction between a line rational breather and a rational breather of DS1⁻ at a)* $t = -50$, *b)* $t = -20$, *c)* $t = -5$, *d)* $t = 0$, *e)* $t = 10$, *f)* $t = 50$. *The rational breather propagates transversally to the direction of the line breather.*

Reality condition. Choose $w_a, w_b, h, \theta \in \mathbb{R}$ and $\hat{\kappa}_1, \hat{\kappa}_2 \in \mathbb{R} \setminus \{0\}$. Moreover, assume

$$\overline{\hat{d}_{2k}} = \hat{d}_{2k-1}, \quad \overline{\alpha_{v_{2k-1}}} = \alpha_{u_{2k}}, \quad \overline{\alpha_{v_{2k}}} = \alpha_{u_{2k-1}}, \qquad k = 1, 2. \tag{7.3.17}$$

Put $\rho = -\operatorname{sign}(\hat{\kappa}_1 \hat{\kappa}_2)$. With (7.3.17), it can be seen that the degenerated functions ψ and ψ^* obtained in the considered limit satisfy the reality condition $\psi^* = \rho\,\overline{\psi}$. Therefore, the following degenerated functions give the dromion solution of DS1$^\rho$

$$\begin{aligned} \psi(\xi, \eta, t) &= \hat{A}\, e^{\mathrm{i}\theta}\, \frac{e^{z_1+z_3}}{\varphi(\xi, \eta, t)}, \\ \phi(\xi, \eta, t) &= \frac{1}{2}\, \partial_{\xi\xi} \ln\{\varphi(\xi, \eta, t)\} + \frac{1}{2}\, \partial_{\eta\eta} \ln\{\varphi(\xi, \eta, t)\} + \frac{h}{4}, \end{aligned} \tag{7.3.18}$$

where

$$\varphi(\xi, \eta, t) = 1 + A_1\, e^{2\,\mathrm{Re}(z_1)} + A_2\, e^{2\,\mathrm{Re}(z_3)} + A_3\, e^{2\,\mathrm{Re}(z_1)+2\,\mathrm{Re}(z_3)}.$$

Here z_k is a linear function of the variables ξ, η, t given by

$$z_1 = -\,\mathrm{i}\, \frac{\hat{\kappa}_1}{\alpha_{v_1}}\, \xi - \mathrm{i}\, \frac{\hat{\kappa}_1^2}{\alpha_{v_1}^2}\, \frac{t}{2} - \hat{d}_1, \qquad z_3 = -\,\mathrm{i}\, \frac{\hat{\kappa}_2}{\alpha_{u_3}}\, \eta - \mathrm{i}\, \frac{\hat{\kappa}_2^2}{\alpha_{u_3}^2}\, \frac{t}{2} - \hat{d}_3.$$

The constants $\hat{A}, A_1, A_2$ and A_3 are given by

$$\hat{A} = |\hat{\kappa}_1 \hat{\kappa}_2|^{1/2}\, \frac{w_a\, w_b}{(\alpha_{v_3} - \alpha_{u_1})\, \alpha_{v_1} \alpha_{u_3}}, \qquad A_1 = \frac{w_a}{4\,\mathrm{Im}(\alpha_{v_1})\,\mathrm{Im}(\alpha_{u_1})},$$

$$A_2 = \frac{w_b}{4\,\mathrm{Im}(\alpha_{v_3})\,\mathrm{Im}(\alpha_{u_3})}, \qquad A_3 = A_1\, A_2 + \frac{w_a\, w_b}{4\,\mathrm{Im}(\alpha_{v_1})\,\mathrm{Im}(\alpha_{u_3})}\, \frac{1}{|\alpha_{u_1} - \alpha_{v_3}|^2}\,.$$

Moreover, in the case where $A_1 > 0$, $A_2 > 0$ and $A_3 > 0$, functions (7.3.18) are smooth solutions of DS1$^\rho$.

Remark 7.3.7. i) The functions (7.3.18) define a family of dromion solutions of DS1$^\rho$ depending on 6 complex parameters $\hat{d}_1, \hat{d}_3, \alpha_{u_1}, \alpha_{v_1}, \alpha_{u_3}, \alpha_{v_3}$ and 6 real parameters $w_a, w_b, \hat{\kappa}_1, \hat{\kappa}_2, h, \theta$.
ii) In the case where $\alpha_{u_1}, \alpha_{v_3} \in \mathbb{R}$, one gets localized breathers, namely, the solution oscillates with respect to the time variable (modulus of ψ is constant with respect to t).

Example 7.3.6. *Figure 7.13 shows the evolution in time of the dromion solution of DS1$^-$ for the following choice of parameters:* $w_a = 1$, $w_b = 2$, $\hat{\kappa}_1 = \hat{\kappa}_2 = 1$, $\alpha_{u_1} = 2 + \mathrm{i}$, $\alpha_{v_1} = -1 + \mathrm{i}$, $\alpha_{u_3} = 1 + 3\mathrm{i}$, $\alpha_{v_3} = 2\mathrm{i}$, $\hat{d}_1 = \hat{d}_3 = h = 0$.

Different degenerations can be investigated for larger values of g. The performed functions lead to particular solutions such as dromions which move along sets of straight and curved trajectories, as well as oscillating dromion solutions. We do not discuss these solutions here.

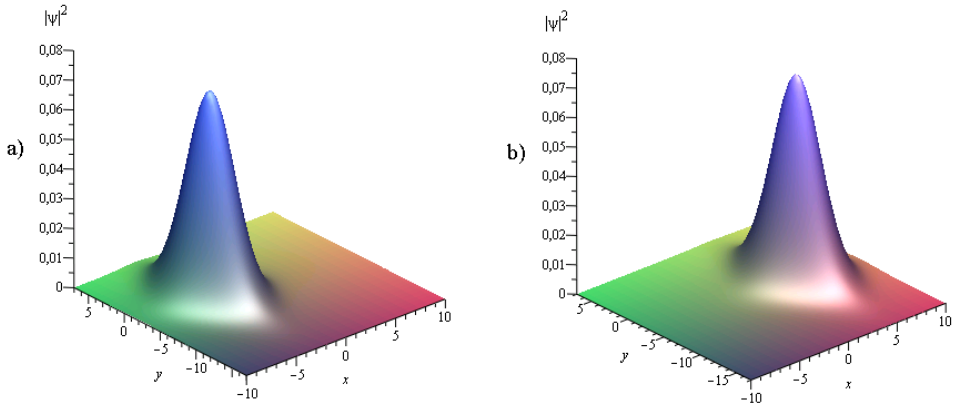

Figure 7.13: *A dromion solution of DS1⁻ at a) $t = -5$, b) $t = 10$.*

Lump of DS2$^-$.

The lump solutions were discovered in [111] for the KP1 equation, and have been extensively studied. Arkadiev et al. [18] have constructed a family of travelling waves (the lump solutions) of DS2$^-$ that we rediscover here.

Let us consider functions ψ, ψ^*, ϕ given in (7.3.1), assume $g = 2$ and put $A = |\kappa_1\kappa_2|^{1/2}|w_a - w_b|^{-1}$. Moreover, consider the following transformation which leaves the system (6.4.2) invariant:

$$\begin{aligned}
\psi(\xi,\eta,t) &\to \psi\left(\xi+\beta_1\,t,\eta+\beta_2\,t,t\right)\exp\left\{-\mathrm{i}\left(\beta_1\,\xi+\beta_2\,\eta+\left(\beta_1^2+\beta_2^2\right)\tfrac{t}{2}\right)\right\},\\
\psi^*(\xi,\eta,t) &\to \psi^*\left(\xi+\beta_1\,t,\eta+\beta_2\,t,t\right)\exp\left\{\mathrm{i}\left(\beta_1\,\xi+\beta_2\,\eta+\left(\beta_1^2+\beta_2^2\right)\tfrac{t}{2}\right)\right\},\\
\phi(\xi,\eta,t) &\to \phi\left(\xi+\beta_1\,t,\eta+\beta_2\,t,t\right),
\end{aligned} \tag{7.3.19}$$

where $\beta_i = \mu_i\,\kappa_i^{-1}$ for some $\mu_i \in \mathbb{C}$, $i = 1, 2$.

Degeneration. Choose a small parameter $\epsilon > 0$ and define $d_k = \mathrm{i}\pi + \epsilon\,\hat{d}_k$, for $k = 1, 2$, and

$$\begin{aligned}
w_{v_1} &= w_a + \epsilon\,\alpha_{v_1}, \qquad & w_{u_1} &= w_a + \epsilon\,\alpha_{u_1},\\
w_{v_2} &= w_b + \epsilon\,\alpha_{v_2}, \qquad & w_{u_2} &= w_b + \epsilon\,\alpha_{u_2}.
\end{aligned}$$

Moreover, put $\kappa_k = \epsilon^2\,\hat{\kappa}_k$, and $\mu_k = \epsilon^2\,\hat{\mu}_k$ for $k = 1, 2$. Now take the limit $\epsilon \to 0$ in (7.3.19). The functions ψ and ϕ obtained in this limit are given in (7.3.20).

Reality condition. Choose $w_a, w_b \in \mathbb{C}$ such that $\overline{w_a} = -\,w_b$ or $w_a, w_b \in \mathbb{R}$. Take $h, \theta \in \mathbb{R}$ and assume

$$\overline{\hat{\kappa}_1} = \hat{\kappa}_2, \quad \overline{\hat{\mu}_1} = \hat{\mu}_2, \quad \overline{\hat{d}_1} = \hat{d}_2, \quad \overline{\alpha_{v_1}} = \alpha_{v_2}, \quad \overline{\alpha_{u_1}} = \alpha_{u_2}.$$

With this choice of parameters, it can be seen that the functions ψ and ψ^* obtained in the limit considered here satisfy the reality condition $\psi^* = -\,\overline{\psi}$.

The solutions. Therefore, the following degenerated functions describe smooth solutions of DS2$^-$

$$\psi(x,y,t) = \frac{\hat{A}\, e^{\mathrm{i}\theta}}{\hat{B} + |z_1|^2} \exp\left\{-\mathrm{i}\left(2\,\mathrm{Re}(\beta_1\,\xi) + \mathrm{Re}(\beta_1^2)\,t\right)\right\},$$
$$\phi(x,y,t) = \frac{1}{2}\,\partial_{\xi\xi} \ln\left\{\hat{B} + |z_1|^2\right\} + \frac{1}{2}\,\partial_{\overline{\xi}\overline{\xi}} \ln\left\{\hat{B} + |z_1|^2\right\} + \frac{h}{4}, \tag{7.3.20}$$

where $\xi = x + \mathrm{i}y$ and $\beta_1 = \hat{\mu}_1\,\hat{\kappa}_1^{-1}$. Here $z_1 = \mathrm{i}\,\hat{V}_{a,1}\,(\hat{\kappa}_1\,\xi + \hat{\mu}_1\,t) - \hat{d}_1$ and

$$\hat{V}_{a,1} = -\frac{\alpha_{u_1} - \alpha_{v_1}}{\alpha_{u_1}\alpha_{v_1}}, \qquad \hat{A} = \frac{|\hat{\kappa}_1|\,|\alpha_{u_1} - \alpha_{v_1}|^2}{|w_a - w_b|\,\alpha_{v_1}\,\overline{\alpha_{u_1}}}, \qquad \hat{B} = \frac{|\alpha_{u_1} - \alpha_{v_1}|^2}{(w_b - w_a)^2}\,.$$

Simplifications. To simplify (7.3.20), put

$$\hat{d}_1 = -\frac{\mathrm{i}\,\mu}{\hat{V}_{a,1}\,\hat{\kappa}_1}, \quad \nu = \frac{\alpha_{u_1}\overline{\alpha_{v_1}}}{|\hat{\kappa}_1|\,|w_a - w_b|}, \quad \lambda = \beta_1,$$

for arbitrary $\mu \in \mathbb{C}$. In this way, functions (7.3.20) become

$$\psi(x,y,t) = \nu\,\frac{\exp\{-2\mathrm{i}\,\mathrm{Re}(\lambda\,\xi) - \mathrm{i}\,\mathrm{Re}(\lambda^2)\,t + \mathrm{i}\theta\}}{|\xi + \lambda\,t + \mu|^2 + |\nu|^2},$$
$$\phi(x,y,t) = \frac{1}{2}\,\partial_{\xi\xi} \ln\left\{|\xi + \lambda\,t + \mu|^2 + |\nu|^2\right\} + \frac{1}{2}\,\partial_{\overline{\xi}\overline{\xi}} \ln\left\{|\xi + \lambda\,t + \mu|^2 + |\nu|^2\right\} + \frac{h}{4}, \tag{7.3.21}$$

where $\xi = x + \mathrm{i}y$. Here λ, ν, μ are arbitrary complex constants, and $\theta, h \in \mathbb{R}$. Solutions (7.3.21) coincide with the lump solution previously obtained in [18].

Example 7.3.7. *Figure 7.14 shows the evolution in time of the lump solution of DS2$^-$ for the following choice of parameters:* $\lambda = -1 + \mathrm{i}$, $\nu = 2$, $\mu = 2\mathrm{i}$, $h = 0$.

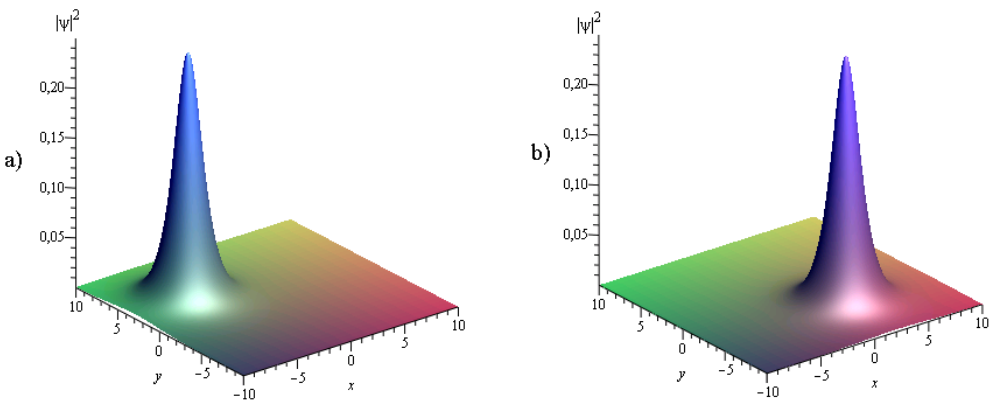

Figure 7.14: *A lump solution of DS2$^-$ at a) $t = -5$, b) $t = 2$.*

7.4 Outlook

Various classes of solutions to the multi-component NLS equation and the DS equations in terms of elementary functions have been presented as limiting cases of algebro-geometric solutions discussed in Chapter 6. We did not construct all families of solutions that can be found in the literature, but we believe that different degenerations will lead to interesting new or known solutions that are not presented here.

In particular, future investigations might address bright multi-solitons of n-NLS with inelastic collision. This novel type of inelastic collision, which is not observed in $1+1$ dimensional soliton systems, follows from a family of bright soliton solutions having more independent parameters than the ones presented here with standard elastic collision. We also believe that this kind of solutions arises from algebro-geometric solutions after suitable degenerations.

Chapter 8

On the numerical evaluation of algebro-geometric solutions

In the case of hyperelliptic surfaces, efficient algorithms exist even for almost degenerate surfaces. This allows the numerical study of solitonic limits. For general real Riemann surfaces, the choice of a homology basis adapted to the anti-holomorphic involution is important for a convenient formulation of the solutions and smoothness conditions. Since existing algorithms for algebraic curves produce a homology basis not related to automorphisms of the curve, we study symplectic transformations to an adapted basis and give explicit formulae for M-curves.

As examples we discuss solutions of the Davey-Stewartson equations (6.4.1) and the multi-component nonlinear Schrödinger equations (6.3.1) investigated in Chapter 6. We first consider the hyperelliptic case and study concrete examples of low genus, also in almost degenerate situations. Finally, we consider examples of non-hyperelliptic real Riemann surfaces and discuss symplectic transformations needed to construct smooth solutions.

8.1 Hyperelliptic case

In this section we consider concrete examples for the solutions, in terms of multi-dimensional theta functions, to the DS and n-NLS equations on hyperelliptic Riemann surfaces. We first review the numerical methods to visualize the solutions and discuss how to test the accuracy.

8.1.1 Computation on real hyperelliptic curves

The simplest example of algebraic curves are hyperelliptic curves,

$$\mu^2 = \begin{cases} \prod_{i=1}^{2g+2}(\lambda - \lambda_i), & \text{without branching at infinity} \\ \prod_{i=1}^{2g+1}(\lambda - \lambda_i), & \text{with branching at infinity} \end{cases},$$

where g is the genus of the Riemann surface, and where we have for the branch points $\lambda_i \in \mathbb{C}$ the relations $\lambda_i \neq \lambda_j$ for $i \neq j$. If the number of finite branch points is odd, the curve is branched at infinity. Recall that all Riemann surfaces of genus 2 are hyperelliptic, and that the involution σ which interchanges the sheets, $\sigma(\lambda, \mu) = (\lambda, -\mu)$, is an automorphism on any hyperelliptic curve. A vector of holomorphic differentials for these surfaces is given by $(1, \lambda, \ldots, \lambda^{g-1})^t \, \mathrm{d}\lambda/\mu$. For a real hyperelliptic curve the branch points are either real or pairwise conjugate. As we

saw in Example 3.1.1, if all branch points λ_i are real and ordered such that $\lambda_1 < \ldots < \lambda_{2g+2}$, the hyperelliptic curve is an M-curve with respect to both anti-holomorphic involutions τ_1 and τ_2 defined in the example. The other case of interest in the context of smooth solutions to n-NLS^s and DS are real curves without real branch point. For the involution τ_1, a curve given by $\mu^2 = \prod_{i=1}^{g+1}(\lambda - \lambda_i)(\lambda - \overline{\lambda}_i)$, with $\lambda_i \in \mathbb{C} \setminus \mathbb{R}$, $i = 1, \ldots, g+1$, in this case is dividing (two points whose projections onto $\mathbb{C}$ have respectively a positive and a negative imaginary part cannot be connected by a contour which does not cross a real oval), whereas a curve given by $\mu^2 = -\prod_{i=1}^{g+1}(\lambda - \lambda_i)(\lambda - \overline{\lambda}_i)$ has no real oval, and vice versa for the involution τ_2.

In the following, we will only consider real hyperelliptic curves without branching at infinity and write the defining equation in the form

$$\mu^2 = (\lambda - \xi)(\lambda - \eta) \prod_{i=1}^{g} (\lambda - E_i)(\lambda - F_i).$$

It is possible to introduce a convenient homology basis on the related surfaces, see Figure 8.1 for the case $\eta = \overline{\xi}$. The simple form of the algebraic relation between μ and λ for hyperelliptic curves makes the generation of very efficient numerical codes possible, see, for instance, [65, 66] for details. These codes allow the treatment of almost degenerate Riemann surfaces, i.e., the case where the branch points almost collide pairwise, where the distance of the branch points is of the order of machine precision: $|E_i - F_i| \sim 10^{-14}$. The homology basis Figure 8.1 is adapted to this kind of degeneration.

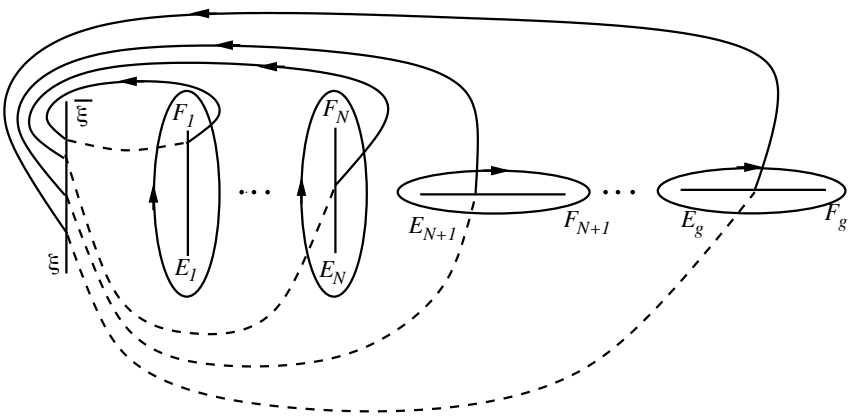

Figure 8.1: *Homology basis on the real hyperelliptic curves, contours on sheet 1 are solid, contours on sheet 2 are dashed. $\mathcal{A}$-cycles are the closed contours entirely on sheet 1.*

The Abel map $\int_a^b \omega$ between two points a and b is computed in the following way: the sheet identified at the point $a = (\lambda(a), \mu(a))$ (where we take for μ the root computed by Matlab) is labeled sheet 1, and at the point $(\lambda(a), -\mu(a))$, sheet 2. Then the ramification point whose projection to the λ-sphere has the minimal distance to $\lambda(a)$ is determined. For simplicity we assume always that this is the point ξ in Figure 8.1 (for another branch point, this leads to the addition of half-periods, see e.g. [23]). This means we compute $\int_a^b \omega$ as $\int_a^b \omega = \int_\xi^b \omega - \int_\xi^a \omega$. The choice of a branch point as the base point of the Abel map has the advantage that a change of

sheet of a point a just implies a change of sign of the integral:

$$\int_{\xi}^{(\lambda(a),\mu(a))} \omega = -\int_{\xi}^{(\lambda(a),-\mu(a))} \omega.$$

To compute the integral $\int_{\xi}^{a} \omega$, one has to analytically continue μ on the connecting line between $\lambda(a)$ and ξ onto the λ-sphere. Whereas the root μ is not supposed to have any branching on the considered path, the square root in Matlab is branched on the negative real axis. To analytically continue μ on the path $[\lambda(a), \xi]$, we compute the Matlab root at some $\lambda_j \in [\lambda(a), \xi]$, $j = 0, \ldots, N_c$ and analytically continue it starting from $\mu(a)$ by demanding that

$$|\mu(\lambda_{j+1}) - \mu(\lambda_j)| < |\mu(\lambda_{j+1}) + \mu(\lambda_j)|.$$

The so defined sheets will be denoted here and in the following by numbers, i.e., a point on sheet 1 with projection $\lambda(a)$ into the base is denoted by $(\lambda(a))^{(1)}$.

Thus the computation of the Abel map is reduced to the computation of line integrals on the connecting line between $\lambda(a)$ and ξ in the complex λ-plane. For the numerical computation of such integrals we use Clenshaw-Curtis integration (see, for instance, [147]): to compute an integral $\int_{-1}^{1} h(x)\,\mathrm{d}x$, this algorithm samples the integrand on the $N_c + 1$ Chebyshev collocation points $x_j = \cos(j\pi/N_c)$, $j = 0, \ldots, N_c$. The integral is approximated as the sum:

$$\int_{-1}^{1} h(x)\,\mathrm{d}x \sim \sum_{j=0}^{N_c} w_j\, h(x_j)$$

(see [147] on how to obtain the weights w_j). It can be shown that the convergence of the integral is exponential for analytic functions h as the ones considered here. To compute the Abel map, one uses the transformation $\lambda \to \lambda(a)(1+x)/2 + \xi(1-x)/2$, to the Clenshaw-Curtis integration variable. The same procedure is then carried out for the integral from ξ to b.

The theta functions are approximated as in [65] as a sum,

$$\Theta_{\mathbb{B}}[\delta](\mathbf{z}) \sim \sum_{m_1=-N_\theta}^{N_\theta} \cdots \sum_{m_g=-N_\theta}^{N_\theta} \exp\left\{\tfrac{1}{2}\langle \mathbb{B}(\mathbf{m}+\delta_1), \mathbf{m}+\delta_1\rangle + \langle \mathbf{m}+\delta_1, \mathbf{z}+2\mathrm{i}\pi\delta_2\rangle\right\}. \tag{8.1.1}$$

The periodicity properties of the theta function (2.2.3) make it possible to write $\mathbf{z} = \mathbf{z}_0 + 2\mathrm{i}\pi\mathbf{N} + \mathbb{B}\mathbf{M}$ for some $\mathbf{N}, \mathbf{M} \in \mathbb{Z}^g$, where $\mathbf{z}_0 = 2\mathrm{i}\pi\alpha + \mathbb{B}\beta$ with $\alpha_i, \beta_i \in \,]-\frac{1}{2}, \frac{1}{2}]$ for $i = 1, \ldots, g$. The value of N_θ is determined by the condition that all terms in (2.2.1) with $|m_i| > N_\theta$ are smaller than machine precision, which is controlled by the largest eigenvalue of the real part of the Riemann matrix (the one with minimal absolute value since the real part is negative definite), see [65, 67].

To control the accuracy of the numerical solutions, we use essentially two approaches. First we check the theta identity (6.1.1), which is the underlying reason for the studied functions being solutions to n-NLS^s and DS, at each point in the spacetime. This test requires the computation of theta derivatives not needed in the solution (which slightly reduces the efficiency of the code since additional quantities are computed), but provides an immediate check whether the solution satisfies (6.1.1) with the required accuracy. Since this identity is not implemented in the code, it provides a strong test. This ensures that all quantities entering the solution are computed with the necessary precision. In addition, the solutions are computed on Chebyshev collocation points

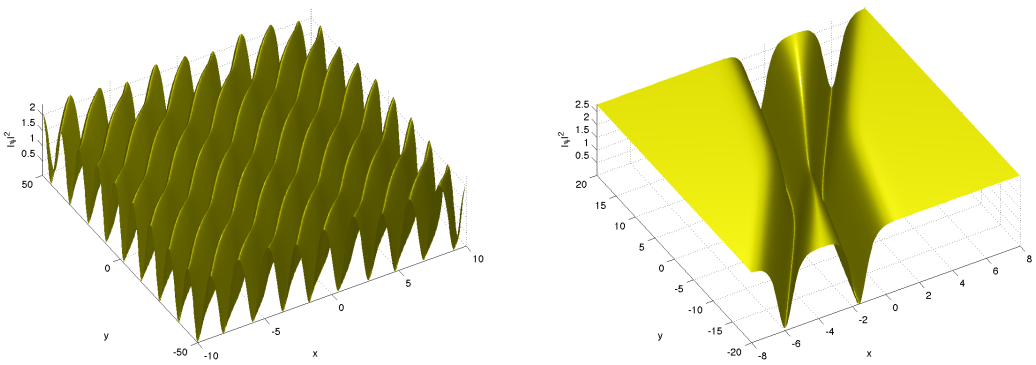

Figure 8.2: *Solution (6.4.10) to the DS1$^+$ equation at $t = 0$ on a hyperelliptic curve of genus 2 with branch points $-2, -1, 0, \epsilon, 2, 2+\epsilon$ and $a = (-1.9)^{(1)}$, $b = (-1.1)^{(2)}$ for $\epsilon = 1$ on the left and $\epsilon = 10^{-10}$, the almost solitonic limit, on the right.*

(see, for instance, [147]) for each of the physical variables. This can be used for an expansion of the computed solution in terms of Chebyshev polynomials, a so-called spectral method having in practice exponential convergence for analytic functions as the ones considered here. Since the derivatives of the Chebyshev polynomials can be expressed linearly in terms of Chebyshev polynomials, a derivative acts on the space of polynomials via a so called differentiation matrix. With these standard Chebyshev differentiation matrices (see [147]), the solution can be numerically differentiated. The computed derivatives allow to check with which numerical precision the PDE is satisfied by a numerical solution. With these two independent tests, we ensure that the shown solutions are correct to much better than plotting accuracy (the code reports a warning if the above tests are not satisfied to better than 10^{-6}).

8.1.2 Solutions to the DS equations

The elliptic solutions are the well known travelling wave solutions and will not be discussed here. The simplest examples we will consider for the DS solutions are given on hyperelliptic curves of genus 2. As we saw in Section 6.4.2, for DS1$^\rho$ reality and smoothness conditions imply that the branch points of the curve are either all real (M-curve) or all pairwise conjugate (dividing curve). The points a and b must project to real points on the λ-sphere and must be stable under the anti-holomorphic involution τ (we use here $\tau = \tau_1$, as defined in Example 3.1.1 except for DS2$^-$). For DS2$^\rho$, we have $\tau a = b$ where the projection of a onto the λ-sphere is the conjugate of the projection of b. For DS2$^+$ the curve must have only real branch points (M-curve), whereas for DS2$^-$ it must have no real oval.

For DS we will mainly give plots for fixed time since for low genus, the solution is essentially travelling in one direction. For higher genus, we show a more interesting time dependence in Figure 8.9.

We first consider the defocusing variants, DS1$^+$ and DS2$^+$ on M-curves. In genus 2 we study the family of curves with the branch points $-2, -1, 0, \epsilon, 2, 2+\epsilon$ for $\epsilon = 1$ and $\epsilon = 10^{-10}$. In the former case the solutions will be periodic in the (x, y)-plane, in the latter almost solitonic

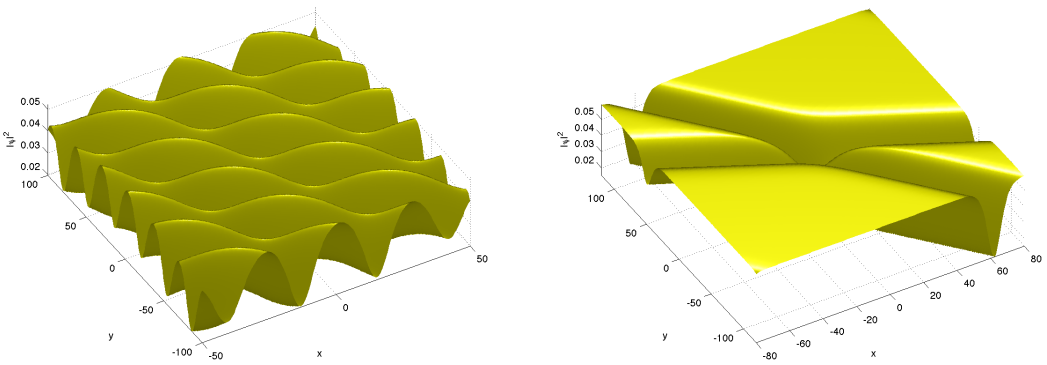

Figure 8.3: *Solution (6.4.20) to the DS2$^+$ equation at $t = 0$ on a hyperelliptic curve of genus 2 with branch points $-2, -1, 0, \epsilon, 2, 2+\epsilon$ and $a = (-1.5+2\mathrm{i})^{(1)}$, $b = (-1.5-2\mathrm{i})^{(2)}$ for $\epsilon = 1$ on the left and $\epsilon = 10^{-10}$, the almost solitonic limit, on the right.*

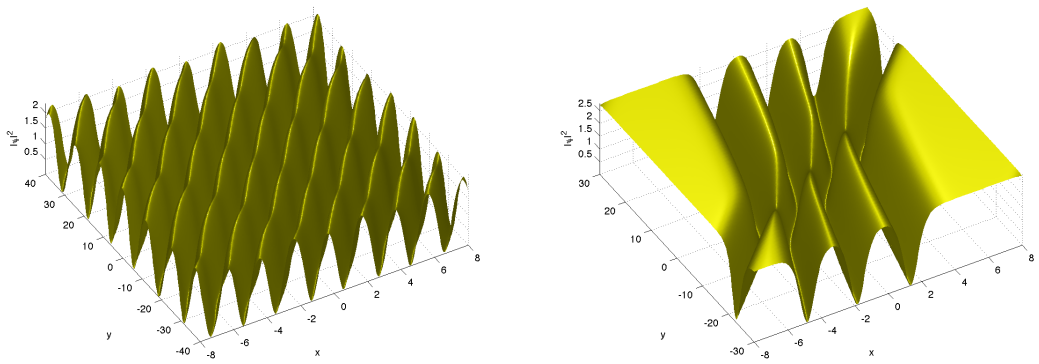

Figure 8.4: *Solution (6.4.10) to the DS1$^+$ equation at $t = 0$ on a hyperelliptic curve of genus 4 with branch points $-4, -3, -2, -2+\epsilon, 0, \epsilon, 2, 2+\epsilon, 4, 4+\epsilon$ and $a = (-3.9)^{(1)}$, $b = (-3.1)^{(2)}$ for $\epsilon = 1$ on the left and $\epsilon = 10^{-10}$, the almost solitonic limit, on the right.*

since the Riemann surface is almost degenerate (in the limit $\epsilon \to 0$ the surface degenerates to a surface of genus 0, and the resulting solutions have been discussed in more detail in Chapter 7). To obtain nontrivial solutions in the solitonic limit, we use $\mathbf{d} = \frac{1}{2}\left[\begin{smallmatrix}1 & 1\\ 0 & 0\end{smallmatrix}\right]^t$ in all examples. In Figure 8.2 it can be seen that these are in fact *dark solitons*, i.e., the solutions tend asymptotically to a non-zero constant and the solitons thus represent 'shadows' on a background of light. The well known features from soliton collisions for (1+1)-dimensional integrable equations, namely, the propagation without change of shape, and the unchanged shape and phase shift after the collision, can be seen here in the (x, y)-plane.

The corresponding solutions to DS2$^+$ can be seen in Figure 8.3. We only show the square modulus of the solution here for simplicity. For the real and the imaginary part of such a solution for the DS1$^-$-case, see Figure 8.6.

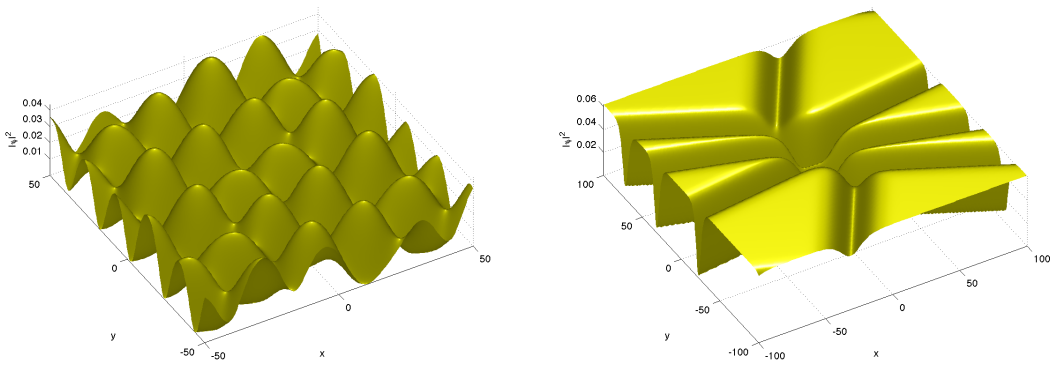

Figure 8.5: *Solution (6.4.20) to the DS2$^+$ equation at $t = 0$ on a hyperelliptic curve of genus 4 with branch points $-4, -3, -2, -2+\epsilon, 0, \epsilon, 2, 2+\epsilon, 4, 4+\epsilon$ and $a = (-1.5+2\mathrm{i})^{(1)}$, $b = (-1.5-2\mathrm{i})^{(1)}$ for $\epsilon = 1$ on the left and $\epsilon = 10^{-10}$, the almost solitonic limit, on the right.*

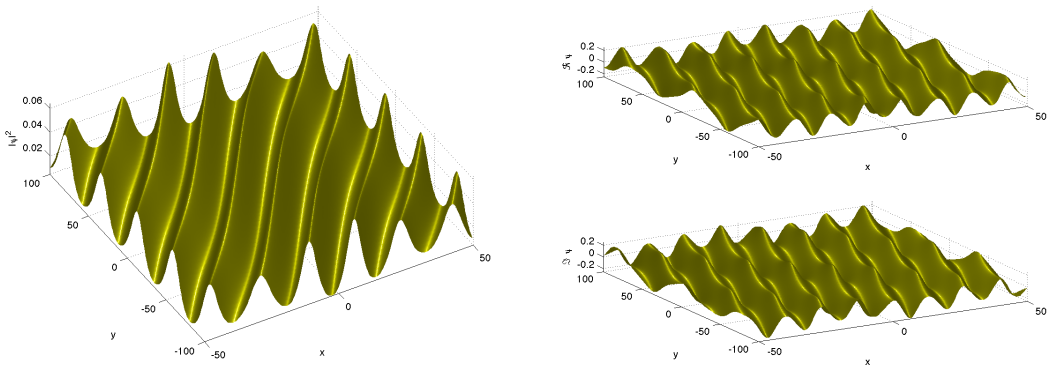

Figure 8.6: *Solution (6.4.10) to the DS1$^-$ equation at $t = 0$ on a hyperelliptic curve of genus 2 with branch points $-2 \pm \mathrm{i}$, $-1 \pm \mathrm{i}$, $1 \pm \mathrm{i}$ and $a = (-4)^{(1)}$, $b = (-3)^{(2)}$. The square modulus of the solution is shown on the left, real and imaginary parts on the right.*

In the same way one can study on a genus 4 hyperelliptic curve the formation of the dark 4-soliton for these two equations. We consider the curve with branch points $-4, -3, -2, -2+\epsilon, 0, \epsilon, 2, 2+\epsilon, 4, 4+\epsilon$ for $\epsilon = 1$ and $\epsilon = 10^{-10}$, and use $\mathbf{d} = \frac{1}{2}\left[\begin{smallmatrix}1&1&1&1\\0&0&0&0\end{smallmatrix}\right]^t$. The DS1$^+$ solutions for this curve can be seen in Figure 8.4. The corresponding solutions to DS2$^+$ is shown in Figure 8.5.

Solutions to the focusing variants of these equations can be obtained on hyperelliptic curves with pairwise conjugate branch points. For such solutions the solitonic limit cannot be obtained as above since the quotient of theta functions in (6.4.10) and (6.4.20) tends to a constant in this case. To obtain the well-known *bright solitons* (solutions tend to zero at spatial infinity) in this way, the hyperelliptic curve has to be completely degenerated (all branch points must collide pairwise to double points) which leads to limits of the form '0/0' in the expression for the solutions (6.4.10), (6.4.20) which are not convenient for a numerical treatment; see Chapter 7

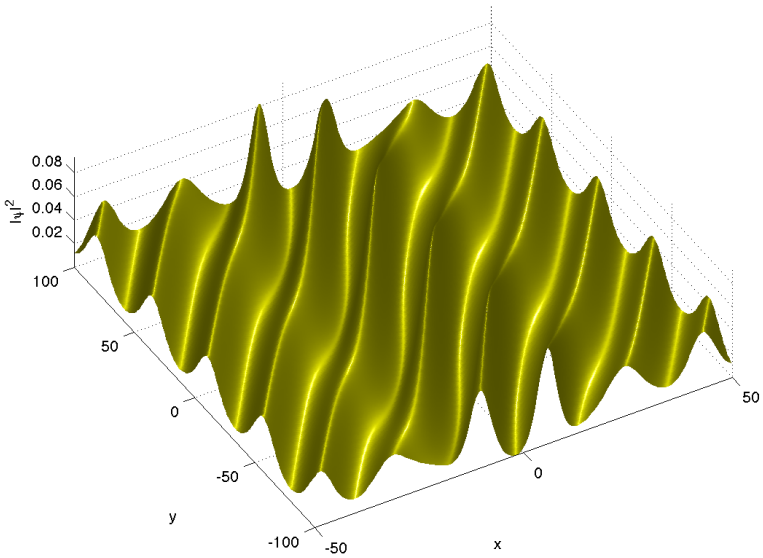

Figure 8.7: *Solution (6.4.10) to the DS1⁻ equation at* $t = 0$ *on a hyperelliptic curve of genus 4 with branch points* $-2 \pm \mathrm{i}$, $-1 \pm \mathrm{i}$, $\pm\mathrm{i}$, $1 \pm \mathrm{i}$, $2 \pm \mathrm{i}$ *and* $a = (-4)^{(1)}$, $b = (-3)^{(2)}$.

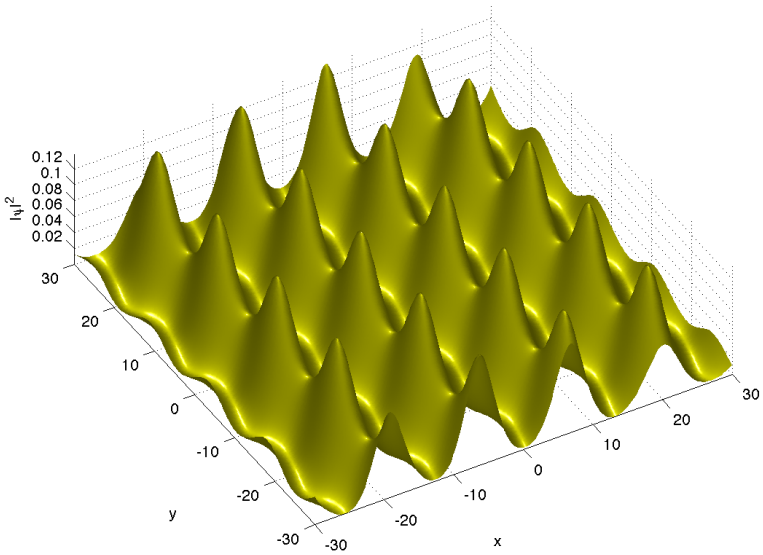

Figure 8.8: *Solution to the DS2⁻ equation at* $t = 0$ *on a hyperelliptic curve of genus 2 with branch points* $-2 \pm \mathrm{i}$, $-1 \pm \mathrm{i}$, $1 \pm \mathrm{i}$ *and* $a = (-1.5 + 2\mathrm{i})^{(1)}$, $b = (-1.5 - 2\mathrm{i})^{(2)}$.

for an analytic discussion. Therefore we only consider non-degenerate hyperelliptic curves here. To obtain smooth solutions, we use $\mathbf{d} = 0$. A solution in genus 2 of the DS1$^-$ equation is studied on the curve with the branch points $-2 \pm \mathrm{i}, -1 \pm \mathrm{i}, 1 \pm \mathrm{i}$ in Figure 8.6.

A typical example of a DS1$^-$ solution on a hyperelliptic curve of genus 4 with branch points $-2 \pm \mathrm{i}, -1 \pm \mathrm{i}, \pm\mathrm{i}, 1 \pm \mathrm{i}, 2 \pm \mathrm{i}$ is shown in Figure 8.7.

Smooth solutions to DS2$^-$ can be obtained on Riemann surfaces without real oval for points a and b satisfying $\tau a = b$. As mentioned above, hyperelliptic curves of the form $\mu^2 = -\prod_{i=1}^{2g+2}(\lambda - \lambda_i)$ with pairwise conjugate branch points have no real oval for the standard involution τ_1 as defined in Example 3.1.1. On the other hand, surfaces defined by the algebraic equation $\mu^2 = \prod_{i=1}^{2g+2}(\lambda - \lambda_i)$ have no real oval for the involution τ_2 (see Example 3.1.1). We will consider here τ_2 for the same curves as for DS1$^-$. An example for genus 2 can be seen in Figure 8.8. An example for a DS2$^-$ solution of genus 4 can be seen in Figure 8.9.

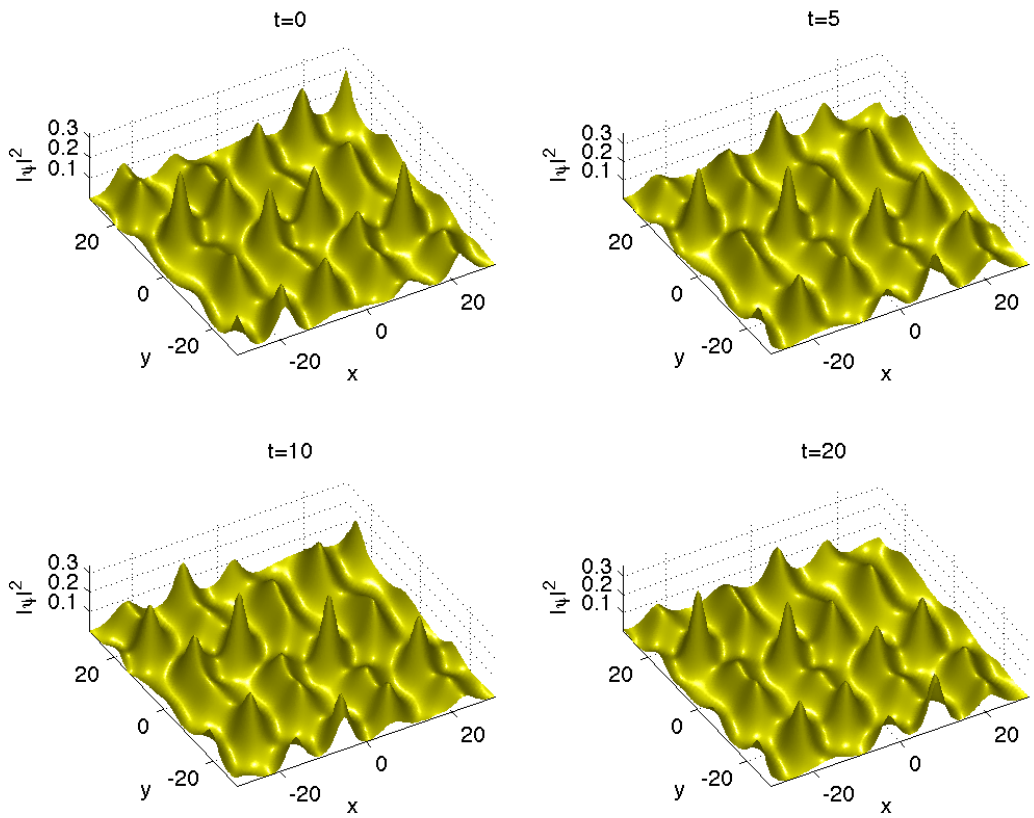

Figure 8.9: *Solution to the DS2$^-$ equation for several values of t on a hyperelliptic curve of genus 4 with branch points* $-2 \pm \mathrm{i}$, $-1 \pm \mathrm{i}$, $\pm\mathrm{i}$, $1 \pm \mathrm{i}$, $2 \pm \mathrm{i}$ *and* $a = (-1.5 + 2\mathrm{i})^{(1)}$, $b = (-1.5 - 2\mathrm{i})^{(2)}$.

8.1.3 Solutions to the n-NLS^s equation

As we saw in Section 6.3, a straightforward way to obtain solutions to the n-NLS^s equation is given on an $(n+1)$-sheeted branched covering of the complex plane, an approach that will be studied in more detail in the next section. As can be seen from the proof of Theorem 6.3.1, the crucial point in the construction of the solutions (6.3.14) of n-NLS^s is the fact that $\sum_{k=1}^{n+1} \mathbf{V}_{a_k} = 0$. This implies that it is also possible to construct smooth theta-functional n-NLS^s solutions on hyperelliptic surfaces by introducing constants γ_k via $\sum_{k=1}^{n+1} \gamma_k \mathbf{V}_{a_k} = 0$, see Theorem 6.3.4.

As an example we consider, as for DS in genus 2, the family of curves with the branch points $-2, -1, 0, \epsilon, 2, 2+\epsilon$ for $\epsilon = 1$ and $\epsilon = 10^{-10}$. In the former case the solutions will be periodic in the (x,t)-plane, in the latter almost solitonic. To obtain nontrivial solutions in the solitonic limit, we use $\mathbf{d} = \frac{1}{2}\left[\begin{smallmatrix}1 & 1\\ 0 & 0\end{smallmatrix}\right]^t$ in all examples.

In Figure 8.10 we show the case $a_1 = (-1.9)^{(1)}$, $a_2 = (-1.1)^{(1)}$ and $a_3 = (-1.8)^{(1)}$, which leads to a solution of 2-NLS$^{\hat{s}}$ with $\hat{s} = (-1,-1)$. Interchanging a_2 and a_3 in the above example, we obtain a solution to 2-NLS$^{\hat{s}}$ with $\hat{s} = (1,-1)$ in Figure 8.11.

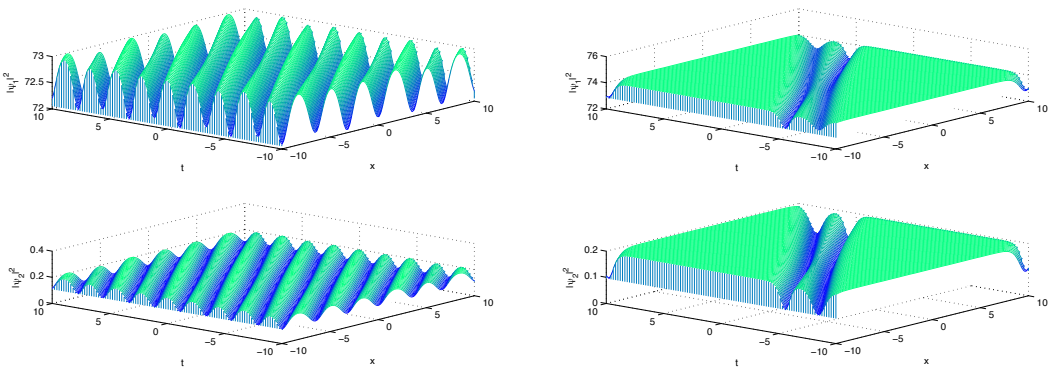

Figure 8.10: *Solution (6.3.39) to the 2-NLS$^{\hat{s}}$ equation with $\hat{s} = (-1,-1)$ on a hyperelliptic curve of genus 2 with branch points $-2, -1, 0, \epsilon, 2, 2+\epsilon$ and $a_1 = (-1.9)^{(1)}$, $a_2 = (-1.1)^{(1)}$ and $a_3 = (-1.8)^{(1)}$ for $\epsilon = 1$ on the left and $\epsilon = 10^{-10}$, the almost solitonic limit, on the right.*

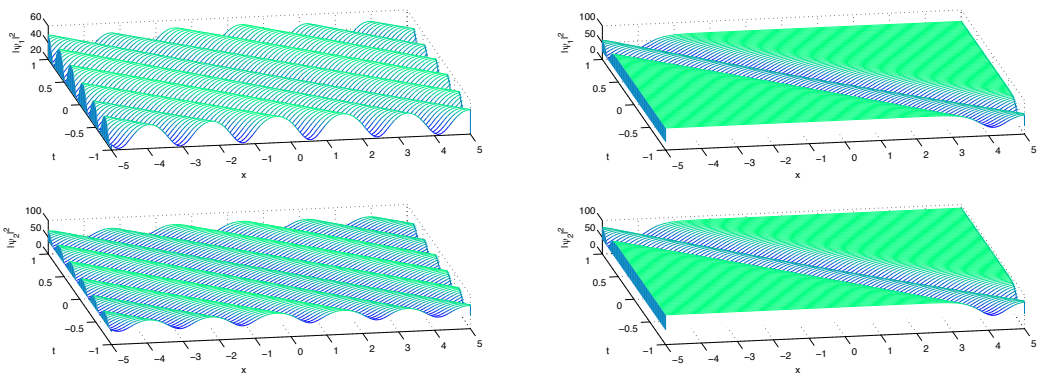

Figure 8.11: *Solution (6.3.39) to the 2-NLS$^{\hat{s}}$ equation with $\hat{s} = (1,-1)$ on a hyperelliptic curve of genus 2 with branch points $-2, -1, 0, \epsilon, 2, 2+\epsilon$ and $a_1 = (-1.9)^{(1)}$, $a_2 = (-1.8)^{(1)}$ and $a_3 = (-1.1)^{(1)}$ for $\epsilon = 1$ on the left and $\epsilon = 10^{-10}$, the almost solitonic limit, on the right.*

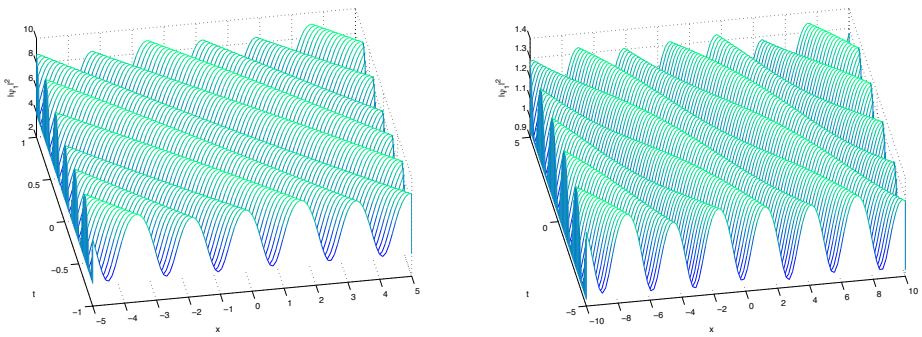

Figure 8.12: *Solution to the 4-NLS$^{\hat{s}}$ equation on a hyperelliptic curve of genus 4 with branch points* $-4, -3, -2, -2+\epsilon, 0, \epsilon, 2, 2+\epsilon, 4, 4+\epsilon$ *and* $\epsilon = 1$ *for* $a_1 = (-3.9)^{(1)}$, $a_2 = (-3.7)^{(1)}$, $a_3 = (-3.5)^{(1)}$, $a_4 = (-3.3)^{(1)}$ *and* $a_5 = (-3.1)^{(1)}$, *which leads to* $\hat{s} = (1, -1, 1, -1)$, *on the left, and for* $a_1 = (-3.9)^{(1)}$, $a_2 = (-3.7)^{(1)}$, $a_3 = (-3.5)^{(1)}$, $a_4 = (-3.1)^{(1)}$ *and* $a_5 = (-3.3)^{(1)}$, *which leads to* $\hat{s} = (-1, 1, -1, -1)$ *on the right.*

Solutions of 4-NLS$^{\hat{s}}$ can be studied in the same way on the hyperelliptic curve of genus 4 with branch points $-4, -3, -2, -2+\epsilon, 0, \epsilon, 2, 2+\epsilon, 4, 4+\epsilon$. We use $\mathbf{d} = \frac{1}{2}\left[\begin{smallmatrix}1&1&1&1\\0&0&0&0\end{smallmatrix}\right]^t$ and the points $a_1 = (-3.9)^{(1)}$, $a_2 = (-3.7)^{(1)}$, $a_3 = (-3.5)^{(1)}$, $a_4 = (-3.3)^{(1)}$ and $a_5 = (-3.1)^{(1)}$. Since the vectors $\mathbf{V}_{a_j}$ and $\mathbf{W}_{a_j}$ are very similar in this case, the same is true for the functions ψ_j. Therefore, we will only show the square modulus of the first component ψ_1 in Figure 8.12 for

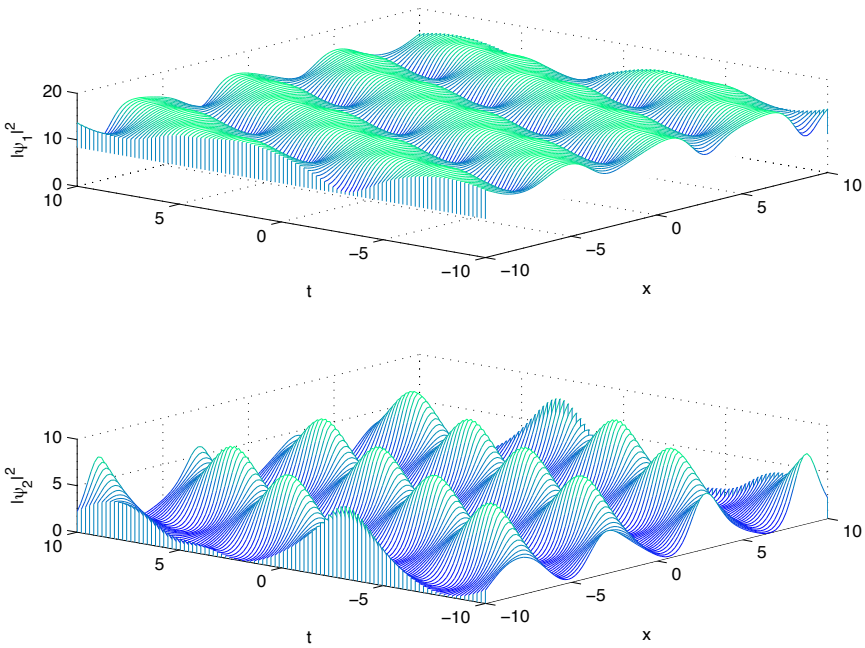

Figure 8.13: *Solution to the 2-NLS$^{\hat{s}}$ equation with* $\hat{s} = (1, 1)$ *on a hyperelliptic curve of genus 2 with branch points* $-2 \pm \mathrm{i}$, $-1 \pm \mathrm{i}$, $1 \pm \mathrm{i}$ *and* $a_1 = (-1.9)^{(1)}$, $a_2 = (-1.8)^{(2)}$ *and* $a_3 = (-1.1)^{(1)}$.

$\hat{s} = (1, -1, 1, -1)$ on the left. Interchanging a_4 and a_5 in this case, one gets a solution to 4-NLS$^{\hat{s}}$ with $\hat{s} = (-1, 1, -1, -1)$ which can be seen on the right of Figure 8.12. The almost solitonic limit $\epsilon = 10^{-10}$ produces well known solitonic patterns as shown for instance for the DS equation in the previous subsection.

Hyperelliptic solutions of n-NLS$^{\hat{s}}$ with $\hat{s}_j = 1$, $j = 1, \ldots, n$, can be constructed on a curve without real branch point. To get smooth solutions, we use $\mathbf{d} = 0$. A solution of the 2-NLS$^{\hat{s}}$ equation is studied on the curve of genus 2 with the branch points $-2\pm\mathrm{i}, -1\pm\mathrm{i}, 1\pm\mathrm{i}$ in Figure 8.13.

A typical example for a hyperelliptic 4-NLS$^{\hat{s}}$ solution with $\hat{s} = (1, 1, 1, 1)$ can be obtained on a curve of genus 4 with branch points $-2 \pm \mathrm{i}, -1 \pm \mathrm{i}, \pm\mathrm{i}, 1 \pm \mathrm{i}, 2 \pm \mathrm{i}$, as shown in Figure 8.14.

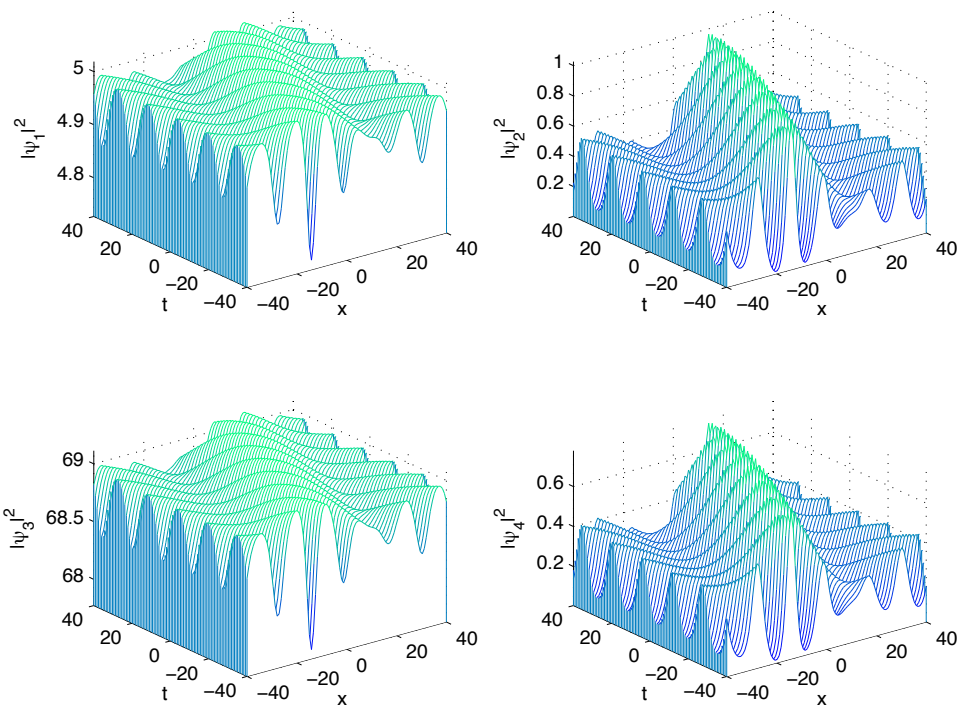

Figure 8.14: *Solution to the 4-NLS$^{\hat{s}}$ equation with $\hat{s} = (1, 1, 1, 1)$ on a hyperelliptic curve of genus 4 with branch points $-2 \pm \mathrm{i}$, $-1 \pm \mathrm{i}$, $\pm\mathrm{i}$, $1 \pm \mathrm{i}$, $2 \pm \mathrm{i}$ and $a_1 = (-3.9)^{(1)}$, $a_2 = (-3.7)^{(2)}$, $a_3 = (-3.5)^{(1)}$, $a_4 = (-3.3)^{(2)}$ and $a_5 = (-3.1)^{(1)}$.*

8.2 General real algebraic curves

The quantities entering theta-functional solutions of the DS and n-NLS^s equations are related to compact Riemann surfaces. Since all compact Riemann surfaces can be defined via compactified non-singular algebraic curves, convenient computational approaches as [39, 40] and [67] are based on algebraic curves: differentials, homology basis and periods of the Riemann surface can be obtained in an algorithmic way. We refer the reader to the cited literature for details.

In this part we are interested in non-singular real algebraic curves of the form

$$\sum_{n=1}^{N}\sum_{m=1}^{M} a_{mn}x^m y^n = 0, \quad x, y \in \mathbb{C}, \tag{8.2.1}$$

with $a_{mn} \in \mathbb{R}$, on which we consider the anti-holomorphic involution given by $\tau(x, y) = (\overline{x}, \overline{y})$. The identification of the sheets of the covering defined by the algebraic curve (8.2.1) via the projection map $(x, y) \mapsto x$, is done, as in the hyperelliptic case, by analytic continuation of the roots y_i, $i = 1, \ldots, N$, for some non-critical point x_b on the x-sphere, along a set of contours specified in [67]. In the context of real algebraic curves for which solutions of n-NLS^s and DS are discussed here, an additional problem is to establish the action of the anti-holomorphic involution τ on points on different sheets. A typical problem is to find points $a \in \mathcal{R}_g$ and $b \in \mathcal{R}_g$ with the same projection onto the x-sphere such that $\tau a = b$. To this end, the roots y_i, $i = 1, \ldots, N$, identified at $x = x_b$, are analytically continued to the points projecting to $x(a)$ on the x-sphere. It is then established which pairs of points in the different sheets satisfy $\tau a = b$.

In contrast to the hyperelliptic curves of the previous section, it is not possible for general curves to introduce a priori a basis of the homology. Thus the cited codes use an algorithm by Tretkoff and Tretkoff [148] which produces a homology basis for a given branching structure of the covering which is in general not adapted to possible automorphisms of the curve. In the context of theta-functional solutions to integrable PDEs one is often interested in real curves. As discussed in Chapter 6, the Vinnikov basis (i.e., the canonical homology basis which satisfies (3.2.1)) is convenient in this context. Since solutions and smoothness conditions for n-NLS^s and DS equations are formulated in this basis, a symplectic transformation relating the computed basis to the Vinnikov basis needs to be worked out. This transformation is discussed in the present section and will be applied to examples of real algebraic curves.

8.2.1 Symplectic transformation

Let $\mathcal{R}_g$ be a real compact Riemann surface of genus g and τ an anti-holomorphic involution defined on it. Let $(\nu_1, \ldots, \nu_g)$ be a basis of holomorphic differentials such that

$$\overline{\tau^* \nu_j} = \nu_j, \qquad j = 1, \ldots, g \tag{8.2.2}$$

(recall that τ^* denotes the action of τ lifted to the space of holomorphic differentials). For an arbitrary canonical homology basis $(\mathcal{A}, \mathcal{B})$, let us denote by $P_{\mathcal{A}}$ and $P_{\mathcal{B}}$ the matrices of $\mathcal{A}$ and $\mathcal{B}$-periods of the differentials ν_j:

$$(P_{\mathcal{A}})_{ij} = \int_{\mathcal{A}_i} \nu_j, \qquad (P_{\mathcal{B}})_{ij} = \int_{\mathcal{B}_i} \nu_j, \qquad i, j = 1, \ldots, g. \tag{8.2.3}$$

In what follows $(\mathcal{A},\mathcal{B})$ denotes the Vinnikov basis. From (8.2.2) and (3.2.1) we deduce the action of the complex conjugation on the matrices $P_{\mathcal{A}}$ and $P_{\mathcal{B}}$:

$$(P_{\mathcal{A}})_{ij} \in \mathbb{R}, \tag{8.2.4}$$

$$\overline{P_{\mathcal{B}}} = -P_{\mathcal{B}} + \mathbb{H}P_{\mathcal{A}}. \tag{8.2.5}$$

Denote by $(\tilde{\mathcal{A}},\tilde{\mathcal{B}})$ the homology basis on $\mathcal{R}_g$ produced by the Tretkoff-Tretkoff algorithm. As we saw in (2.1.2), there exists a symplectic matrix $\begin{pmatrix} A & B \\ C & D \end{pmatrix} \in Sp(2g,\mathbb{Z})$ such that

$$\begin{pmatrix} A & B \\ C & D \end{pmatrix}\begin{pmatrix} \tilde{\mathcal{A}} \\ \tilde{\mathcal{B}} \end{pmatrix} = \begin{pmatrix} \mathcal{A} \\ \mathcal{B} \end{pmatrix}. \tag{8.2.6}$$

From the symplectic transformation (8.2.6) we obtain the following transformation law between the matrices $P_{\tilde{\mathcal{A}}}, P_{\tilde{\mathcal{B}}}$ and $P_{\mathcal{A}}, P_{\mathcal{B}}$ defined in (8.2.3):

$$\begin{pmatrix} A & B \\ C & D \end{pmatrix}\begin{pmatrix} P_{\tilde{\mathcal{A}}} \\ P_{\tilde{\mathcal{B}}} \end{pmatrix} = \begin{pmatrix} P_{\mathcal{A}} \\ P_{\mathcal{B}} \end{pmatrix}. \tag{8.2.7}$$

Therefore, by (8.2.4) one gets

$$A\,\mathrm{Re}\left(P_{\tilde{\mathcal{A}}}\right) + B\,\mathrm{Re}\left(P_{\tilde{\mathcal{B}}}\right) = P_{\mathcal{A}} \tag{8.2.8}$$

$$A\,\mathrm{Im}\left(P_{\tilde{\mathcal{A}}}\right) + B\,\mathrm{Im}\left(P_{\tilde{\mathcal{B}}}\right) = 0, \tag{8.2.9}$$

and by (8.2.5)

$$C\,\mathrm{Re}\left(P_{\tilde{\mathcal{A}}}\right) + D\,\mathrm{Re}\left(P_{\tilde{\mathcal{B}}}\right) = \frac{1}{2}\,\mathbb{H}P_{\mathcal{A}} \tag{8.2.10}$$

$$C\,\mathrm{Im}\left(P_{\tilde{\mathcal{A}}}\right) + D\,\mathrm{Im}\left(P_{\tilde{\mathcal{B}}}\right) = \mathrm{Im}\left(P_{\mathcal{B}}\right). \tag{8.2.11}$$

According to (8.2.8), the matrix $A\,\mathrm{Re}\left(P_{\tilde{\mathcal{A}}}\right) + B\,\mathrm{Re}\left(P_{\tilde{\mathcal{B}}}\right)$ is invertible, since the matrix $P_{\mathcal{A}}$ of $\mathcal{A}$-periods of a basis of holomorphic differentials is always invertible. Moreover, since the Riemann matrix $\mathbb{B} = 2\mathrm{i}\pi\, P_{\mathcal{B}}\,(P_{\mathcal{A}})^{-1}$ has a (negative) definite real part, which is equal to $-2\pi\,\mathrm{Im}(P_{\mathcal{B}})\,\mathrm{Im}((P_{\mathcal{A}})^{-1})$ for the real matrix $P_{\mathcal{A}}$ here, then by (8.2.11) the matrix $C\,\mathrm{Im}\left(P_{\tilde{\mathcal{A}}}\right) + D\,\mathrm{Im}\left(P_{\tilde{\mathcal{B}}}\right)$ is also invertible.

Lemma 8.2.1. *The matrices $A,B,C,D \in \mathcal{M}_g(\mathbb{Z})$ solving (8.2.8)-(8.2.11) satisfy:*

$$A^t = Im\left(P_{\tilde{\mathcal{B}}}\right)\left[C\,Im\left(P_{\tilde{\mathcal{A}}}\right) + D\,Im\left(P_{\tilde{\mathcal{B}}}\right)\right]^{-1} \tag{8.2.12}$$

$$B^t = -Im\left(P_{\tilde{\mathcal{A}}}\right)\left[C\,Im\left(P_{\tilde{\mathcal{A}}}\right) + D\,Im\left(P_{\tilde{\mathcal{B}}}\right)\right]^{-1} \tag{8.2.13}$$

$$C^t = \frac{1}{2}\,A^t\mathbb{H} - Re\left(P_{\tilde{\mathcal{B}}}\right)\left[A\,Re\left(P_{\tilde{\mathcal{A}}}\right) + B\,Re\left(P_{\tilde{\mathcal{B}}}\right)\right]^{-1} \tag{8.2.14}$$

$$D^t = \frac{1}{2}\,B^t\mathbb{H} + Re\left(P_{\tilde{\mathcal{A}}}\right)\left[A\,Re\left(P_{\tilde{\mathcal{A}}}\right) + B\,Re\left(P_{\tilde{\mathcal{B}}}\right)\right]^{-1}. \tag{8.2.15}$$

Proof. Multiplying equality (8.2.9) from the left by the matrix C^t, we deduce from (2.1.3) and (2.1.4) that

$$\begin{aligned}
&C^t A \operatorname{Im}\left(P_{\tilde{\mathcal{A}}}\right) + C^t B \operatorname{Im}\left(P_{\tilde{\mathcal{B}}}\right) = 0\\
&C^t A \operatorname{Im}\left(P_{\tilde{\mathcal{A}}}\right) + (A^t D - \mathbb{I}_g) \operatorname{Im}\left(P_{\tilde{\mathcal{B}}}\right) = 0\\
&A^t C \operatorname{Im}\left(P_{\tilde{\mathcal{A}}}\right) + A^t D \operatorname{Im}\left(P_{\tilde{\mathcal{B}}}\right) = \operatorname{Im}\left(P_{\tilde{\mathcal{B}}}\right),
\end{aligned}$$

which leads to (8.2.12). Equality (8.2.13) can be checked analogously with (2.1.3) and (2.1.5). To prove (8.2.14), multiply equality (8.2.10) from the left by the matrix A^t. Using (2.1.3) and (2.1.4) one gets

$$\begin{aligned}
&A^t C \operatorname{Re}\left(P_{\tilde{\mathcal{A}}}\right) + A^t D \operatorname{Re}\left(P_{\tilde{\mathcal{B}}}\right) = \frac{1}{2} A^t \mathbb{H} P_{\mathcal{A}}\\
&C^t A \operatorname{Re}\left(P_{\tilde{\mathcal{A}}}\right) + (\mathbb{I}_g + C^t B) \operatorname{Re}\left(P_{\tilde{\mathcal{B}}}\right) = \frac{1}{2} A^t \mathbb{H} P_{\mathcal{A}}\\
&C^t \left(A \operatorname{Re}\left(P_{\tilde{\mathcal{A}}}\right) + B \operatorname{Re}\left(P_{\tilde{\mathcal{B}}}\right)\right) = \frac{1}{2} A^t \mathbb{H} P_{\mathcal{A}} - \operatorname{Re}\left(P_{\tilde{\mathcal{B}}}\right),
\end{aligned}$$

which by (8.2.8) leads to (8.2.14). Identity (8.2.15) can be proved analogously. □

Remark 8.2.1. Lemma 8.2.1 implies that it is sufficient to know the matrices A and B (or C and D) to determine the symplectic matrix in (8.2.7). In practice, this means that a convenient ansatz for one of the matrices has to be found. The others then follow from the relations in Lemma 8.2.1.

Thus to construct these matrices one first checks which of the matrices $\operatorname{Re}\left(P_{\tilde{\mathcal{A}}}\right)$, $\operatorname{Re}\left(P_{\tilde{\mathcal{B}}}\right)$, $\operatorname{Im}\left(P_{\tilde{\mathcal{A}}}\right)$, $\operatorname{Im}\left(P_{\tilde{\mathcal{B}}}\right)$ are invertible. This way a matrix can be identified (e.g. A) in terms of which the others can be expressed. The task is thus reduced to provide an ansatz for this matrix such that the others will have entire components. We illustrate this approach at the example of the Trott curve below.

Proposition 8.2.1. *Let $(\tilde{\mathcal{A}}, \tilde{\mathcal{B}})$ be the canonical homology basis obtained with the Tretkoff-Tretkoff algorithm; we denote with a tilde the quantities expressed in this basis. Under the change of homology basis (8.2.6), solutions of n-NLS^s and DS equations given in (6.3.14) and (6.4.10), (6.4.20) respectively, which are expressed in the basis satisfying (3.2.1), transform as follows: the vector $\mathbf{d}$ appearing in the solutions becomes $(2\mathrm{i}\pi)^{-1}\,\tilde{\mathbb{K}}^t\,\mathbf{d}$ where $\tilde{\mathbb{K}} = 2\mathrm{i}\pi A + B\,\tilde{\mathbb{B}}$, and the theta function $\Theta = \Theta_{\mathbb{B}}$ with zero characteristic, transforms to the theta function $\Theta_{\tilde{\mathbb{B}}}[\tilde{\delta}]$ with characteristic $\tilde{\delta} = [\tilde{\delta}_1, \tilde{\delta}_2]$ given by*

$$\tilde{\delta}_1 = \frac{1}{4}\, diag\left(B^t \mathbb{H} B - 2\, Re\left(P_{\tilde{\mathcal{A}}}\right) \tilde{\mathbb{M}}^{-1} Im\left(P^t_{\tilde{\mathcal{A}}}\right)\right) \tag{8.2.16}$$

$$\tilde{\delta}_2 = \frac{1}{4}\, diag\left(A^t \mathbb{H} A - 2\, Re\left(P_{\tilde{\mathcal{B}}}\right) \tilde{\mathbb{M}}^{-1} Im\left(P^t_{\tilde{\mathcal{B}}}\right)\right) \tag{8.2.17}$$

where

$$\tilde{\mathbb{M}} = Im\left(P^t_{\tilde{\mathcal{B}}}\right) Re\left(P_{\tilde{\mathcal{A}}}\right) - Im\left(P^t_{\tilde{\mathcal{A}}}\right) Re\left(P_{\tilde{\mathcal{B}}}\right). \tag{8.2.18}$$

Moreover, the real constant h appearing in (6.4.11), (6.4.21) and (6.4.7) becomes $h + \tilde{h}$ where $Im(\tilde{h})$ is given by

$$Im(\tilde{h}) = \frac{1}{2} \ln\left\{\left|\frac{\Theta_{\tilde{\mathbb{B}}}[\tilde{\delta}](\tilde{\mathbf{Z}} + \tilde{\mathbf{r}})}{\Theta_{\tilde{\mathbb{B}}}[\tilde{\delta}](\tilde{\mathbf{Z}} - \tilde{\mathbf{r}})}\right|\right\} - Im(\tilde{G}_3), \tag{8.2.19}$$

with $\tilde{\mathbf{Z}} = \mathrm{i}(\tilde{\mathbf{W}}_a - \tilde{\mathbf{W}}_b)$*, and the vectors* $\mathbf{N}, \mathbf{M}$ *defined in (3.3.9) become* $A^t\mathbf{N} + C^t\mathbf{M}$ *and* $B^t\mathbf{N} + D^t\mathbf{M}$ *respectively.*

Proof. Under the change of the canonical homology basis (8.2.6), the vector $\omega = (\omega_1, \ldots, \omega_g)^t$ of normalized holomorphic differentials transforms as

$$\omega = 2\mathrm{i}\pi\,(\tilde{\mathbb{K}}^t)^{-1}\,\tilde{\omega}, \tag{8.2.20}$$

where $\tilde{\mathbb{K}} = 2\mathrm{i}\pi A + B\,\tilde{\mathbb{B}}$. According to the transformation law (2.2.5) of theta functions, it can be checked after straightforward calculations, that under this change of homology basis, quantities (2.3.11), (2.3.12) and (6.1.2), (6.1.3) transform as:

$$q_1(a,b) = \tilde{q}_1(a,b) + \frac{1}{2}\,\tilde{\mathbf{V}}_a^t\,(\tilde{\mathbb{K}}^t)^{-1}B\,\tilde{\mathbf{V}}_b, \tag{8.2.21}$$

$$q_2(a,b) = \tilde{q}_2(a,b)\,\exp\left\{-\tilde{\mathbf{r}}^t\,(\tilde{\mathbb{K}}^t)^{-1}B\,\tilde{\mathbf{r}}\right\}, \tag{8.2.22}$$

$$K_1(a,b) = \tilde{K}_1(a,b) + \frac{1}{2}\left(\tilde{\mathbf{V}}_a^t\,(\tilde{\mathbb{K}}^t)^{-1}B\,\tilde{\mathbf{r}} + \tilde{\mathbf{r}}^t\,(\tilde{\mathbb{K}}^t)^{-1}B\,\tilde{\mathbf{V}}_a\right), \tag{8.2.23}$$

$$K_2(a,b) = \tilde{K}_2(a,b) - \frac{1}{2}\left(\tilde{\mathbf{W}}_a^t\,(\tilde{\mathbb{K}}^t)^{-1}B\,\tilde{\mathbf{r}} + \tilde{\mathbf{r}}^t\,(\tilde{\mathbb{K}}^t)^{-1}B\,\tilde{\mathbf{W}}_a\right) - \tilde{\mathbf{V}}_a^t\,(\tilde{\mathbb{K}}^t)^{-1}B\,\tilde{\mathbf{V}}_a. \tag{8.2.24}$$

We deduce that solutions of the n-NLS^s and DS equations given in (6.3.14) and (6.4.10), (6.4.20), respectively, transform as follows: the vector $\mathbf{d}$ becomes $(2\mathrm{i}\pi)^{-1}\,\tilde{\mathbb{K}}^t\,\mathbf{d}$, and the theta function $\Theta = \Theta_{\mathbb{B}}$ with zero characteristic, transforms to the theta function $\Theta_{\tilde{\mathbb{B}}}[\tilde{\delta}]$ with characteristic $\tilde{\delta}$. To compute the vectors of the characteristic $\tilde{\delta}$ we consider the inversion of the symplectic matrix in (8.2.6), which leads to

$$\begin{pmatrix}\tilde{\mathcal{A}}\\ \tilde{\mathcal{B}}\end{pmatrix} = \begin{pmatrix} D^t & -B^t \\ -C^t & A^t\end{pmatrix}\begin{pmatrix}\mathcal{A}\\ \mathcal{B}\end{pmatrix}.$$

Since the characteristic used in Chapter 6 to construct algebro-geometric solutions of n-NLS^s and DS is zero, we get with (2.2.8)

$$\begin{pmatrix}\tilde{\delta}_1\\ \tilde{\delta}_2\end{pmatrix} = \frac{1}{2}\,\mathrm{Diag}\begin{pmatrix}D^tB\\ C^tA\end{pmatrix}$$

(note that D^tB and C^tA are symmetric matrices). Substituting (8.2.12) and (8.2.13) in (8.2.14) (resp. (8.2.15)), it can be checked that

$$C^tA = \frac{1}{2}\left(A^t\mathbb{H}A - 2\,\mathrm{Re}\left(P_{\tilde{\mathcal{B}}}\right)\tilde{\mathbb{M}}^{-1}\,\mathrm{Im}\left(P_{\tilde{\mathcal{B}}}^t\right)\right),$$
$$D^tB = \frac{1}{2}\left(B^t\mathbb{H}B - 2\,\mathrm{Re}\left(P_{\tilde{\mathcal{A}}}\right)\tilde{\mathbb{M}}^{-1}\,\mathrm{Im}\left(P_{\tilde{\mathcal{A}}}^t\right)\right),$$

with

$$\tilde{\mathbb{M}} = \mathrm{Im}\left(P_{\tilde{\mathcal{B}}}^t\right)\mathrm{Re}\left(P_{\tilde{\mathcal{A}}}\right) - \mathrm{Im}\left(P_{\tilde{\mathcal{A}}}^t\right)\mathrm{Re}\left(P_{\tilde{\mathcal{B}}}\right).$$

Moreover, the real constant h appearing in the solutions of the Davey-Stewartson equations becomes $h + \tilde{h}$, where $\tilde{h}$ is given by

$$\tilde{h} = -\tilde{\mathbf{V}}_a^t\,(\tilde{\mathbb{K}}^t)^{-1}B\,\tilde{\mathbf{V}}_a - \tilde{\mathbf{V}}_b^t\,(\tilde{\mathbb{K}}^t)^{-1}B\,\tilde{\mathbf{V}}_b. \tag{8.2.25}$$

Notice that the construction of these solutions given in Chapter 6 allows to express the imaginary part of the constant $\tilde{h}$ (8.2.25) in terms of the characteristic $\tilde{\delta}$. Namely, since the reality condition

$$\psi^* = \rho\,\overline{\psi} \tag{8.2.26}$$

is satisfied for the Vinnikov basis, where the function $\psi^*(\xi,\eta,t)$ is defined in (6.4.4), it also holds for the computed basis. Therefore, putting $\xi=\eta=0$, $t=2$, $\mathbf{d}=0$, and taking the modulus of each term in (8.2.26) expressed in the computed basis, one gets:

$$\left|\frac{\Theta_{\tilde{\mathbb{B}}}[\tilde{\delta}](\tilde{\mathbf{Z}}-\tilde{\mathbf{r}})}{\Theta_{\tilde{\mathbb{B}}}[\tilde{\delta}](\tilde{\mathbf{Z}})}\exp\{-\mathrm{i}\,(\tilde{G}_3+\tilde{h})\}\right| = \left|\frac{\Theta_{\tilde{\mathbb{B}}}[\tilde{\delta}](\tilde{\mathbf{Z}}+\tilde{\mathbf{r}})}{\Theta_{\tilde{\mathbb{B}}}[\tilde{\delta}](\tilde{\mathbf{Z}})}\exp\{\mathrm{i}\,(\tilde{G}_3+\tilde{h})\}\right|$$

where $\tilde{\mathbf{Z}} = \mathrm{i}(\tilde{\mathbf{W}}_a - \tilde{\mathbf{W}}_b)$. We deduce that

$$\mathrm{Im}(\tilde{h}) = \frac{1}{2}\,\ln\left\{\left|\frac{\Theta_{\tilde{\mathbb{B}}}[\tilde{\delta}](\tilde{\mathbf{Z}}+\tilde{\mathbf{r}})}{\Theta_{\tilde{\mathbb{B}}}[\tilde{\delta}](\tilde{\mathbf{Z}}-\tilde{\mathbf{r}})}\right|\right\} - \mathrm{Im}(\tilde{G}_3). \tag{8.2.27}$$

□

Remark 8.2.2. *In the case where the spectral curve is an M-curve, i.e.* $\mathbb{H}=0$*, the vectors of characteristic (8.2.16) and (8.2.17) do not depend explicitly on the symplectic matrix appearing in the change of homology basis and are uniquely defined by:*

$$\tilde{\delta}_1 = \frac{1}{2}\,diag\left(Re\left(P_{\tilde{\mathcal{A}}}\right)\left[Im\left(P^t_{\tilde{\mathcal{B}}}\right)Re\left(P_{\tilde{\mathcal{A}}}\right) - Im\left(P^t_{\tilde{\mathcal{A}}}\right)Re\left(P_{\tilde{\mathcal{B}}}\right)\right]^{-1} Im\left(P^t_{\tilde{\mathcal{A}}}\right)\right) \tag{8.2.28}$$

$$\tilde{\delta}_2 = \frac{1}{2}\,diag\left(Re\left(P_{\tilde{\mathcal{B}}}\right)\left[Im\left(P^t_{\tilde{\mathcal{B}}}\right)Re\left(P_{\tilde{\mathcal{A}}}\right) - Im\left(P^t_{\tilde{\mathcal{A}}}\right)Re\left(P_{\tilde{\mathcal{B}}}\right)\right]^{-1} Im\left(P^t_{\tilde{\mathcal{B}}}\right)\right). \tag{8.2.29}$$

It would be possible to compute the theta-functional solutions in the Vinnikov basis once the symplectic transformation between this basis and the basis determined by the code is known. However, since this symplectic transformation is not unique, the found Vinnikov basis leads in general to a Riemann matrix for which the theta series converges only slowly, i.e., the value N_θ in (8.1.1) has to be chosen very large. To avoid this problem, we compute the theta function always in the typically more convenient Tretkoff-Tretkoff basis with the characteristic of the theta functions given by (8.2.16)-(8.2.18).

8.2.2 Trott curve

The Trott curve [149] given by the algebraic equation

$$144\,(x^4+y^4) - 225\,(x^2+y^2) + 350\,x^2y^2 + 81 = 0 \tag{8.2.30}$$

is an M-curve with respect to the anti-holomorphic involution τ defined by $\tau(x,y)=(\overline{x},\overline{y})$, and is of genus 3. Moreover, this curve has real branch points only (and 28 real bitangents, namely, tangents to the curve in two places). Our computed matrices of $\tilde{\mathcal{A}}$ and $\tilde{\mathcal{B}}$-periods read[1]

$$P_{\tilde{\mathcal{A}}} = \begin{pmatrix} 0.0235\mathrm{i} & 0.0138\mathrm{i} & 0.0138\mathrm{i} \\ 0 & 0.0277\mathrm{i} & 0 \\ -0.0315 & 0 & 0.0250 \end{pmatrix},$$

[1]For the ease of representation we only give 4 digits here, though at least 12 digits are known for these quantities.

$$P_{\tilde{\mathcal{B}}} = \begin{pmatrix} -0.0315 + 0.0235\mathrm{i} & 0.0138\mathrm{i} & -0.0250 + 0.0138\mathrm{i} \\ 0 & -0.025 + 0.0277\mathrm{i} & 0.0250 \\ -0.0235\mathrm{i} & 0.0138\mathrm{i} & 0.0138\mathrm{i} \end{pmatrix}.$$

The Trott curve being an M-curve, the vectors of the characteristic $\tilde{\delta}$ satisfy (8.2.28) and (8.2.29), which leads to $\tilde{\delta} = \frac{1}{2}[\begin{smallmatrix} 0 & 0 & 0 \\ 1 & 1 & 0 \end{smallmatrix}]^t$.

A possible choice of a symplectic transformation bringing the computed basis to the Vinnikov basis is:

$$A = \begin{pmatrix} 1 & 0 & 0 \\ 0 & 1 & 0 \\ 0 & 0 & 1 \end{pmatrix}, \quad B = \begin{pmatrix} -1 & 0 & 0 \\ 0 & -1 & 0 \\ 0 & 0 & 0 \end{pmatrix}, \quad C = \begin{pmatrix} 1 & 0 & 0 \\ 0 & 1 & 0 \\ 0 & 0 & 0 \end{pmatrix}, \quad D = \begin{pmatrix} 0 & 0 & 0 \\ 0 & 0 & 0 \\ 0 & 0 & 1 \end{pmatrix}.$$

Note that the matrices A, B, C, D are not unique since the action (3.2.1) of the anti-holomorphic involution on the basic cycles allows for permutations of $\mathcal{A}_j$-cycles for instance. These matrices can be computed as follows. Since the Trott curve is an M-curve, one has $\mathbb{H} = 0$. Moreover, the matrix $\mathrm{Im}(P_{\tilde{\mathcal{B}}})$ being invertible here, by (8.2.9) one gets:

$$B = -A \,\mathrm{Im}\left(P_{\tilde{\mathcal{A}}}\right) \left(\mathrm{Im}\left(P_{\tilde{\mathcal{B}}}\right)\right)^{-1}. \tag{8.2.31}$$

With (2.1.3) and (2.1.4) it follows that

$$A^t \left(D + C \,\mathrm{Im}\left(P_{\tilde{\mathcal{A}}}\right) \left(\mathrm{Im}\left(P_{\tilde{\mathcal{B}}}\right)\right)^{-1}\right) = \mathbb{I}_3. \tag{8.2.32}$$

The computed matrix $\mathrm{Im}\left(P_{\tilde{\mathcal{A}}}\right) \left(\mathrm{Im}\left(P_{\tilde{\mathcal{B}}}\right)\right)^{-1}$ being (within numerical precision) equal to

$$\mathrm{Im}\left(P_{\tilde{\mathcal{A}}}\right) \left(\mathrm{Im}\left(P_{\tilde{\mathcal{B}}}\right)\right)^{-1} = \begin{pmatrix} -1 & 0 & 0 \\ 0 & -1 & 0 \\ 0 & 0 & 0 \end{pmatrix},$$

and with $C, D \in \mathcal{M}_3(\mathbb{Z})$, we get from (8.2.32) that $\det A = 1$. Since $A \in \mathcal{M}_3(\mathbb{Z})$, the condition $\det A = 1$ implies $A \in Gl_3(\mathbb{Z})$. For any $A \in Gl_3(\mathbb{Z})$, one can see from (8.2.31), (8.2.14) and (8.2.15) that $B, C, D \in \mathcal{M}_3(\mathbb{Z})$, and therefore that the matrices A, B, C, D give a solution of (8.2.8)-(8.2.11). The choice $A = \mathbb{I}_3$ leads to the above matrices.

The Trott curve has real fibers and can thus be used to construct solutions to the 3-NLS equation via the projection map $f : (x, y) \mapsto x$, which is a real meromorphic function of degree 4 on the curve. We consider the points on the curve stable with respect to τ and projecting to the point with $x = 0.1$ in the x-sphere, and choose $\mathbf{d} = 0$. The corresponding solution to the 3-NLS equation can be seen in Figure 8.15.

A solution to the DS1$^+$ equation on this curve can be constructed for points a and b stable with respect to the involution τ. The solution for $a = (-0.2)^{(1)}$, $b = (0.2)^{(2)}$ and the choice $\mathbf{d} = 0$ can be seen in Figure 8.16.

Similarly, a solution to the DS2$^+$ equation can be obtained for points a and b subject to $\tau a = b$. For $a = (0.1 + \mathrm{i})^{(1)}$ and $b = (0.1 - \mathrm{i})^{(1)}$ we get Figure 8.17.

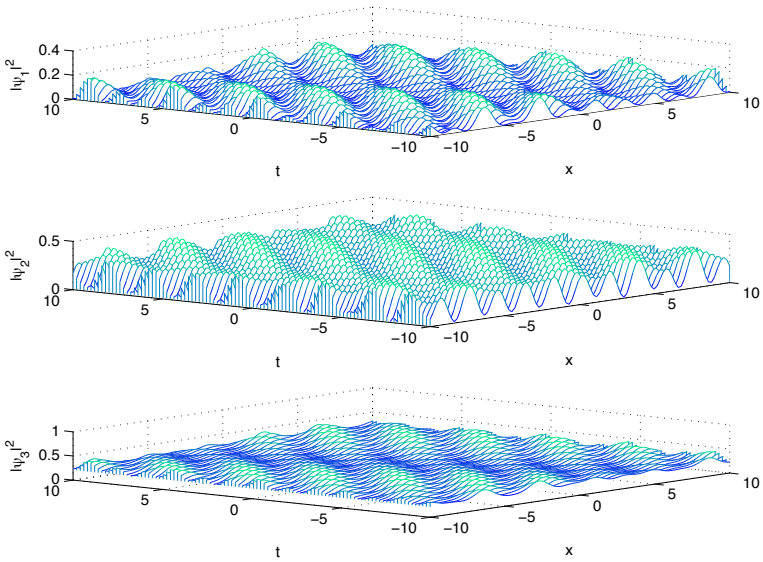

Figure 8.15: *Solution (6.3.14) to the 3-NLS^s equation on the Trott curve for the points with $x = 0.1$ on the x-sphere. The sheets are identified at the points projecting to $x = -1.0129, (0.9582\mathrm{i}, -0.9582\mathrm{i}, 0.1146\mathrm{i}, -0.1146\mathrm{i})$. The vector of signs equals $s = (1, -1, -1)$ from top to bottom.*

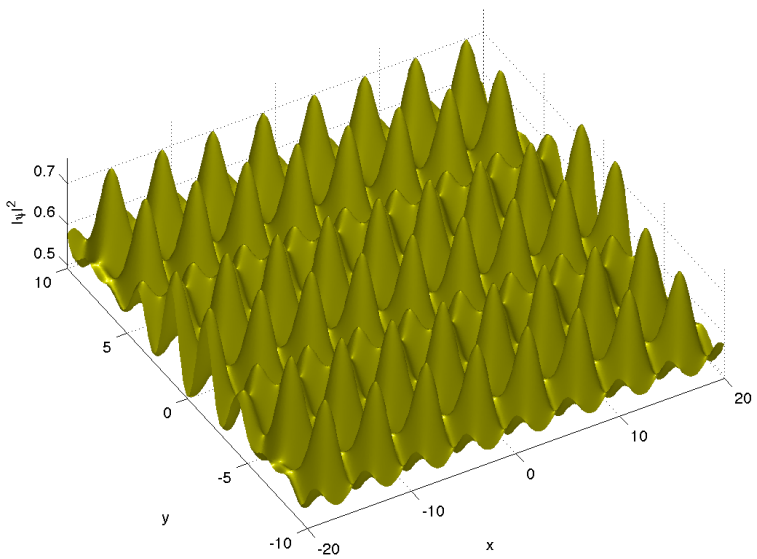

Figure 8.16: *Solution to the DS1$^+$ equation on the Trott curve for the points $a = (-0.2)^{(1)}$ and $b = (0.2)^{(2)}$ at $t = 0$.*

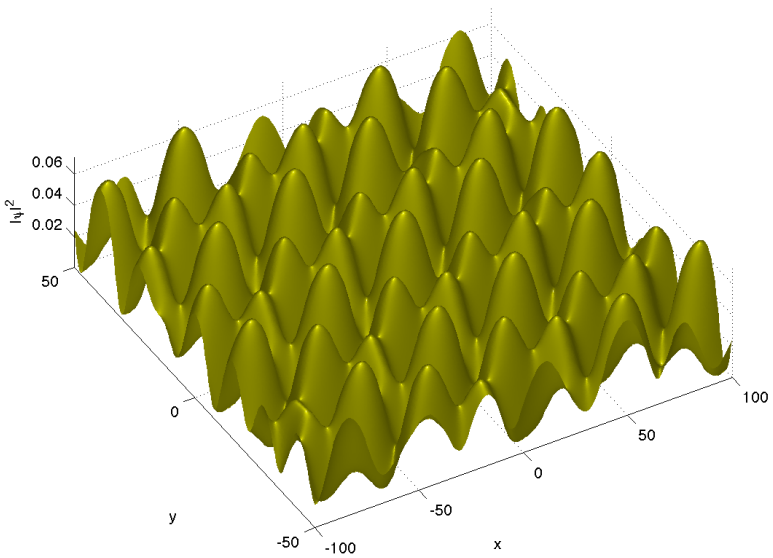

Figure 8.17: *Solution to the DS2$^+$ equation on the Trott curve for the points* $a = (0.1 + \mathrm{i})^{(1)}$ *and* $b = (0.1 - \mathrm{i})^{(1)}$ *at* $t = 0$.

8.2.3 Dividing curves without real branch point

We consider the curve given by the equation

$$30x^4 - 61x^3y + 41y^2x^2 - 43x^2 - 11y^3x + 42xy + y^4 - 11y^2 + 9 = 0 \tag{8.2.33}$$

which was studied in [47] and [150]. It is a genus 3 curve, dividing with respect to the anti-holomorphic involution τ, without real branch point. This curve admits two real ovals. In this case the matrix $\mathbb{H}$ has the form

$$\mathbb{H} = \begin{pmatrix} 0 & 1 & 0 \\ 1 & 0 & 0 \\ 0 & 0 & 0 \end{pmatrix}.$$

The period matrices computed by the code read

$$P_{\tilde{\mathcal{A}}} = \begin{pmatrix} -0.2721 - 0.0977\mathrm{i} & -0.3193 + 0.1914\mathrm{i} & -1.0668 + 0.4293\mathrm{i} \\ 0.2721 + 0.0977\mathrm{i} & -0.3193 - 0.3341\mathrm{i} & -1.0668 - 0.4316\mathrm{i} \\ 0.2721 - 0.0977\mathrm{i} & 0.4676 - 0.3341\mathrm{i} & 0.7992 - 0.4316\mathrm{i} \end{pmatrix},$$

$$P_{\tilde{\mathcal{B}}} = \begin{pmatrix} -0.2721 - 0.2932\mathrm{i} & -0.3193 + 0.3341\mathrm{i} & -1.0668 + 0.4316\mathrm{i} \\ 0.2721 + 0.2932\mathrm{i} & -0.3193 - 0.7169\mathrm{i} & -1.0668 - 1.2903\mathrm{i} \\ 0.2721 - 0.0977\mathrm{i} & 0.4676 + 0.1914\mathrm{i} & 0.7992 + 0.4293\mathrm{i} \end{pmatrix}.$$

After some calculations, one finds that the following matrices A, B, C, D provide a solution of (8.2.8)-(8.2.11):

$$A = \begin{pmatrix} -1 & 2 & -1 \\ 2 & -1 & 0 \\ 0 & 2 & -1 \end{pmatrix}, B = \begin{pmatrix} 1 & 0 & 1 \\ 0 & 1 & 0 \\ 1 & 0 & 0 \end{pmatrix}, C = \begin{pmatrix} 1 & -1 & -1 \\ -1 & 1 & -1 \\ 0 & 0 & 1 \end{pmatrix}, D = \begin{pmatrix} 0 & 1 & 1 \\ 1 & 0 & 1 \\ 0 & 0 & -1 \end{pmatrix}.$$

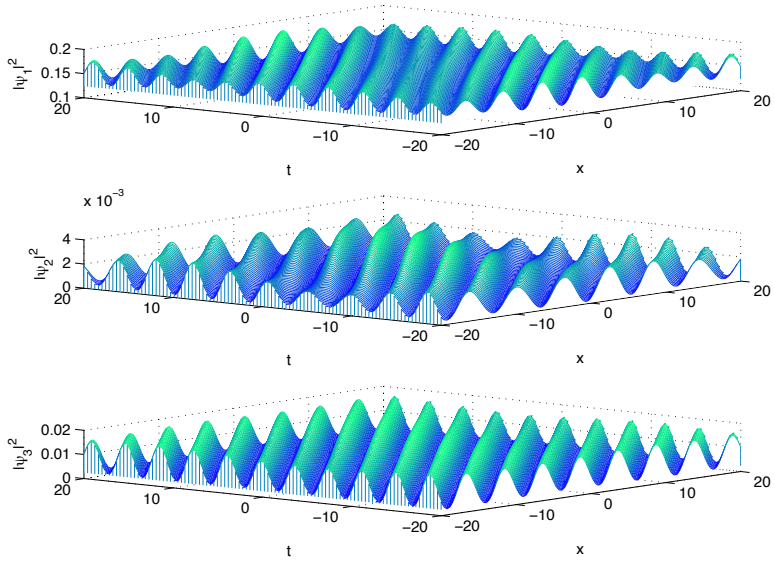

Figure 8.18: *Solution to the 3-NLS^s equation on the dividing curve (8.2.33) of genus 3 for the points with $x = 2.5$ on the x-sphere. The sheets are identified at the fiber over* $-2.1404 + 0.4404\mathrm{i}, (-12.2492+2.0113\mathrm{i}, -5.1634+1.3519\mathrm{i}, -4.5915+0.9380\mathrm{i}, -1.5405+0.5429\mathrm{i})$. *The vector of signs is* $s = (1, 1, 1)$.

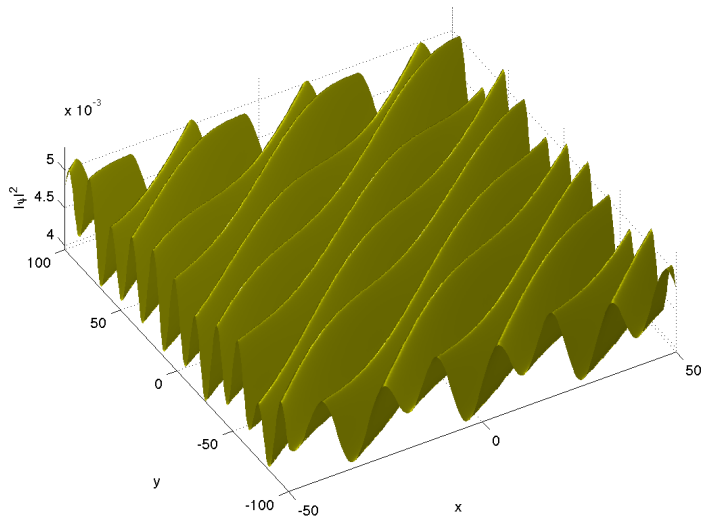

Figure 8.19: *Solution to the DS1$^-$ equation on the dividing curve (8.2.33) of genus 3 for the points* $a = (-4)^{(1)}$ *and* $b = (-3)^{(2)}$ *at* $t = 0$.

From (8.2.16) and (8.2.17) one gets for the characteristic: $\tilde{\delta} = \frac{1}{2}[\begin{smallmatrix} 0 & 0 & 1 \\ 1 & 1 & 0 \end{smallmatrix}]^t$.

The curve (8.2.33) has real fibers and can thus be used to construct solutions to the focusing 3-NLS equation. We consider the points on the curve with $x = 2.5$ and stable with respect to τ, and we choose $\mathbf{d} = 0$. The corresponding solution to the focusing 3-NLS equation can be seen in Figure 8.18.

A solution to the DS1$^-$ equation can be constructed by choosing the points $a = (-4)^{(1)}$ and $b = (-3)^{(2)}$ see Figure 8.19.

8.2.4 Fermat curve

The Fermat curves

$$y^n + x^n + 1 = 0, \qquad n > 2, \quad n \text{ even}, \tag{8.2.34}$$

are real curves without real oval with respect to τ. We consider here the curve with $n = 4$ that has genus 3. The matrix $\mathbb{H}$ has the form

$$\mathbb{H} = \begin{pmatrix} 0 & 1 & 0 \\ 1 & 0 & 0 \\ 0 & 0 & 0 \end{pmatrix},$$

and we find

$$P_{\tilde{\mathcal{A}}} = \begin{pmatrix} 0.9270 & -0.9270\mathrm{i} & -0.9270\mathrm{i} \\ 0 & 0 & -1.8541\mathrm{i} \\ 0.9270\mathrm{i} & -0.9270 & -0.9270\mathrm{i} \end{pmatrix},$$

$$P_{\tilde{\mathcal{B}}} = \begin{pmatrix} 0.9270 + 0.9270\mathrm{i} & 0.9270 - 0.9270\mathrm{i} & 0 \\ 0 & -0.9270 + 0.9270\mathrm{i} & 0.9270 - 0.9270\mathrm{i} \\ -0.9270 & -0.9270\mathrm{i} & -0.9270\mathrm{i} \end{pmatrix}.$$

The following matrices A, B, C, D provide a solution of (8.2.8)-(8.2.11):

$$A = \begin{pmatrix} 0 & 1 & 1 \\ 1 & 0 & 0 \\ 0 & 0 & 1 \end{pmatrix}, B = \begin{pmatrix} -1 & -2 & -1 \\ 0 & 0 & -1 \\ -1 & -1 & 0 \end{pmatrix}, C = \begin{pmatrix} 0 & 1 & 0 \\ 0 & 0 & 1 \\ 1 & -1 & 0 \end{pmatrix}, D = \begin{pmatrix} 0 & 0 & -1 \\ 0 & -1 & 0 \\ 0 & 0 & 1 \end{pmatrix},$$

which leads to the characteristic: $\tilde{\delta} = \frac{1}{2}[\begin{smallmatrix} 0 & 0 & 1 \\ 0 & 1 & 0 \end{smallmatrix}]^t$.

To construct a solution of the DS2$^-$ equation on the Fermat curve, we choose the points $a = (-1.5 + \mathrm{i})^{(1)}$ and $b = (-1.5 - \mathrm{i})^{(3)}$. The resulting solution for the choice $\mathbf{d} = 0$ can be seen in Figure 8.20.

8.3 Outlook

In this chapter we have presented the state of the art of the numerical evaluation of solutions to integrable equations in terms of multi-dimensional theta functions associated to real Riemann surfaces by using an approach via real algebraic curves. It was shown that real hyperelliptic curves parametrized by the branch points can be treated with machine precision for a wide range of the parameters. Even almost degenerate situations where the branch points coincide pairwise can be handled as long as at least one cut stays finite. This approach to real hyperelliptic curves [65, 66] is being generalized to arbitrary hyperelliptic curves.

As discussed in [67], the main difficulty for general algebraic curves is the correct numerical identification of the branch points. The case of degenerations for given branch points has not yet been studied numerically, but is planned for the future. In what concerns the solutions (6.3.14) to n-NLS^s and similar solutions to the DS and the Kadomtsev-Petviashvili equations, the main problem in the context of real Riemann surfaces is to find the symplectic transformation leading to the homology basis introduced in [150], for which the solutions of the studied equations, with regularity conditions, can be conveniently formulated. This problem has been reduced to find a single $g \times g$-matrix for given periods and real ovals, the latter encoded by the matrix $\mathbb{H}$. For M-curves, where the matrix $\mathbb{H}$ vanishes, a general formula for the characteristic (8.2.16)-(8.2.18) could be given. In the general case, an algorithm along the lines indicated in the previous section to find the transformation will be based on a sufficiently general ansatz for one of the matrices entering the symplectic transformation which is the subject of future work.

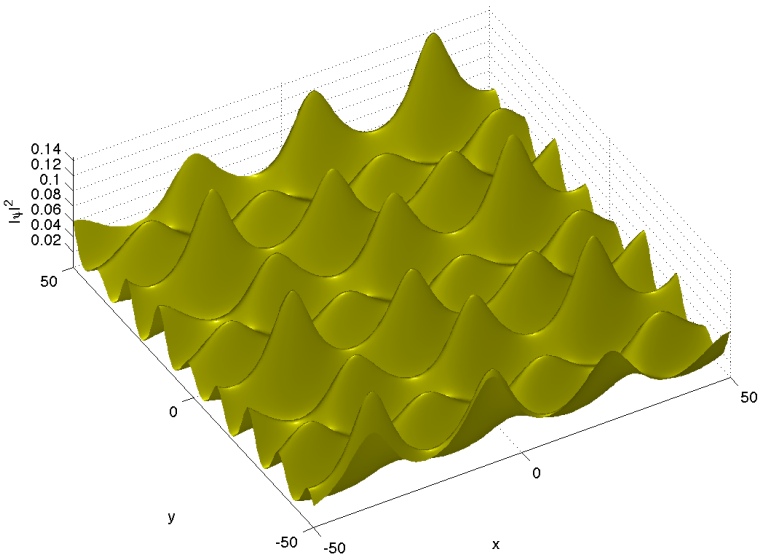

Figure 8.20: *Solution to the DS2$^-$ equation on the Fermat curve (8.2.34) of genus 3 for the points* $a = (-1.5 + \mathrm{i})^{(1)}$ *and* $b = (-1.5 - \mathrm{i})^{(3)}$ *at* $t = 0$.

Outlook

Fay identities, Gowdy universes and Einstein-Maxwell equations

The approach based on Fay's identity to generate solutions to integrable PDEs will be applied to further interesting equations as the stationary axisymmetric Einstein-Maxwell equations which reduce to Ernst equations in the electro-vacuum case. Relevant objects in astrophysics would be disks with strong magnetic fields. An explicit solution would allow us to study the role of strong magnetic fields in astrophysically interesting objects such as neutron stars. It was shown by Korotkin [91] that the corresponding solutions are given on three-sheeted Riemann surfaces where several branch points are parametrized by the physical coordinates. Such solutions have not been studied at all so far. Ernst equations also appear in the context of so-called Gowdy universes. In contrast to the standard Ernst equation they are not studied on $\mathbb{R}^2$ but on spaces with different topology, e.g. $\mathbb{T}^2$. This leads to different regularity requirements for the solutions. The formation of singularities for regular initial data is of particular interest in this context. For this question, a formulation of the initial value problem in terms of a Riemann-Hilbert problem will be studied.

Hurwitz spaces and random matrices

The remarkable property of algebro-geometric solutions to the Ernst equations is that some of the branch points depend on the physical coordinates. Thus modular properties of Riemann surfaces will be important in this context. This is best discussed in terms of Hurwitz spaces, i.e. the space of meromorphic functions on a Riemann surface. The discoveries will also be applicable in the context of random matrix theory. This theory has a wide range of applications in physics and mathematics. Today random matrices are an important tool in physics in 2D quantum gravity, statistical physics and string theory as well as in mathematics in the problem of Laplacian growth, intersection theory on moduli spaces and number theory, see [64] for references. Hurwitz spaces occur here in the context of the partition function in the limit of diverging matrix size, see [56]. A better understanding of Hurwitz spaces would make a study of the little explored case of interacting two-matrix models possible. Hurwitz spaces also occur in the context of Frobenius manifolds which are used to solve the Witten-Dijkgraf-Verlinde-Verlinde equation. This equation is of central importance among others in topological conformal quantum field theory, Gromov-Witten invariants and singularity theory.

Theta functions and Hurwitz spaces

The biggest obstacle for an extensive use of multi-dimensional theta functions in praxis has so far been the difficulty in evaluating these functions and other characteristic quantities on Riemann surfaces numerically. Though at least on hyperelliptic surfaces all important quantities are explicitly known in terms of integrals on the surface, the dependence on the branch points and the number of integrals to be determined are a problem. Several approaches to the numerical treatment of theta functions have been realized, see [39, 40] for references. These two codes are distributed along with Maple. Whereas these codes are an important step to provide general access to multi-dimensional theta functions, they are not efficient enough to study their modular dependence. To discuss solutions to the Ernst equation where the periods have to be calculated for each point of the spacetime, in [65, 66, 90] a spectral code to treat hyperelliptic theta functions has been given. This code computes periods even on almost degenerate Riemann surfaces in fractions of a second on an average computer to the order of machine precision. In collaboration with C. Klein and V. Shramchenko, a generalization of these codes to general algebraic curves would allow among others the visualization of solutions to the electro-magnetic Ernst equations.

Bibliography

[1] M.J. Ablowitz, D.J. Kaup, A.C. Newell, H. Segur, *Nonlinear evolution equation of physical significance*, Phys. Rev. Lett. **31**, 125–127 (1973).

[2] M.J. Ablowitz, D.J. Kaup, A.C. Newell, H. Segur, *The inverse scattering transform - Fourier analysis for nonlinear problems*, Stud. Appl. Math. **53**, 249 (1974).

[3] M.J. Ablowitz, B. Prinari, A.D. Trubatch, *Integrable Nonlinear Schrödinger Systems and their Soliton Dynamics*, Dynamics of PDE, **1**, No.3, 239–299 (2004).

[4] M.J. Ablowitz, H. Segur, *Solitons and the Inverse Scattering Transform*, SIAM, Philadelphia, PA (1981).

[5] N.N. Akhmediev, V.M. Eleonskii, N.E. Kulagin, *First-order exact solutions of the nonlinear Schrödinger equation*, Teoret. Mat. Fiz. **72**, 2:183–196 (1987). English translation: Theoret. Math. Phys. **72**, 2:809–818 (1987).

[6] N. Akhmediev, J. Soto-Crespo, A. Ankiewicz, *Extreme waves that appear from nowhere: On the nature of rogue waves*, Phys. Lett. A **373**, (25) 2137–2145 (2009).

[7] M.S. Alber, *N-component integrable systems and geometric asymptotics*, In Integrability: The Seiberg-Witten and Whitham equations (H.W. Braden and I.M. Krichever, editors). Gordon and Breach Science Publishers, Singapore, 213–228 (2000).

[8] M.S. Alber, R. Camassa, F. Fedorov, D.D. Holm, J.E. Marsden, *On billiard solutions of nonlinear PDE's*, Phys. Lett. A **264**, 171–178 (1999).

[9] M.S. Alber, R. Camassa, D.D. Holm, J.E. Marsden, *The geometry of peaked solitons and billiard solutions of a class of integrable PDE's*, Lett. Math. Phys. **32**, 137–151 (1994).

[10] M.S. Alber, R. Camassa, D.D. Holm, J.E. Marsden, *On the link between umbilic geodesics and soliton solutions of nonlinear PDE's*, Proc. Roy. Soc. **450**, 677–692 (1995).

[11] M.S. Alber, R. Camassa, F. Fedorov, N. Yu., D.D. Holm, J.E. Marsden, *On billiard solutions of nonlinear PDE's*, Phys. Lett. A **264**, 171–178 (1999).

[12] M.S. Alber, R. Camassa, F. Fedorov, N. Yu., D.D. Holm, J.E. Marsden, *The complex geometry of weak piecewise smooth solutions of integrable nonlinear PDE's of shallow water and Dym type*, Comm. Math. Phys. **221**, 197–227 (2001).

[13] M.S. Alber, F. Fedorov, N. Yu, *Wave solutions of evolution equations and Hamiltonian flows on nonlinear subvarieties of generalized Jacobians*, J. Phys. A **33**, 8409–8425 (2000).

[14] M.S. Alber, F. Fedorov, N. Yu, *Algebraic geometrical solutions for certain evolution equations and Hamiltonian flows on nonlinear subvarieties of generalized Jacobians*, Inverse Problems **17**, 1017–1042 (2001).

[15] Andonowati, N. Karjanto, E. Van Groesen, *Extreme wave phenomena in down-stream running modulated waves*, Appl. Math. Model. **31**, 1425–1443 (2007).

[16] D. Anker, N.C. Freeman, *On the Soliton Solutions of the Davey-Stewartson Equation for Long Waves*, Proc. R. Soc. London A **360**, 529 (1978).

[17] E. Arbarello, *Fay's trisecant formula and a characterization of Jacobian Varieties*, Proceedings of Symposia in Pure Mathematics **46** (1987).

[18] V.A. Arkadiev, A.K. Pogrebkov, M.C. Polivanov, *Inverse scattering transform and soliton solutions for Davey-Stewartson II equation*, Physica D **36**, 189–197 (1989).

[19] V.I. Arnold, *Mathematical methods of classical mechanics*, vol. **60** of Graduate Texts in Mathematics. Springer-Verlag, New York (1989). Translated from the 1974 Russian original by K. Vogtmann and A. Weinstein, corrected reprint of the second (1989) edition.

[20] W. Beals, D. Sattinger, J. Szmigielski, *Acoustic scattering and the extended Korteweg de Vries hierarchy*, Adv. Math. **140**, 190–206 (1998).

[21] W. Beals, D. Sattinger, J. Szmigielski, *Multi-peakons and a theorem of Stietjes*, Inverse Problems **15**, L1–L4 (1999).

[22] W. Beals, D. Sattinger, J. Szmigielski, *Multipeakons and the classical moment*, Adv. in Math. **154**, no. 2, 229–257 (2000).

[23] E. Belokolos, A. Bobenko, V. Enolskii, A. Its, V. Matveev, *Algebro-geometric approach to nonlinear integrable equations*, Springer Series in nonlinear dynamics (1994).

[24] A.I. Bobenko, C. Klein, (ed.), *Computational Approach to Riemann Surfaces*, Lect. Notes Math. **2013** (2011).

[25] L.A. Bordag, A.I. Bobenko, *Periodic Multiphase Solutions of the Kadomtsev-Petviashvili-equation*, J. Phys. A: Math. and General **22**, p. 1259 (1989).

[26] M. Boiti, J. Leon, L. Martina, F. Pempineili, *Scattering of localized solitons in the plane*, Phys. Lett. A **132**, 432–439 (1988).

[27] M. Boiti, L. Martina, F. Pempinelli, *Multidimensional localized solitons*, Chaos Solitons Fractals **5**, (12): 2377–2417 (1995).

[28] F. Calogero, *An integrable Hamiltonian system*, Phys. Lett. A **201**, 306–310 (1995).

[29] F. Calogero, J.P. Françoise, *Solvable quantum version of an integrable Hamiltonian system*, J. Math. Phys. **37**, (6) 2863–2871 (1996).

[30] R. Camassa, *Characteristic variables for a completely integrable shallow water equation*, In: Boiti, M. et al. (eds.) Nonlinearity, Integrability and All That: Twenty Years After NEEDS'79. Singapore: World Scientific (2000).

[31] R. Camassa, D.D. Holm, *An integrable shallow water equation with peaked solitons*, Phys. Rev. Lett. **71**, (11) 1661–1664 (1993).

[32] R. Camassa, D.D. Holm, J.M. Hyman, *A new integrable shallow water equation*, Adv. Appl. Mech. **31**, 1–33 (1994).

[33] D.Y. Chen, *Introduction to Solitons*, Science Press, Beijing, (2006).

[34] I.V. Cherednik, *Reality conditions in "finite-zone" integration*, Dokl. Akad. Nauk SSSR, **25**, No. 5, 1104–1108 (1980); English translation: Sov. Phys. Dokl., **25**, 450–452 (1980).

[35] A. Clebsch, *Zur Theorie der binären Formen sechster Ordnung und zur Dreitheilung der hyperelliptischen Funktionen*, Abh. der k. Ges. Wiss. zu Göttingen **14**, 1–59 (1869).

[36] A. Clebsch, P. Gordan, *Theorie der Abelschen Funktionen*, Teubner, Leipzig (1866).

[37] E. Date and S. Tanaka, *Analogue of inverse scattering theory for the discrete Hill's equation and exact solutions for the periodic Toda lattice*, Prog. Theoret. Phys. **56**, 457–465 (1976).

[38] A. Davey, K. Stewartson, *On three-dimensional packets of surface waves*, Proc. R. Soc. Lond. A **388**, 101–110 (1974).

[39] B. Deconinck, M. Van Hoeij, *Computing Riemann matrices of algebraic curves*, Physica D **28**, 152–153 (2001).

[40] B. Deconinck, M. Heil, A. Bobenko, M. Van Hoeij, M. Schmies, *Computing Riemann Theta Functions*, Mathematics of Computation **73**, 1417 (2004).

[41] B. Deconinck, M. Patterson, *Computing with plane algebraic curves and Riemann surfaces: the algorithms of the Maple package "algcurves"*, in A.I. Bobenko, C. Klein, (ed.), *Computational Approach to Riemann Surfaces*, Lect. Notes Math. **2013** (2011).

[42] A. Degasperis, *Solitons*, Am. J. Phys. **66**, 486–497 (1998).

[43] L.A. Dmitrieva, *Finite-gap solutions of the Harry Dym equation*, Phys. Lett. A **182**, 65–70 (1993).

[44] L.A. Dmitrieva, *The higher-times approach to multisoliton solutions of the Harry Dym equation*, J. Phys. A **26**, 6005–6020 (1993).

[45] O. Dolgopolova, E. Zverovich, *Explicit construction of global uniformization of an algebraic correspondence* (Russian), Sibirsk. Mat. Zh. **41**, 72–87 (2000), ii (translated in Siberian Math. J. **41**, 61–73 (2000)).

[46] P. Dubard, P. Gaillard, C. Klein, V.B. Matveev, *On multi-rogue wave solutions of the NLS equation and positon solutions of the KdV equation*, Eur. Phys. J. Special Topics **185**, 247–258 (2010).

[47] B.A. Dubrovin, *Matrix finite-zone operators*, Revs. Sci. Tech. **23**, 20–50 (1983).

[48] B.A. Dubrovin, *Theta functions and non-linear equations*, Usp. Mat. Nauk **36**, No. 2, 11–80 (1981) (English translation: Russ. Math. Surv. **36**, No. 2, 11–92 (1981)).

[49] B.A. Dubrovin, I.M. Krichever, S.P. Novikov, *Integrable systems*, Dynamical systems 4, Itogi Nauki i Tekhniki, Fund, invest., VINITI Akad. Nauk SSSR (1985).

[50] B.A. Dubrovin, V.B. Matveev, S.P. Novikov, *Nonlinear equations of Korteweg-de Vries type, finite-zone linear operators, and Abelian varieties*, Russian mathematical surveys **31**, 59–146 (1976).

[51] B.A. Dubrovin, S. Natanzon, *Real theta function solutions of the Kadomtsev-Petviashvili equation*, Math. USSR Irvestiya **32**:2, 269–288 (1989).

[52] S.N. Eilenberger, *An Introduction to Difference Equations*, Springer, New York (1996).

[53] D. Eisenbud, N. Elkies, J. Harris, R. Speiser, *On the Hurwitz scheme and its monodromy,* Compositio Mathematica **77**, No.1, 95–117 (1991).

[54] V. Eleonskii, I. Krichever, N. Kulagin, *Rational multisoliton solutions to the NLS equation*, Soviet Doklady 1986 sect. Math. Phys. **287**, 606–610 (1986).

[55] J. Elgin, V. Enolski, A. Its, *Effective integration of the nonlinear vector Schrödinger equation*, Physica D **225**, (22) 127–152 (2007).

[56] B. Eynard, A. Kokotov, D. Korotkin, $1/N^2$ *correction to free energy in hermitian two-matrix model*, Nucl. Phys. B **694**, 443 (2004).

[57] L. Faddeev, L. Takhtajan, *Hamiltonian Methods in the Theory of Solitons*, Springer, Berlin (1987).

[58] H.M. Farkas, I. Kra, *Riemann surfaces*, Graduate Texts in Mathematics **71**, Springer-Verlag, Berlin - Heidelberg - New York (1980).

[59] H.M. Farkas, *On Fay's trisecant formula*, J. Analyse Math. **44** (1984).

[60] J. Fay, *Theta functions on Riemann surfaces*, Lecture Notes in Mathematics **352** (1973).

[61] H. Flaschka, *The Toda lattice*, Phys. Rev. B9, 1924 (1974); *The Toda lattice II*, Progr. Theor. Phys. **51**, 703–716 (1974).

[62] A.S. Fokas, B. Fuchssteiner, *Symplectic structures, their Bäcklund transformations and hereditary symmetries*, Physica D **4**, 47–66 (1981/82).

[63] A.S. Fokas, P.M. Santini, *Dromions and a boundary value problem for the Davey-Stewartson 1 equation*, Physica D **44**, 99 (1990).

[64] P.J. Forrester, N.C. Snaith, J.J.M. Verbaarshot, *Developments in random matrix theory*, J. Phys. A **36**, R1 (2003).

[65] J. Frauendiener, C. Klein, *Hyperelliptic theta functions and spectral methods*, J. Comp. Appl. Math. (2004).

[66] J. Frauendiener, C. Klein, *Hyperelliptic theta functions and spectral methods: KdV and KP solutions*, Lett. Math. Phys. **76**, 249–267 (2006).

[67] J. Frauendiener, C. Klein, *Algebraic curves and Riemann surfaces in Matlab*, in A. Bobenko and C. Klein (ed.), *Riemann Surfaces –Computational Approaches*, Lecture Notes in Mathematics **2013** (Springer) (2011).

[68] N.C. Freeman, *Soliton Solutions of Non-linear Evolution Equations*, IMA J. Appl. Math. **32**, 125 (1984).

[69] N.C. Freeman, J.J.C. Nimmo, *A method of obtaining the N-soliton solution of the Boussinesq equation in terms of a wronskian*, Phys. Lett. A **95**, 1 (1983).

[70] C.S. Gardner, J.M. Greene, R. Miura, M. Kruskal, *Method for Solving the Korteweg-de Vries Equation*, Comm. Appl. Math. **27**, 97 (1974).

[71] F. Gesztesy, H. Holden, *Soliton Equations and Their Algebro-Geometric Solutions*, Volume I: (1+1)-Dimensional Continuous Models, Cambridge studies in advanced mathematics, volume **79**. Cambridge: Cambridge University Press (2003).

[72] A. Göpel, Crelle's Journ. f. Math. **35**, 277 (1847).

[73] B.H. Gross, J. Harris, *Real algebraic curves*, Ann. sci. Ecole Norm. Sup. (4) **14**, 157–182 (1981).

[74] R.C. Gunning, *Some identities for Abelian integrals*, Amer. J. Math. **108** (1985).

[75] A. Harnack, *Ueber die Vieltheiligkeit der ebenen algebraischen Curven*, Math. Ann. **10**, 189–199 (1876).

[76] K.L. Henderson, D.H. Peregrine, J.W. Dold, *Unsteady water wave modulations: fully nonlinear solutions and comparison with the nonlinear Schrödinger equation*, Wave Motion **29**, 341–361 (1999).

[77] R. Hirota, *Exact Solution of the Korteweg-de Vries Equation for Multiple Collisions of solitons*, Phys. Rev. Lett. **27**, 1192 (1971).

[78] J.K. Hunter, Y.X. Zheng, *On a completely integrable nonlinear hyperbolic variational equation*, Physica D **79** 361–86 (1994).

[79] A.R. Its, *Inversion of hyperelliptic integrals and integration of nonlinear differential equations*, Vestn. Leningr. Gos. Univ. **7**, No. 2, 37–46 (1976).

[80] A.R. Its, V.P. Kotlyarov, *Explicit formulas for solutions of the Nonlinear Schrödinger equation*, Dokl. Akad. Nauk Ukrain. SSR, Ser. A, No. 11, 965–968 (1976), (Russian).

[81] A. Its, V. Matveev, *Schrödinger operators with the finite-band spectrum and the N-soliton solutions of the Korteweg-de Vries equation*, (Russian) Teoret. Mat. Fiz. **23**, No. 1, 51–68 (1975).

[82] A.R. Its, A.V. Rybin, M.A. Salle, *Exact integration of nonlinear Schrödinger equation*, Teore. i Mat. Fiz., **74**, N. 1, 29–45 (1988).

[83] C.G.J. Jacobi, Crelle's Journ. f. Math. **9**, 394 (1832).

[84] M. Kac, P. Van Moerbeke, *A complete solution of the periodic Toda problem*, Proc. Nat. Acad. **72** (1975).

[85] C. Kalla, *New degeneration of Fay's identity and its application to integrable systems*, preprint arXiv:1104.2568v1 (2011).

[86] C. Kalla, *Breathers and solitons of generalized nonlinear Schrödinger equations as degenerations of algebro-geometric solutions*, J. Phys. A : Math. Theor. **44** (2011).

[87] C. Kalla, C.Klein, *On the numerical evaluation of algebro-geometric solutions to integrable equations*, preprint hal-00601630 (2011).

[88] T. Kanna, M. Lakshmanan, P. Tchofo Dinda, N. Akhmediev, *Soliton collisions with shape change by intensity redistribution in mixed coupled nonlinear Schrödinger equations*, Phys. Rev. E **73** (2006).

[89] C. Klein, D. Korotkin, V. Shramchenko, *Ernst equation, Fay identities and variational formulas on hyperelliptic curves*, Math. Res. Lett. **9**, 1–20 (2002).

[90] C. Klein, O. Richter, *Ernst Equation and Riemann Surfaces*, Lecture Notes in Physics **685** (Springer) (2005).

[91] D. Korotkin, *Finite-gap solutions of the stationary axisymmetric Einstein equation*, Theor. Math. Phys. **77** 1018–1031 (1989).

[92] D. Korotkin, V. Shramchenko, *Riemann-Hilbert problem for Hurwitz Frobenius manifolds: regular singularities*, preprint arXiv:0909.0543 (2009).

[93] D.J. Korteweg, G. de Vries, *On the change of form of long waves advancing in a rectangular canal, and on a new type of long stationary waves*, Philos. Mag. Ser. 5, **39**, 422–443 (1895).

[94] V.A. Kozel, V.P. Kotlyarov, *Almost periodic solutions of the equation* $u_{tt} - u_{xx} + \sin(u) = 0$, Dokl. Akad. Nauk Ukrain. SSR Ser. A no. **10** , 878–881 (1976). In Russian.

[95] A. Krazer, *Lehrbuch der Thetafunktionen*, Teubner, Leipzig (1903).

[96] I.M. Krichever, *Algebro-geometric construction of the Zakharov-Shabat equations and their periodic solutions*, Sov. Math. Dokl. **17**, 394–397, (1976).

[97] I.M. Krichever, *Integration of nonlinear equations by the methods of algebraic geometry*, Funkts. Anal. Prilozh. **11**, No. 1, 15–31 (1977) (English translation: Funct. Anal. Appl. **11**, 12–26 (1977)).

[98] I.M. Krichever, *Methods of algebraic geometry in the theory of non-linear equations*, Usp. Mat. Nauk **32**, No. 6, 183–208 (1977) (English translation: Russ. Math. Surv. **32**, No. 6, 185–213 (1977)).

[99] I.M. Krichever, *Algebraic curves and nonlinear difference equations*, Russian Math. Surveys **334**, 255–256 (1978).

[100] I.M. Krichever, *Nonlinear equations and elliptic curves*, Rev. of Science and Technology **23**, 51–90 (1983).

[101] I.M. Krichever, *Algebro-geometric spectral theory of the Schrödinger difference operator and the Peierls model*, Soviet Math. Dokl. **26**, 194–198 (1982).

[102] I.M. Krichever, *The Peierls model*, Funct. Anal. Appl. **16**, 248–263 (1982).

[103] I.M. Krichever, *The averaging method for two-dimensional integrable equations*, (Russian) Funktsional. Anal. i Prilozhen. **22**, No. 3, 37–52, 96 (1988); translation in Funct. Anal. Appl. **22** (1988), No. 3, 200–213 (1989).

[104] I.M. Krichever, *Algebraic-geometrical methods in the theory of integrable equations and their perturbations*, Acta Appl. Math. **39**, 93–125 (1995).

[105] I.M. Krichever, S.P. Novikov, *Holomorphic bundles over Riemann surfaces and the Kadomtsev-Petviashvili (KP) equation. I*, Funkts. Anal. Prilozh. **12**, No. 4. 41–52 (1978) (English translation: Funct. Anal. Appl. **12**, 276–286 (1978)).

[106] P.D. Lax, *Integrals of nonlinear equations of evolution and solitary waves*, Comm. Pure. Appl. Math. **31**, 467–490 (1968).

[107] P.D. Lax, *Periodic solutions of the KdV equation*, Communications on pure and applied mathematics **28**, 141–188 (1975).

[108] Y.C. Ma, *The perturbed plane-wave solutions of the cubic Schrödinger equation*, Stud. Appl. Math. **60**, 1:43–58 (1979).

[109] S.V. Manakov, *On the theory of two-dimensional stationary self-focusing of electromagnetic waves*, Sov. Phys. JETP **38**, 248 (1974).

[110] S.V. Manakov, *Complete integrability and stochastization of discrete dynamical systems*, Soviet Phys. JETP **40**, 269–274 (1974).

[111] S.V. Manakov, V.E. Zakharov, L.A. Bordag, A.R. Its, V.B. Matveev, *Two Dimensional Solitons of the Kadomtsev-Petviashvili Equation and Their Interaction*, Phys. Lett. A **63**, 205 (1977).

[112] T. Malanyuk, *Finite-gap solutions of the Davey-Stewartson equations*, J. Nonlinear Sci. **4**, No. 1, 1–21 (1994).

[113] Y. Matsuno, *Multiperiodic and multisoliton solutions of a nonlocal nonlinear Schrödinger equation for envelope waves*, Phys. Lett. A **278**, 53 (2000).

[114] V.B. Matveev, M.A. Salli, *Darboux Transformations and Solitons*, Springer Series in Nonlinear Dynamics, Springer-Verlag, Berlin (1991).

[115] M. McConnell, A. Fokas, B. Pelloni, *Localized coherent solutions of the DSI and DSII equations–a numerical study*, Mathematics and Computers in Simulation **69**, no. 5-6, 424–468 (2005).

[116] S. McCullough, *The trisecant identity and operator theory*, Integral Equations Operator Theory **25**, 104–128 (1996).

[117] H.P. McKean, A. Constantin, *A shallow water equation on the circle*, Comm. Pure Appl. Math. Vol LII, 949–982 (1999).

[118] H.P. McKean, P. Van Moerbeke, *The spectrum of Hill's equation*, Inventiones Math. **30**, 217–274 (1975).

[119] P. Van Moerbeke, D. Mumford, *The spectrum of difference operators and algebraic curves*, Acta Math. **143**, 97–154 (1979).

[120] D. Mumford, *An algebro-geometric construction of commuting operators and of solutions to the Toda lattice equation, Korteweg-de Vries equation and related non-linear equations*, Intl. Symp. Algebraic Geometry, 115–153, Kyoto (1977).

[121] D. Mumford, *Tata Lectures on Theta. I and II.*, Progress in Mathematics **28** and **43**, respectively. Birkhäuser Boston, Inc., Boston, MA (1983 and 1984).

[122] A.C. Newell, *Solitons in Mathematics and Physics*, Society for Industrial and Applied Mathematics, Philadelphia (1985).

[123] J.J.C. Nimmo, N.C. Freeman, *The use of Bäcklund transformations in obtaining N-soliton solutions in Wronskian form*, J. Phys. A: Math. Gen. **17**, 1415 (1984).

[124] S.P. Novikov, *The periodic problem for the Korteweg-de Vries equation*, Functional analysis and its applications **8**, 54–66 (1974).

[125] D.P. Novikov, *Algebraic-geometrical solutions of the Harry–Dym equations*, Sibirskii Matematicheskii Zhurnal **40**, 159–163, (Russian) English transl. in: Siberian Math. Journal **40**, 136–140 (1999).

[126] S. Novikov, S. Manakov, L. Pitaevskii, V. Zakharov, *Theory of Solitons - The Inverse Scattering Method*, Consultants Bureau: New York (1984). (original Russian edition 1980)

[127] A.R. Osborne, M. Onorato, M. Serio, *The nonlinear dynamics of rogue waves and holes in deep-water gravity wave trains*, Phys. Lett. A **275**, 386–393 (2000).

[128] R.S. Palais, *The symmetries of solitons*, Bull. Amer. Math. Soc. **34**, 339–403 (1997).

[129] D.H. Peregrine, *Water waves, nonlinear Schrödinger equations and their solutions*, J. Austral. Math. Soc. Ser. B **25**, 1:16–43 (1983).

[130] A.D. Polyanin, V.F. Zaitsev, *Handbook of Nonlinear Partial Differential Equations*, Chapman and Hall/CRC, Boca Raton (2004).

[131] C. Poor, *Fay's trisecant formula and cross-ratios*, American mathematical society **114**, No. 3 (march 1992).

[132] E. Previato, *Hyperelliptic quasi-periodic and soliton solutions of the nonlinear Schrödinger equation*, Duke Math. J. **52**, 329–377 (1985).

[133] R. Radhakrishnan, M. Lakshmanan, *Bright and dark soliton solutions to coupled nonlinear Schrödinger equations*, J. Phys. A, Math. Gen. **28**, 2683–2692 (1995).

[134] R. Radhakrishnan, M. Lakshmanan, *Inelastic Collision and Switching of Coupled Bright Solitons in Optical Fibers*, Phys. Rev. E **56**, 2213 (1997).

[135] R. Radha, M. Lakshmanan, *Localized Coherent Structures and Integrability in a Generalized* $(2+1)$*-Dimensional Nonlinear Schrödinger Equation*, Chaos, Solitons and Fractals **8**, p. 17 (1997).

[136] R. Radhakrishnan, R. Sahadevan, M. Lakshmanan, *Integrability and singularity structure of coupled nonlinear Schrödinger equations*, Chaos, Solitons and Fractals **5**, No. 12, 2315–2327 (1995).

[137] A. Raina, *Fay's Trisecant Identity and Conformal Field Theory*, Commun. Math. Phys. **122**, 625 (1989).

[138] G. Rosenhain, Crelle's Journ. f. Math. **40**, 319 (1850).

[139] J.S. Russell, Report on waves. Proc. Roy. Soc. Edinburgh, 319–320 (1844).

[140] P.M. Santini, *Energy exchange of interacting coherent structures in multidimensions*, Physica D **41**, 26–54 (1990).

[141] T. Shiota, *Characterization of Jacobian varieties in terms of soliton equations*, Invent. Math. **83**, 333–382 (1986).

[142] H. Stahl, *Theorie der Abel'schen Functionen*, Teubner, Leipzig (1896).

[143] M. Tajiri, T. Arai, *Periodic soliton solutions to the Davey-Stewartson equation*, Proc. Inst. Math. Natl. Acad. Sci. Ukr. **30**, 1:210–217 (2000).

[144] G. Teschl, *Jacobi Operators and Completely Integrable Nonlinear Lattices*, Math. Surv. and Monographs **72**, Amer. Math. Soc., Rhode Island (2000).

[145] M. Toda, *Theory of Nonlinear Lattices*, 2nd enl. ed., Springer, Berlin (1989).

[146] M. Toda, *Theory of Nonlinear Waves and Solitons*, Kluwer, Dordrecht (1989).

[147] L.N. Trefethen, *Spectral Methods in Matlab*, SIAM, Philadelphia, PA (2000).

[148] C.L. Tretkoff, M.D. Tretkoff, *Combinatorial group theory, Riemann surfaces and differential equations*, Contemporary Mathematics **33**, 467–517 (1984).

[149] M. Trott, *Applying Groebner Basis to Three Problems in Geometry*, Mathematica in Education and Research **6**, (1) 15–28 (1997).

[150] V. Vinnikov, *Self-adjoint determinantal representations of real plane curves*, Math. Ann. **296**, 453–479 (1993).

[151] N. Yoshida, K. Nishinari, J. Satsuma, K. Abe, *A new type of soliton behavior of the Davey-Stewartson equations in a plasma system,* J. Phys. A **31**, 3325 (1998).

[152] N.J. Zabusky, M.D. Kruskal, *Interaction of solitons in a collisionless plasma and the recurrence of initial states*, Physics Rev. Lett. **15**, 240–243 (1965).

[153] V. Zakharov, S. Manakov, *On the complete integrability of a nonlinear Schrödinger equation*, Teoret. Mat. Fiz. **19**:3, 332–343 (1974).

[154] V.E. Zakharov, A.B. Shabat, *Exact theory of two-dimensional self-focusing and one-dimensional self-modulation of waves in nonlinear media*, Soy. Phys. JETP **34**, 62–69 (1972).

[155] V.E. Zakharov, A.B. Shabat, *A scheme for integrating the nonlinear equations of mathematical physics by the method of the inverse scattering problem*, I., Funct. Anal. Appl. **8**, 226–235 (1974).

[156] V. Zakharov, E. Schulman, *To the integrability of the system of two coupled nonlinear Schrödinger equations*, Physica D **4**, 270–274 (1982).

Index

Abel map, 23
Abel's theorem, 23
Abelian differential, 21
    normalized, 22
    of the first kind, 21
    of the second kind, 21
    of the third kind, 21
    period, 21
    polar period, 21
Abelian function, 24
algebraic curve, 17
    dividing, 33
    hyperelliptic, 18
    M-curve, 33
    non-singular, 18
    real, 14
analytic continuation
    numerical, 133
    paths for, 142

Baker-Akhiezer function, 4
base point, 23
bidifferential, 26
branch cuts, 105
branch number, 19
branch point, 18
breather, 108
    rational, 108

Camassa-Holm equation, 8
canonical basis of cycles, 20
chain, 19
characteristic, 23
    half integer, 23
    non-singular, 24
    odd, 24
Chebyshev polynomials, 134
collision, 104
    elastic, 104
covering
    m-sheeted, 19
    holomorphic, 18
    ramified, 18
critical point, 78
cross-ratio
    on a Riemann surface, 27
    on the sphere, 27
cusp-like singularity, 46
cuspon, 59
cycle, 19

Davey-Stewartson equations, 11
degenerate
    hyperelliptic curve, 55
    Riemann surface, 98
divisor, 23
    degree, 23
    linearly equivalent, 23
    principal, 23
    theta, 25
dromion, 123
Dym type equation, 8

elliptic
    function, 25
    integral, 25
    surface, 83
essential singularity, 5

Fay's identity, 27
finite-gap potential, 4
fundamental group, 78

gap, 7
genus, 18

half-period, 132
Hamiltonian, 1
Harnack's inequality, 33
holomorphic mapping, 18
    branch number, 19
    branch point, 18
    degree, 19
    fiber, 73
homology basis
    canonical, 20
    symplectic transformation, 20
homology group
    first, 19
    relative, 35
hyperelliptic
    curve, 18
    involution, 30
    surface, 97

integrable system, 1
intersection index, 20
inverse scattering transform method, 2
involution
    anti-holomorphic, 33
    hyperelliptic, 30

Jacobi inversion problem, 24
Jacobian, 23

Kadomtsev-Petviashvili equation, 5
Korteweg-de Vries equation, 3

Lax pair, 2
Liouville integrable system, 1
local parameter, 18
lump, 123

M-curve, 33
meromorphic function
    on a Riemann surface, 18
    on the sphere, 102
    real, 75
multi-component nonlinear Schrödinger equation, 10

nonlinear Schrödinger equation, 4

peakon, 61
period, 21
period lattice, 23
polar period, 21
prime form, 25

ramification point, 78
real oval, 33
residue (of a differential), 21
Riemann matrix, 22
Riemann sphere, 27
Riemann surface, 17
    hyperelliptic, 30
    real, 33
    real dividing, 33
    with punctures, 35
Riemann theta function, 25
Riemann's bilinear identity, 21

Schottky problem, 13
Schottky uniformization, 13
Sine-Gordon equation, 30
soliton, 3
    bright, 104
    dark, 104
solitonic limit, 55
    almost, 135
spectral curve, 2
spinor, 26
symplectic transformation, 20

theta divisor, 25
theta function
    Riemann, 25
    with characteristic, 23
Toda lattice equation, 31
Tretkoff-Tretkoff algorithm, 142
Trott curve, 146

uniformization map, 98

Vandermonde determinant, 85
vector of Riemann constants, 25
Vinnikov basis, 34

Wronskian, 4

Abstract

Fay's identity on Riemann surfaces is a powerful tool in the context of algebro-geometric solutions to integrable equations. This relation generalizes a well-known identity for the cross-ratio function in the complex plane. It allows to establish relations between theta functions and their derivatives. This offers a complementary approach to algebro-geometric solutions of integrable equations with certain advantages with respect to the use of Baker-Akhiezer functions. It has been successfully applied by Mumford et al. to the Korteweg-de Vries, Kadomtsev-Petviashvili and sine-Gordon equations.

Following this approach, we construct algebro-geometric solutions to the Camassa-Holm and Dym type equations, as well as solutions to the multi-component nonlinear Schrödinger equation and the Davey-Stewartson equations. Solitonic limits of these solutions are investigated when the genus of the associated Riemann surface drops to zero. Moreover, we present a numerical evaluation of algebro-geometric solutions of integrable equations when the associated Riemann surface is real.